THE AGE, ORIGIN AND PATHWAY OF SUBSURFACE STORMFLOW IN A STEEP HUMID HEADWATER CATCHMENT

A Thesis

Presented for the Degree of

Doctor of Philosophy in Geography

at the University of Canterbury

Christchurch, New Zealand

by

J.J. McDonnell

University of Canterbury

1988

ERRATA

PAGE	READS	SHOULD READ
xvii p1 L6	"Of the 7 events"	"Of the 6 events"
xvii p1 L8	"averaged 10%"	"averaged 90%"
52 p1 L6	"runoff exceeded the slope"	"runoff plotted above the slpoe"
p1 L11	"3 of 13 storms"	"4 of the 11 storms"
p1 L12	"API_7=32.2mm"	"API_7=31.2mm"
p1 L13	"4 plotted"	"5 plotted"
51 p1 L13	"below 90% volumetric water conteht"	"below 90%saturation"
45 p3 L27	"Qo=(Co-Cn/Co-Cn)Qs"	"Qo=[(Cs-Cn)/(Co-Cn)]Qs"
215 p1 L7/8	"Never the less ... context	delete
220 p1 L13	"representing 35%"	"representing 44%"

p = page L = lines from top of page

ACKNOWLEDGEMENTS

Many individuals, institutions and funding agencies contributed to the completion of this research, and I would like to thank them formally for their help.

The research was funded through the American Geophysical Union (in the form of a Horton Research Grant), New Zealand Commonwealth Scholarship and Fellowship Programme, University Grants Committee and the University of Canterbury Geography Department. The Institute of Nuclear Sciences and Forest Research Centre are also thanked for their analytical services and logistical support throughout the study.

Early discussion and/or correspondence with Drs. B. Clothier, J. Laronne, C. Taylor, V. Kennedy, M. Sklash, P. Germann, J. Buttle and Prof. O. Slaymaker was very useful and much appreciated. Throughout the research, Drs. M. Bonell, M. Stewart, R. Jackson and A. Pearce provided input and guidance on the research results and interpretations. Dr. M. Stewart, in particular, contributed to the isotopic modelling, and his thoughts and ideas enhanced the interpretation of isotopic results. Dr. I. Owens is thanked for his supervision, administration of the research grant and critical review of written material. Drs. G. Buchan and K. Cameron provided valuable input on soil physics interpretations in the final stages.

Many individuals assisted with the construction or design of the field instrumentation, including: P. Weir, P. Tyree, W. Gallagher, R. McGregor, and Drs. R. Jackson, B. Clothier, C. Trotter and M. Sklash. Particular thanks go to Dr. M. Sklash who loaned his Scanivalve and Cygnus water sampler to the project. The use of this equipment greatly enhanced collected data. P. Weir's early help with data logging, computing and electronic design greatly assisted a 'quick' field set-up. Many people

assisted me in the field, most notably: K. McDonnell, Dr. I. Owens, M. Single, R. Begg, S. Parker, Prof. O. Slaymaker, Dr. M. Bonell, J. Gray, J. Payne and S. Kitchingmen. J. Gray performed all laboratory water chemistry analysis, while K. McDonnell conducted most of the field water chemistry analysis, including computer input and data reduction. Dr. G. Buchan is thanked for loan of his soil testing equipment and related advice. A. Dyer and T. Shatford are thanked for their help in producing the figures. Dr. P. Goodson and K. McDonnell are thanked for their painstaking proofreading of the thesis. L. Rowe is thanked for his assistance in the final stages. The rainfall frequency data he so willingly provided improved the final interpretations considerably.

Finally, I would like to thank Kathleen for not only providing outstanding assistance in the field and laboratory, but also for much motivational and emotional support throughout the research.

Christchurch 16 December 1988

Jeff McDonnell

TABLE OF CONTENTS

LIST OF FIGURES

LIST OF TABLES

LIST OF SYMBOLS

A intercept of the regression line.

A amplitude of the δD input sine curve, $^{o}/_{oo}$.

API antecedent precipitation index, mm.

B amplitude of the δD output sine curve, $^{o}/_{oo}$.

B slope of the regression line.

BD bulk density, g cm^{-3}.

C tracer concentration, $^{o}/_{oo}$, $\mu S\ cm^{-1}$, or ppm.

Cl chloride, ppm.

d slit width, mm.

D deuterium.

D_{sg} deep soil water and groundwater, $^{o}/_{oo}$, $\mu S\ cm^{-1}$, ppm.

DF delayed flow, mm.

EC electrical conductivity, $\mu S\ cm^{-1}$.

f(t) fraction of water of any given age t, d.

g acceleration due to gravity, m s^{-2}.

h water depth, mm.

h' pressure differential, Pa.

H wetted depth, mm.

ID inside diameter, mm.

Ii rainfall intensity during sampling increment, mm hr^{-1}.

K hydraulic conductivity, mm hr^{-1}.

K_{sat} saturated hydraulic conductivity, mm hr^{-1}.

L porous cup thickness, mm.

n new water (subscript).

o old water (subscript).

o osmotic potential, cm H_2O.

OD outside diameter, mm.

P precipitation, mm.

P porosity, %.

ρ_f fluid density, g cm^{-3}.

Pi fractionally collected rain, mm.

p_w density of water, g cm^{-3}.

Q discharge, mm hr^{-1}, or ml min^{-1}.

Q' rate of outflow (from well permeameter), mm^3 hr^{-1}.

QF quickflow, mm.

R radius, mm.

R D/H.

RO runoff, mm.

s stream water (subscript).

S_w shallow soil water concentration, ‰, µS cm^{-1}, ppm.

SL suction lysimeter.

SMOW standard mean ocean water.

t time, s, d.

T mean age of water, d.

ν dynamic viscosity, N m^{-2}.

v flux, mm hr^{-1}.

V_{sub} subsurface velocity, mm hr^{-1}.

x_w weighted mean.

z elevational potential, cm.

z measurement height, mm, cm, m.

δ delta notation for D concentrations.

θ volumetric water content, %.

θ phase lag, days.

ψ matric potential, cm H_2O.

ϕ total potential, cm.

‰ per mil difference, used with δ notation.

ABSTRACT

A combined recording tensiometric, hydrometric, chemical and stable isotope tracing approach was used to identify the age, origin and pathways of subsurface stormflow in a small (3.8 ha) catchment in the Tawhai State Forest, Westland, New Zealand. Eleven storm runoff events were intensively monitored during the August to December 1987 study period. Of the 7 events suitable for isotopic mass balance hydrograph separation, the volume fraction of groundwater, or pre-event water, averaged 10% of stormflow volumes. New water contribution could be accounted for by saturation overland flow and headwater subsurface flow. Hillslope flow was dominated by old water contributions of between 70 and 100%, which increased downslope. Within storm deuterium variations in rainfall were high (4.4 to 93.5‰), reflecting changes in air mass trajectory and rainfall intensity. Soil water and groundwater deuterium concentrations showed a dampened response to rainfall input, and mean residence time varied from approximately 12 to 100 days, depending on soil depth, slope position and distance downslope.

Soil physics analyses were conducted in valley-bottom near-stream, midslope hollow and upslope hollow locations. Tensiometric results showed that the unsaturated zone overlying near-stream groundwater was rapidly changed to positive matric potential due to the limited storage characteristics of the local soils. This response produced an early and steady increase in old water exfiltration into the stream channel as a groundwater ridge developed along the channel margin. As rainfall depth increased above approximately 10 mm, contributions from mid-slope and upslope hollows dominated channel stormflow, and most of the subsurface water was delivered to first order channels via continuous pipes occurring at the mineral soil-bedrock interface.

Limited storage effects augmented the development of a perched water-table in the mid-slope hollow, which was quickly dissipated by lateral pipeflow. Bypass flow down cracks was observed during some events with high (8 to 14 mm hr^{-1}) short-term rainfall intensity bursts. The relatively low frequency of high hourly rainfall intensities, however, ensures that bypassing is not a regular occurrence in the M8 catchment. Results from ten hillslope water injection experiments in various slope positions showed that input water isotopic signatures attained an old water status very quickly, due to mixing with a near-saturated soil matrix along crack and pipe walls.

The major implications of this work are twofold: (i) it has demonstrated that stream-based isotopic and chemical tracing can be reconciled with hillslope-oriented hydrometric work, and (ii) it has revealed some of the important runoff processes that link the idea of macropore flow with the notion of old water displacement, and which satisfies information on soil water physics and water isotopic concentrations.

1 INTRODUCTION

1.1 RATIONALE FOR HILLSLOPE HYDROLOGICAL RESEARCH

Since the early work of Horton (1933), hydrologists have examined the rates and pathways of runoff production in an attempt to model water transfer through catchments of various sizes. For flood routing, relatively simple assumptions regarding runoff pathways have been adequate for successful modelling. However, as water quality considerations are incorporated into many distributed catchment models (e.g. the SHE model; Beven et al., 1980), more detailed understanding of water movement pathways, residence times and water origin is required for successful model implementation. This is particularly true for acid rain and contaminant transport investigations, in which details of not only the magnitude of water flux, but also its complete movement history within the catchment, are important.

Runoff rates and pathways vary considerably in time and space, and to date, three basic mechanisms have been observed which pertain to specific local environmental, storm and antecedent wetness conditions (Ward, 1984). Hortonian overland flow, based on Horton's (1933) infiltration theory, operates under specific conditions where rainfall rates exceed the current infiltration capacity of the soil. This situation results in rapid flow over the soil surface and into the stream channel. Betson (1964) incorporated this process into his 'partial area' concept, and showed that overland flow from only a small area of the catchment was required to supply the hydrograph peak.

A number of studies during the late 1960s and early 1970s questioned the understanding of Hortonian overland flow, and showed that for many forested environments with suitable soil conditions and slope angles, subsurface stormflow (Whipkey, 1965)

may completely generate the storm hydrograph. This process was considered by Hewlett (1961), when he combined the idea of subsurface stormflow together with that of an expanding channel network, into the 'variable source area concept'. Subsequent studies by Dunne and Black (1970a) showed that overland flow in most temperate upland areas occurred because of a rising groundwater table adjacent to the stream channel. Saturation overland flow is then produced when rain falls on to these surface saturated zones. Resulting rapid flow toward the channel is matched by a return flow component, consisting of both soil water and groundwater.

Although general conceptual models of runoff production for most environments are now available, we still do not have a complete understanding of many detailed processes. One example is that of groundwater-streamflow interaction and the role of soil macropores (non-capillary channels) in this process. As the fate of environmental contaminants becomes more problematic, detailed knowledge of both groundwater recharge and exfiltration into stream channels is required for proper management. If macropores are important under these conditions, then traditional models considering only soil matrix flow will have to be revised.

1.2 STATEMENT OF PROBLEM

The key to solving the above and other related problems is through fundamental research into the rainfall-runoff process. At present, further progress in understanding processes of storm runoff generation in humid headwater catchments is hampered by discrepancies often found between the different approaches to quantifying water movement. Results from chemical and natural isotope separations of streamwater into old (pre-event) and new (event) water sources often appear to contradict results from hydrometric studies of pathways of water movement on hillslopes.

Rodhe (1987) and others note that there is a gap between detailed investigations of single hillslopes (Anderson and Burt, 1978a) and the basin input-ouput studies (e.g. Bottomley et al., 1986) in which isotopes are used as tracers; and "no studies have been reported where the two types of investigation have been performed in the same basin" (Rodhe, 1987, p.41).

As a result, the importance of rapid throughflow of event water through macropores, versus translatory displacement of old water in subsurface runoff, remains poorly understood, largely due to inherent biases contained in specific field techniques. To increase our knowledge of groundwater-streamflow interaction, the above process must be examined, since it forms the major pathway of water movement in many small headwater catchments, and in part determines the residence time and chemical changes of subsurface water.

The critical questions in hillslope hydrology at present are: (i) can slope-oriented hydrometric studies be reconciled with stream-oriented isotopic tracing studies, and if so, (ii) can a mechanism satisfying both data sets be developed? This thesis addresses these questions by employing a combined soil physics, hydrometric, chemical and isotopic tracing approach, in an attempt to reconcile the broad hydrometric versus stream-oriented approaches and to provide comprehensive evidence of both runoff response mechanisms and water origin.

1.3 PRESENTATION FORMAT

1.3.1 Thesis format

Seven sections comprise the remainder of this thesis. Section 2 outlines the general processes of subsurface stormflow in terms of the physics of water flux in soil. It then reviews some of the studies that have documented subsurface flow under natural field conditions. Rapid flux mechanisms are also

described as they relate to interpretations from different approaches. Finally, the objectives of the thesis are fully outlined, particularly as they relate to previous work in the study catchment.

Section 3 describes the field site and general data collection and analysis procedures. The recording tensiometer network for measuring soil matric potential changes, is treated in some detail, and the section outlines new developments in recording techniques developed in this thesis research. Isotopic and chemical tracing techniques are also presented, and the mass balance equation and hydrograph separation procedures are fully explained.

Sections 4, 5 and 6 comprise the main results of the study. Section 4 focuses on the age and origin of subsurface flow, by showing data on the various isotopic, chemical and water volume inputs, outputs and reservoir storages. Both long-term (6 month) and short-term (within storm) analyses are conducted. Section 5 investigates the pathways of subsurface water movement at various sites using soil physics approaches. Relationships between near-stream, mid-slope and upslope areas are described and related to streamflow and throughflow response. Section 6 describes a series of 10 hillslope tracer experiments, in which tagged water was applied to the soil surface and traced to a downslope soil face. Results are discussed as they relate to natural events described in the preceding two sections.

Section 7 forms the main discussion of the research and outlines a general model of storm runoff production in humid headwater catchments. Hydrometric, chemical, isotopic and soil physics data are combined into a general description of catchment runoff behaviour. Geomorphological implications are discussed, particularly as they relate to subsurface water movement and

debris flow initiation. The final section reviews the major findings and presents some suggestions for future research, both in the study catchment and elsewhere.

1.3.2 Definition of terms

Various terms have been proposed to describe the runoff processes and mechanisms of soil water and groundwater movement. This thesis will follow the general terminology of Kirkby (1978) and Hewlett (1982). The terms given below are those which are not always clearly defined or else their definitions vary from author to author.

Capillary-fringe. Zone of tension saturation (i.e. where matric potential <0 cm H_2O but soil volumetric water content is near saturation).

Event water. Rainfall entering the catchment or stream channel during a storm event.

Exfiltration. Return flow of groundwater to the soil surface.

Groundwater. Water in soil or bedrock with matric potential at or above 0 cm H_2O. The term may apply to a long-term unconfined aquifer, or to transient groundwater developed on a hillslope for only a few hours.

Macropore. Structural void space within soil >3 mm diameter, capable of conducting water independently of the soil matrix. Two broad categories include: biologically created channels such as plant root cavities or faunal tunnels and soils with cracks along pedal faces.

Macropore flow. Subsurface stormflow through macropores.

Matric potential. A term used to express the specific potential energy of soil water, relative to that of water in a standard reference state.

Pre-event water. Soil water, groundwater and stream water in the catchment prior to rainfall.

Quickflow. Part of the stream hydrograph above the 0.0055 l ha^{-1} hr^{-1} line developed by Hewlett and Hibbert (1967). Relates only to rapidity of stream response and not to water origin.

Soil water. Water in soil with matric potential less than 0 cm H_2O. Soil water may be rapidly converted to groundwater by increases in matric potential.

Subsurface flow. Saturated or unsaturated (i.e. groundwater or soil water, respectively) water movement in soil in a downslope direction.

Subsurface stormflow. Subsurface flow which contributes to streamflow and the quickflow portion of the hydrograph.

Throughflow. Subsurface stormflow, generally moving laterally along a low permeability boundary. Different to translatory flow in that flow moves through soil, without significant displacement processes.

Translatory flow. Pre-event soil water or groundwater displaced by rainfall-induced subsurface flow to become part of storm runoff in stream channel.

Water-table. Surface of an unconfined groundwater body, at which matric potential is 0 cm H_2O.

1.3.3 Units

SI units are used in this thesis. In some cases, however, non-SI units are adopted for clarity or for ease of comparison with other published work.

For example, matric potential, elevational potential and total potential are each defined with regard to a unit quantity of water. The units of potential corresponding to three methods of specifying a unit quantity of water in the SI system are (Hanks and Ashcroft, 1986): (i) J Kg^{-1} if quantity of water is expressed as a mass, (ii) N m^{-2} if quantity of water is expressed

as a volume, or (iii) m = cm H_2O if quantity is expressed as a weight. Weight is the most convenient method of specifying the unit of water and is generally used in soil physics literature. Although cm (cm H_2O) is non-SI (i.e. not mm or m), it is used throughout the thesis for convenience and ease of comparison with other published work. Similarly, any other vertical or horizontal distance measurements associated with measured potentials (soil depth, depth of tensiometer bulbs etc) are also given in cm for ease of comparison.

All flow and flux data follow the SI format, except for pit throughflow. In this case, ml min^{-1} is used as the unit of discharge, because of the low and often intermittent flows involved.

2 SUBSURFACE FLOW: PROCESSES AND STUDIES

Subsurface flow on hillslopes has been measured directly using throughflow pits (Whipkey, 1965) and natural seepage faces (Weyman, 1973), and indirectly using soil water potentials and equations of flow in porous media (Harr, 1977). Stream-oriented studies have quantified subsurface water volumes indirectly using isotopic (Sklash and Farvolden, 1979) and chemical (Pilgrim et al., 1978) tracing techniques. The following sections explore the mechanisms of subsurface stormflow in relation to the theory of water flux in natural soils and previous attempts to quantify its movement. Each of the techniques is critically examined and its limitations discussed in an effort to show the importance of an holistic approach in identifying the runoff process.

It is important to note that different types of field experiments have proposed subsurface flow mechanisms relating to their sphere of inquiry. Throughflow pit investigations, for example, have generally shown that macropore flow of new water is the most important runoff producing mechanism. On the other hand, isotope tracing investigations have argued towards a displacement-type capillary-fringe flow mechanism to explain large old water volumes in the stream storm hydrograph. Figure 2.1 summarises some of these studies and their conclusions regarding the type of flow process operating.

2.1 WATER FLUX IN SOIL

Subsurface water movement may occur within three physically distinct zones: saturated, unsaturated and tension-saturated. Below the water table, the saturated zone maintains fluid pressures greater than atmospheric so that matric potentials (ψ) are positive. All the soil pores are filled with water (except for possibly some trapped air) and the moisture content (θ)

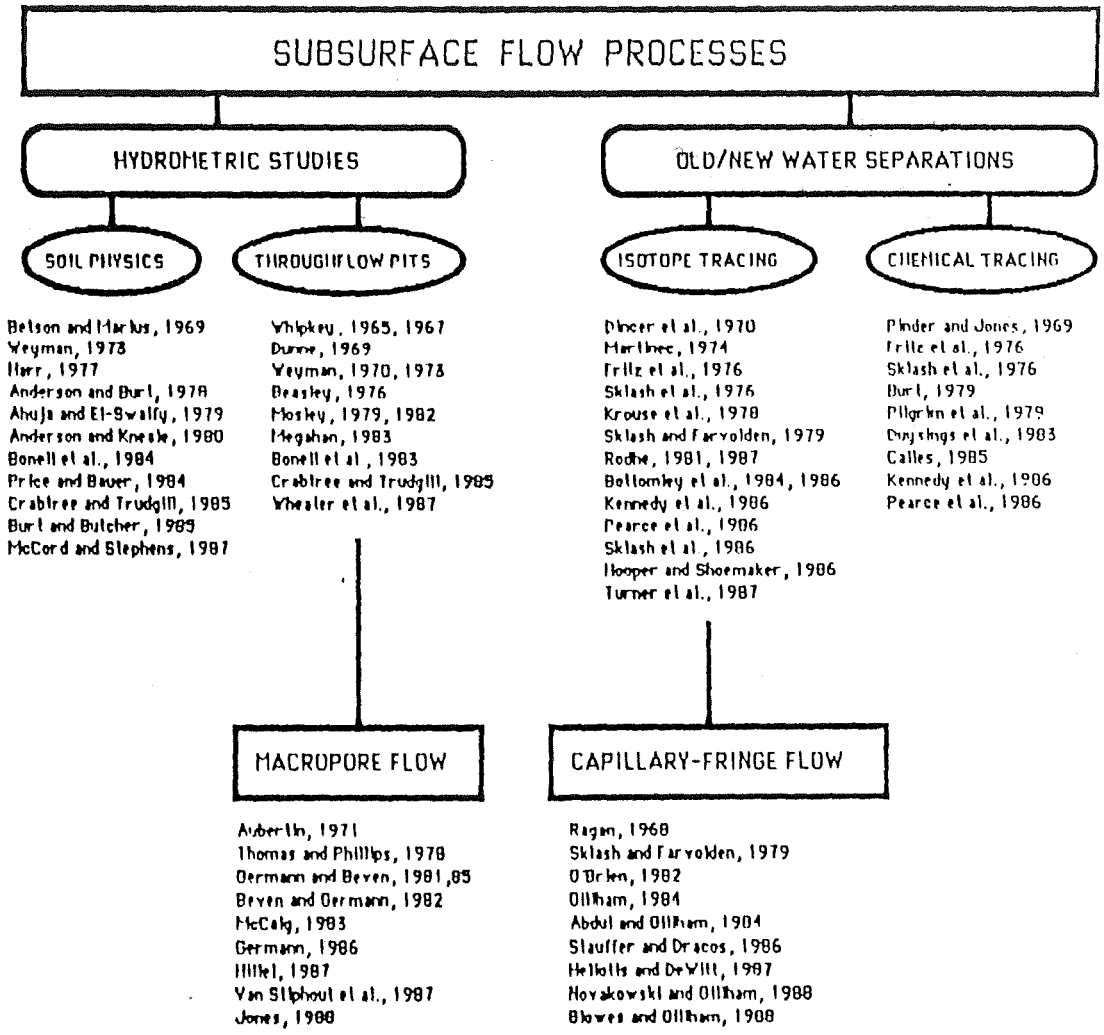

Figure 2.1 Summary of investigations into subsurface flow processes, highlighting processes and rapid response mechanisms.

equals the porosity (P). The other significant factor is that the hydraulic conductivity (K) is constant and is not a function of ψ (Freeze and Cherry, 1979).

Above the water table, the unsaturated zone is partially saturated and $\theta < P$. The fluid pressure is less than atmospheric and therefore $\psi < 0$. Under these conditions, the hydraulic conductivity and the moisture content are both functions of the matric potential ψ. Immediately above the water table, the tension-saturated zone is somewhere midway between the characteristics of the saturated versus unsaturated zone, with fully saturated pores, but with $\psi < 0$.

2.1.1 Laminar flow

The movement of subsurface water on a hillslope is governed by the hydraulic conductivity and gradient of the total potential of the soil, as expressed by Darcy's Law:

$$Q = -KA\, d\phi/dl \qquad (2.1)$$

where: K is the hydraulic conductivity, A is the cross-sectional area and $d\phi/dl$ is the gradient of the total potential. The total potential (ϕ) for water at any point within the soil can be defined as:

$$\phi = \psi + z + o \qquad (2.2)$$

where z is the height above an arbitrary datum (or elevational potential), ψ is the matric potential recorded on a tensiometer (or height above z to which water will stand in a piezometer tube) and o is the osmotic potential (generally ignored in non-arid environments).

2.1.2 Quasi-turbulent flow

Although Darcy's Law is valid for flow in porous media where water movement is driven by gravity and matric potentials, a number of studies have demonstrated that water may flow in large pores, partially independent of the hydraulic conditions of the

smaller pores (Germann and Beven, 1981). In this case, a preferred flow through macropores may occur, where gravity is the only driving force. The relationship between the radius R of a cylindrical pore and the capillary potential ψ with which water is held, defines the minimum dimensions of macropores (Germann and Beven, 1981):

$$\psi = -2\sigma/Rp_w g \qquad (2.3)$$

where: σ is the surface tension at the air-water interface, p_w is the density of water, g is the acceleration due to gravity, and ψ is in units of length. Germann and Beven (1981) note that ψ=-10.0 mm roughly approximates the boundary between macropores and micropores, with an equivalent radius of c.1.5 mm.

Macropores maintain a quasi to fully turbulent flow regime where the equations for describing the flow are those normally employed for open channels or pipes (Atkinson, 1978). The flow through a hollow soil cylinder is generally determined using the Hagen-Poisuille equation applied to gravity induced flow in a vertical channel (Childs, 1969):

$$q = (\pi p_f g R^4)/(8\nu) \qquad (2.4)$$

where: q is the flow rate, p_f is the fluid density, g is the acceleration due to gravity, R is the radius of the tube, and ν is the dynamic viscosity. The solute or isotopic flux into such a tube (assuming no lateral diffusion) is qC_1 where C_1 is the concentration of applied solution or isotopic concentration.

If macropore flow is through natural ped faces or small slit openings in the soil structure, then the gravity induced flow is (Childs, 1969):

$$p = (p_f g d^3)/(12\nu) \qquad (2.5)$$

where: p is the flow rate per unit length of slit and d is the slit width. Since these parameters are almost impossible to

measure in a field situation, various modelling approaches have been developed (e.g. Jones, 1988; Beven and Germann, 1981b).

2.2 HYDROMETRIC APPROACHES TO MEASURING SUBSURFACE FLOW

2.2.1 Throughflow pits

Artificial throughflow pits excavated across a hillslope, with troughs 0.5 (Wheater et al., 1987) to 49 m wide (Megahan, 1983), have been used in many studies of subsurface flow on hillslopes. The construction of throughflow pit systems has generally been based either on the Whipkey (1965) or Knapp (1973) design. Slope angles have ranged from 2° (Weyman, 1973) to 45° (Mosley, 1982) with saturated hydraulic conductivities (K_{sat}) in the order of 0.07 mm hr^{-1} (Mosley, 1979) to 1180 mm hr^{-1} (Dunne, 1969), and lag times between the centre of a burst of rainfall and peak subsurface stormflow from 0.8 hr (Whipkey, 1967) to 80 hr (Weyman, 1973). Dunne (1978) noted that these lag times tend to increase with catchment or plot size and are c.40 times longer than those of Hortonian overland flow for catchments in the range 0.1-1.0 km^2.

Other investigators have used natural troughs at the hillslope base (Weyman, 1973; Megahan, 1983), large inclined laboratory soil plots (Hewlett and Hibbert, 1963; Nutter, 1971; Anderson and Burt, 1978a) and artificial sprinkling (Corbett et al., 1975; Mosley, 1979; 1982) when examining subsurface water movement to pit face.

(a) Unsaturated flow distortion

Any artificial trough or pit excavated in the side of a hillslope, will inevitably alter or interrupt the subsurface water flux. Despite some improvements more sophisticated trough studies have offered (e.g. Megahan, 1983), throughflow pits by their own presence change the rate, direction and magnitude of hillslope water flux. This is because positive pore water

pressures (and therefore a saturated soil face) are required for any pit seepage. When this occurs, a saturated wedge is initiated upslope of the face, inducing an upslope artificially saturated wedge. The magnitude of this saturated wedge may vary in time and space, and control the local K_{sat} (Atkinson, 1978), hydraulic gradient and resulting throughflow hydrograph.

Throughflow pits may also distort the net of hydraulic potential on the slope, so that they receive drainage from areas laterally away from the pit itself (Whipkey and Kirkby, 1978; Atkinson, 1978). Under wet antecedent conditions, the pit face may produce a draw-down effect on the total potentials around the pit, extending the contributing area laterally away from the pit face. Under dry antecedent conditions, Whipkey and Kirkby (1978) note that the build-up to saturation required to drain water from the pit, produces upslope hydraulic gradients which divert water away from the face. The pit contributing area, therefore, varies with pit discharge and antecedent wetness conditions.

Nevertheless, throughflow pits are used extensively in hillslope investigations and are the only direct means of obtaining subsurface flow measurements. Isotopic information from pit throughflow was collected by Sklash et al. (1986) but was not related to the hillslope hydrograph. In fact, no previous studies known to the author have combined throughflow discharge with throughflow water isotopic information, in determining the relative importance of rainfall versus pre-event soil water and groundwater.

2.2.2 Soil water physics approaches

Whereas throughflow pit investigations have sought to monitor hillslope flow directly, soil water physics approaches have attempted to solve mathematically (using Darcy's Law) for flow in hillslope soils. Soil water information has been obtained

from a range of instruments including standard tensiometers (Harr, 1977; Crabtree and Trudgill, 1985; Weyman, 1973), recording tensiometers (Anderson and Burt, 1978b; Ahuja and El-Swaify, 1979), piezometers (Betson et al., 1968; Bonell et al., 1984) and moisture content information (McCord and Stevens (1987). These studies have concentrated on determining the rates, magnitude and direction of subsurface water movement in relation to saturated and unsaturated conditions and resulting changes in K.

As soil drains and the remaining water is held in progressively smaller pores at progressively lower potentials, the total conductive volume becomes less and K decreases rapidly. Wellings and Bell (1982) note that a reduction in volumetric water content of only a few percent can cause a reduction in K of 3-5 orders of magnitude in certain soils (especially coarser textured). Several soil physics investigations have attempted to identify the controls on saturated zone development, given its important role in hillslope flow. These studies have been conducted in material ranging from dune sand (McCord and Stevens, 1987) to silty clay (Ahuja and El-Swaify, 1979) and till (Lundin, 1982), and under saturated (Anderson and Kneale, 1980a) and unsaturated (Burt and Butcher, 1985) conditions. Recording (Anderson and Burt, 1977) and non-recording tensiometers (Harr, 1977) have been used to determine hydraulic gradients within soil plots, as have maximum rise piezometers (Bonell et al., 1984) and soil moisture sensors (McCord and Stephens, 1987).

(a) Unsaturated zone heterogeneity

Heterogeneity of unsaturated zone parameters, such as surface infiltration (Horton, 1933), antecedent moisture conditions (Weyman, 1973), hillslope topography (Anderson and Burt, 1978c), and soil structure (Whipkey, 1965), greatly affects

soil K and resulting subsurface flow. Most soil physics approaches, while monitoring small plots in some detail, have made assumptions of isotropicity and homogeneity when moving from the plot scale to the small catchment scale. Stephenson and Freeze (1974) showed that variable soil properties greatly affected the application of the Freeze (1972b) model even on a simple subsurface system. Price and Bauer (1984) suggest that even small-scale heterogeneities can induce significant changes in soil water motion, and caution against oversimplifying unsaturated zone processes.

Soil water physics approaches, while plagued with difficulties relating to soil heterogeneity, are the only method of quantifying moisture relations in the soil and resulting water movement pathways. Again, soil water physics approaches, while sometimes used in conjunction with throughflow pit investigations, have not been combined with isotopic tracing data. As a result, soil water response to storm rainfall has not been related to soil water origin.

2.3 STREAM-BASED TRACING

2.3.1 Chemical tracing

The relationship between hydrological and chemical properties in small catchments has been recognised for some time (Brown, 1986). Many studies have demonstrated the relationship between average annual flow and average annual concentration of total dissolved solids (Langbein and Dawdy, 1964), soluble salts (Durum, 1953), silica concentration (Edwards, 1973), nitrate (Wellings and Bell, 1980) and several major ions (Walling and Foster, 1975). Acid deposition has also provided the impetus for hillslope soil water-streamwater chemistry relations in the northeast US (e.g. Likens et al., 1977), Scandinavia (e.g. Overrein et al., 1980) and southcentral Canada (e.g. Dillon et

al., 1982). Pinder and Jones (1968) were among the first to separate a stream hydrograph into direct and indirect components, and since then, several studies have sought to identify the sources of storm runoff using naturally occurring chemical tracers (Pilgrim et al., 1978; Duysings et al., 1983). Hillslope chemical tracing has also been conducted (Burt, 1979) and subsurface flow generation has been related to slope soil water solute concentration.

(a) Problems of non-conservation

Pilgrim et al. (1979) showed that the residence time of water in hillslope soils was directly related to dissolved solids concentration, thereby casting doubt on simple mass balance chemistry models for hydrograph separation. Fritz et al. (1976) demonstrated that areal variability of the chemical composition of groundwater within a basin could partly explain the observed time variations in streamwater chemistry. Calles (1985) noted that increased relative contribution of solute poor shallow groundwater could give the misleading impression of large rainwater contributions. Similarly, Burt (1979) warned against interpretation of chemical data collected at few sampling locations in terms of details of hydrological processes within a catchment, while Bache (1984) examined the role of the hillslope soil in determining streamwater composition in relation to subsurface flow pathways.

2.3.2 Isotopic tracing

Stable isotopes are constituent parts of natural water molecules, and as such, are free from the problems of non-conservation experienced in chemical tracing techniques. This makes them excellent tracers of water movement and origin. Environmental isotopes (^{3}H, ^{14}C, ^{18}O and D) have been applied to hydrological modelling of soil-moisture transport (Allison et

al., 1984), mixing and evapotranspiration in large lakes and swamps, glacial ice movement (Dansgaard, 1964), groundwater flow (Maloszewski and Zuber, 1982), and transport of contaminants in groundwater (Egboka, 1985). Several studies have applied environmental isotope tracers (particularly ^{18}O and D) to hydrograph separation based on groundwater (pre-event water) and rain water (event water) components (Fritz et al., 1976; Sklash et al., 1976; Sklash and Farvolden, 1979; Kennedy et al., 1986; Pearce et al., 1986; Sklash et al., 1986) or snowmelt (Dincer et al., 1970; Martinec, 1975; Rodhe, 1981). These studies have been performed in a wide variety of hydrogeological and physiographic environments and in response to both rain and snowmelt events. Results indicate that groundwater can form a major component (from <20% [Krouse et al., 1978] to 90% [Jacks et al., 1986]) in storm and snowmelt hillslope runoff (e.g. Sklash et al., 1986) and streamflow (e.g. Sklash and Farvolden, 1979).

(a) Assumptions when using stable isotopes

The use of stable isotope tracers is based on the assumption and requirement that old water (soil water and groundwater) and new water (rain and snowmelt) have distinct isotopic signatures. A number of simplifications are also made: (i) groundwater and stream baseflow maintain the same isotopic composition prior to an event, (ii) baseflow signatures are the same before and after an event has occurred, (iii) there is no significant surface storage water contribution to the stream, (iv) there is no areal or temporal variation in new water input (rain or snowmelt), (v) soil water contributions to streamflow (as opposed to groundwater contributions) are negligible. Sklash and Farvolden (1979; 1980) discussed these points in relation to water sampling and hydrograph separation. Recently, Kennedy et al. (1986) have questioned the validity of these assumptions and have suggested

that previous 'groundwater' separations should be re-examined in the light of problems of rainfall isotopic variability, groundwater/baseflow isotopic inconsistencies, and large soil water contributions.

2.4 A RAPID FLUX MECHANISM

Although Freeze (1972a) argued mathematically that there are stringent topographic and K_{sat} limitations on the occurrence of rapid subsurface stormflow, the studies listed in sections 2.2 and 2.3 show that subsurface stormflow is an important and widespread phenomenon. A major problem in both hydrometric and isotope-chemical tracing approaches, has been to explain a mechanism by which subsurface flow can cause a rapid contribution to stormflow. Hydrometric studies, particularly pit throughflow investigations, have emphasised the role of soil macropores in conducting water rapidly downslope, while the role of the capillary-fringe has been emphasised in isotopic tracing studies as a means of promoting rapid groundwater (pre-event) flow into the stream channel.

2.4.1 Macropore flow

Many studies over the past decade have identified preferred flow along macropores, indicating that rapid new water flow in the unsaturated zone may occur under conditions of non-equilibrium between soil moisture content and moisture potential (Beven and Germann, 1982). Recent literature has emphasised the importance of macropores in generating rapid subsurface runoff, in the order of 5.5 m hr^{-1} (Hammermeister et al., 1982a), 15 m hr^{-1} (Rahe et al., 1978) and 33.3 m hr^{-1} (Mosley, 1982) via turbulent non-Darcy type flow in large soil pipes (Jones, 1971) decaying root channels (Aubertin, 1971), soil cracks (Bouma and Wosten, 1979) and animal burrows (Omoti and Wild, 1979).

The effect of macropores on solute infiltration and transport has been examined (e.g. Skopp et al., 1981), but macropore effects on isotopic separations of storm runoff have not yet been addressed. Several authors have commented on the amount of soil water displacement that occurs during macropore flow in a structured soil. Thomas and Phillips (1979) note that the amount of displacement that occurs (i.e. total displacement, partial displacement or complete bypassing), is a function of the rate of macropore flow versus volume of flow in the soil matrix. This relationship is governed by the rainfall rate, soil structure, pore size distribution, clay orientation and soil water content. In a structured clay loam soil, Van Stiphourt et al. (1987) found that at ψ=-1000 cm H_2O (i.e. antecedent ψ in soil matrix), bypass flow averaged 45% of applied rainfall (20-35 mm hr^{-1}), and at ψ= -200 cm H_2O, bypass flow averaged 70%. Kneale and White (1984) examined rainfall intensity effects on bypassing and found that if intensity increased above a threshold of 2.2 mm hr^{-1}, bypass flow occurred down cracks in 9 cm cores of dry, cracked clay loam soil. Furthermore, they noted that although the absolute magnitude of water adsorption by the peds increased with higher rainfall intensity, the ratio of bypass flow to absorption also increased to an output/input ratio of 55% for a 21.9 mm hr^{-1} rainfall intensity.

(a) Downslope connectivity

Many macropore studies have been affected to an unknown extent by unnatural boundary conditions such as plot boundary trenches (Whipkey, 1965), or artificial rainfall rates orders of magnitude greater than natural storm rainfall (Mosley, 1979; 1982). Even more problematic is the notion of downslope continuity of the macropore network and resulting flow. Although the influence of macropores on infiltration rates has been shown

under many conditions (e.g. Hillel, 1987), there is little experimental evidence to show that macropores may conduct water laterally downslope with a sufficient degree of connectivity to overcome losses to the matrix and produce rapid stream response. Burt (1985) notes that resolution of this problem is fundamental to improvements in the understanding of subsurface stormflow, since K is directly proportional to the presence or absence of macropores.

2.4.2 Capillary-fringe flow

Water movement in the capillary-fringe has been attributed to rapid water table rise (O'Brien, 1982), cavernous weathering (Conca and Astor, 1987), diurnal water table fluctuations resulting from atmospheric pressure changes (Turk, 1975) and salt weathering (Cooke et al., 1982). Recently, it has been shown that the capillary-fringe can have a significant effect on subsurface flow initiation. On the basis of soil water physical principles (Gillham, 1984), computer simulations (Sklash and Farvolden, 1979) and limited field evidence (Ragan, 1968; Novakowski and Gillham, 1988), it has been proposed that groundwater ridges in the valley bottoms (Sklash and Wilson, 1982) and saturated wedges on the lower slopes (Sklash et al., 1986) develop quickly as a capillary-fringe response, thereby increasing hydraulic gradients and promoting increased gravity drainage of old water toward the stream channel. The mechanism is important for two reasons: (i) it provides explanation of why isotopic tracing studies observe such large old water volumes in storm runoff, and (ii) it emphasises the importance of matrix flow in generating translatory subsurface water movement (cf. Hewlett and Hibbert, 1967).

(a) Field limitations

The capillary-fringe effect has only been clearly demonstrated in laboratory models. Abdul and Gillham (1984) showed in a 1.4 x 0.8 x 1.2 m sand packing that if the capillary-fringe extends to the ground surface, the addition of a very small amount of infiltrating rain can trigger a rapid conversion from tension to pressure saturation. They noticed that the height of the water table rise associated with the conversion was much greater than would be expected on the basis of normal specific yield values for sandy materials. Stauffer and Dracos (1986) extended the Abdul and Gillham (1984) work into a layered sand packing and confirmed Abdul and Gillham's results. They also demonstrated the importance of the initial moisture conditions on capillary-fringe response, and showed that solute transport was dominated by advective transport mechanisms which were strongly influenced by the layering of the sand packing.

The applicability of these physical models to real hillslopes and field soils may be questionable given the latter's heterogeneity. Zaltsberg (1986) provided field data to show that the height of the capillary-fringe very rarely extended to the ground surface for material ranging from sandy clays to coarse sand and till. Recent field investigations by Novakowski and Gillham (1988) and Heliotis and DeWitt (1987) have shown that under low relief wetland conditions, the capillary-fringe can in fact extend to the ground surface and does generate a ridging of groundwater and increased gravity flow. It remains to be seen, however, whether this process is applicable to upland areas.

2.5 THE MAIMAI DEBATE

Significant work into the subsurface runoff process in a highly responsive catchment on the west coast of New Zealand (M8), has yielded conflicting results regarding the importance of

new water macropore flow versus old water translatory movement in throughflow transmission. This catchment is at the forefront of the subsurface flow controversy because it is "apparently highly suited to rapid throughflow (macropore flow) of storm rainfall" (Pearce et al., 1986, p.1272), and yet old water dominates the storm hydrograph by 75-96% (Sklash et al., 1986).

2.5.1 The hydrometric work

Mosley (1979) conducted a hydrometric study of stormflow generation mechanisms in the M8 catchment (3.8 ha) and a 0.3 ha sub-watershed. Precipitation, throughfall and streamflow were measured for 12 storm events. In addition, hillslope subsurface flow was measured at 7 throughflow pits within the 0.3 ha subwatershed (Figure 2.2) in a variety of soil and topographic positions. Each pit was excavated down to bedrock, and a 1 m trough was installed to intercept subsurface flow.

Results indicated that subsurface flow could account for total streamflow throughout the storm hydrograph and no overland flow was observed (except in limited areas along the channel). Gravimetric soil moisture analyses during rain events identified vertical water movement in the soil profile, and in a downslope direction. A saturated wedge developed in the soil mantle, whose shape was modified by the topography of the bedrock surface.

For the series of natural rain events, Mosley noted: (i) hillslope hydrographs maintained a close coincidence of peaks (Figure 2.3) with lag times in the order of 1.0-1.9 hr, (ii) throughflow increased in a downslope direction (as illustrated in Figure 2.3), indicating that flow moved considerable distances through the soil during the hydrograph rise, and (iii) throughflow pit faces displayed points of concentrated seepage and high outflow rates, where at a mid-slope site "water gushed at maximum rates of the order of 20 l sec^{-1} through two pipes at

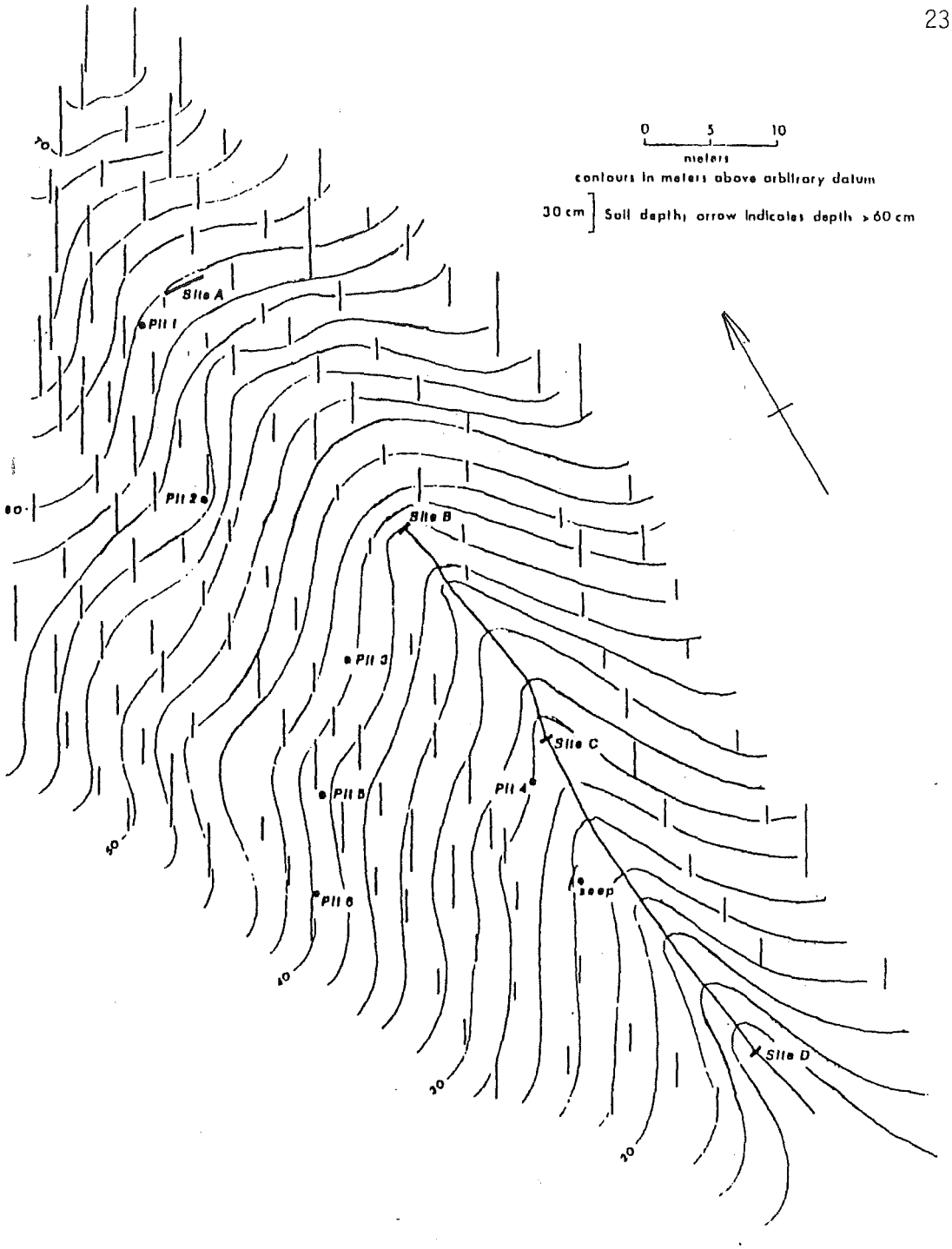

Figure 2.2 Topographic map of the M8 0.3 ha subwatershed showing pit and seepage locations (from; Mosley, 1979).

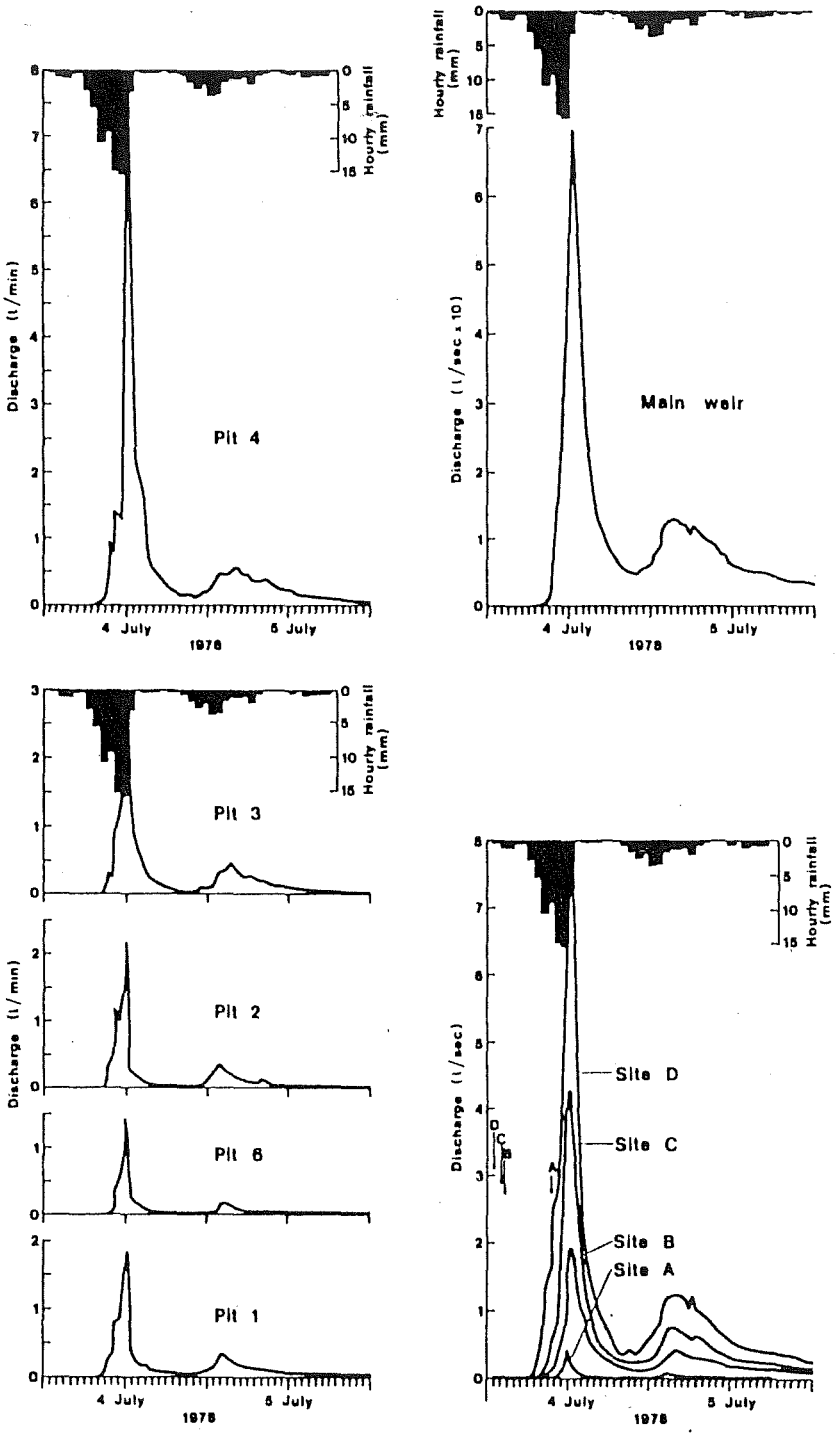

Figure 2.3 Subsurface flow and catchment runoff for 04-05 July 1978 storm (from; Mosley, 1979).

the base of the B horizon" (Mosley, 1979, p.800). Mosley inferred that this water appeared in the downslope areas and stream channel.

Four tracer trials were then conducted at the pit sites at the end of a 33 mm rainfall event, to explore the role of macropores in hillslope flow. Rhodamine B and sodium dichromate dye were applied to the soil surface through a 150 mm diameter cylinder under a variety of application rates. Additional tracer experiments were conducted toward the end of a 26 hr, 82 mm precipitation event. In this case, 1 l of rhodamine B dye was simply sprinkled on to the soil surface 1m upslope from the pit face.

In each case, maximum subsurface flow dye travel velocities were up to 300 times greater than the K_{sat} (252 mm hr^{-1}) for mineral soil. Mosley concluded that "this bypassing, combined with the sensitive and rapid response of subsurface flow to variations in precipitation (and tracer input) suggests that flow through macropores rather than through the soil matrix contributes to channel stormflow. This flow was of new water, and no evidence for translatory flow was observed" (Mosley, 1979, p.806).

2.5.2 The isotopic work

Pearce et al. (1986) conducted an isotopic and chemical tracing study in the MB catchment to examine the origin of subsurface storm runoff in the catchment. From a series of long-term (1977-1980) observations of ^{18}O , EC and Cl in streamflow, groundwater, and rain, they showed that the catchment outflow reflected a well-mixed reservoir with mean residence times in the order of 4 months. Subsequent analysis of an 11 April 1979 storm event revealed that only 3% of storm runoff could be considered new water. ^{18}O concentrations in storm runoff varied only

slightly from antecedent conditions, and did not reflect inputs of new water. The isotope data combined with the solute chemistry results showed that for small events under moderately wet antecedent conditions, macropore flow of new water (as suggested by Mosley, 1979) could not explain streamflow response in the catchment.

The anomalous results of Pearce et al. (1986) led to a more intensive isotopic and chemical tracing study of hillslope and low-order stream response in the M8 catchment. Sklash et al. (1986) reactivated 6 of Mosley's (1979) 8 throughflow pits and examined the ^{18}O, δD, EC and Cl concentrations in pit and streamflow for 3 small September 1983 storms. In each case, new water contributions to stormflow were small (<25%) and could be accounted for by saturation overland flow. Hillslope response varied according to slope position, with upslope sites producing larger new water contributions (30-40%) than downslope sites (<10%). Table 2.1 shows that for a 21 September 1983 event, Pits 1-3 and Site A averaged 30-45% new water, while Pit 5 and the Seep only produced 6 and 8% respectively. Sklash et al. (1986) argue that throughflow from the upslope pit sites would normally continue to flow downslope to the stream channel, undergoing further mixing with stored water from other locations and possibly with other newly infiltrated water.

The Sklash et al. work explicitly refuted Mosley's interpretations, by indicating that a macropore rapid flux mechanism was not required to explain rainwater contributions to storm runoff because old water (both stored vadose and phreatic water) constituted 70-92% of the channel stormflow.

Table 2.1. Old and new water peak discharge contributions to throughflow, from Sklash et al. (1986) 21 September 1983 M8 storm.

Site	Flow δD °/oo	Old δD °/oo	New δD °/oo	Old Water %	New Water %
Pit 1	-43.1	-12.2	-33.7	70	30
Pit 2	-43.1	-12.2	-31.4	62	38
Pit 3	-43.1	-12.2	-29.2	55	45
Site A	-42.3	-12.2	-32.9	69	31
Pit 5	-45.5	-12.2	-43.5	94	6
Seep	-44.0	-12.2	-41.3	92	8
Site D	-39.1	-12.2	-32.4	75	25

2.5.3 Is there a consensus?

There is agreement between the hydrometric and isotope tracing studies conducted in M8, that subsurface stormflow dominates the production of storm runoff in all events yielding more than a few millimeters of runoff (Pearce and McKerchar, 1979; Mosley, 1979; Pearce et al., 1986). There is no agreement, however, regarding the importance of various hillslope flow mechanisms.

Mosley (1979) may have induced macropore flow by his high rate of tracer application. During Mosley's experiments, 6-23 l of water was applied 1 to 3 m upslope from the pit faces, simulating storm input rates in the order of years to decades. Mosley acknowledged that the conditions were clearly 'artificial', but except in the immediate vicinity of the cylinder, he considered the movement of dye to be similar to that of water applied by an intense rainfall event. Clearly, however, the soil matric potential conditions in this situation would be unrealistic given the fact that the dyed water was applied to the soil surface through a 150 mm diameter cylinder pressed into the humus layer. This situation would lead to a greater potential for macropore flow through an unsaturated matrix, than would be the

case under lower intensity events wetting the entire hillslope section. In fact, Thomas and Phillips (1979) have shown that macropore flow is directly proportional to applied input rate.

Secondly, Mosley (1979) assumed downslope continuity of the macropore network to route the water 'several tens of meters' rapidly downslope to the stream channel. There are clearly problems with this concept, both in terms of soil structural characteristics at Maimai and in other 'macropore environments' (e.g. Plynlimon, U.K.; Jones (1971)). There is also a lack of evidence to suggest a sufficient degree of downslope connectivity.

Sklash et al. (1986), on the other hand, examined storm events with return periods from 4 weeks to 6 months. It is possible that they were exploring a completely different scale of hydrologic operation in their hillslope study, as compared to Mosley's injection trials. Given the size of the soil water store and the estimated residence time for water in the catchment by Pearce et al. (1986), they argue that only events with return periods of years to decades would have substantial components of new water in the storm hydrograph. It seems possible that the return period of Mosley's simulated events is in the order of several years.

Apart from limited maximum rise piezometer data, Sklash et al. (1986) provide no evidence of a capillary-fringe or groundwater ridging response to explain the large old water volumes in the channel, even though they cite this process to explain old water volumes in storm runoff. In fact, as discussed in section 2.4.2, there is no field evidence from any instrumented catchment to suggest that this may be a viable explanation under field conditions. In summary, it appears that there are shortcomings in each study, and that macropore flow (if

it does occur) may augment a capillary-fringe groundwater ridging mechanism (if it does occur) by accelerating infiltration and moving water quickly to depth and into the capillary-fringe zone.

2.6 OUTLINE OF PRESENT STUDY

This thesis outlines the development and results of a physically-based field experiment designed to test specific hypotheses on the nature of runoff production in a steep, humid headwater catchment (M8). The broad objectives of this research are to: (i) develop a more complete understanding of water movement on hillslopes in relation to solute transport and streamflow generation, (ii) identify the controlling mechanisms facilitating these processes, and (iii) document any implications for catchment geomorphological development.

Since previous studies in the M8 catchment have already documented certain aspects of the stated objectives, specific hypotheses are tested in an effort to resolve any discrepancies and to provide better understanding of key mechanisms. In particular, the process of macropore-groundwater-streamflow interaction is examined by field experimentation and theoretical generalisation. Although not specifically answered within the main body of the text, each question is referred to in section 8.1.

1. How do the areal and temporal isotopic variations of subsurface water in the catchment affect isotopic signatures at the basin outflow?

   (i) What are the between and within storm rain isotopic variations and how do they affect subsurface isotopic signatures?

   (ii) Is the subsurface reservoir fully mixed isotopically, or are there downslope or depth variations?

2. Is there enough old water in a discharge position to account for the old water component in a runoff event?

(i) Is soil water isotopically similar to groundwater?

(ii) What are the isotopic mixing processes and can they explain the large old water component in storm runoff?

3. What role does the capillary-fringe play in initiating saturated wedge and groundwater ridging phenomena?

(i) Does the capillary-fringe effect operate similarly in both hillslope and near-stream locations?

(ii) Is there a relationship to capillary-fringe response and rainfall intensity or antecedent wetness conditions?

(iii) Does groundwater ridging occur?

4. What are the relationships between surface/subsurface macroporosity and rapid groundwater table rise?

(i) Does macropore infiltration augment capillary-fringe water table rise?

(ii) Are near-stream and mid-slope zones linked in terms of subsurface response, or do near-stream groundwater tables operate independently of catchment runoff?

The following chapters outline the methods, results and conclusions of the experiment in relation to the previous MB experiments and current international literature on hillslope hydrology. A range field techniques are employed in order to examine the age, origin and pathway of water movement. While elements of soil physics and isotope geochemistry are utilised, only those aspects which provide direct or circumstantial evidence for addressing the above hydrological goals, are considered in detail.

3 FIELD SITE AND DATA COLLECTION PROCEDURES

3.1 THE M8 CATCHMENT

3.1.1 Location

The study was carried out in one of eight small catchments established by the Forest Research Centre of the New Zealand Forest Service. The Maimai experimental watersheds are located in the Tawhai State Forest (45 05'S, 171 48'E), North Westland, and have been monitored since 1974 (Pearce et. al., 1976; 1980; Pearce and McKerchar, 1979; O'Loughlin et al., 1980; 1982; Figure 3.1).

Mean annual gross rainfall in the study area is approximately 2600 mm, producing approximately 1550 mm of runoff from 1950 mm of net rainfall (Rowe, 1979). Pearce and McKerchar (1979) note that the catchments are highly responsive to storm rainfall, with 1000 mm (65%) of the mean annual runoff and 39% of the total annual rainfall (P) in the form of quickflow (QF), as defined by Hewlett and Hibbert's (1967) separation method.

3.1.2 Physiography and soils

The M8 catchment is underlain by a firmly compacted, moderately weathered, early Pleistocene conglomerate, known as the Old Man Gravels. This unit has been described as "effectively impermeable" (Mosley, 1979, p.795), and "poorly to moderately permeable" (Pearce et al., 1976, p.150).

Slopes are short (<30 m) and steep (mean 34°), with a local relief of 100-150 m. Catchment side-slopes consist of regular spurs of Old Man Gravel bedrock and linear hollows infilled with matrix-rich colluvium. Soils in the catchment have developed from the underlying soft, weathered conglomerate and colluvium and are broadly classified as Blackball Hill soils (N.Z. Soil Bureau, 1968; Mew et al., 1975). They show large spatial variability in

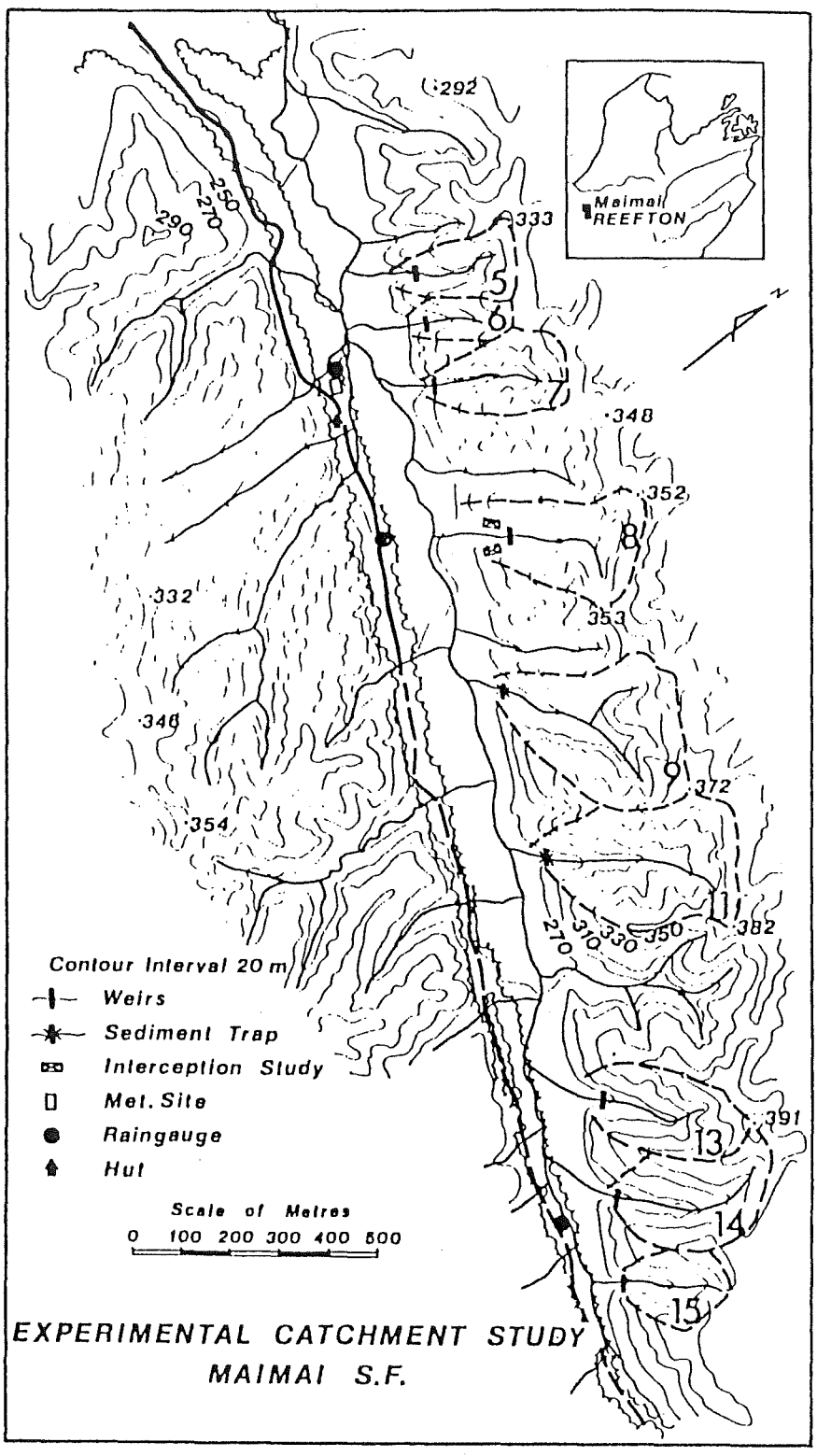

Figure 3.1 The Maimai study area, North Westland, New Zealand (from; Pearce and McKerchar, 1979).

depth (mean 0.6 m, range 0.2-1.8 m) and character (from podsolized Yellow Brown Earth [YBE], to mottled YBE, to gley soils), and are dominantly stoney throughout their profiles. Mineral soil horizons are overlain by a thick (mean 170 mm) well-developed upper humic horizon. Webster (1977) reported average infiltration capacity of the humic layer and average saturated hydraulic conductivity of the upper mineral soil in the order of 6100 mm hr^{-1} and 250 mm hr^{-1} respectively.

McKie (1978) separated the soils belonging to the Blackball Hill group into 7 soil profile classes according to their parent material, slope angle, vegetation and drainage (Table 3.1). Generally, there is a strong relationship between soil type and slope position as they relate to drainage and soil development processes. The common profile features of the dominant soil profile classes (2,4 and 5) were derived by McKie from a selection of most commonly occurring properties found in a number of described profiles, whereas the features of the less widespread classes (1,3,6 and 7) were based on a representative profile. Further reference to these soil pedological characteristics, as they relate to soil water movement and K_{sat} measurements, will be made in section 5.1.

Table 3.1. M8 soil profile classes compiled from data in McKie (1978).

Class	Slope position	Slope °	Drainage
1. Shallow podzols	upper nose	15-30	well
2. Podzols	nose and sideslopes	30-40	well
3. Gley podzols	upper hollows	20-40	imperfect
4. Podzolised lowland YBE	sideslopes, upper nose	25-35(75%) 36-50(30%)	moderate
5. Mottled YBE	valley basin hollows	26-35(70%) 10-26(30%)	imperfect
6. Shallow gley	near-stream (limited)	15-35	poor
7. Gley	near-stream	15-35	very poor

3.2 HYDROMETRIC MONITORING

3.2.1 General instrument deployment

Figure 3.2 shows the deployment of all hydrometric devices, tensiometer plots and water sampling locations within the main M8 catchment and 0.3 ha subcatchment. Three main physiographic areas were instrumented in some detail: a near-stream zone between the catchment outflow and Site D, a midslope hollow zone (Pit 5), and an upslope hollow zone (Pit A). All instruments were installed 09 May to 05 June 1987, while data recording commenced on 28 August. Weekly site visits and data downloading were conducted from 11 September to 12 November. More intensive on-site 'field seasons' were conducted 28 August to 10 September and 13 November to 17 December.

Figure 3.3 shows a schematic representation of the recording network, controlled and monitored by a Campbell CR21X micrologger. Thirty-two electronically multiplexed tensiometers were installed at Pit 5. Twenty-four tensiometers, linked to a Scanivalve unit, were installed at the near-stream site (31 August to 20 November) and then moved to the Pit A site for the duration of the experiment (23 November to 16 December). Mini 10:1 v-notch weirs were linked to Pit A, Pit 5 and Seep outflow. Data was stored in a Campbell SM64 Solid State Memory Module and downloaded to a field portable Zenith Z181 computer via a Campbell SM232 interface. The following sections describe the instrument network and detail important instrument design and performance characteristics.

3.2.2 Rainfall and streamflow

A tipping bucket raingauge recorded 10 min precipitation totals throughout the study season. Streamflow was recorded at the basin outflow using a Forest Research Centre 90° degree

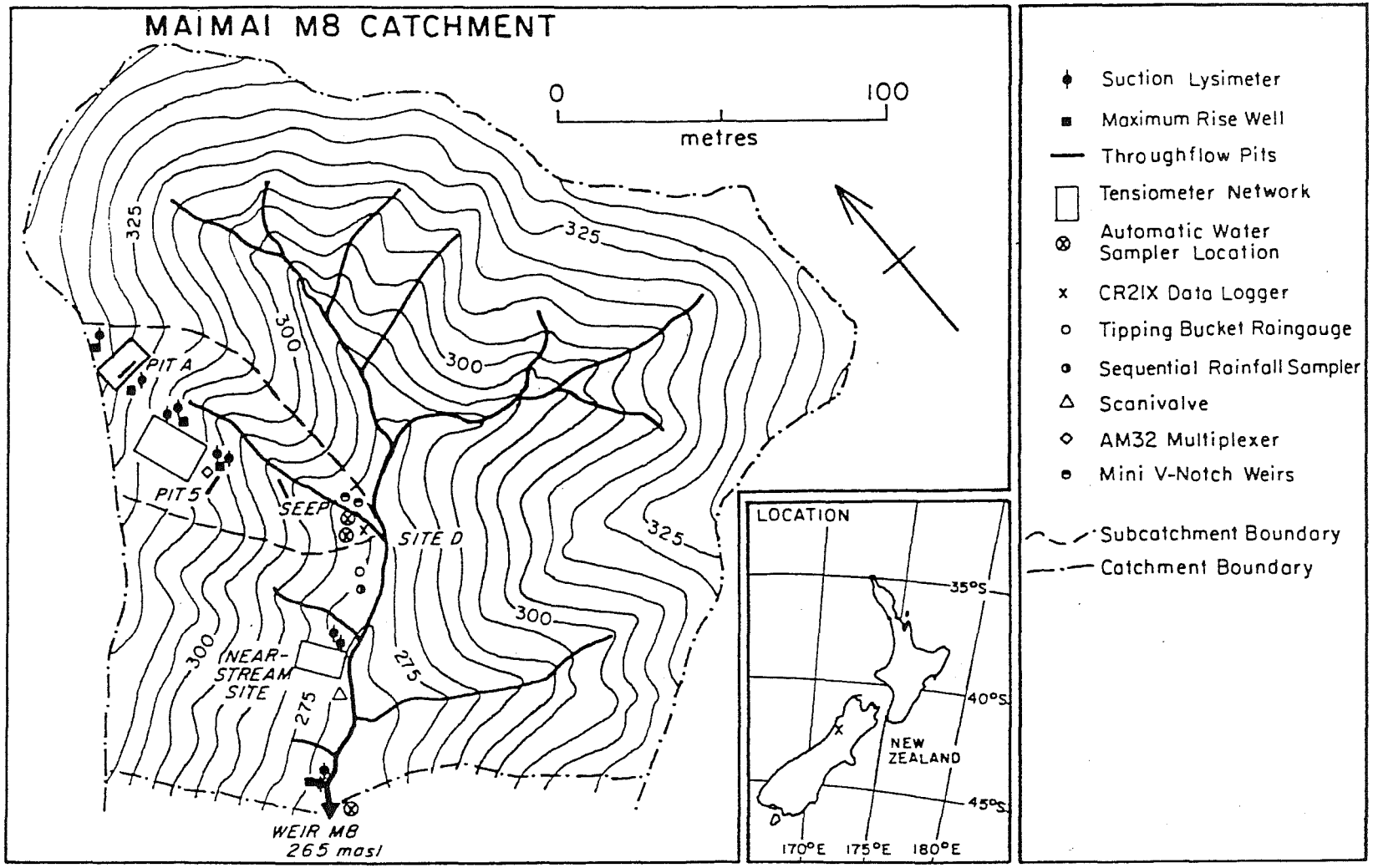

Figure 3.2 M8 catchment showing locations of hydrometric instrumentation and sampling sites.

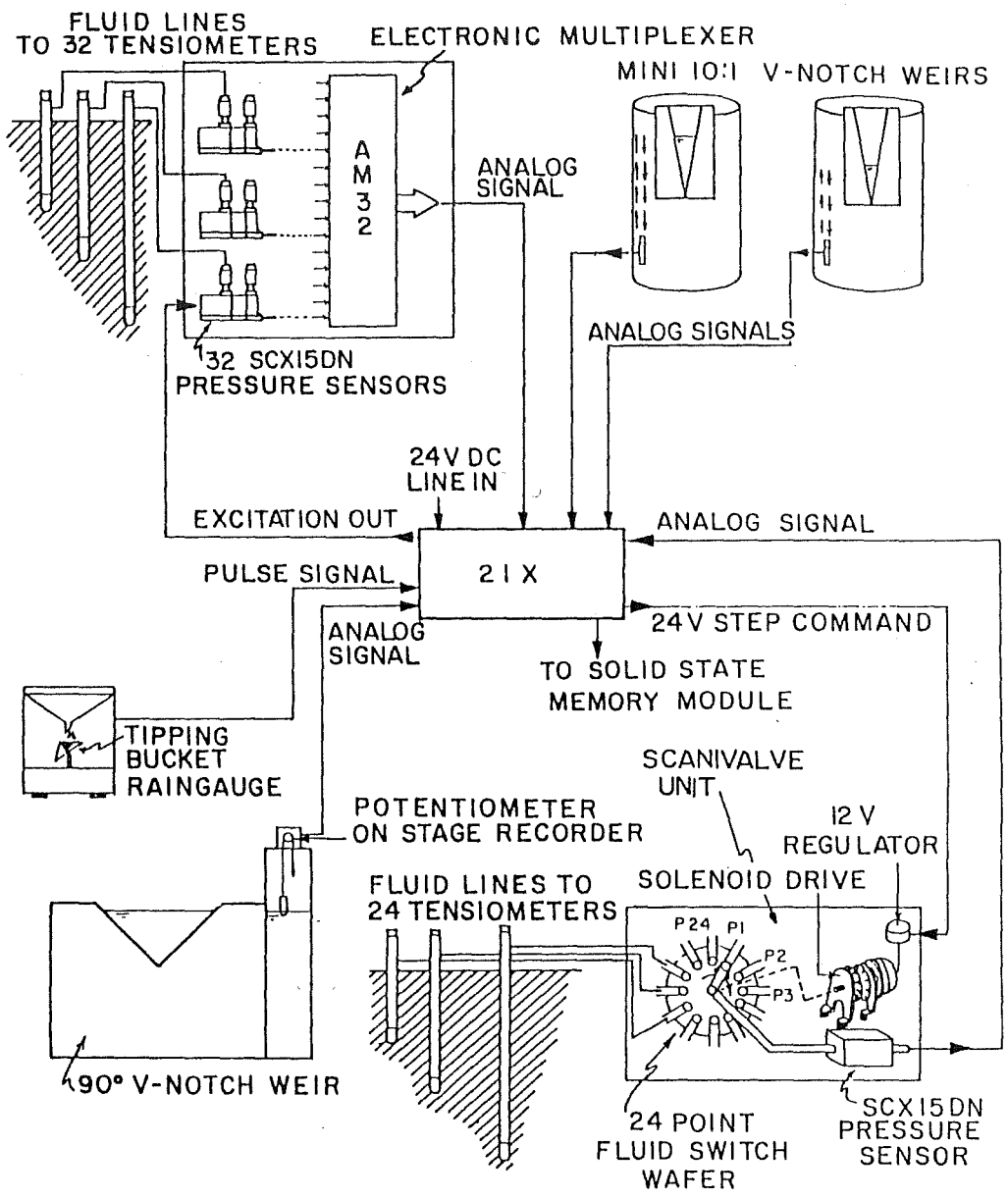

Figure 3.3 Schematic representation of the electronic recording network.

v-notch weir and Leopold Stevens recorder fitted with a low-torque, 10-turn, 1 K-ohm potentiometer. Stage height fluctuations induced changes in the resistance of the potentiometer, and this resistance change was recorded as a voltage output on the CR21X.

3.2.3 Hillslope throughflow

Throughflow was continuously monitored at 3 topographic hollow sites within the M8 catchment: Pit A, Pit 5 and the Seep (see Figure 3.2). Table 3.2 lists the local site characteristics of the pit locations and Figure 3.4 shows an idealised view of the soil-landscape relationships at each site. Although individual pits were located in different sub-hollows within the 0.3 ha 1st order subcatchment, their relative slope positions are compared in Figure 3.4. Pit A represents an upslope hollow site, approximately 10 m from the catchment divide. Although the longitudinal slope of the hollow is 40°, side-slopes into the hollow are only 15°. Pit 5 represents a mid-slope hollow site, where soil depths and hollow side-slopes are greater. This site maintains a highly concave longitudinal and sideslope profile. The Seep site represents a downslope hollow site, where slopes are steeper and soil are shallow (0.3 m). Outflow from the Seep flows directly into an incised 1st order channel, draining the subcatchment.

Each of these sites was monitored by Mosley (1979) and Sklash et al. (1986). Mosley (1979) originally constructed the pits by excavating a pit face 2-3 m long and digging down through the soil into the Old Man Gravels. A cement trough 1 m long (3.3 m at Pit A) was constructed at the pit base to intercept subsurface flow seeping from the soil mantle. In this study, the pit troughs were re-cemented and 25 mm ID garden hose was connected to the trough to route the water downslope into storage

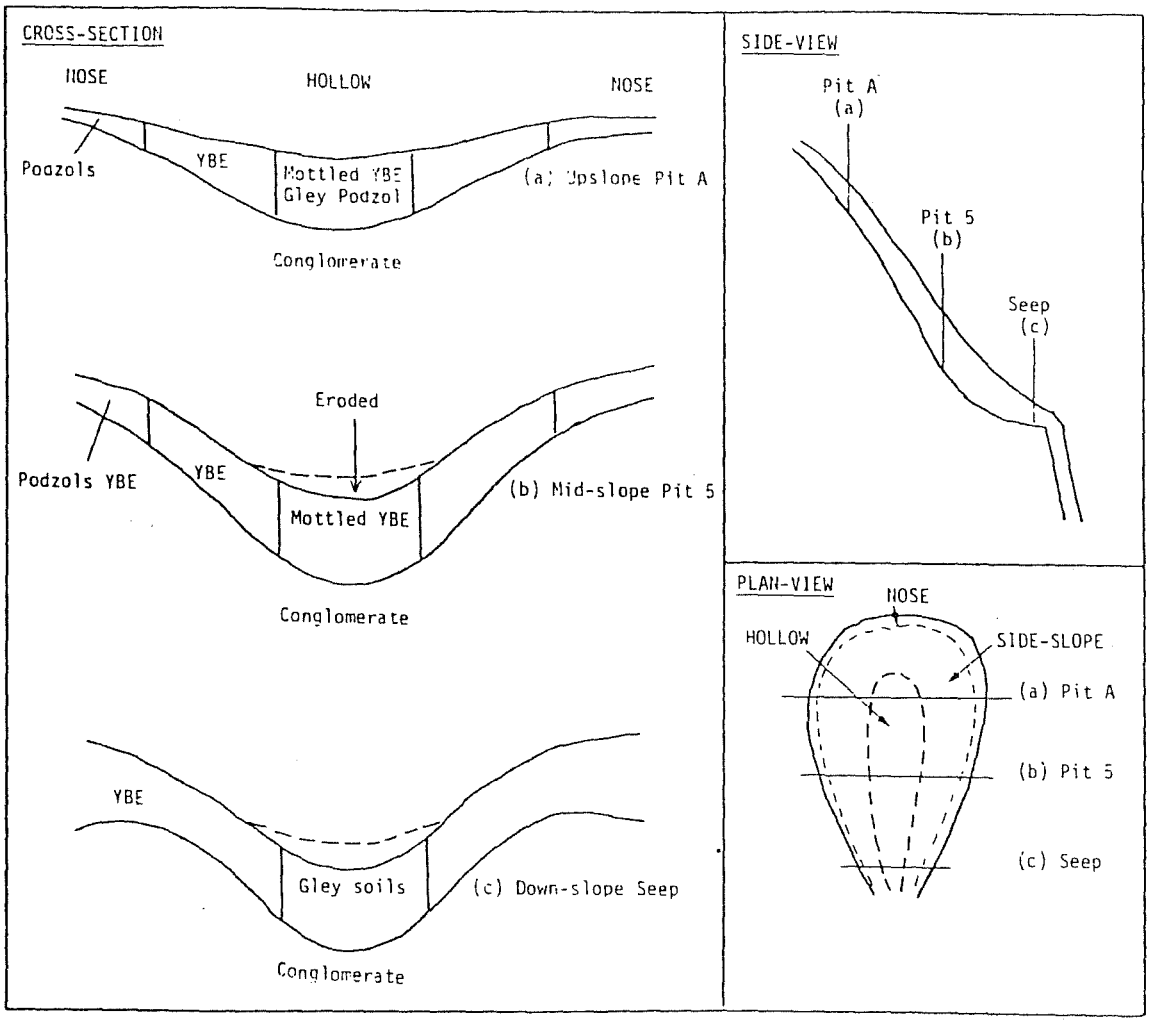

Figure 3.4 Relative slope positions of monitored throughflow pit sites. Soil-landscape data and terminology from, McKie (1978).

containers. Plastic sheeting was placed over the pit faces to prevent rain water mixing with the throughflow.

Table 3.2. Throughflow pit site characteristics.

Site	Area m^2	Soil Depth** m	Slope °	Topographic Position
Pit A	97*	0.6	40	upslope hollow
Pit 5	383*	1.5	35	mid-slope hollow
Seep	1128#	0.3	25	downslope hollow

** At pit face.
* Computed from EDM site survey.
# Computed from topographic map in Mosley (1979, p.797).

Flow from the hillslope pits was monitored using a mini 10:1 v-notch weir systems, mounted directly on to 210 l storage drums (design by B. Fahey, personal communication, 1987). Ministry of Works N.Z. underwater pressure sensors (0-0.5 m, absolute transducers) were used to monitor stage height in the drums for flow computation. Power was supplied to the sensors from the 24 V DC supply, while 10 min signals were stored in the CR21X.

3.2.4 Soil hydraulic conductivity

A well permeameter was developed and used to examine the spatial variability of K_{sat} in the M8 catchment (Figure 3.5). The device was constructed and modified after the Guelph permeameter (Talsma and Hallam, 1980; Reynolds and Elrick, 1985), to allow rapid in situ measurement of soil hydraulic conductivity. The device used little water, permitted easy set-up and allowed calculation of K_{sat} based on steady-rate infiltration theory and techniques (e.g. Phillip, 1968). Normally, only small quantities of water were required per measurement (0.5-2.0 l), and in most cases measurements were made within 15-60 min.

The method allowed estimation of K_{sat} by measuring the steady-state rate of water flow out of a 300 mm shallow well of

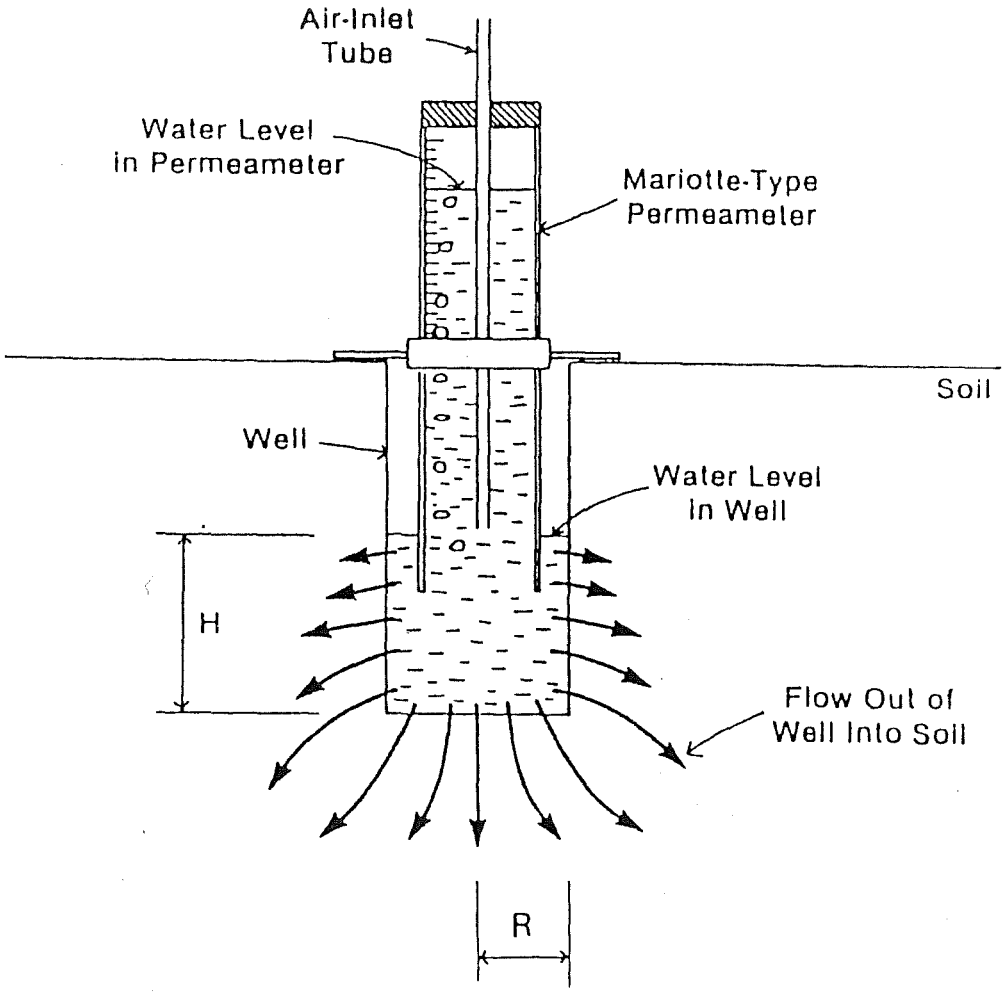

Figure 3.5 Simplified view of well permeameter method (from; Elrick et al., 1984).

radius R (32 mm) in which a constant depth of water H (157 mm) was maintained. Flow from the small well into the unsaturated soil rapidly achieved a steady-state within a finite wetted region, with this small saturated zone encased within a larger unsaturated envelope. The formula used for calculating K_{sat} was an expanded version of the Zanger (1953) solution, used by Bonell et al. (1983):

$$K_{sat} = Q'/2\pi H^2 [\ln(H/R + (H/R)^2 + 1) - 1] \qquad (3.1)$$

where: Q' is the rate of outflow into the augered hole ($mm^3\ hr^{-1}$), H is the constant water depth in the auger hole, and R is the radius of the hole. Measured K_{sat} values using the above apparatus and equation 3.1 are probably more representative of 'field saturated' hydraulic conductivity rather than true K_{sat}. Nevertheless, these values will be treated as roughly equivalent to K_{sat} values of the M8 soils, in the absence of laboratory permeameter data.

3.2.5 Soil analyses

(a) Bulk density and porosity

Laboratory analyses of soil bulk density and porosity were carried out on soil cores (50 mm diameter, 15-20 mm deep) extracted from the throughflow pit faces. Brass rings (55 mm diameter) were pressed horizontally into an exposed vertical face at selected depths. The inside wall of the ring was coated with grease to ensure a good seal between the soil core and ring wall. Ringed cores were taken back to the laboratory and trimmed to equal the ring equivalent volume (i.e. no excess soil protruding out from the ring face). Trimmed ringed cores were placed in a tray of standing water (slightly shallower than the ring depth), and allowed to absorb water for 24 hr. These were then weighed and placed into ovens for drying. Soil cores were oven dried at 105° C for 24 hr and then weighed once again, this time without

the ring. All of the core volumes decreased enough so that cores were easily removed from the rings, which were then weighed separately.

Bulk density (BD) is defined as the mass per unit volume of dry soil expressed as:

BD = weight oven-dry soil/volume of soil (3.2)

Porosity (P) is defined as the ratio of pore volume to total soil volume:

P = [(particle density - BD)/particle density] X 100% (3.3)

Particle density for porosity measurements was assumed to be 2.65 g cm^{-3} for the mineral (B_{2t}) horizon.

(b) Moisture release characteristics

The soil moisture release characteristic is defined as the relationship between water content (θ) and ψ. A Tension Table apparatus (Klute, 1986) was employed using facilities at Lincoln College, Department of Soil Science. Separate soil cores were extracted (as described above) at the same locations. Cores were taken back to the laboratory and prepared in the usual manner. A thin gauze mesh was wrapped around each ringed core face to prevent any loss of sample during analysis. Ringed cores were allowed to stand in a water bath (as described above) for 24 hr and then weighed. Ringed cores were then placed at 10 cm of tension on the apparatus and allowed to equilibrate for 3 days, before weighing again. This process continued at 20, 30, 50 and 100 cm suction intervals until a drainage curve (in the ψ range 0 to -100 cm H_2O) was established. Equilibration times were progressively increased with suction, to a maximum of about 7 days at the final suction. After the final suction equilibration, rings were separately weighed to allow determination of actual core weight.

3.3 RECORDING TENSIOMETRY

3.3.1 Introduction

Recording of soil matric potential (ψ) was essential for investigation of capillary-fringe response and saturated/unsaturated flow in hillslope soils. While many electronic and recording tensiometer systems have been developed using stationary tensiometer-transducer systems (Watson, 1967), capacitance manometer systems (Thony and Vachaud, 1980), and portable tensiometer-transducer systems (Marthaler et al., 1983; Mullins et al., 1986), few recording systems have been designed to address the magnitude and direction of water movement over the entire hillslope scale.

In this experiment, tensiometers had to be deployed in sufficient numbers with adequate time resolution of recording technique to assess ψ changes in response to precipitation. Burt (1978) described a fluid switch wafer system in which 22 tensiometers and 2 water references were multiplexed to a single pressure transducer connected to a chart recorder. Subsequent studies (Anderson and Burt, 1978b; Ahuja and El-Swaify, 1979; Crabtree and Trudgill, 1985) used this technique for monitoring hillslope soil water movement.

The rationale behind the selection of fluid multiplexing systems in previous studies was based on the high cost of accurate pressure sensors. Recent developments in electronic data acquisition and cheap thermally stable pressure transducers, however, provided additional possibilities for rapid response recording of multiple tensiometers. New electronic multiplexers are able to scan multiple tensiometers at rates in excess of solenoid stepper drives used in fluid switching techniques.

Tensiometers were made from 20 mm OD Perspex pipe. Standard Soil Moisture Corp. 1 bar (1 MPa) porous ceramic round-bottom

neck top cups (655X1-B1M1) were cemented to the pipes after they had been cut to the desired length. Soil Moisture Corp. clamp assemblies (2326) allowed coupling of the 4.7 mm OD nylon tubing to the pressure sensors.

3.3.2 Pressure sensor characteristics

Sensym model SCX15DN 0-15 psi (0-1.04x10^5 Pa) pressure sensors were used in the recording tensiometer systems. The SCX15DN provided a cost-effective compensated sensor with high accuracy over a wide temperature range. Temperature induced offset shift calibrations were conducted for 37 sensors with measurements of the difference in output offset voltage at 35.5 +/-0.5° C and 3.0 +/-0.5° C, at an excitation voltage of 12 V DC. Absolute shift (and standard deviation) averaged 95 (86) μV, with maximum 300 μV shift recorded on a single sensor. Response time was very rapid (100 μsec) with repeatability in the order of 0.2-0.5% full scale output.

3.3.3 Tensiometer multiplexing

(a) Electronic multiplexing

A Campbell Scientific AM32 multiplexer was used to multiplex 30 tensiometer and 2 water reference leads to 32 SCX15DN sensor inputs, and then into one differential analog channel on the CR21X. The system was configured such that all transducers were mounted on a single circuit board and housed in a waterproof container. Power was supplied to the unit from a remote 24 V DC supply, regulated down to 12 V DC at the transducer box.

(b) Fluid multiplexing

A Scanivalve fluid switch wafer (W0602/1p-24T) and solenoid stepper drive (WSS-24) were used to timeshare 22 tensiometers and two water references to a single SCX15DN pressure sensor. In previous applications of this system, 555 timing circuits were used to activate a stepping relay output direct to a chart

recorder. In this case, the system was reconfigured to link with the CR21X micrologger for control of the stepper drive rate, drive initiation and signal recording. In addition to more efficient data reduction, this system offered more flexibility in scanning rate and programming.

3.3.4 Plot locations

Figure 3.6 shows the layout of the upslope Pit A (fluid multiplexed), mid-slope Pit 5 (electronically multiplexed) and near-stream (fluid multiplexed) recording tensiometer grids. Tensiometer pipes were inserted vertically down through the soil profile at approximately 28, 52, 97 and 140 cm depths, with cluster spacings of 1-2.5 m.

3.4 ISOTOPE AND CHEMICAL TRACING

3.4.1 Introduction

The tracer concentrations of streamwater were interpreted using a two component mass balance separation. Isotope concentrations in water samples were expressed as per mil ($^{o}/_{oo}$) differences relative to the international standard, SMOW (Standard Mean Ocean Water) as defined by Craig (1961):

$$\delta D = [(R_{sample} - R_{SMOW})/R_{SMOW}] \times 1000^{o}/_{oo} \qquad (3.4)$$

where δD is the relative concentration expressed in the conventional δ-notation, and R is the D/H ratio. By combining a water mass balance with an isotopic mass balance, the storm hydrograph was separated (using the notation from equation 3.4) by:

$$Qs = Qo + Qn \qquad (3.5)$$

combined with

$$Qs\ Cs = Qo\ Co + Qn\ Cn \qquad (3.6)$$

gives

$$Qo = (Co-Cn/Co-Cn)\ Qs \qquad (3.7)$$

and

Figure 3.6 Schematic diagram of tensiometer deployment for Pit A fluid multiplexed tensiometers (A), Pit 5 electronically multiplexed tensiometers (B), and near-stream fluid multiplexed tensiometers (C).

A

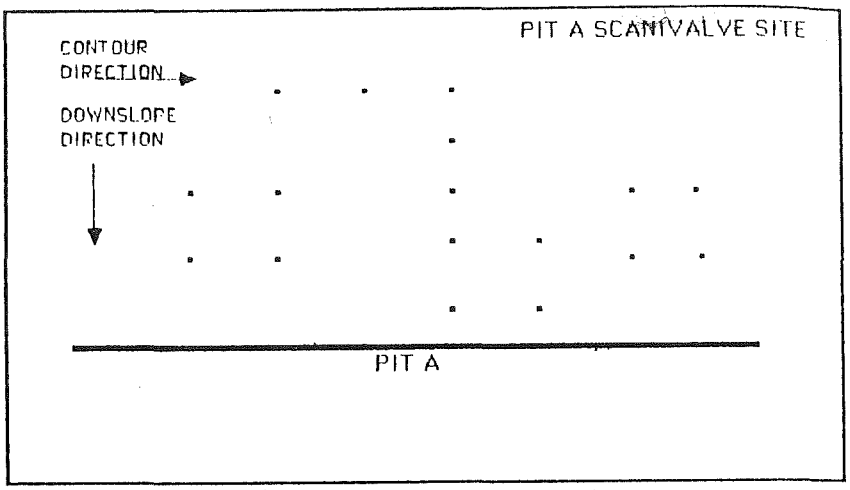
PIT A SCANIVALVE SITE
CONTOUR DIRECTION
DOWNSLOPE DIRECTION
PIT A

B

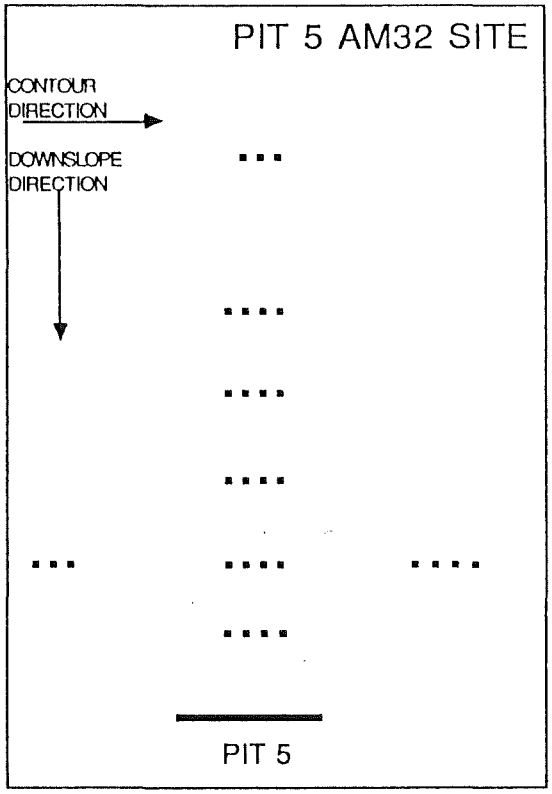
PIT 5 AM32 SITE
CONTOUR DIRECTION
DOWNSLOPE DIRECTION
PIT 5

C

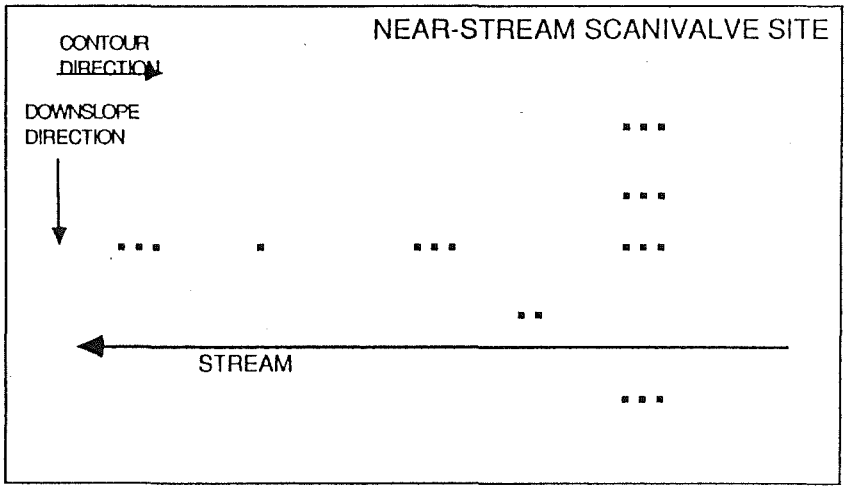
NEAR-STREAM SCANIVALVE SITE
CONTOUR DIRECTION
DOWNSLOPE DIRECTION
STREAM

$$Qn = Qs - Qo \qquad (3.8)$$

where: Qs, Qo and Qn represent current streamflow, old water (stored subsurface water), and new water (rainfall) volumes respectively, and Cs, Co and Cn are the corresponding tracer concentrations. Water samples were also analysed for electrical conductivity (EC) and chloride (Cl) in order to augment isotopic interpretations of water origin.

3.4.2 Sequential precipitation sampling

Rain samples were collected sequentially within the catchment at 2.5 mm, 5 mm and then successive 9.2 mm increments. The collection system was modified after Kennedy et al. (1979) and consisted of a 410 mm diameter funnel, connected at the base to a series of 0.3 l, 0.6 l and then successive 1.0 l bottles. Specially designed glass fittings were constructed and arranged so that each bottle filled before any rain flowed into the following bottle (Figure 3.7). An air outlet tube maintained a vacuum within each bottle and prevented any mixing between sequential rain samples. A tipping bucket device was located adjacent to the unit to allow determination of bottle filling time in relation to rain depth and intensity.

3.4.3 Soil water and groundwater sampling

Soil water and groundwater were sampled at various intervals using standard Soil Moisture Corp. 40 mm diameter porous cup suction lysimeters. These tubes were inserted at 20, 40 and 80 cm depths in different slope positions within the M8 catchment. A small hand pump was connected to the device and a 20" Hg (67.7 KPa) vacuum was established within the tube. Soil water and groundwater were drawn in through the porous cup and were recovered by re-attaching the hand pump and pumping the water into a collection bottle. Water was extracted at weekly intervals

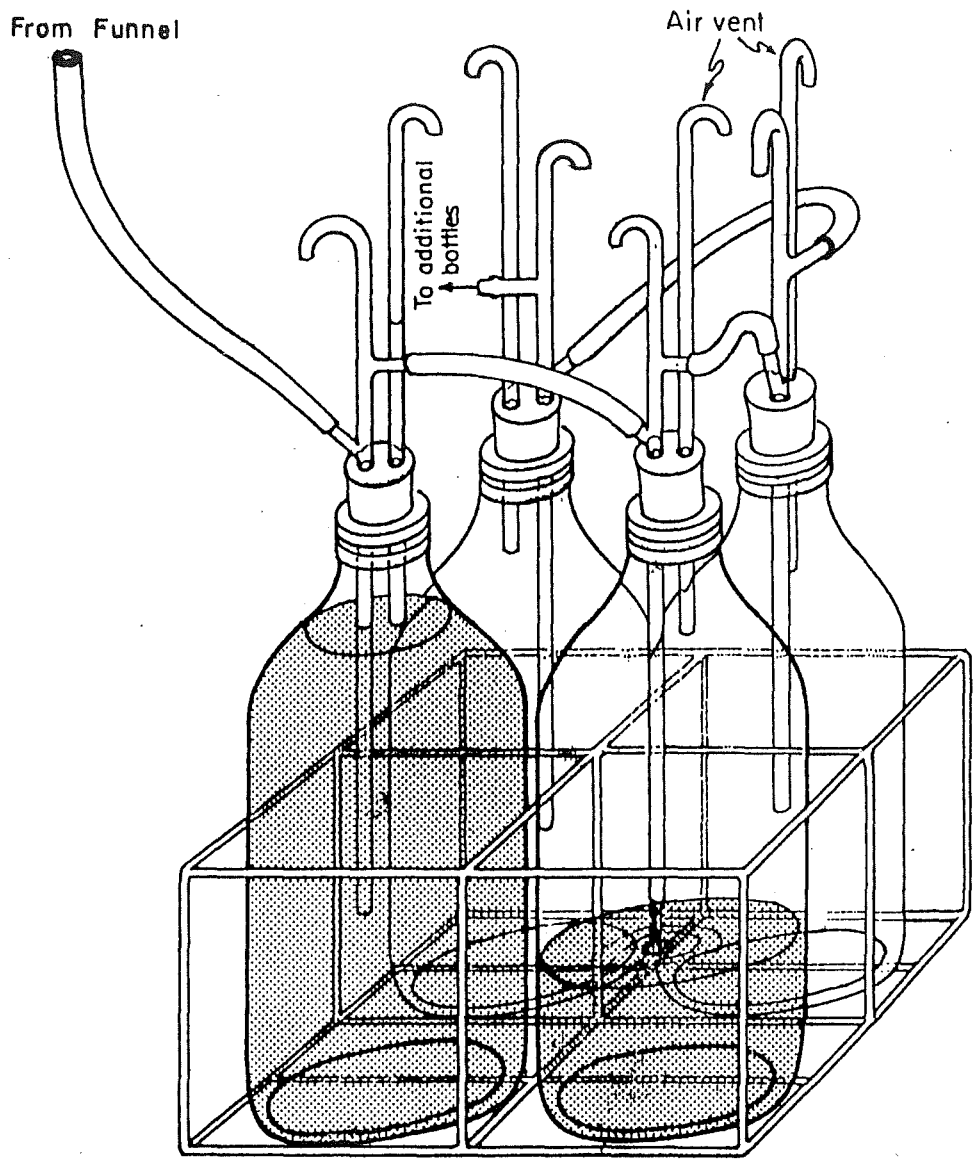

Figure 3.7 Diagrammatic sketch of collector used for sequential rain sampling (modified after Kennedy et al., 1979).

(August - October, 1987) and then at daily intervals during the main field season (November and December 1987).

Simple maximum rise piezometers were constructed using a polystyrene float in a 20 mm OD perspex tube. These were located adjacent to each suction lysimeter location to provide data on water table height at the time of sampling. This information allowed determination of saturated (phreatic zone) versus unsaturated (vadose zone) water sampling.

3.4.4 Streamflow and throughflow collection

Electronically operated vacuum-type automatic 24-bottle liquid samplers (A.L.S. Ltd., 4BSEC and 3BSEC) were used to sample throughflow and streamflow at discrete intervals through a storm hydrograph. The bottles were evacuated simultaneously to a vacuum of about 640 mm Hg (4800 Pa) by a hand-operated pump. Each bottle was connected to a separate rubber tube trapped by a pinch valve, which was then triggered in sequence by a mechanical clock. The clock mechanism was programmed for 2, 4 and 8 hr sampling rates (depending on storm conditions, man-power availability etc.) and was triggered by a remote float switch mounted within the weir stilling wells.

3.4.5 Deuterium, electrical conductivity and chloride analyses

Environmental isotope analyses were conducted at the Institute of Nuclear Sciences, Lower Hutt. Deuterium samples were prepared by the zinc reduction method (Coleman et al., 1982) and analyses run on a V.G. Micromass 602 mass spectrometer. Solute chemistry analyses were conducted at the Forest Research Centre, Christchurch. Electrical conductivity was measured in the laboratory and in the field using portable Metrohm and pHox conductivity meters, while chloride was analysed using an automated mercuric thiocyanate-ferric nitrate method (A.P.H.A.,

1976). Deuterium samples were sealed in 30 ml bottles to prevent evaporation and resulting isotopic fractionation. Chloride and electrical conductivity samples were stored in 0.25 l bottles and cooled or frozen until time of analysis. This procedure eliminated microbial action which can lead to changes in total dissolved solid concentrations.

4 THE ORIGIN OF THROUGHFLOW AND STREAMFLOW - HYDROMETRIC ISOTOPIC AND CHEMICAL CONSIDERATIONS

4.1 SUMMARY OF INTENSIVELY MONITORED 1987 EVENTS

Since much of the hydrometric response data are similar to earlier investigations in the M8 catchment, results are not analysed here in detail, but form the background for the more detailed isotopic analysis in this section and soil physics analysis in section 5. Seventeen storm event hydrographs (greater than about 10 mm of runoff) occurred between 02 September 08 and December 1987. Eleven storms had sufficient data coverage to be analysed for water volume relationships, runoff depths and quickflow characteristics (Table 4.1). Although M8 was very responsive to rain events yielding more than a few millimeters of quickflow, QF/P varied from 16.7 to 62.2%. Using the rationale of Hewlett and Hibbert (1967) and assuming M8 soils are rarely drop below 90% volumetric water content (Mosley, 1979), approximately 25 to 75% of the catchment area produced quickflow in these events. This area exceeds the maximum extent of near-stream surface saturated zones (<7%) and shows the importance of subsurface stormflow in generating most of the runoff.

Table 4.1. Summary of M8 1987 study period runoff events ranked by runoff total (R).

Rank	Date	API$_7$ mm	P mm	Q_{pk} mm hr^{-1}	R mm	QF mm	QF/R %	QF/P %
1	13 October	35.1	104.0	6.4	80.8	64.4	79.9	62.2
2	28 November	3.2	63.1	1.5	36.8	31.7	86.1	50.2
3	07 October	4.7	68.6	0.9	36.1	30.6	84.8	44.6
4	10 October	31.2	43.0	0.9	30.7	14.5	47.7	33.7
5	29 October	4.7	58.2	2.8	30.6	29.0	94.8	49.9
6	13 November	4.6	33.9	1.1	15.7	13.1	83.4	38.6
7	30 September	0.7	26.0	0.8	14.3	11.4	79.9	43.8
8	03 December	39.5	29.4	0.9	14.0	9.2	65.7	31.3
9	26 November	1.6	47.3	0.9	9.8	9.1	92.8	19.2
10	24 October	0.0	30.5	0.3	6.4	5.1	79.7	16.7
11	08 November	3.2	26.4	0.8	5.6	4.6	82.1	17.4

Gross P is used throughout this thesis and is assumed to be roughly equivalent to net P after logging. R/P was modified by antecedent wetness conditions. In storms with a high 7-day antecedent precipitation index (API_7; defined by $\sum_{i=1}^{7} P_i/i$, where Pi is the total gross precipitation on the ith day beforehand), runoff exceeded the slope of the regression line between total storm rainfall and total storm runoff (Figure 4.1A). The R^2 in Figure 4.1A is 0.86, which shows that conditions between storms were not the same. If conditions were identical for each event (i.e. equal API, rain intensity etc.), then the R^2 value would be close to unity. In this case, 3 of the 13 storms plotted substantially above the separation line (API_7=32.2 mm to API_7=39.5 mm) and 4 plotted substantially below the line (API_7=0 mm to API_7=4.7 mm), indicating that low API_7 storms had a lower runoff response. A plot of total storm rainfall versus QF/R substantiates this hypothesis by clearly showing the division in QF/R response based on API_7 (Figure 4.1B). In each case, storm events with high API_7 maintained QF/R>80%. This shows that for high API_7 storms, baseflow is relatively high prior to the event and this high value is incorporated into the QF calculation, yielding a higher relative proportion of quickflow to total runoff. The anomalous positioning of the 30 September storm cannot be explained.

4.2 RAINFALL ISOTOPIC INPUT

Rain input characteristics are described below, as they relate to monitored storm hydrograph events. Rain data are described, both from a long-term perspective (as it relates to the soil water store, section 4.3.1) and within storm perspective (as it relates to storm hydrograph analysis, section 4.4).

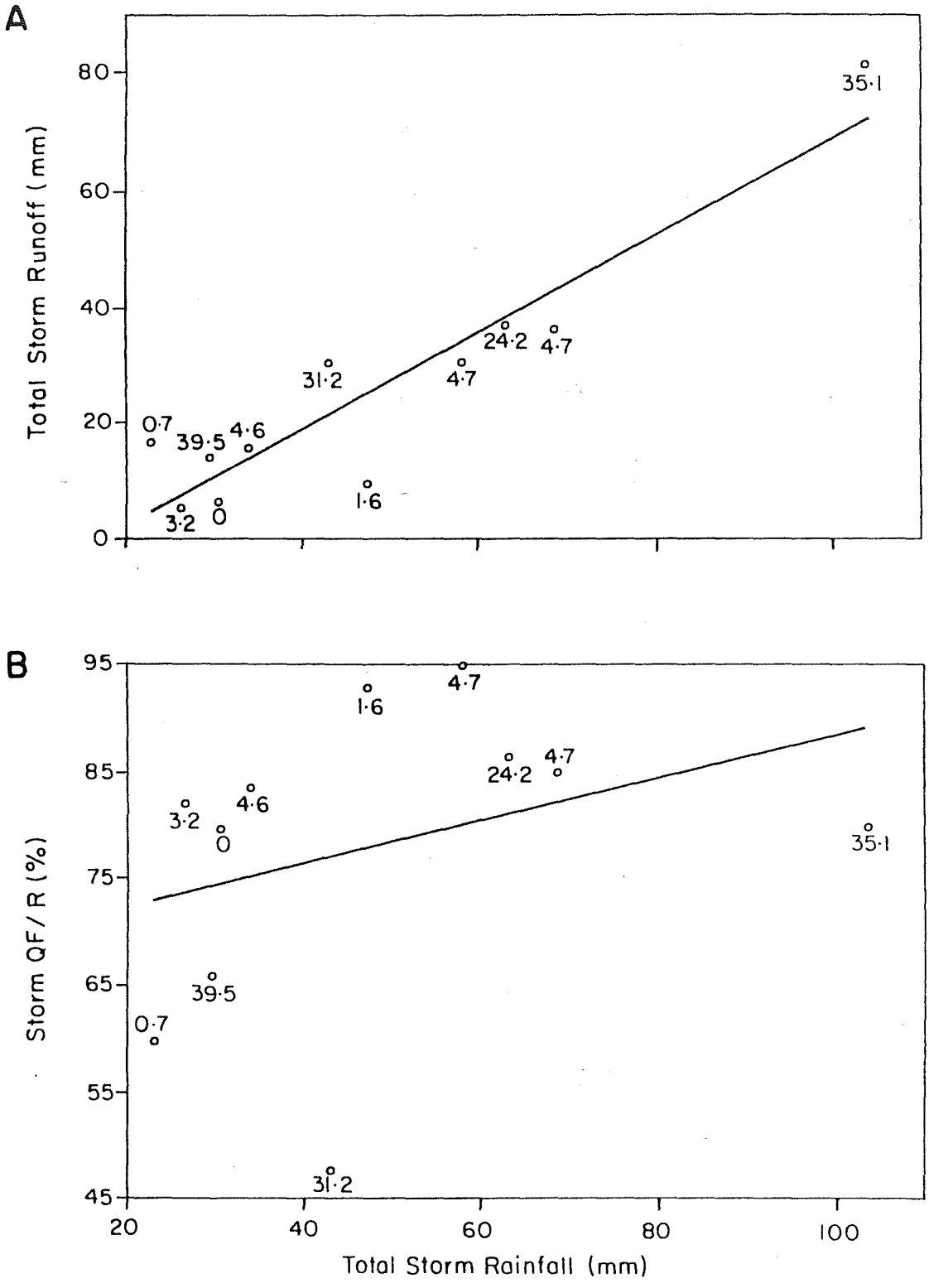

Figure 4.1 Total storm rainfall versus total storm runoff (A) and storm QF/R (B) for monitored 1987 events.

4.2.1 Between storm δD variability

Seventeen individual rainfall events including those associated with the runoff events outlined in Table 4.1 were analysed for isotopic and chemical variability. Mean rainfall depth was 39.2 mm (SD=23.8 mm, range 14-97 mm), mean duration was 29hr (SD=18.2 hr, range 5-69 hr), and all return periods were in the 1-6 month range, except for a 13 October event with a return period of 2-5 yr. Figure 4.2 shows the high variability of δD, Cl and EC between storm events and no clear seasonal or time-related dependence. Average (and standard deviation) storm δD, EC and Cl were -37.8 (17.0) °/₀₀, 9.4 (8.8) μS cm^{-1}, and 2.174 (2.518) ppm respectively.

Rainfall depth, duration and intensity varied considerably between events, reflecting the local synoptic conditions and direction of storm passage. Generally, the rain events were protracted with low intensities (<2 mm hr^{-1}), interspersed with very short higher intensity bursts of 5-12 mm hr^{-1}. The δD, EC and Cl compositions for bulk rain varied depending on air mass history and storm trajectory. Table 4.2 illustrates the differences in bulk δD, EC and Cl for the 17 events and clearly shows the dependence of δD concentration on the amount of terrestrial versus oceanic air mass contact. A simple t-test for unpaired data shows that the difference between δD in southwesterly and westerly storms (i.e. long oceanic contact; mean -23.6 and -20.1°/₀₀ respectively) and northwesterly and northerly storms (i.e. long terrestrial contact; mean -51.9 and -38.0°/₀₀ respectively), is significant at the 0.05 level. It was anticipated that δD would be correlated with both EC and Cl, because ocean derived rainfall would be expected to have higher Cl and lower EC than terrestrially derived rainfall. Linear

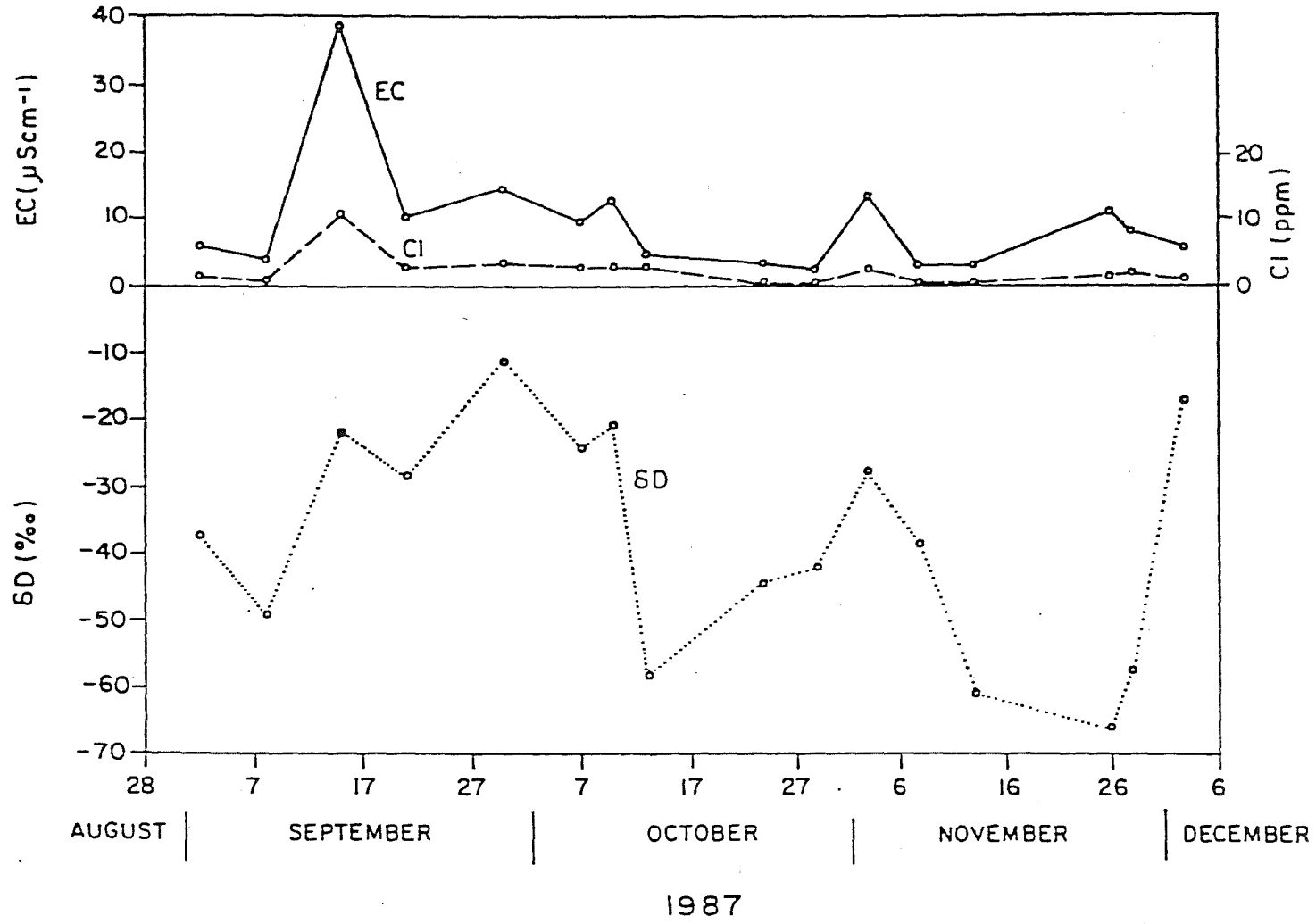

Figure 4.2 Variations in total storm rainfall δD, EC and Cl for 1987 study season.

regression showed no significant relationships; R^2 was only 0.181 and 0.203 for Cl and EC respectively.

4.2.2 Within storm δD variability

Average within storm variability (and standard deviation) of δD, EC and Cl was -34 (-27.3) °/₀₀, 16.5 (16.6) μS cm^{-1}, and 4.965 (4.891) ppm respectively, and related to a number of local climatological factors associated with the event. Seven storm events had sufficient rainfall depths to be sequentially sampled at a rate fine enough to determine relationships between rain chemistry and local synoptic conditions. Two of the 7 events showed classic rain-out (Miyake et al., 1968) of Cl and EC (e.g. 30 September event; Figure 4.3). In this case, a 26 mm westerly rain event moved over the Tasman Sea and then about 30 km inland until reaching the M8 catchment (Figure 4.3A). Rainfall intensity was steady and showed a progressive depletion in EC from 44.8 to c.5.2 μS cm^{-1} over a 9 hr period (Figure 4.3B). Similar effects were observed in Cl chemistry, with a progressive depletion from a very high value of 15.08 ppm (reflecting oceanic history) to 0.520 ppm. In this case, δD values remained relatively constant, -14.4 to -8.1°/₀₀, irrespective of rainfall chemistry fluctuations.

Only one event (02 September) showed any significant correlation between rainfall chemistry and rain isotopic composition. Figure 4.4A shows the correspondence between EC, Cl and δD for the complete storm duration. In this case, the air parcels that arrived at M8, originated inland and followed a north, northwest, then westerly trajectory. Chemical and isotopic concentrations reflect this overall movement and show high R^2 values between EC and δD (R^2=0.768, n=9) and Cl and δD (R^2=0.659), n=9 (see Figures 4.4B and 4.4C).

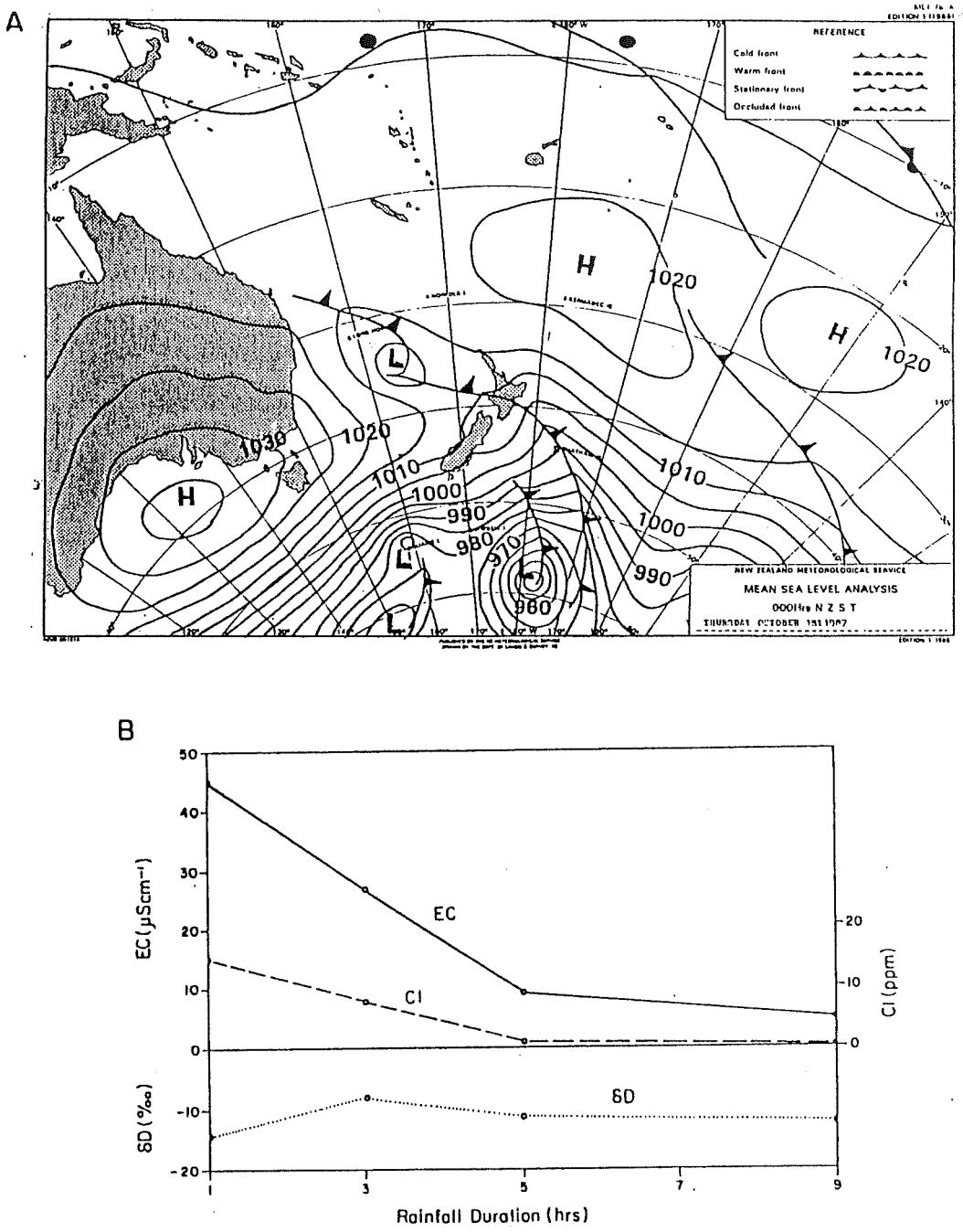

Figure 4.3 30 September 1987 event showing westerly storm trajectory (A) and associated rain-out of δD, EC and Cl (B).

Figure 4.4 Storm rainfall variations for the 02 September event, including chemical and isotopic relationships to rainfall depth (A) and δD correlations with EC (B) and Cl (C).

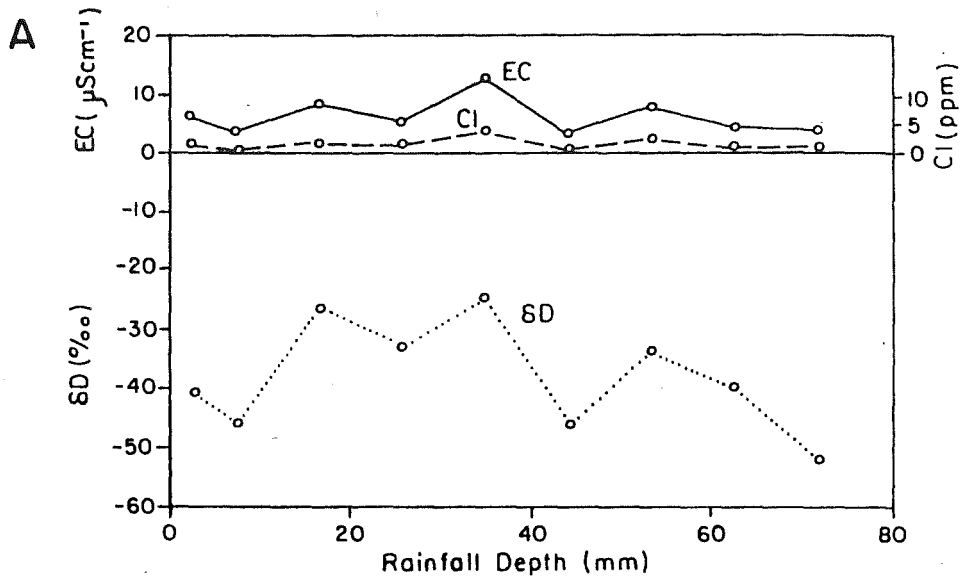
A
EC (μScm⁻¹)
20
10
0
-10
-20
-30
-40
-50
-60
EC
Cl
10
5
0
Cl (ppm)
δD (‰)
δD
0
20
40
60
80
Rainfall Depth (mm)

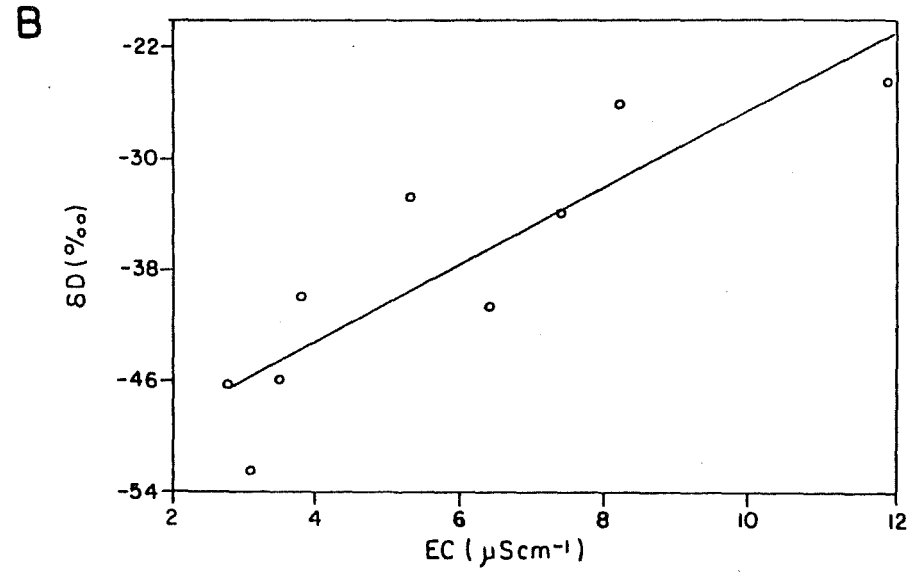
B
-22
-30
-38
-46
-54
δD (‰)
2
4
6
8
10
12
EC (μScm⁻¹)

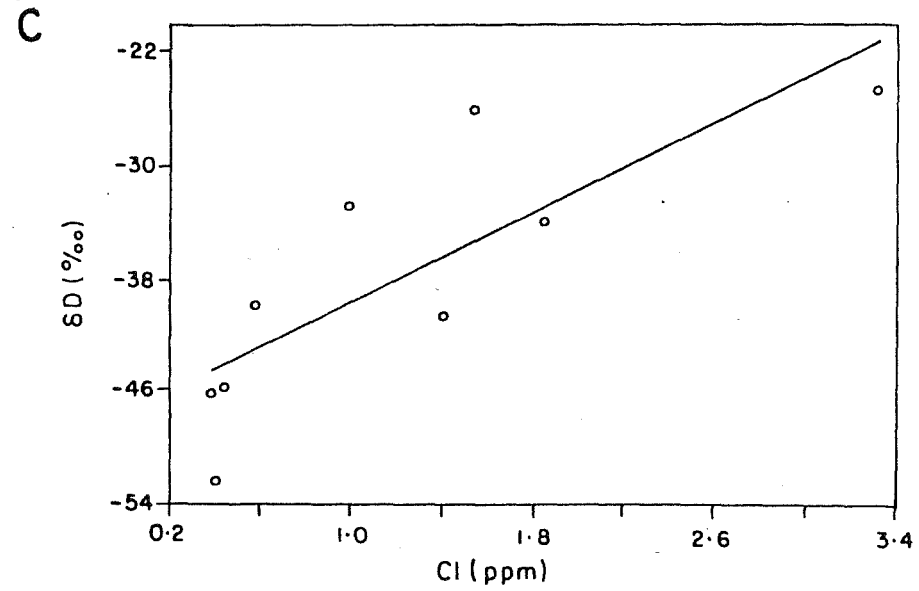
C
-22
-30
-38
-46
-54
δD (‰)
0·2
1·0
1·8
2·6
3·4
Cl (ppm)

4.2.3 Correlations with air mass trajectory

Variations in EC, Cl and particularly δD were strongly related to within storm changes in air mass trajectory. Quantitative relationships were not established because of poor weather map resolution and lack of nearby wind speed and direction data. A qualitative example of storm passage effects on within storm rain δD variations, however, is shown in Figure 4.5. In this case, a southwesterly disturbance yielded approximately 8 mm of rain (constant δD=-35°/₀₀) over an 18hr period before veering northwest. For the next 16 hr, the northwest air movement yielded approximately 28 mm of rain of much lighter isotopic composition (c. δD=-85 to -105°/₀₀). At approximately 34 hr storm duration, the depression moved back to a southwesterly orientation, yielding a further 3 mm of rain at δD= c.-40°/₀₀.

Table 4.2. Summary of weighted mean rain δD, EC and Cl for storms of different wind direction.

-----SW------			------W-----			-----NW-----			-----W-----		
δD	EC	Cl	δD	EC	Cl	δD	EC	Cl	δD	EC	Cl
-21.6	38.7	10.6	-11.1	14.6	3.6	-37.5	5.9	1.2	-38.3	3.1	0.3
-28.4	10.4	2.8	-24.3	9.7	2.6	-49.3	3.9	0.6			
-20.7	12.9	2.7	-27.8	13.4	2.5	-58.3	4.4	2.8			
			-17.1	5.8	1.0	-44.2	3.5	0.3			
						-42.1	2.4	0.3			
						-60.7	3.1	0.3			
						-65.8	10.9	1.3			
						-57.1	8.1	1.8			

*δD=°/₀₀, EC=uS cm^{-1}, Cl=ppm

4.3 SOIL WATER AND GROUNDWATER ISOTOPIC RESERVOIRS

Eleven suction lysimeters were deployed within M8 (see section 3.2.1) to monitor soil water and groundwater δD, EC and Cl concentration through time and space. Table 4.3 gives the characteristics of each site including depth, distance to the stream channel and distance to the catchment divide.

Figure 4.5 The effects of air mass trajectory on rainfall δD characteristics for the period 27-29 November.

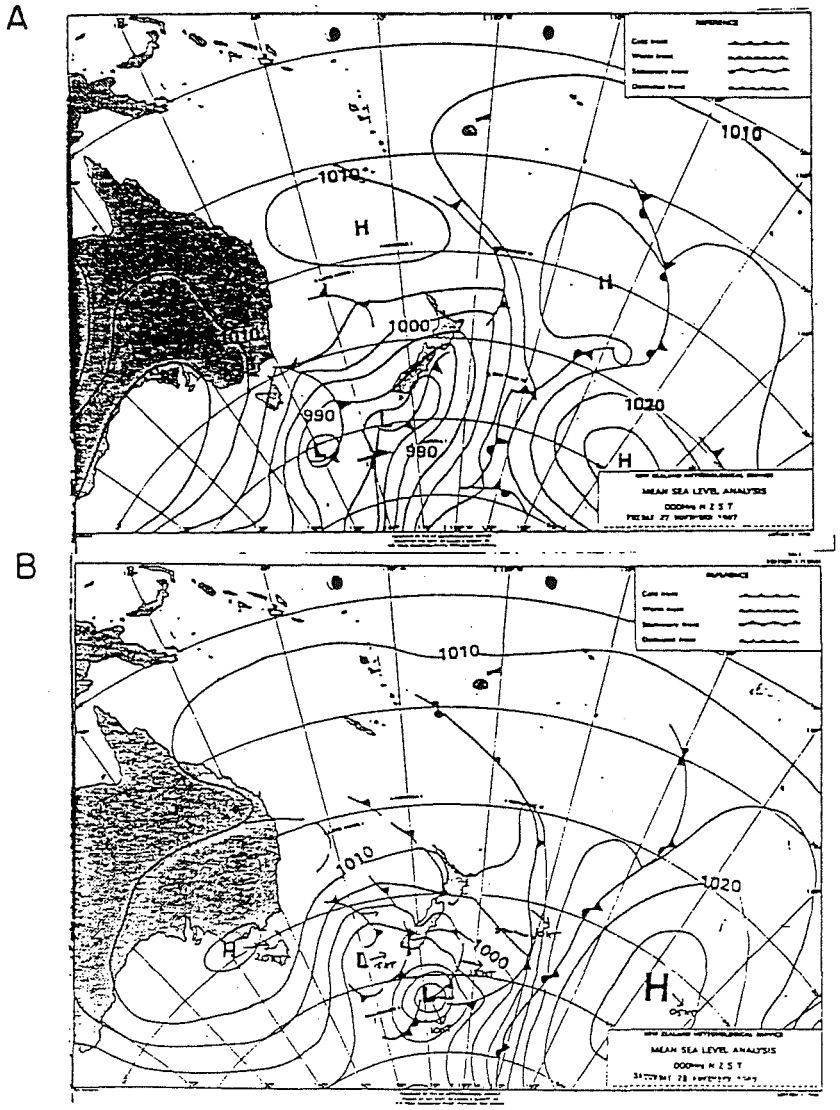
A
B
1010
1000
990
980
1020
H
L
MEAN SEA LEVEL ANALYSIS

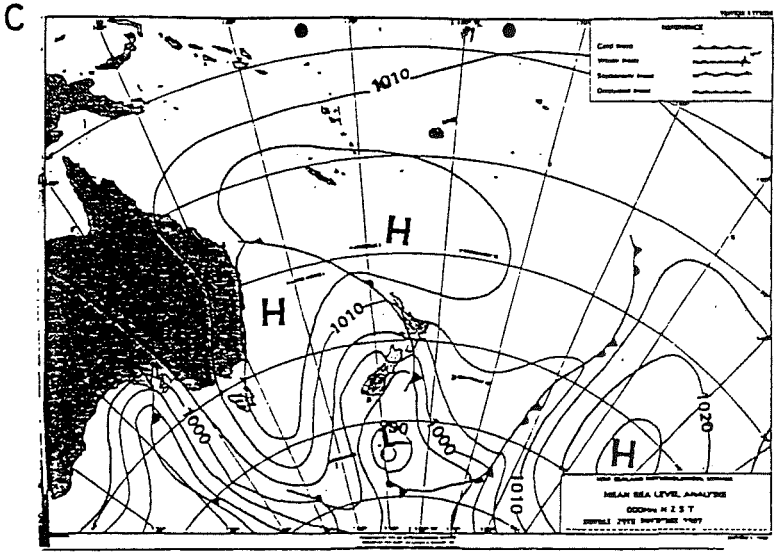
C
1010
1000
990
1020
H
L
MEAN SEA LEVEL ANALYSIS

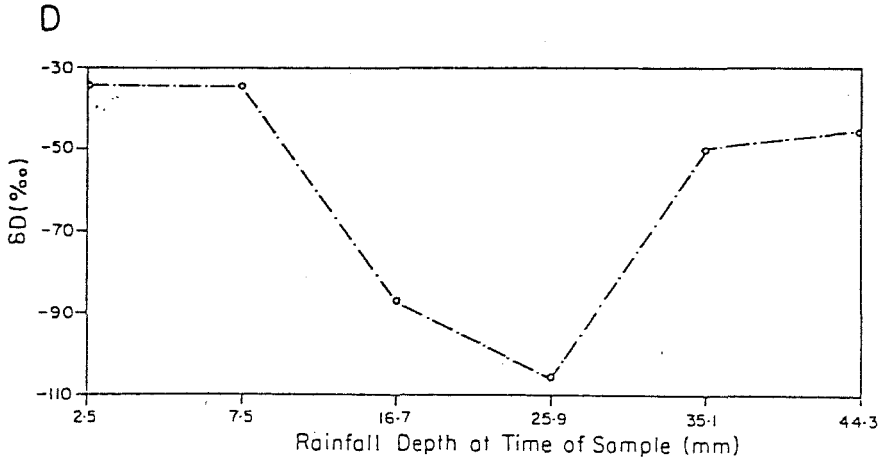
D
-30
-50
-70
-90
-110
δD(‰)
2·5
7·5
16·7
25·9
35·1
44·3
Rainfall Depth at Time of Sample (mm)

4.3.1 Spatial and temporal δD variability

Suction lysimeter δD results for the entire study season are shown in Figure 4.6 (including some spot samples from Pit A, Pit 5 and M8 baseflow), and illustrate varying responses to the rainfall δD input (note different sampling times; Figure 4.6A). All sites show a somewhat dampened response to the sinusoidal high amplitude rain δD input, but vary according to slope position and depth within the profile.

Table 4.3. Suction lysimeter depths and site characteristics.

SL #	Depth mm	Distance to channel m	Distance to divide m
1	40	5	65
2	80	5	65
3	80	30	40
4	20	30	40
5	40	30	40
6	40	25	15
7	30	35	5
8	40	1	75
9	80	1	75
10	40	40	25
11	80	40	25

SL1 (not shown in Figure 4.6 because of limited data coverage) exhibited a peak related to, but much smaller than and delayed from, the high (i.e. less negative) δD values of rainfall around 29 September to 06 October. SL2 shows a steady increase in δD with little significant variation around it. This increase is presumably due to the seasonal increase of δD from winter to summer (or there may be a sharper transition at 27 October). Near Pit 5, SL3 and SL5 show similar small δD variations, but SL5 generally has higher δD-values. This is probably because SL3 contains more old (i.e. winter-derived) water, or possibly (but less likely) because of soil evaporation. SL4 has the largest

Figure 4.6 Variations in rainfall (A), suction lysimeter samples (B-D,F) and M8 baseflow δD (E) for the 1987 study period.

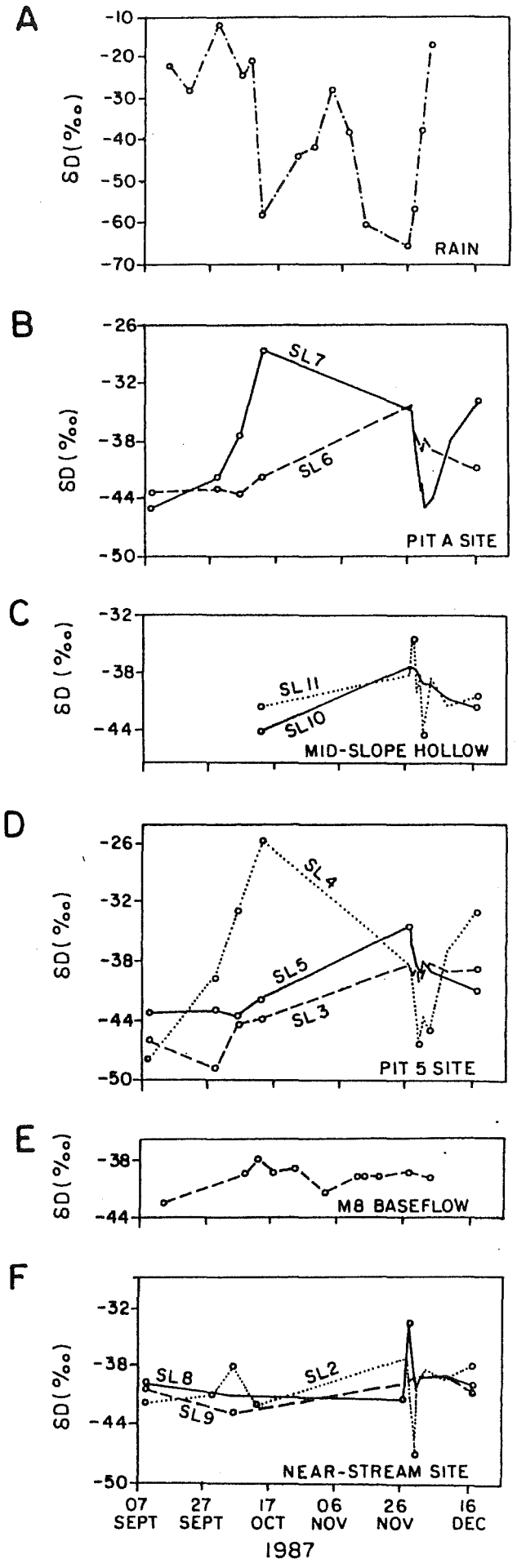
A
-10
-20
-30
-40
-50
-60
-70
δD(‰)
RAIN
B
-26
-32
-38
-44
-50
δD(‰)
SL7
SL6
PIT A SITE
C
-32
-38
-44
δD (‰)
SL11
SL10
MID-SLOPE HOLLOW
D
-26
-32
-38
-44
-50
δD(‰)
SL4
SL5
SL3
PIT 5 SITE
E
-38
-44
δD(‰)
M8 BASEFLOW
F
-32
-38
-44
-50
δD(‰)
SL8
SL9
SL2
NEAR-STREAM SITE
07 SEPT
27 SEPT
17 OCT
06 NOV
26 NOV
16 DEC
1987

variation and follows the rainfall pattern closely, but with smaller amplitude and a lag of about 10 days. Pit 5 throughflow δD follows the SL3 and SL5 curves, although it is not clear which is favoured. SL6, SL7 and PitA δD values show increasing response to rainfall in that order. SL6 is very dampened, while Pit A may be as responsive as SL4.

SL8 and SL9 and M8 baseflow show essentially no variation apart from a long term steady increase in δD value (as for SL2). By fitting a trend line by eye, it appears that there is a tendency for SL8 to have higher δD than SL9. SL10 and SL11 appear to be most similar to SL3 and SL5 and perhaps SL6. All of them are quite dampened compared to rainfall.

To test the description of suction lysimeter δD response through time and to reinforce any spatial trends in the data (i.e. downslope or with increasing depth), a simple multivariate cluster analysis (Everitt, 1974) was performed using the data shown in Figure 4.6. Figure 4.7 depicts the relationships between each suction lysimeter site in the form of phenograms, based on the nearest neighbour Euclidean distance method (Systat, 1985). Three groups can be detected: SL5, SL10, SL6 and then SL3 (Group A) amalgamated at the shortest distance and are therefore the most similar sites. SL8, SL9 and SL11 (Group B) joined shortly after Group A and show some spatial correlation with Group A after half distance. SL7 and SL4 (Group C) show no spatial correlation to Groups A or B, but remain isolated throughout the entire distance and form a distinct grouping.

The quantitative groupings established by the cluster analysis are consistent with the previous description of δD trends. Group A seems to represent a mid-slope, mid-profile location, in which suction lysimeter δD response is intermediate between both high and low amplitude sites (as described earlier).

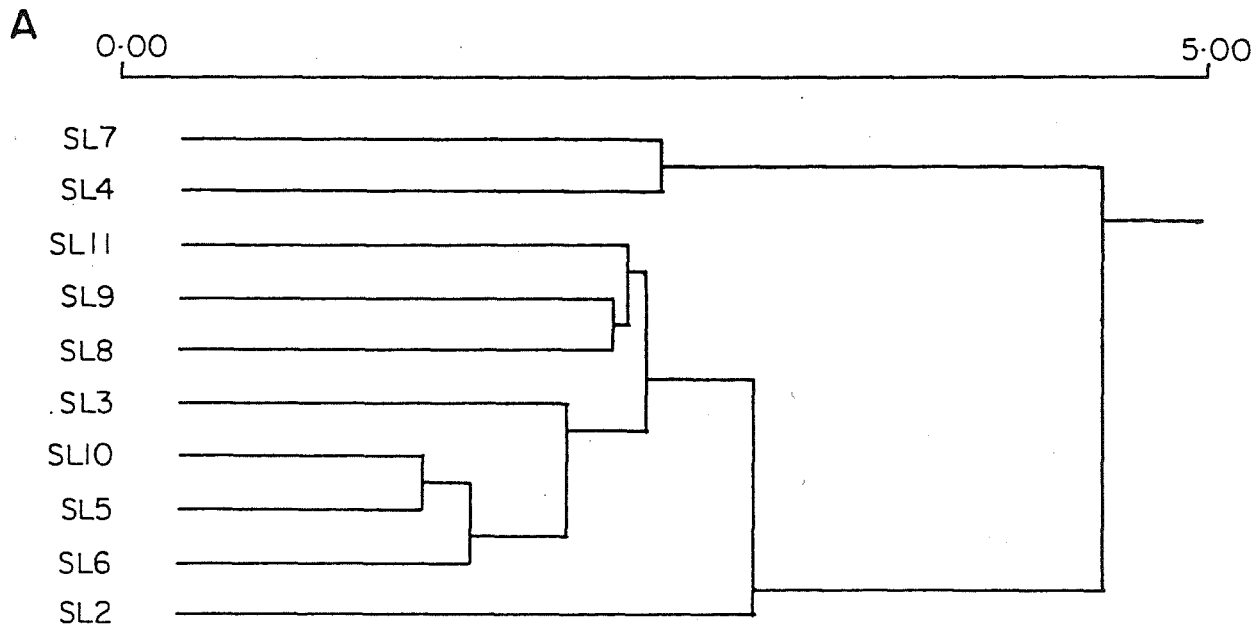

Figure 4.7 Phenogram showing relationships between suction lysimeter sites for the 1987 study period.

Group B is more representative of a near-stream site, or deep suction lysimeter in a slope hollow. This group would maintain the lowest amplitude of response, and also longest lag between rain input and suction lysimeter δD shift. Group C is clearly a shallow soil zone: one with a large amplitude in δD values through time, similar to the rainfall δD input.

4.3.2 Suction lysimeter δD response through an event

The 26-28 November rain event was intensively sampled to examine the suction lysimeter δD response on a much shorter time-scale and to see if longer-term patterns persisted. Daily suction lysimeter and rainfall δD values are plotted in Figure 4.8. Because suction lysimeter samples were extracted on an irregular time series (i.e. during daylight hours within a 0800 to 1800 hr working day) and filled at varying rates (c.1-5 hr), and because weighted mean rain δD was computed for 2400 to 2400 hr periods, some error was introduced into the lag response. Nevertheless, some general comments and trends can be outlined.

Phenograms for the daily time series (Figure 4.8) are shown in Figure 4.9, and indicate that although the rates of amalgamation shifted, groups identified in the weekly time series remained intact. SL9 was an exception to this pattern and moved from Group B into Group A. SL3, SL9, SL10, SL6 and SL5 (in that order) amalgamated first and therefore maintained the closest similarity. These values remained relatively unchanged isotopically through the period (Figure 4.8). SL4 and SL7 (Group C) showed the highest δD fluctuations, in response to rain δD input. Daily rainfall δD values are shown in Figure 4.8A. Rain δD shifted from -72.9‰ to a peak of -40.4‰ (28 November), before dropping to c.-112‰. Group C values showed decreasing δD through time, but did not show any sensitivity to large variations observed in rain signal. Part of this may be due to

Figure 4.8 Variations in rainfall (A) and suction lysimeter samples (B-E) for 27 November to 01 December period.

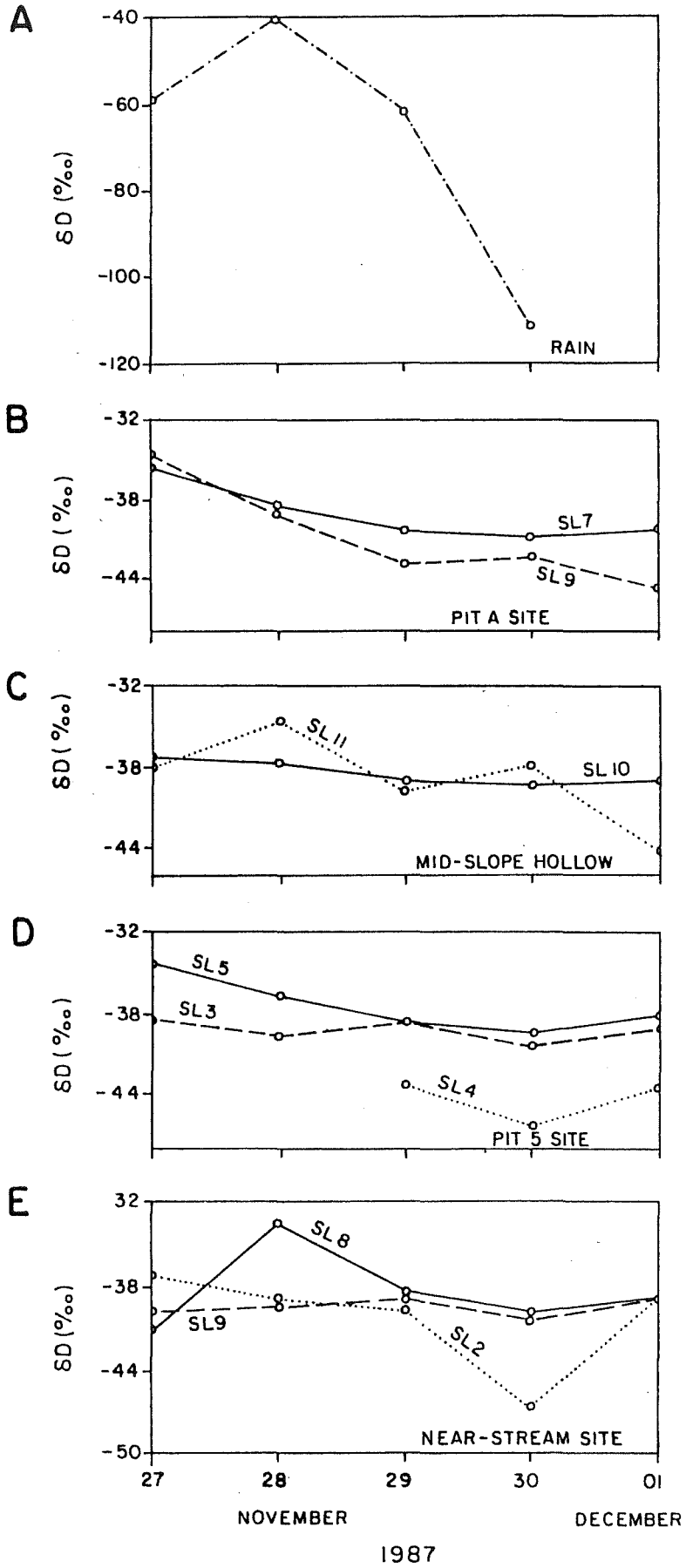
A
-40
-60
-80
-100
-120
δD (‰)
RAIN
B
-32
-38
-44
δD (‰)
SL7
SL9
PIT A SITE
C
-32
-38
-44
δD (‰)
SL 11
SL 10
MID-SLOPE HOLLOW
D
-32
-38
-44
δD (‰)
SL5
SL3
SL4
PIT 5 SITE
E
32
-38
-44
-50
δD (‰)
SL8
SL9
SL2
NEAR-STREAM SITE
27
28
29
30
01
NOVEMBER
DECEMBER
1987

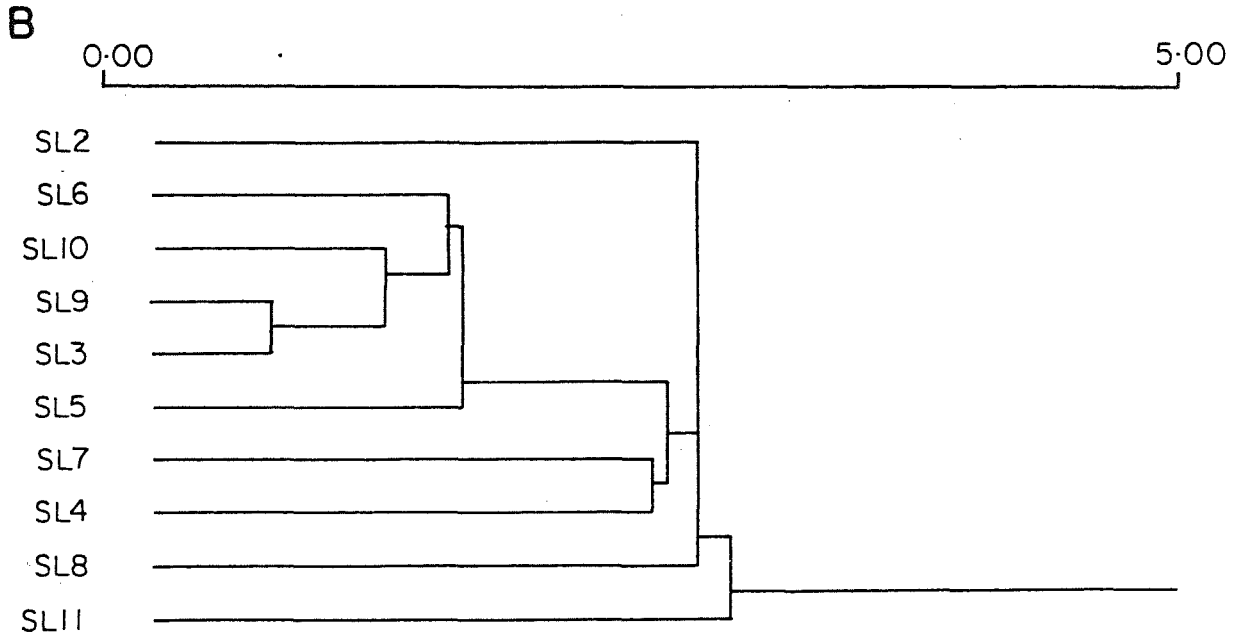

Figure 4.9 Phenogram showing relationships between suction lysimeter sites for the 27 November to 01 December period.

the fact that rain δD shifted very close to the pre-storm SL4 and SL7 value, negating suction lysimeter δD response. Nevertheless, a trend toward rain δD was apparent, indicating substantial new water in the shallow soil zone (<25 cm). Group B sites (SL8 and SL11) were again intermediate between both Group A and B, in terms of the amplitude of response (Figure 4.8) to rain δD. In this case, however, SL8 and SL11 shifted away from the rain signal on 28 November, and then returned to a constant unchanged signal for the rest of the event. This initial movement may be a result of heavier (less negative) water being displaced downward through the profile, in response to the initial wetting front caused by the rainfall burst. δD values from shallow soil locations seem to confirm this postulation (i.e. SL7=c.-35‰).

4.3.3 Reservoir mixing models

(a) Simple volumetric mixing

For shallow soil zones where δD response to rain δD is high (i.e. SL4, SL7), simple volumetric mixing may be applicable. Water from a rainfall event (new water) is added to pre-existing soil water (old water), as given by the previous suction lysimeter sample, to produce the resulting suction lysimeter sample. The fraction (x) of new water is given by:

$$x = (\delta_{SL} - \delta_{SL_0})/(\delta_R - \delta_{SL_0}) \qquad (4.1)$$

where: δ_{SL_0} and δ_{SL} are the δD values of the suction lysimeter samples before rain, after rain, and δD_R represents current rainfall δD. The water is considered to drain out between rainfalls so that total input equals total output (Figure 4.10).

Results for SL4 vary from 21 to 69% new water (depending reasonably on the magnitude and intensity of rain), and have a weighted mean value of 46% (Table 4.4). Some of the results have been combined (see brackets in last column of Table 4.4) because rainfall prior to the current suction lysimeter sample still

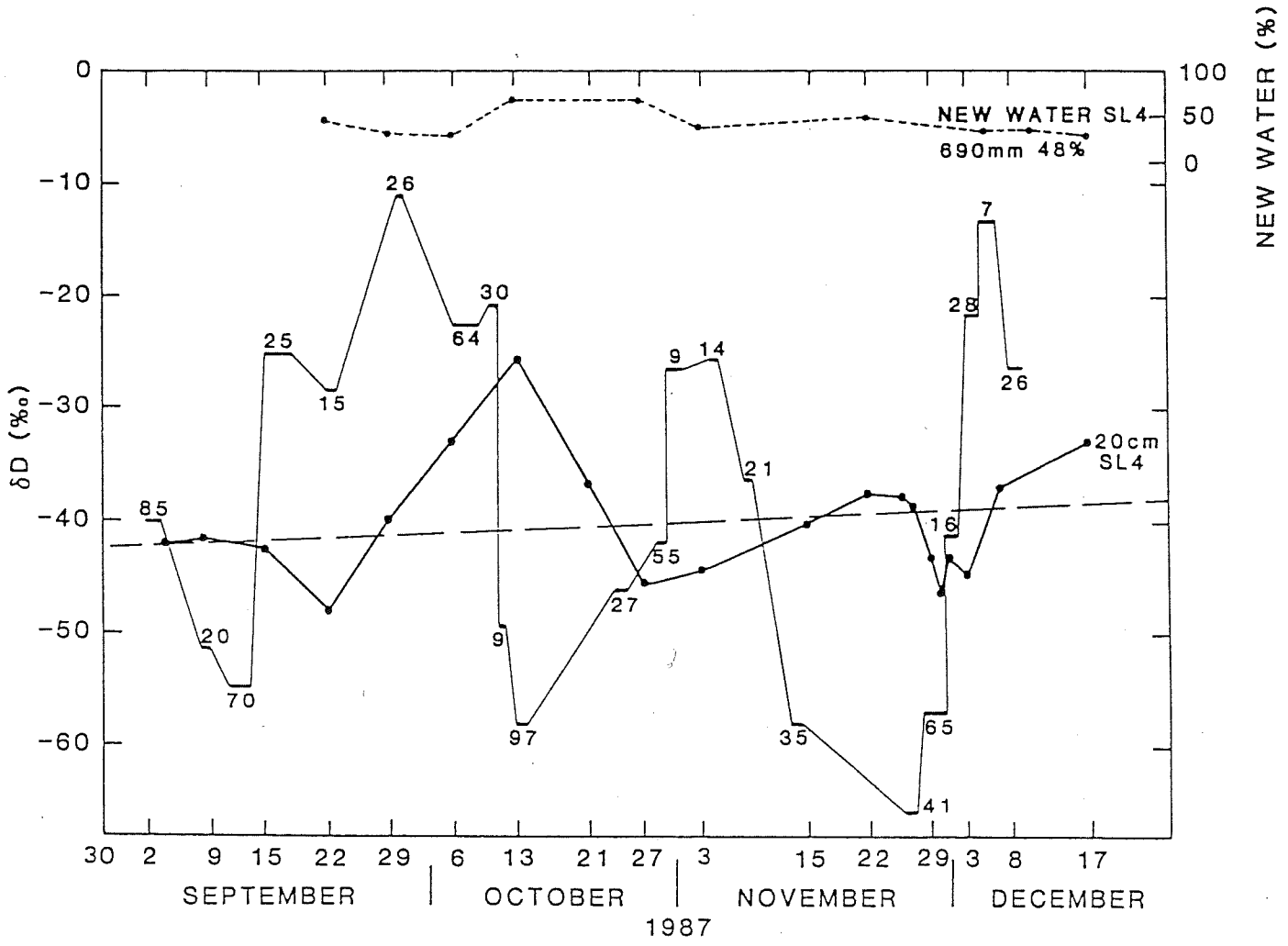

Figure 4.10 Deuterium variations in storm rainfall and suction lysimeter (SL4) samples showing new water percentage estimates.

Table 4.4. Calculation of new water input for SL4.

Date	Suction Lysimeter δSL_o ‰	δSL ‰	Rainfall Depth mm	δR ‰	New Water %	(mm	‰)
4-8 September	-42.0	-41.6	85	-40.1	21		
8-15 September	-41.6	-42.5	20	-51.4	9	90	-54.0
15-22 September	-42.5	-48.0	70	-54.8	45	52%	
22-29 September	-48.0	-39.8	25	-25.0	36		
29,6-9 October	-39.8	-33.0	41	-17.2	30		
6-13 October	-33.0	-25.5	94	-21.9	68		
13-21 October	-25.5	-36.6	106	-57.3	35	133	-55.0
21-27 October	-36.6	-45.8	27	-46.0	98	69%	
27,3-11 November	-45.8	-44.3	55	-41.8	38		
3-17 November	-44.3	-40.4	23	-26.0	21	44	-30.9
17-22 November	-40.4	-37.4	21	-36.3	73	51%	
22-30, November	-37.4	-46.2	76	-62.2	35	157	-57.8
30,3-11 December	-46.2	-44.9	81	-53.8	-17	37%	
3-8 December	-44.9	-36.9	28	-21.6	34		
8-17 December	-36.9	-33.0	33	-23.5	29		
		Total	785mm	---	---		
	Total Weighted Mean		---	-42.1‰	46%		

appeared to be having an effect. Rainfall intensity and amount influenced the variations in x. More importantly, rainfall timing in relation to suction lysimeter sampling was important, combined with the prevailing API conditions. The method showed similar results for SL7 data, but was not applicable to other suction lysimeters which had much smaller δD variations through time and therefore less new water influence.

(b) Exponential steady-state model

Rainfall δD for the weekly time series varied from -12 to $-66^{o}/_{oo}$, in a pattern very similar to a sine curve. An exponential model (Eriksson, 1965), used by Maloszewski et al. (1983) and Pearce et al. (1986), takes advantage of the rainfall signal by allowing computation of:

$$T = w^{-1} [(A/B)^2 - 1]^{1/2} \qquad (4.2)$$

$$\text{Cos } \theta = (w^2T^2 + 1)^{-1/2} \qquad (4.3)$$

where: T is the mean age of the water sampled, A and B are the amplitudes of the input and output sine curves, and w is related to the period of oscillation by $w = 2\pi/\text{period}$. θ is the phase lag. For the M8 August to December rainfall, the amplitude was $c.36^{o}/_{oo}$ and period was 34 days. Results for equations 4.2 and 4.3 are given in Table 4.5.

These equations are derived assuming an exponential model (i.e. incoming water is fully mixed with already-present water) and that the amount of water in the system is constant. The exponential distribution is described by:

$$f(t) = 1/T\ e^{-t/T} \qquad (4.4)$$

where: f(t) is the fraction of water of any given age (t). An example of this distribution for SL4 is shown in Figure 4.11. This model can be reconciled with the simple mixing model (equation 4.1) described earlier, by identifying water with residence times between 0 days and 7 days as new water (rainfall)

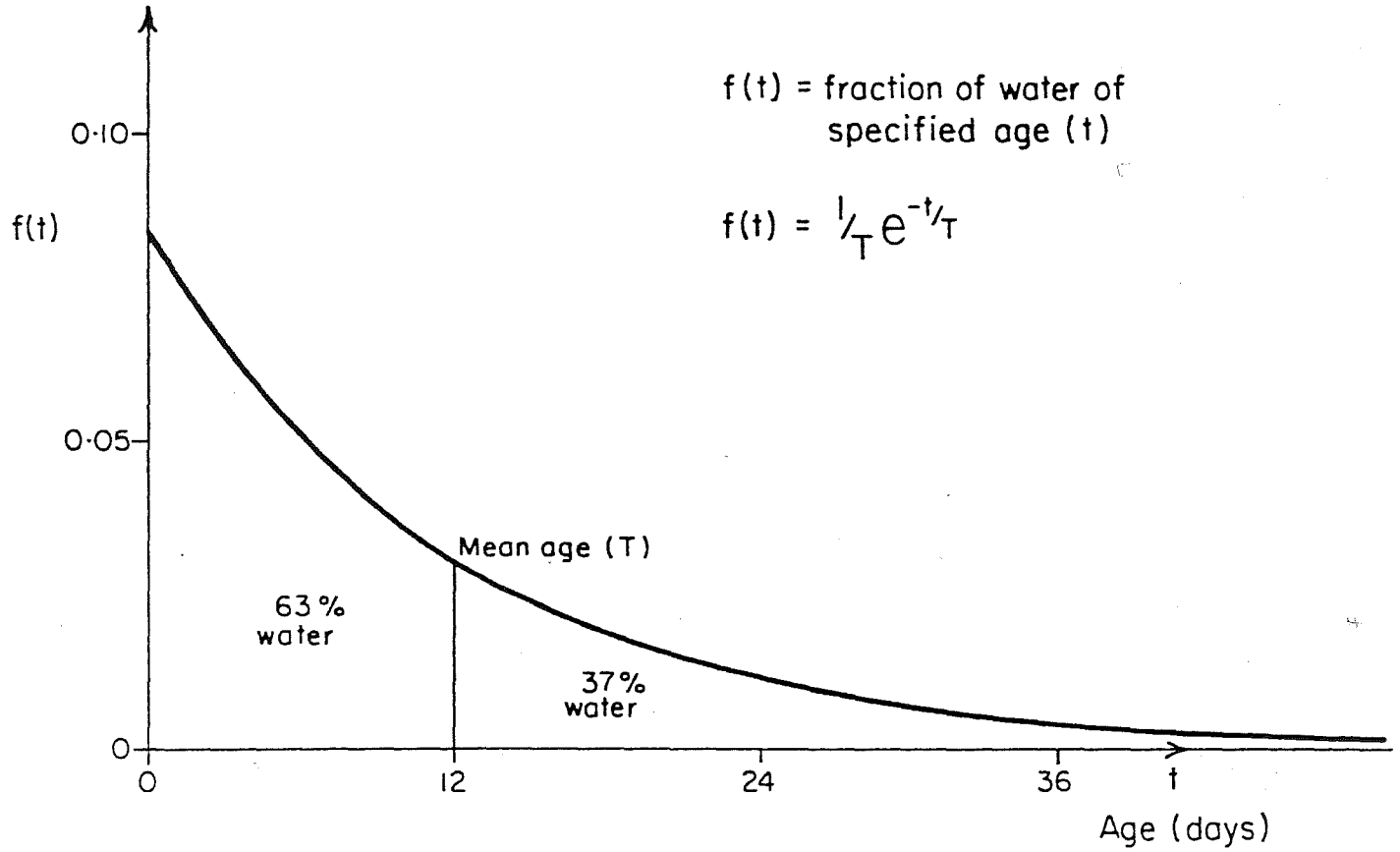

Figure 4.11 Exponential model distribution for suction lysimeter SL4.

and water with residence times from 7 days to n as old water. The fraction of new water can then be calculated by integrating equation 4.1. Table 4.5 plots these results, and shows that the mean age of the old water fraction is T+7 days. These results are in complete agreement with those results of the simple mixing model.

Table 4.5. Exponential model results.

Lysimeter	B ‰	Mean Age (T) days	Expected Lag days	New Water %
SL4, Pit A	15	12	6	44
SL7	12	15	7	37
SL1, 5, 6, 10	4	48	8	14
SL3, 11, Pit 5	2	100	8	7
SL2, 8, 9	<2	>100	8	<7

Results from Table 4.5 can be compared with the throughflow results of Sklash et al. (1986), who identified two groups. Group 1 sites were ephemeral Pits 1, 2 and 3 and Site A (named Pit A in the present study) which had 30-40% new water contributions and high EC values because of flushing. Group 2 sites included Pit 5 and the Seep, which showed <10% new water and low EC values. A third group may now be identified. It includes Site D, Stream B and M8 (with 20-30% new water), and contains displaced Group 2 water, together with new water added by direct rainfall on to channel areas. Although the streamflows from the Sklash et al. (1986) study (c.2.5 mm hr^{-1}) were somewhat smaller than the largest flow observed in this study (c.7 mm hr^{-1}), suction lysimeter δD data (Table 4.5) seem to support this concept. This is particularly true for the presence of old water (mean residence times >100 days) at depths near the bottom of slopes.

4.4 THROUGHFLOW AND STREAMFLOW EVENT ISOTOPIC OUTPUTS

4.4.1 Stormflow sensitivity considerations

In a short-term time series like a storm hydrograph, individual sample error is important, as it relates to the significance of differences between pre-storm δD and succeeding stormflow δD values. Replicate δD samples were run on the V.G. Micromass Mass Spectrometer to determine machine experimental accuracy. Repeats of 5 sample groups showed that on any individual measurement, average standard deviation (SD) equals $1^{o}/_{oo}$ at the 0.05 level (i.e. 68% of the normally distributed data lie within $1^{o}/_{oo}$). Pre-storm δD for each storm was computed and then plotted within a $^{+}/_{-}1^{o}/_{oo}$ error band. The error band limit was then projected through the event (Figure 4.12), and succeeding stormflow values fell either within or outside of this range. Those stormflow values within the range were considered identical to pre-storm δD. Values outside this range were also plotted within a $^{+}/_{-}1^{o}/_{oo}$ error band, but if this overlapped with the pre-storm δD error band, then the difference was considered insignificant.

To quantify the arbitrary test described above, a t-test was performed, using dummy storm values compared with the pre-storm δD:

$$t = (x_p - x_d)/(S.E._{(x_p - x_d)}) \qquad (4.5)$$

where: t is the Student's Test value compared with standard tables, x_p and x_d are sample mean of the pre-storm and dummy variable δD respectively, and S.E. is the standard error of the difference between x_p and x_d. Results showed that at the 0.05 level, $^{+}/_{-}2^{o}/_{oo}$ represented the critical level for significant difference between pre-storm and stormflow δD values.

Storm streamflow δD results were subdivided into the 3 categories listed in Table 4.6, according to their streamflow δD

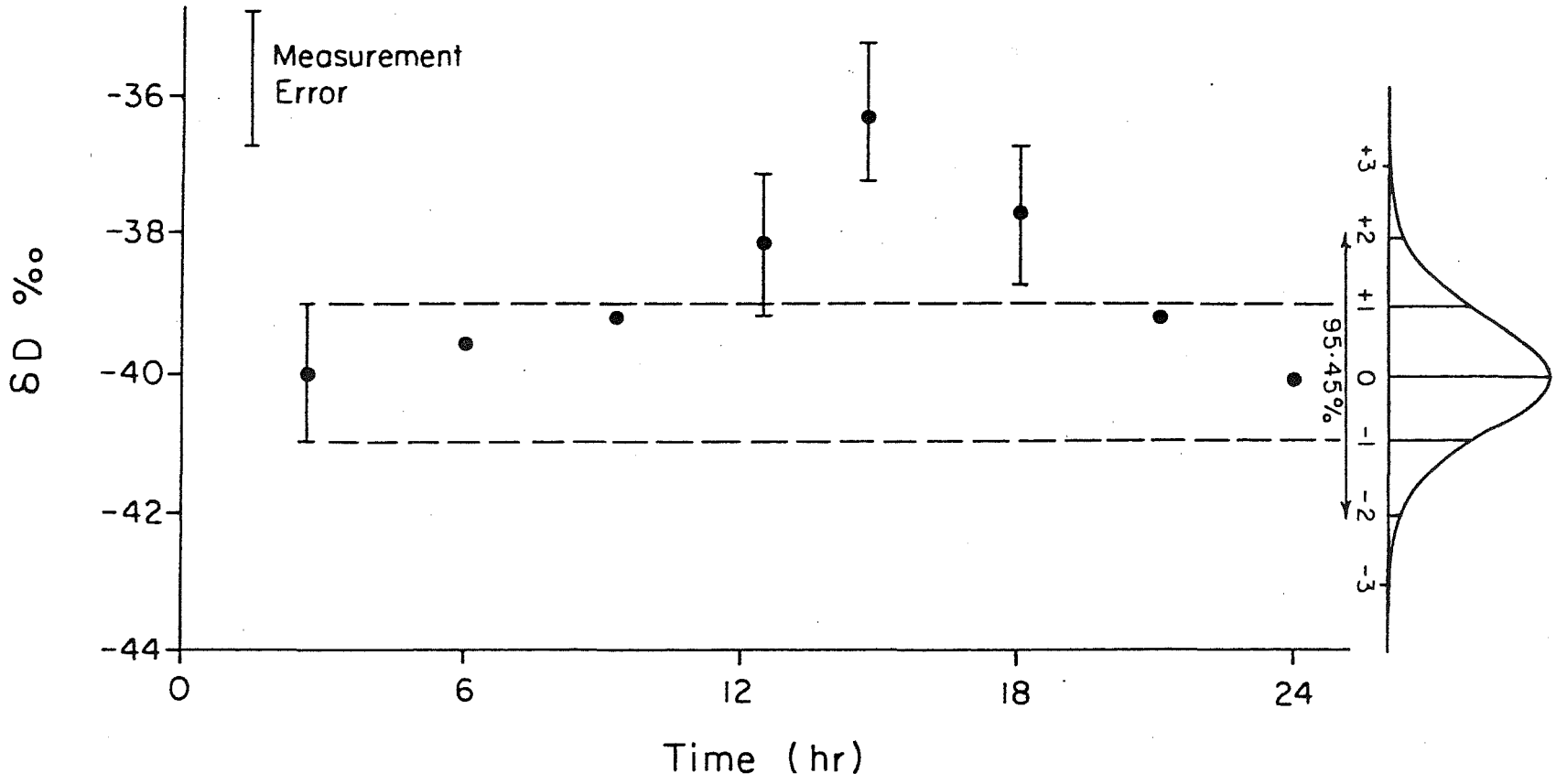

Figure 4.12 Relative error associated with streamflow δD time series.

deflection away from pre-storm δD. Events where weighted mean rain δD equalled pre-storm streamflow δD are not discussed, since isotopic hydrograph separation could not be accomplished.

Table 4.6. Summary of M8 stream δD response to storm rain δD.

Storm streamflow δD response categories		
No δD shift	Rain δD = M8 δD	Normal Deflection
10 October event	03 September event	30 September event
13 November event	20 October event	07 October event
	08 November event	13 October event
	28 November event*	26 November event
	03 December event	

*Rain δD fluctuated through pre-storm M8 δD

4.4.2 Events with no new water input

Two events (10 October and 13 November) showed no detectable new water input into the stream channel. Rainfall and pre-storm flow conditions are given in Table 4.7. Although each event showed large differences between rain δD and pre-storm M8 δD, (i.e. making them suitable for isotopic analysis), stream δD did not deflect away from the pre-storm δD value.

Table 4.7. Rainfall and pre-storm conditions for events with no detectable new water input.

						--x_w RAIN---			--Pre-Storm M8--		
EVENT	RAIN mm	API_7 mm	API_{14} mm	QF/R %	QF/P %	Cl ppm	EC μScm^{-1}	δD ‰	Cl ppm	EC μScm^{-1}	δD ‰
10 Oct.	43	31.2	33.6	48	37	2.672	12.9	-20.7	3.800	17.0	-37
13 Nov.	34	4.1	6.1	83	39	0.316	3.1	-60.7	3.400	21.5	-38

(a) 10 October Event

Forty-three millimetres of rain fell in 2 separate bursts over a 24 hr period on 10 and 11 October (Figure 4.13). Streamflow showed a slow and protracted hydrograph rise, which

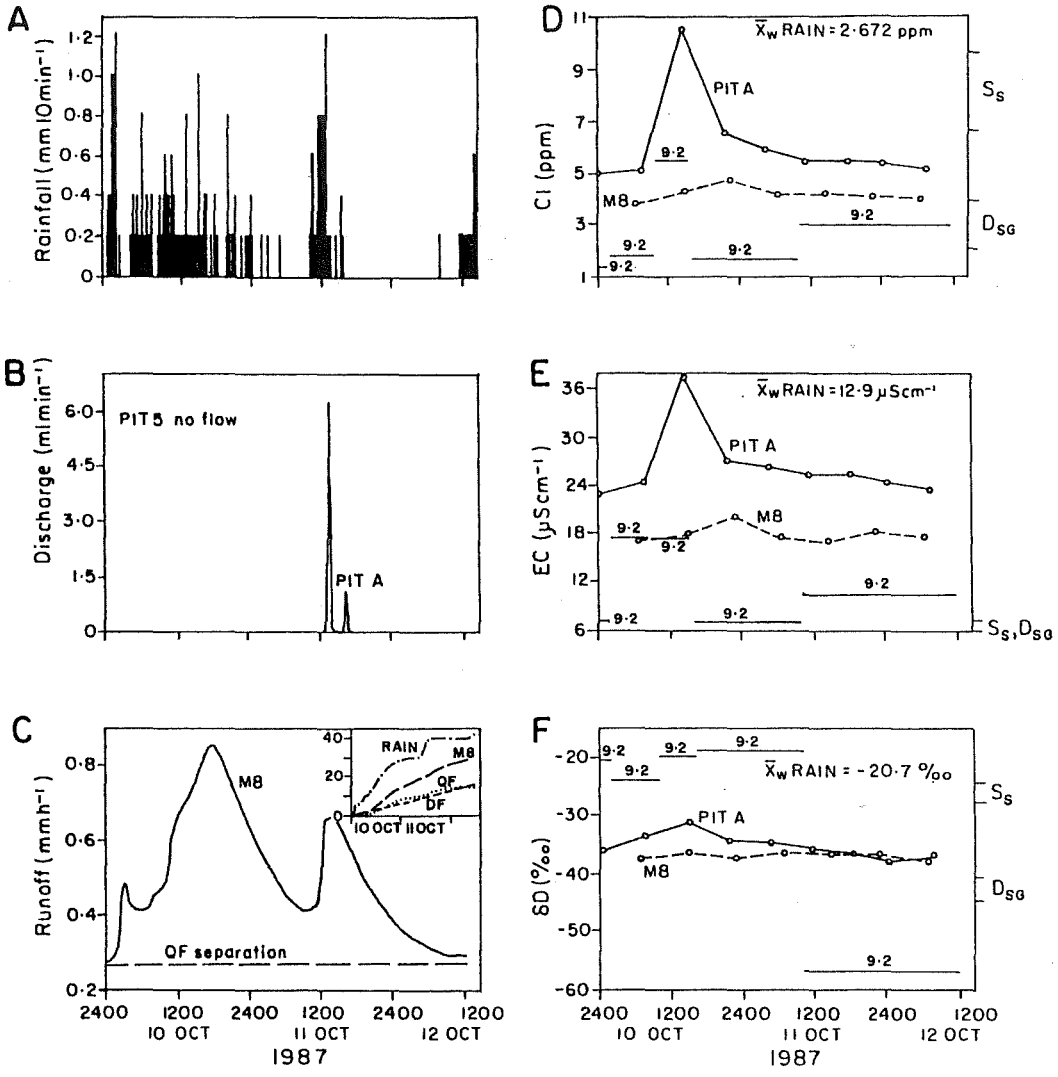

Figure 4.13 Water volume (A-C), chloride (D), electrical conductivity (E) and deuterium (F) relationships for the 10 October event.

peaked at 0.85 mm hr^{-1} at 1800 hr 10 October, followed by a second 0.70 mm hr^{-1} peak at 1800 hr 11 October. Rainfall intensities were low and averaged 3 mm hr^{-1}, with some short higher intensity 10 min bursts of 6 mm hr^{-1}. Weighted mean rain δD was -20.7°/$_{oo}$, and sequential samples stayed within the -17 to -25°/$_{oo}$ range for most of the event. Some lighter -56°/$_{oo}$ rain fell during the later stages of the second rainfall burst, but did not affect the isotopic interpretation for the main stream response.

Pit throughflow data for this storm may be in error. Pit 5 registered no flow, while Pit A showed >6 ml min^{-1} peak discharge (Figure 4.13B). In the previous 07 October event, both Pits 5 and A showed >1000 ml min^{-1} flow. One would expect that given the high antecedent wetness conditions and amount of rainfall in this event, both pits would have yielded greater throughflow. It is assumed that both pits produced more flow than indicated in Figure 4.13B, but for the purpose of isotopic and chemical interpretation, only Pit A produced enough flow to exceed drum flushing rates.

Water samples were extracted at 8 hr intervals for this event. M8 showed no detectable change in streamflow δD throughout the storm. All streamflow samples collected through the hydrograph were within +/-2°/$_{oo}$ of pre-storm (-37°/$_{oo}$) δD. Pit A showed a -4.5°/$_{oo}$ δD deflection toward rain δD, from pre-storm flow δD of -36.1°/$_{oo}$. Since peak δD response was sampled c.3hr before the stream hydrograph peak, Pit A δD would presumably have continued to become less negative until the time of peak streamflow. A mass balance calculation for the 1500hr sample on 10 October indicates c.30% new water contribution to the pit face.

Both Pit A and M8 showed elevated Cl concentrations through the event, away from mean rain Cl of 2.672 ppm. Pit A peaked at 10.500 ppm, c.8 hr before M8 peak of 4.600 ppm. EC variations through the event show increases in total solutes (rather than dilution) for both Pit A and M8. EC peak values coincided with peak Cl concentrations, with Pit A EC shifting from a pre-storm 23 $\mu S\ cm^{-1}$ to peak flow 37 $\mu S\ cm^{-1}$ and M8 from 18.5 to 20.5 $\mu S\ cm^{-1}$. Cl and EC data reinforce the δD data, by showing increases in stormflow concentrations indicating displacement of older soil water and groundwater (which had a substantial period of contact with the soil), rather than dilution by current rainfall. The lack of stream response, as indicated by the slow rate of hydrograph rise, low peak discharge and low QF/R, supports the conclusion that for this storm, no detectable new water contributed to channel stormflow.

(b) 13 November Event

Hydrometric, chemical and isotopic data for the 13 November event are shown in Figure 4.14. Streamflow and pit throughflow responded rapidly to c.8-10 mm hr^{-1} peak 10 min rainfall intensities. Peak catchment runoff was 1.05 mm hr^{-1}, while Pit A and Pit 5 peaked at 3000 and 500 ml min^{-1} respectively. Pit A peak coincided with M8 peak flow, but Pit 5 peak flow occurred after a second small rainfall burst at c.1300 hr 11 October. M8 was sampled at 2 hr intervals, but pit throughflow samples were not obtained for this event. Rainfall showed considerable isotopic variability, but remained lighter than pre-storm M8 δD for the complete duration (x_w=-60.7‰).

M8 showed no detectable δD shift from a pre-storm δD of -39.7‰. M8 Cl and EC concentrations also showed no response through the hydrograph, and reinforce the interpretation that for this event, no new water of any consequence other than that very

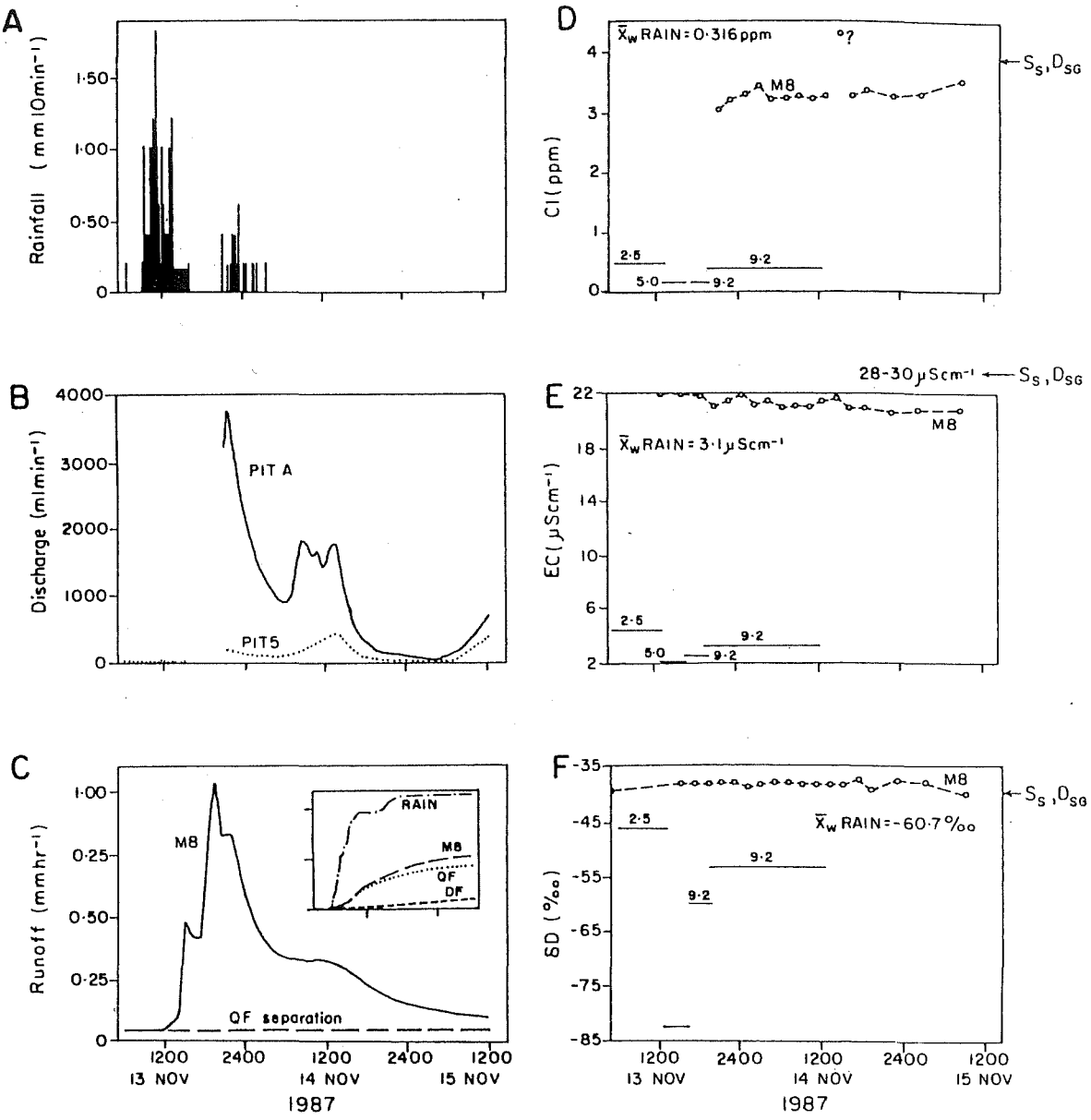

Figure 4.14 Water volume (A-C), chloride (D), electrical conductivity (E) and deuterium (F) relationships for the 13 November event.

small amount falling directly on to the stream, contributed to M8 storm streamflow.

4.4.3 Events with detectable new water input

Four events showed detectable new water input to the storm hydrograph and are listed in Table 4.8.

Table 4.8. Rainfall and pre-storm conditions for events with detectable new water input.

EVENT	RAIN	API_7	API_{14}	QF/R	QF/P	--x_w RAIN--- Cl	EC	δD	--Pre-Storm M8-- Cl	EC	δD
	mm	mm	mm	%	%	ppm	μScm^{-1}	‰	ppm	μScm^{-1}	‰
30 Sep.	26	1.5	4.1	80	44	3.599	14.6	-11.1	4.000	17.0	-39**
07 Oct.	65	4.7	6.2	85	45	2.630	9.7	-24.3	4.200	19.5	-39*
13 Oct.	103	35.1	37.5	80	62	2.842	4.4	-58.3	3.700	17.4	-39
26 Nov.	48	1.5	4.1	93	19	1.273	8.1	-65.8	4.000	23.0	-39

**Estimated sample from long-term baseflow δD series
*From sample at 0520 hr 02 October in long-term baseflow δD series

(a) 30 September Event

Twenty-six millimetres of rain fell during a 9 hr period on 30 September, with a mean intensity of 3 mm hr^{-1} (Figure 4.15). Peak streamflow response (0.8 mm hr^{-1}) lagged the centre of the rainfall burst by c.12 hr, because of very low API conditions (Table 4.8). Data logger problems prevented any hydrometric recording for the complete storm duration. Rainfall and streamflow records were digitised from chart-fitted recorders, but pit throughflow data were unavailable. Rain δD was consistently between -9.0 and -14.5‰, with a weighted mean of -11.1‰.

Streamflow was sampled at 4 hr intervals through the event, with the first sample taken at 1300 hr 30 September. Because of very dry conditions for 2 weeks prior to the event, no streamflow samples were available for a pre-storm (pre-rain) δD value. A δD

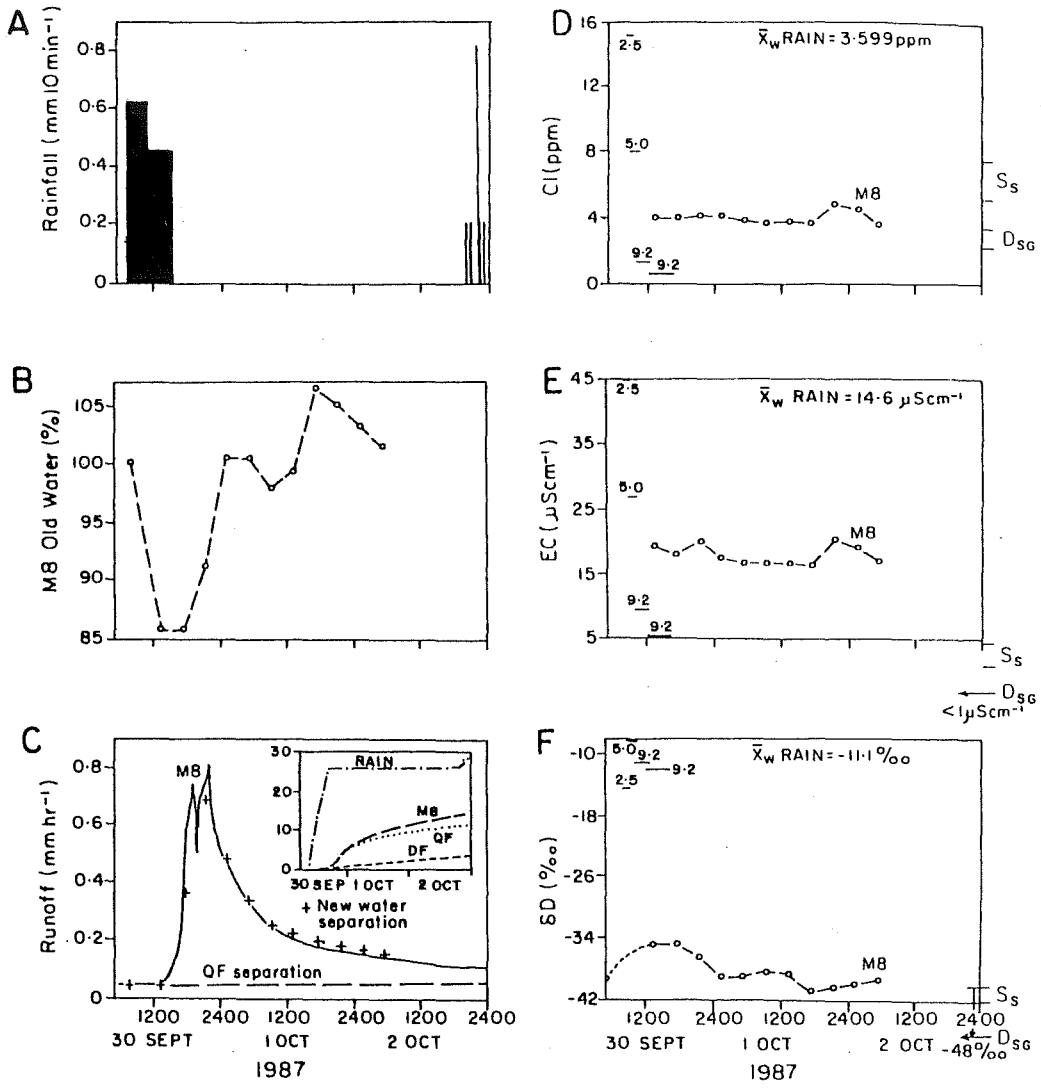

Figure 4.15 Water volume (A-C), chloride (D), electrical conductivity (E) and deuterium (F) relationships for the 30 September event.

of -39°/₀₀ was taken from the long-term baseflow δD series in Figure 4.6E. A mass balance separation of the M8 storm hydrograph is shown in Figure 4.15C. Peak new water input occurred during the rising limb of the hydrograph. Water samples extracted at 1300 hr and 1800 hr 30 September (representing the start of hydrograph rise and mid-rise conditions respectively) showed new water contributions of 14% in each case. At 2400 hr (i.e. peak discharge), new water contributions declined to 9%, and 4 hr later (early recession), new water was not detectable in the hydrograph. These conditions prevailed for the duration of the event.

M8 new water δD values at peak discharge can be accounted for by rain falling on to the stream channel itself and surface saturated zones (groundwater effluent) adjacent to the channel. Both shallow soil water δD and deep soil water and groundwater δD were lighter isotopically (-39 to -48°/₀₀) than pre-storm M8 flow. The rapid shift back to pre-storm δD and then even lighter δD at c.1800 hr 01 October, indicates an increasing deep soil water and groundwater component through the later hydrograph recession. This is also apparent in Figure 4.15C, where old water estimates plot above the M8 hydrograph recession limb, a situation indicating >100% old water.

Without a pre-storm water sample for comparison, water chemistry variations through the 30 September event are difficult to interpret. M8 Cl and EC concentrations remained relatively constant through the event, with some increase in both Cl and EC at c.2400 hr 01 October. These shifts are not easily explained, as rainfall had ceased more than 24 hr previous, and streamflow showed a steady recession. Although mean rain Cl and EC (3.599 ppm and 14.6 $\mu S\ cm^{-1}$ respectively) were well away from pre-storm M8 concentrations, rainfall signatures fluctuated

through the stream value, which further complicates the chemical interpretation. This may in fact account for the flat response, particularly during the early stages of the hydrograph.

(b) 07 October Event

Over the period 06 to 08 October, 65 mm of rain fell in M8 and produced 36 mm of runoff (Figure 4.16). The first 30 mm of rain (1800 hr 06 October to 1800 hr 07 October) maintained average intensities <1.5 mm hr^{-1} and generated only c.7 mm of quickflow. The main streamflow and quickflow response occurred after a more intense 6hr burst (2000 hr 07 October to 0200 hr 08 October), in which peak 10 min rainfall intensities reached 12 mm hr^{-1}. Rainfall δD, EC and CL were sampled in the usual manner, but instrument failure resulted in the loss of 25 mm of rain. Nevertheless, weighted mean rain δD was $-24.3‰$, and fluctuated in the -5 to $-35‰$ range. Synoptic conditions and wind direction remained constant before, during and after the period of data loss, and the mean weighted value is therefore considered representative of lost rain.

M8 streamflow was sampled at 8 hr intervals through the event. Unfortunately, the streamflow peak was missed, but two samples were collected 4 hr before and after peak flow. δD values gradually became heavier through the event, from a pre-storm δD of $-39‰$. This pre-storm value was extracted from the long-term baseflow δD series (Figure 4.6E), and is considered representative of pre-storm M8 δD conditions. Isotopic hydrograph separation is shown in Figure 4.16D. Based on the data, new water contributions to stormflow varied between 13 and 32%, with highest values occurring at 2300 hr 07 October, approximately 4 hr before peak flow.

Because the absolute shift in M8 δD was relatively small (Figure 4.16F), values $+/-1‰$ of the selected pre-storm δD were

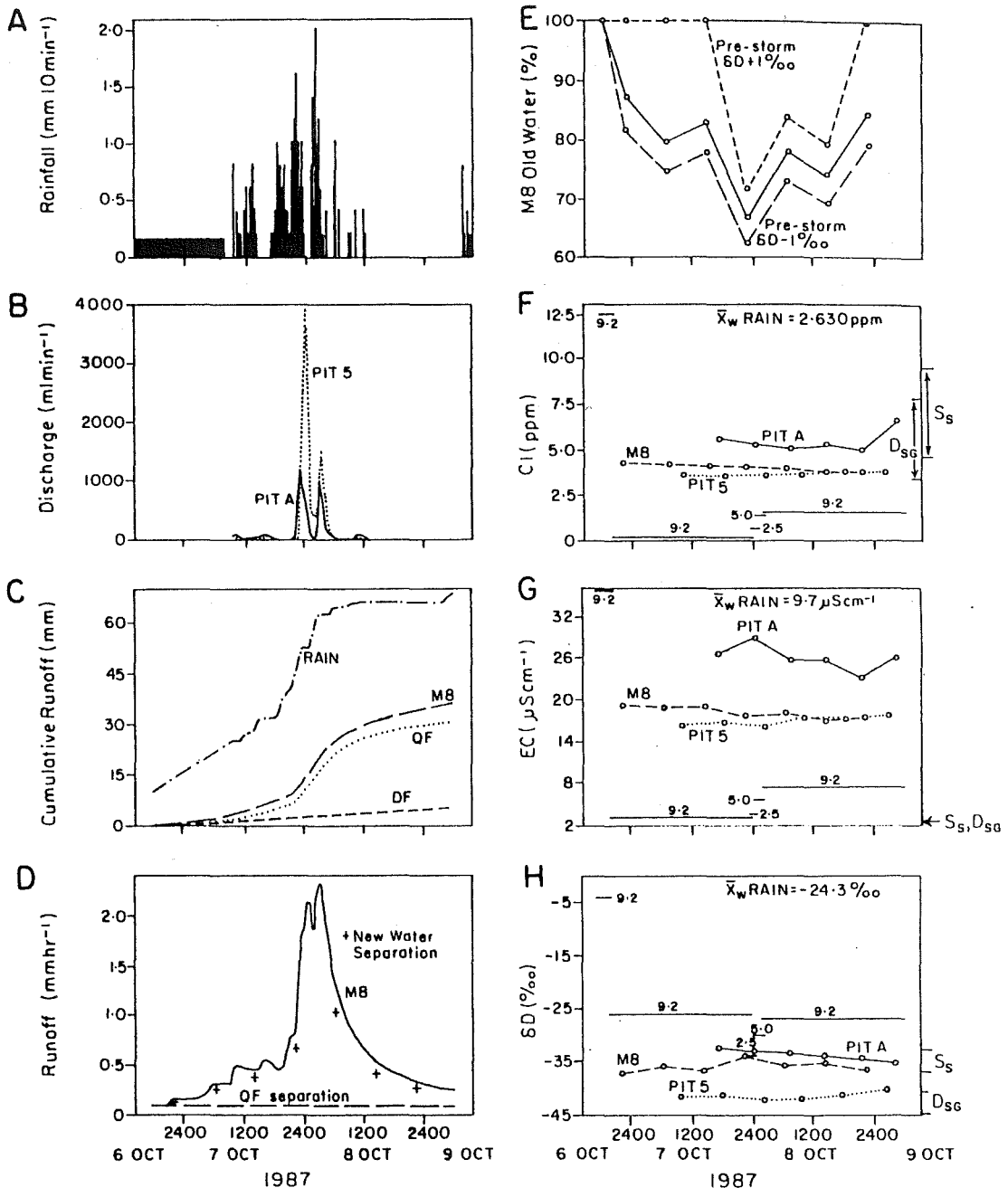

Figure 4.16 Water volume (A-E), chloride (F), electrical conductivity (G) and deuterium (H) relationships for the 07 October event.

inserted into the mass balance calculation. Figure 4.16E shows that only a +/-1°/₀₀ change in pre-storm δD resulted in a +/-5% alteration in peak new water input. More importantly, the shifting of pre-storm δD to a value 1°/₀₀ heavier, caused many of the samples to fall within the +/-1°/₀₀ machine error band, indicating no new water input for much of the event, except during the main hydrograph response 1800 hr 07 October to c.1200 hr 08 October. As a result of these potential errors, cumulative new water discharge (Qn) was not computed.

M8 water chemistry parameters showed very little change through the event. Both Cl and EC showed a gradual decrease in concentration with time (toward rain signatures), but the magnitude of each shift was very low (Cl=0.4 ppm and EC=2.0 μS cm^{-1}). The dilution of Cl and EC indicates some influence of new water on streamwater chemistry, but quantitative estimates are difficult to establish because: (i) a pre-storm sample was not available, and (ii) both Cl and EC are non-conservative, and within storm variations may in fact relate to more complex chemical exchanges, rather than simple two component mixing.

Pit throughflow δD samples were extracted at 7 hr intervals commencing at 1000 hr 07 October for Pit 5 and 1800 hr 07 October for Pit A. Collected samples showed no detectable δD shift through the event. No throughflow occurred prior to the rain event, and therefore no pre-storm samples were available for comparison to subsequent storm samples. Also, no samples were extracted between the time of initial rainfall (1800 hr 05 October) and the first pit samples described above. Pit throughflow was negligible during this period (Figure 4.16B), and δD values would have represented drum storage water rather than any real throughflow.

Pit A peak discharge (4000 ml min^{-1}) occurred at 2400 hr 07 October, with a second peak (c.1500 ml min^{-1}) at 0300 hr 08 October. A water sample was collected at peak flow and showed a δD value of -33.1°/$_{oo}$. If shallow soil water δD (as indicated in Figure 4.16H) is taken as a possible pre-storm δD condition for the pit area, then new water formed c.25% of peak discharge. Pit 5 peak flow coincided with Pit A, but differed in the relative magnitude of each response. In this case, the first response at c.2400 hr (1200 ml min^{-1}) was >3 times less than Pit A, but the second response at 0300 hr (1000 ml min^{-1}) was within 500 ml min^{-1} of Pit A. The magnitude of each response is a function of the upslope contributing area and width of the pit face. Obviously since Pit A face is c.3 times wider, it produces more flow. More importantly, however, Pit 5 response shows increasing input from upslope zones, by its relatively high flow during the second peak. Pit 5 δD response is difficult to interpret, and seems to indicate a δD shift away from storm rainfall and towards deeper groundwater (Figure 4.16H). If the above hydrometric interpretation is correct, then longer residence time deep soil water and groundwater (characteristic of SL3,5,;-44.3 and -43.6°/$_{oo}$ respectively) were displaced by upslope water, undergoing increasing mixing downslope (cf. mechanism described by Sklash et al., 1986).

(c) 13 October Event

The largest rain event of the 1987 study season (return period c.2-5 yr) occurred on 13 October. Ninety-five millimteres of rain fell in two separate bursts, with average rain intensities of 7 mm hr^{-1} (for the first 75 mm burst) and 3 mm hr^{-1} (for the second 20 mm burst; Figure 4.17). API was very high for this event (Table 4.8), and 81 mm of runoff was produced (64 mm in the form of quickflow). Rain δD fluctuated from -25 to

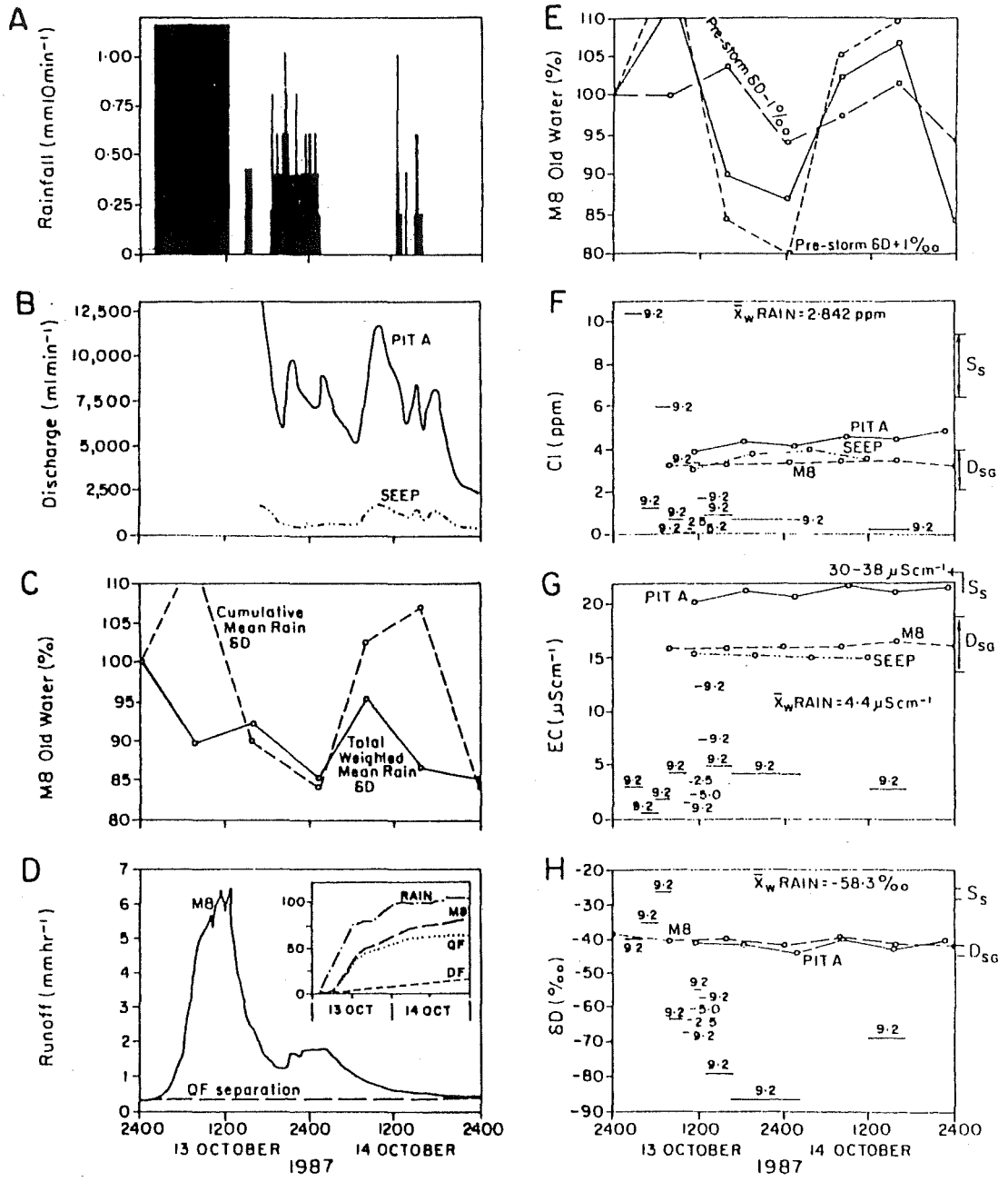

Figure 4.17 Water volume (A-E), chloride (F), electrical conductivity (G) and deuterium (H) relationships for the 13 October event.

-85°/₀₀, with a weighted mean δD of -58.3°/₀₀. Although the first 30 mm of rain was heavier than pre-storm M8 streamflow, the subsequent rain (which produced most of the runoff) was much lighter, making the event suitable for isotopic separation. Instrument failure resulted in loss of all hydrometric data between 0100 hr and 1600 hr 13 October. Rainfall and streamflow data were digitised from existing chart records, but pit throughflow data for this period was not recoverable.

M8 was sampled at 8hr intervals through the event. Peak flow at 1200 hr 13 October was missed, but samples were collected at c.80% peak flow on the hydrograph rising limb and c.40% peak flow on the recession. The second peak (2400 hr) was sampled and showed the maximum δD deflection toward rain δD (-41.6°/₀₀) of all collected samples. Isotopic analysis of the hydrograph rising limb is complicated by large fluctuations in rain δD. Figure 4.17E demonstrates the effect of varying rain δD on estimates of M8 old water percentage estimates. Standard weighting overestimated new water contributions in most cases, especially during the main rising limb, and late recession on 14 October. Using a cumulative weighted mean (discussed fully in Appendix C), better estimates of new water contributions were made by taking into account within storm rain δD variations.

The first three rain δD samples collected averaged -33.8°/₀₀, a value very close to pre-storm M8 δD (-38.7°/₀₀). Mass balance calculations for the 0900 hr sample (Figure 4.17C) show an unrealistic 140% (+/-40%; as per 07 October event discussion) old water input. This value exceeds 100% because M8 δD shifted away from rain δD, possibly indicating increased exfiltration of longer residence time, deep soil water and groundwater (as shown in Figure 4.17H). The next M8 sample showed 10% new water input, and increased to c.15% new water input

during the second smaller hydrograph peak at 2400 hr. These δD values reflect increasingly lighter rain δD. MB Cl and EC variations also showed very little fluctuation in response to distinct rain Cl and EC signatures. Both Cl and EC show a very minor trend toward increases in total concentrations, again reinforcing the notion of negligible new water input (i.e. dilution).

Pit A throughflow response from c.1700 hr onward (i.e. after data loss) showed high discharge rates in excess of 13,000 ml min^{-1}. Peak flow at 2400 hr may have been considerably higher. A pre-storm Pit A δD of $-37^{o}/_{oo}$ was selected for use in the mass balance separation. This value represents Pit A δD on the recession of the 10 October event, and is roughly midway between pre-storm shallow soil water δD and deep soil water and groundwater δD, as indicated in Figure 4.17H. This value is considered possibly lighter than actual pre-storm δD (and therefore apt to underestimate new water), because of the long period of rich δD input on 07 October to 12 October. Results indicate that peak new water inputs (for collected samples) reached 31% at 2300 hr 13 October. Presumably, new water inputs would have exceeded this value at peak throughflow c.1200 hr, possibly by up to 10-20%. Pit A Cl and EC shows a steady increase in concentration through the event, with a slight dilution in the 2300 hr 13 October sample. This corresponds to maximum new water input as defined by the isotopic mass balance, and confirms the increase in new water at this time. The trend toward increasing total solutes, however, does not generally agree with the magnitude of new water response for this storm. Again, non-conservation and lack of data on soil chemistry exchange, limits quantification in this case.

Seep δD was not measured for this event. EC data shows no response to the rainfall input, while Cl concentrations show some increase (<1 ppm) around 2400 hr 13 October. Seep water chemistry generally resembles M8 water chemistry and indicates negligible new water input.

(d) 26 November Event

Forty-seven millimtres of rain fell in two separate bursts on 26 and 27 November. Peak 10 min rainfall intensities in each burst reached c.13mm hr^{-1}, but average intensities were <3 mm hr^{-1} (Figure 4.18). Only 9.8 mm of runoff was produced because of low API conditions (Table 4.8). M8 stream hydrograph response was bimodal and peaked at 0.40 mm hr^{-1} at 1800hr 26 November and 0.68 mm hr^{-1} at 0900 hr 27 November. Approximately 9 mm of quickflow was produced, but QF/P was <20%. The low QF/P value is due partly to the fact that the QF separation line did not intersect the hydrograph receding limb by the end of the event at 0600 hr 28 November. The event was arbitrarily terminated at this point because another rain event commenced at c.0700 hr, producing a separate storm runoff response (named the 28 November event). The events were separated because a >24 hr interval separated major rainfall bursts.

Rain δD fluctuated over 70°/₀₀, but this variation (except for the first 7.5 mm) occurred in the -45 to -105°/₀₀ range, with a weighted mean of -65.8°/₀₀. Although M8 showed some new water input for many of the collected water samples (Figure 4.18D), each was <10%. Peak new water input (8%) occurred during the first hydrograph peak. The second hydrograph peak showed only 4% new water. Again, in this storm, potential errors introduced through pre-event M8 δD selection caused large relative error in new water estimates (as shown in Figure 4.18E). M8 water chemistry showed little variation through the event and supports

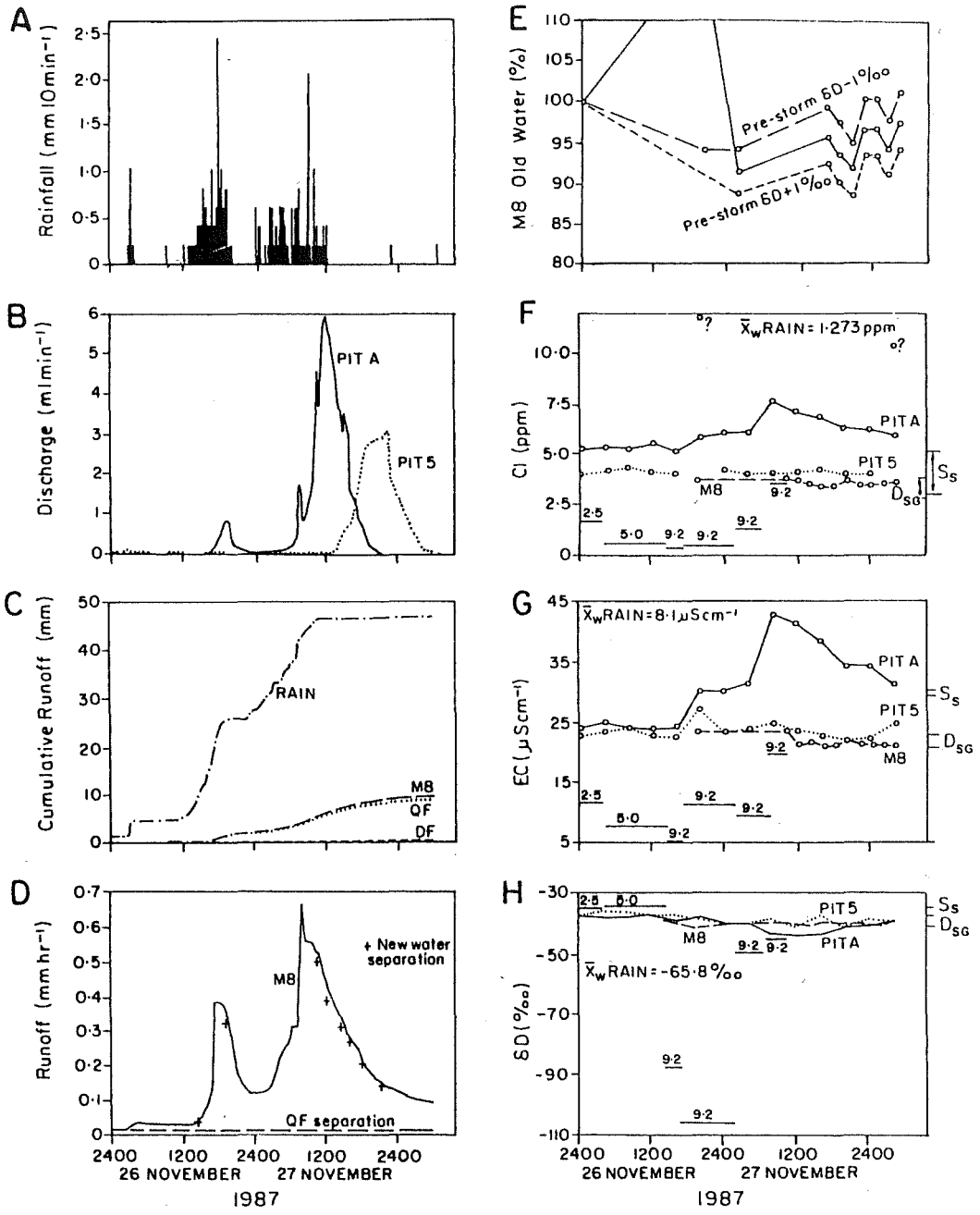

Figure 4.18 Water volume (A-E), chloride (F), electrical conductivity (G) and deuterium (H) relationships for the 26 November event.

the δD interpretation of only a small new water input. Water chemistry data implies some new water input during the second hydrograph response. Without a pre-storm sample, both Cl and EC fluctuations are difficult to quantify, but it appears that dilution of M8 Cl and EC concentrations occurred immediately following peak flow at 1400 hr 27 November. Cl concentration returned to a pre-response value (c.3.8 ppm) after deflection toward rain Cl, but dilute M8 EC concentrations persisted for the duration of the event.

Pit A throughflow peak (600 ml min^{-1}) coincided with the second streamflow peak, while Pit 5 throughflow peak (3000 ml min^{-1}) lagged Pit A by c.12 hr (Figure 4.17B). Pit A showed a large δD deflection from pre-storm δD (c.-37‰) toward rain δD, and peak new water input reached 25%. Pit A water chemistry showed large increases in Cl concentration and EC, indicating increased total solute concentration. Although both of these shifts were away from rain chemistry values, they may indicate the flushing of high Cl and solute-rich soil water, that had been enriched during evaporative conditions preceding the event. As noted earlier, API conditions were low, and warm summer temperatures would have promoted increased evaporative flux, particularly in exposed upslope locations. Pit 5 throughflow δD showed c.14% new water at peak flow. Pit 5 water chemistry showed very little change through the event and mirrored M8 Cl and EC concentrations.

4.5 SUMMARY

Within storm variability of rainfall δD for monitored 1987 events showed strong correlation with air mass trajectory. Variations between events produced measureable variability in subsurface soil water and groundwater during weekly suction lysimeter surveys. The subsurface reservoir in the M8 catchment

is not fully mixed, and the residence time of subsurface water (and its resulting δD value) increases both in a downslope and down-profile direction. Mean ages for shallow soil water in upslope positions averaged around 2 weeks, and increased to >100 days in the downslope and near-stream zones. Long-term (August to December 1987) rainfall δD signatures followed a semi-sinusoidal pattern. Soil water and groundwater signatures followed this pattern, but with measureable lags and dampening of the relative δD shift, with increased soil depth and distance from the catchment divide.

During rain events, MB streamflow response showed negligible flushing of new water. Large within storm rainfall δD shifts were dampened within the soil profile, and showed virtually no effect on channel δD values. Of the 11 intensively monitored events, 2 showed no shift in channel δD from pre-storm values, 5 were unable to be analysed using the mass balance approach because rain δD equalled pre-storm stream δD, and 4 events showed some new water flushing (5-15%). Collected throughflow from the upslope (Pit A), mid-slope (Pit 5) and downslope (Seep) pits showed a progressive decrease in new water inputs with distance from the catchment divide.

5 PATHWAYS OF SUBSURFACE RUNOFF - SOIL PROPERTIES AND SOIL PHYSICS CONSIDERATIONS

5.1 SOIL PHYSICAL CHARACTERISTICS AND HYDROLOGICAL PROPERTIES

5.1.1 Forest floor

Detailed analysis of forest floor characteristics was not conducted in this study. Data from Webster (1977), however, provides a surrogate measure of forest floor characteristics and their potential hydrological properties in the M8 catchment.

The depth of forest humus in M8 varies from 0 to 25 cm and is characterised by an open, fibrous structure, high porosity and high variability in physical properties over very short distances. Webster (1977) showed that average bulk densities and porosities are roughly 0.14 g cm^{-3} and 86% respectively. Water retention tests conducted by Webster showed that the forest floor was capable of retaining large quantities of water. Much of the water above its field capacity of 45% by volume, was held in large macropores which drained readily at low suction (0-20 cm H_2O). The K_{sat} of the forest floor is very high 720 mm hr^{-1} and field tests conducted by Webster (1977) showed that the mean infiltration rate of the forest floor (6,120 mm hr^{-1}) is high enough to absorb even the most intense rainfall bursts.

Hydrologically, the forest floor represents an important reservoir and pathway for subsurface water movement. If the average humus layer depth in the M8 catchment is considered to be 17 cm, and maintains a mean water content of 45% by volume, then the maximum depth of water which may be held in the forest floor, overlying the mineral soil, is 77 mm (or a total of 2950 m^3 of water in the M8 catchment). Because much of the water above field capacity is held by large macropores (which drain at low suctions), any excess rainfall added to the forest floor during a storm event, should therefore drain quickly through the organic

layers. In this respect, only small, temporary changes in water storage would be produced, and Webster (1977) characterised the humus layer as behaving like a large sponge.

5.1.2 Mineral soil macropores

Mosley (1982) identified preferential flow paths at vertical pit faces in the Maimai catchments for a number of dyed water injection experiments (Figure 5.1). Assuming that the vertical faces are acceptable samples of the whole soil profile, Mosley's observations show that there are preferred pathways for flow, along cracks and holes in the soil and along live and dead roots and root channels (macropores). He assumed that all paths shown in Figure 5.1 are active at each pit location, but that their relative importance varies substantially. For instance, Mosley noted that pathways 3 and 7 were dominant for rapid outflow at one particular site, but because only 18% of the input volume appeared as rapid outflow, it seemed that pathways 4 and 5 were followed by the bulk of the water. At another pit site, Mosley found that 40% of the input water passed rapidly through the soil via pathway 6, with the remainder following the other pathways, in particular pathways 4 and 5. Mosley (1982, p.77) concluded that "in view of the great variability from site to site, it was not feasible to quantify the relative importance of the pathways."

(a) Operational definition for this study

Although Mosley's work was rudimentary, he provided visual evidence of macropore flow of dyed water at a pit face. These observations are verified in this study by experiments discussed in section 6. Whipkey (1967) and Aubertin (1971) have also used these simple techniques to identify preferred flow pathways in forest soils. In other investigations of preferential flow along macropores in agricultural soils, various techniques have been

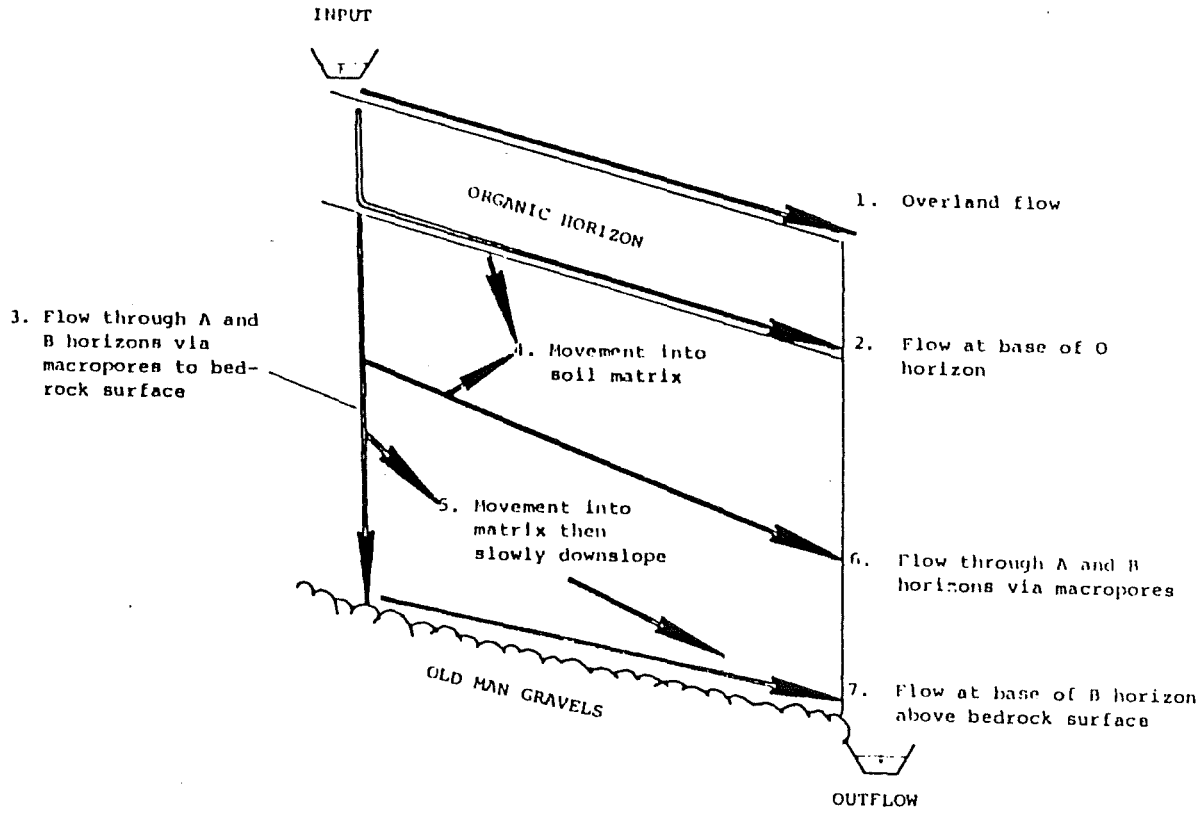

Figure 5.1 Flow pathways identified by Mosley (1982) during dyed water injections at a pit face (from; Mosley, 1982).

used to quantify macroporosity, including: laboratory (Germann and Beven, 1981) and field (Bouma et al., 1981), soil block drainage, tension infiltrometers (Clothier and White, 1981; Wilson and Luxmoore, 1988), and micromorphometry or image analysis (Bouma et al., 1977; 1979; Ringrose-Voase, 1987).

Beven and Germann (1982) noted that the definition of macropore size classes is quite arbitrary and does not necessarily relate to flow processes. Table 5.1 lists some of the size definitions used by various researchers. Recently, Luxmoore (1981) designated three size classes for pores, macro- (>1000 μm), meso- (10-1000 μm) and micro- (<10 μm), where the micropore class corresponds to the soil matrix. In addition to pore size, however, pore structure (including continuity and connectivity) is also of crucial importance to the effective definition of a macropore (Bouma, 1981). As a result, terms such as preferential pathways or macrochannels have been suggested to emphasise the importance of structure on flow dynamics. Bouma et al. (1977) have shown that different numbers and sizes of macropores may be effective under different conditions. Therefore, a relevant definition of macropores for solute infiltration in a ploughed field, may be different to a relevant definition for subsurface flow in a steeply sloping hillslope.

In this thesis, only those pores which are hydrologically effective in terms of channelling flow through the soil and contributing to rapid subsurface flow are of principal concern. In M8 soils, any pore >60 μm may be considered a macropore. This will consist of interaggregate pore space, discontinuous worm or root channels, discontinuous cracks, continuous cracks from the soil surface to the mineral soil base and lateral pipes at the soil-bedrock interface. Local M8 catchment conditions are different to many other areas where macropores have been

identified, because: (i) the soil mass is steeply sloping (average 25° to 40°), (ii) the soil is shallow (average 60 cm) and underlain by impermeable bedrock, (iii) the soil profile is drained at its base by a continuous piping system, and (iv) soils remain within 10% of saturation for most of the year.

Table 5.1. Some definitions of macropores and macroporosity (modified after Beven and Germann, 1982).

Data Source	Matric Potential cm H_2O	Diameter μm
Nelson and Baver, 1940	>-30	
Marshall, 1959	>-100	>30
Brewer, 1964		
Coarse macropores		5000
Medium macropores		2000-5000
Fine macropores		1000-5000
Very fine macropores		75-1000
McDonald, 1967	>-60	
Ranken, 1974	>-10	
Webster, 1977	>-50	
Bullock and Thomasson, 1979	>-50	>60
Reeves, 1980		
Enlarged macrofissures		2000-10000
Macrofissures		200-2000
Luxmoore, 1981	>-3.0	>1000
Beven and Germann, 1981	>-1.0	>3000
Clothier and White, 1981		>750
This study		
Pipes		3000-10000
Cracks		1000-3000

As a result of these conditions, the most hydrologically important macropore types in M8 are considered to be continuous pipes (pathway 7 in Figure 5.1) and cracks (pathway 3 in Figure 5.1), as described below. The dependence of flow rate on the fourth power of the pore radius means that while the presence of these cracks and pipes may make only a very minor contribution to the total soil porosity, nearly all the rapid flow (at or near saturation) is through these channels (Bouma and Anderson, 1973; Scotter, 1978).

(b) Pipes and pipeflow

Evidence from a number of recent field monitoring programmes, particularly in the U.K., has shown that pipeflow can be a substantial contributor to storm quickflow (Jones, 1979; McCaig, 1983; Wilson and Smart, 1984; Jones, 1987). In the M8 catchment, pipes occur at the mineral soil-Old Man Gravel interface and extend laterally downslope over distances of several 10s of metres (Mosley, 1979). This conclusion is supported by the visual observations in this study of pipe outflows at pit faces, along the banks of 1st order channels (Figure 5.2) and by the fact that hillslope runoff increases rapidly in a downslope direction. Conditions that promote pipe development in the M8 catchment seem to relate to: (i) shallow soil depth, (ii) underlying impermeable bedrock, and (iii) root growth and decay.

Large roots extend vertically through the shallow mineral soil (average 60 cm depth), but cannot penetrate the underlying conglomerate. Roots then extend laterally over the conglomerate surface (P. Tonkin, personal communication, 1988) for up to several metres. Watson (1988, unpublished data) has shown that maximum lateral length of 25-year-old P. radiata root systems in Mangatu Forest, North Island, New Zealand is 10.4 m. Pipes formed in this manner and by subsequent decay of root networks may be enlarged by eluviation. Conditions promoting this process in the M8 catchment would include: high rainfall, rapid movement of infiltrating water to depth (discussed below), steep slopes and high hydraulic gradients, potentially dispersive soil at the mineral soil base and the presence of pipe outlets at the 1st order channel bank.

As a result of this process, a well-connected pipe network has become established in M8, which conducts a large percentage

Figure 5.2 Pipe outflows identified along the bank of a 1st order channel in the M8 catchment.

of subsurface stormflow. From limited visual observations at pit faces and along 1st order stream banks, pipes range from 3-100 mm in diameter.

(c) Cracks and bypass flow

In well-structured soils like the clay-rich mottled and gleyed soils in the the M8 hollows, flow through continuous cracks, defined as channelling (Beven, 1981), short-circuiting (Bouma et al., 1981) or bypassing (Smettem et al., 1983; Van Stiphourt et al., 1987), may result in a deeper penetration of rainfall and solutes than is predicted by uniform displacement (Thomas et al., 1978). The term 'bypass flow' will be used in this thesis to describe the vertical movement of free water along continuous cracks (from the mineral soil surface to its base), through an unsaturated or partially saturated soil matrix.

The rate and occurrence of bypass flow will be determined by: (i) total rainfall depth and intensities, (ii) pre-storm soil moisture content, and (iii) soil matrix K_{sat}. Bypass flow is a two-domain flow process, whereby water movement in vertical cracks is driven by gravity, independent of the soil matrix, in which flow is driven by both gravity and matric (especially capillary) forces. Germann (1986) gives an example of this two-domain flow process. A bacterial transport model based exclusively on matrix flow concepts, predicted the advancement of the micro-organisms to a maximum depth of 0.2 m, and the time required to reach that depth was more than 2 weeks. In contrast to these results, Smith et al. (1985) observed the arrival of the bacteria at 0.28 m depth in well-structured soil columns within 17-50 min after the microbial suspension had been applied to the soil surface. The discrepancy clearly indicates that "flow processes different from matrix flow are to be expected under certain input and soil conditions" (Germann, 1986, p.3).

At the Pit 5 site, soil was excavated upslope from the pit face to identify any vertical cracking. Regularly-spaced vertical cracks, roughly 1-3 mm wide, were observed extending from the mineral soil surface to the Old Man Gravel interface. These cracks showed signs of organic staining along their walls and fine 'hair-like' root structures along their entire length. This evidence, together with dye tracer experimental results (discussed in section 6), suggest that water regularly moves through these channels. Maimai soils, while never significantly dropping below 90% saturation, do occasionally encounter dry periods (of about 3 weeks), when surface cracking can occur (P. Tonkin, personal communication, 1988). In many hillslope hollow zones, upper mineral soils are organic-rich, particularly in mid-slope hollows. Mineral soil surfaces in some situations develop hydrophobicity, which increases the susceptibility to surface cracking.

5.1.3 Pit face mineral soil matrix characteristics

(a) Bulk density and porosity

Soils were sampled at the near-stream, Pit 5 and Pit A sites. In each case, samples were biased toward stone-free and root-free portions of the horizon, because of sampling difficulty. Much of the profile at each site was stoney, and therefore proper undisturbed cores were difficult to extract. Horizon boundaries at each site were distinct, and the Old Man Gravel surface formed an impermeable underlying layer.

Soil depth at the Pit A face was 45 cm, and textural and structural variability was very high. Two horizons overlying the Old Man Gravel surface were identified:

OH horizon 0-18 cm
dark brown fibrous humus
many small roots

B_{2g} horizon 18-45 cm

light grey strongly gleyed silty clay

many 0.5-1.5 cm clasts, with stained exterior surfaces

Three core samples were taken at 25 cm depth, using the technique described in section 3.2.5. The 25 cm depth was the only portion of the profile where clasts could be avoided. Over 10 core extractions were attempted before 3 proper cores were taken.

Soil depth at the Pit 5 face was 135 cm and again textural and structural variability was high. Three horizons overlying the Old Man Gravel surface were identified:

OH horizon 0-30 cm

dark brown fibrous humus

many small roots

A_{2g} horizon 30-60 cm

medium brown silt loam

medium granular structure

B_{2g} horizon 60-135 cm

dark yellow brown silty clay

medium granular/crumb structure

Three cores were easily extracted at 36 cm depth below the surface (called Pit 5 upper). Three additional cores were extracted with some difficulty at 105 cm (called Pit 5 lower).

A soil pit was dug at the near-stream recording tensiometer site, 7 m from the stream channel. Soil was excavated down to the Old Man Gravel surface. Soil depth was 48 cm, with 29.5 cm of moderately gleyed and 18 cm strongly gleyed soil. Three horizons overlying the Old Man Gravel surface were identified:

OF horizon 0-0.5 cm

decomposing leaves

B_1 horizon 0.5-30 cm

dark grey moderately gleyed silty clay

B_{2g} horizon 30-48 cm

light grey strongly gleyed silty clay

many 0.5-1.5 cm clasts embedded in matrix

Three soil cores were extracted at 25 cm (called near-stream upper), and 3 additional cores were extracted at 40 cm. All cores were difficult to extract (similar to Pit A), because of profile stoniness.

Table 5.2 lists the average bulk density and porosity values obtained from the analysis described in section 3.2.5. Particle-size analysis was not performed because of the high variability in soil characteristics both vertically through the profile and areally through the catchment. From data in McKie (1978), it can be inferred that Pit 5 and Pit A sand-silt-clay percentages are very roughly 55-25-20% (Pit 5) and 25-30-45% (Pit A). The values listed in Table 5.2 are interpreted with caution, bearing in mind the limitations associated with the data in terms of core representativeness of general profile conditions.

Pit A and the lower near-stream site showed moderately high bulk densities (1.2-1.5 g cm^{-3}) and low porosities (44.7-62.7%), indicative of a clay-rich, poorly drained matrix. The Pit 5 upper and lower zone showed much higher porosities (77-79.6%) and exceptionally low bulk densities (0.5-0.6 g cm^{-3}), reflecting an aggregated soil structure with high organic content. At each location, porosity decreased and bulk density increased with depth.

The low bulk density values at the Pit 5 site may reflect the disturbing influences of long-term subsurface water exfiltration at the pit face. The pit was orginally excavated in 1978, and therefore soil structural conditions at the pit face may have altered over the subsequent decade. A fresh face at the

Table 5.2. Soil properties at selected sites within the M8 catchment.

Location	Depth cm	Bulk Density g cm^{-3}	Porosity %
Pit A	25	1.5 (0.2)	44.7 (8.3)
Pit 5 Upper	36	0.5 (0.1)	79.6 (4.2)
Pit 5 Lower	105	0.6 (0.1)	77.0 (2.5)
Near-stream Upper	25	1.0 (0.1)	62.7 (2.7)
Near-stream Lower	35	1.2 (0.1)	53.3 (3.2)

() Indicates standard deviation

Pit 5 site was excavated roughly 10 cm upslope of the orginal face excavated in 1978, but this may not have been far enough away for a true representation of in situ subsoil bulk density. Another possible explanation for the low bulk density values obtained relates to 'infilling' of former macropores. McKie (1978) also observed low bulk density values in many Maimai soil samples. P. Tonkin (personal communication, 1988) notes that this may be due to soil development where a macropore has been filled with soil during colluvial processes on the hillslope.

(b) Moisture release characteristics

In this study, pore size distributions of extracted cores were not computed because of biases in sampling outlined above, and because of the influence of local soil structural characteristics. Large, well-spaced macropores are not reliably sampled by small cores. Even if they could be adequately sampled, the biggest macropores would give up water at only a few centimetres of suction, and so may not be detected by the tension tables. The drainage curves shown in Figure 5.3 represent results from measurements on samples considered representative of capillary pore space of the soil matrix. Any holes, cracks,

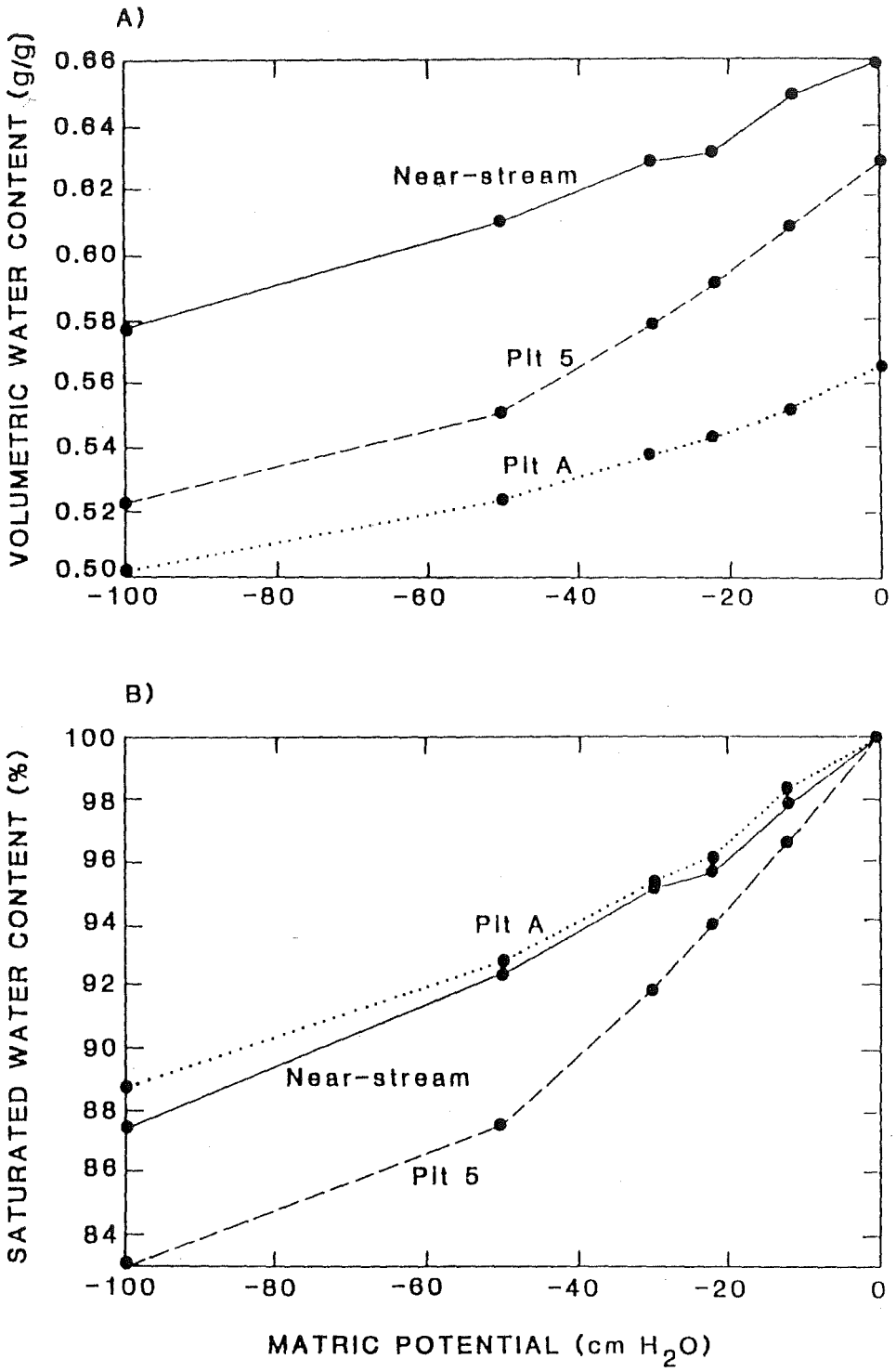

Figure 5.3 Moisture release characteristics for selected M8 soils.

exposed root channels or organically-stained cracks were avoided during core extraction.

Average soil moisture release curves for the Pit A, Pit 5 and near-stream zone are shown in Figure 5.3. Separate replicate cores were taken for this analysis on a subsequent site visit. Only one depth was sampled for each site because of sampling difficulty and previous site disturbance from core extraction. Three replicate cores were extracted from the Pit A, Pit 5 and near-stream site (as described above), at 25, 70 and 35 cm depths below the surface respectively. Again, these cores (and resulting moisture release curves) are biased toward the stone-free and root-free part of the soil horizon. In addition, these cores are probably atypical of much of the profile, simply because of sampling bias. Tension-table measurements (as described in section 3.2.5) were only conducted in the 0 cm H_2O to -100 cm H_2O range, since ψ in all sites in M8 rarely went beyond -100 cm H_2O, even under dry antecedent conditions.

Porosity and bulk density values for the cores extracted for moisture release information are shown in Table 5.3. Pit A and near-stream zones showed very similar results to those in Table 5.2 for similar profile depths. Pit 5, however, showed considerable divergence between the two sets of measurements, with approximately 10% lower porosity and 0.3 g cm^{-3} higher bulk density values for the second sampling run. This may relate to pit face conditions outlined above. Cores extracted for moisture release determination, were sampled 2 months after the initial samples (used for Table 5.2 measurements) were extracted. The Pit 5 face was re-excavated another 20-50 cm upslope before cores were extracted. The second set of cores is probably more representative of actual subsoil conditions.

Table 5.3. Soil properties of cores taken for moisture release information.

Location	Depth cm	Bulk Density g cm^{-3}	Porosity %
Pit A	25	1.5 (0.004)	42.6 (0.2)
Pit 5	70	0.9 (0.05)	67.5 (1.9)
Near-stream	35	1.3 (0.06)	52.1 (2.3)

() Indicates standard deviation

Starting at 0 cm H_2O, decreasing ψ overcomes capillary forces maintaining saturation and the largest pores drain, followed by successively smaller and smaller pores. In each case, the slope of the ψ-θ line is steepest during the initial drainage stage (0 cm H_2O to -50 cm H_2O), which represents drainage from capillary pores >60 μm in diameter (Gradwell, 1978; Danielson and Sutherland, 1986). It is assumed here that the extracted cores have a roughly similar capillary pore-size distribution to that quoted in Gradwell (1978) for Southern yellow-brown earths, where: pores draining in the ranges 0 to -50 cm H_2O and -50 to -100 cm H_2O constituted respectively 6.2% and 1.0% of the total soil volume for the middle subsoil region. Degree of saturation (θ_m) versus ψ is plotted in Figure 5.3B. In this case, θ_m is >87% (in the 0 to -100 cm H_2O range) for the near-stream and Pit A sites. The Pit 5 soil core shows a lower θ_m for the complete drainage curve, but especially at ψ<-20 cm H_2O. This possibly relates to the low bulk density at the Pit 5 location and highly aggregated soil structure.

In terms of capillary-fringe characteristics, M8 soils do not exhibit the horizontal tension-saturated zones characteristic of other soils like silt loams or fine sands. Nevertheless, it should be noted that matric potential will be highly sensitive tc water addition, because of the small differential water capacity,

or 'limited storage effect'. The effects of this phenomenon will be discussed in the following sections on tensiometric response to storm rainfall.

5.1.4 K_{sat}-topographic relationships

Six K_{sat} measurements were conducted, using the methodology outlined in section 3.2.4, in different slope positions within the M8 catchment. Vertical K_{sat} measurements are assumed to be equivalent to horizontal K_{sat} at each location. Although this cannot be so on a large scale if macropore geometry is anisotropic between vertical and horizontal (as suggested in the previous sub-section), it may be approximately so on the small scale of measurement of a Guelph permeameter, if macropores are not intercepted by the wetted volume.

Table 5.4 shows that K_{sat} varies over 2 orders of magnitude between hollow (location 1 and 4) and nose (location 3 and 6) sites, which have mean values (and standard deviations) of 2 (1) mm hr^{-1} and 210 (140) mm hr^{-1} respectively. These values are within the range of laboratory permeameter K_{sat} results for 20 samples (topographic location unknown) listed in Webster (1977). Her K_{sat} values ranged from 5.4 to 583.2 mm hr^{-1} with a mean value of 265 mm hr^{-1}. Clearly these samples were biased toward

Table 5.4. M8 K_{sat} variability for different slope positions (cf. Table 3.1).

Location	K_{sat} mm hr^{-1}
1. Upslope hollow	3
2. Upslope ridge	119
3. Mid-slope nose	141
4. Mid-slope hollow	2
5. Mid-slope side-slope	8
6. Lower slope nose	370

sideslope and nose slope zones, as indicated by the mean value; however, they verify the range of values obtained in this investigation. The effect of K_{sat} variability on the rates and direction of water movement in the catchment is addressed in section 7.2.5.

5.2 NEAR-STREAM TENSIOMETRIC RESPONSE TO STORM RAINFALL

Tensiometer numbers and porous cup depths for the near-stream location are shown in Figure 5.4. Depending on local soil depths, tensiometers were installed at depths of approximately 15, 40 and 80 cm. These depths were rarely achieved and were adjusted if roots or stones interfered with augering. Site numbers are also shown, and will be referred to in the following discussion on tensiometric response to storm rainfall.

Tensiometer porous cups were embedded in the soil matrix (away from cracks and pipes) and are assumed to provide information on soil matrix conditions only. By combining the soil matric potential data with storm rainfall, streamflow and hillslope discharge, inferences may be made regarding the nature of subsurface flow. Soil physics considerations are aimed at identifying the rate of development and longevity of the water-table, hydraulic gradients and resulting subsurface water movement. Macropore flow in cracks and pipes, while not directly related to tensiometric response to storm rainfall, can be inferred from soil profile wetting patterns and hillslope discharge. The following three storms are discussed in detail: a low magnitude rainfall on 24 October, a moderate magnitude rainfall on 29 October and a high magnitude rainfall on 13 October.

5.2.1 Low magnitude rainfall: 24 October event

A 12-hr 25-mm rainfall event occurred on 24 October, with

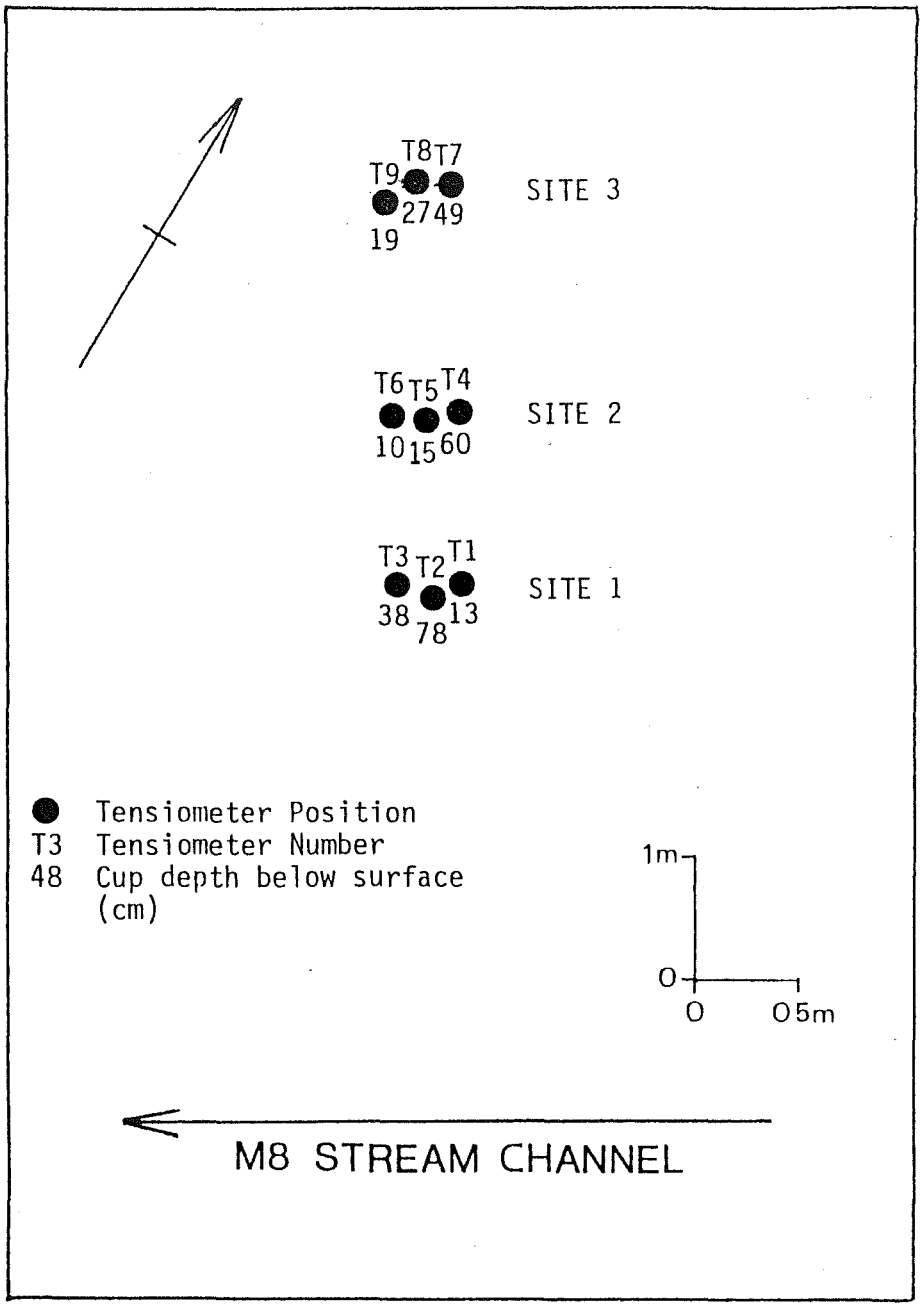

Figure 5.4 Tensiometer numbering and porous cup depths for the near-stream site.

6 mm hr^{-1} peak 10 min rainfall intensity. Rainfall-runoff relationships are shown in Figure 5.5 and illustrate a rapid hydrograph rise followed by a steep recession. A bimodal stream hydrograph was produced because of a second burst of rainfall at 0600 hr. A total of 6.4 mm of runoff was produced, 80% of which was in the form of quickflow. Antecedent conditions were relatively dry and API_7 and API_{14} were 0 and 14.6 mm respectively. Pit throughflow response lagged behind stream response, in which both Pit A and Seep peak discharge (6000 ml min^{-1} and 160 ml min^{-1} respectively) coincided with the second hydrograph peak.

Soil matric potential is plotted as a continuous function of time for tensiometric Sites 1-3 (Figure 5.5). Each site responded rapidly to the rainfall input, and peak ψ coincided with the second peak streamflow response. At all sites, vertical unsaturated drainage had occurred prior to the event, and the complete soil profile was unsaturated, with no detectable water-table at depth. Each site showed very similar ψ response characteristics and maintained constant low magnitude water potentials (-20 to 55 cm H_2O) for over 24 hr after the event, indicating further drainage through this zone from upslope areas.

For the rest of this 24 October event discussion, 5 arbitrary time intervals are examined in detail: 1800 hr 23 October (t_0), 2200 hr 23 October (t_1), 0230 hr 24 October (t_2), 0830 hr 24 October (t_3), and 1200 hr 25 October (t_4). At Site 1 (Figure 5.5D), rate of ψ response decreased with depth below the surface. T1 (13 cm) responded very rapidly and shifted from a pre-storm ψ of -70 cm H_2O to approximately -10 cm H_2O for the duration of the event. T2 (78 cm) and T3 (38 cm) peaked around 9 hr after T1 and showed a slower rise to peak. At Site 2, ψ response characteristics followed a similar pattern to Site 1,

Figure 5.5 Rainfall-runoff relationships and near-stream tensiometric response for the 24 October event.

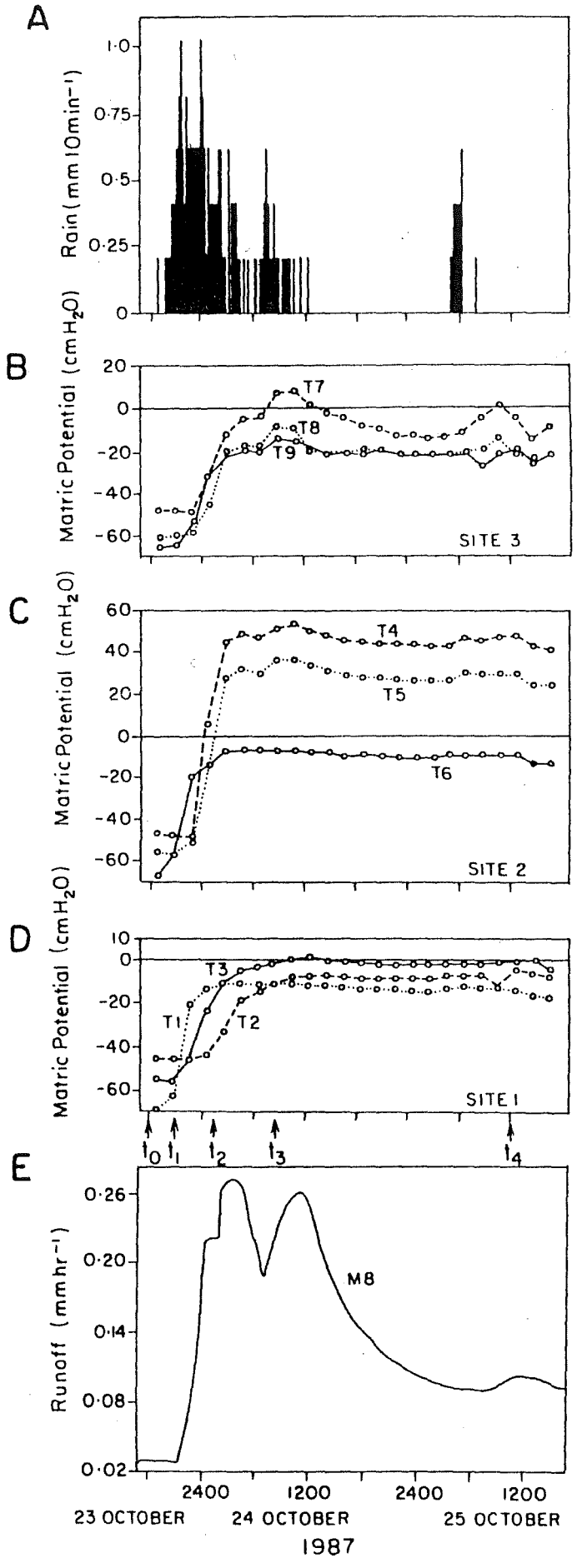
A
Rain (mm 10min⁻¹)
1·0
0·75
0·5
0·25
0
B
Matric Potential (cmH2O)
20
0
-20
-40
-60
T7
T8
T9
SITE 3
C
Matric Potential (cmH2O)
60
40
20
0
-20
-40
-60
T4
T5
T6
SITE 2
D
Matric Potential (cmH2O)
10
0
-20
-40
-60
T1
T2
T3
SITE 1
t0 t1 t2 t3 t4
E
Runoff (mm hr⁻¹)
0·26
0·20
0·14
0·08
0·02
M8
2400
1200
2400
1200
23 OCTOBER
24 OCTOBER
25 OCTOBER
1987

with some ψ lag with depth. Unsaturated conditions before the event were rapidly changed to positive ψ for tensiometers T4 (60 cm) and T5 (15 cm), between time t_0 and t_2. At Site 3, ψ response to rainfall was lagged with depth down through the soil profile, and showed a significant decline after peak ψ at t_3. These changes resemble stream hydrograph changes, suggesting that Site 3 may be characteristic of much of the stream response, while Sites 1 and 2 are transmission zones which translate the slope base subsurface water to the stream channel.

Figure 5.6 shows matric potential plotted as a function of depth at different times during wetting (t_0-t_3) and drainage (t_4). Strong flow conditions were produced during the main wetting period, with mainly lateral moisture potential gradients. At Site 1, readings are consistent with a wetting front propagating downward between t_0 and t_1. From t_2 onward, tensiometers in the lower profile (especially T2 at 78 cm) responded rapidly, as available storage was filled and perched water-table conditions developed at the mineral soil-Old Man Gravel interface.

At Site 2, soil depths were shallower than Site 1, and a water-table was developed to within 20 cm of the soil surface (Figure 5.6). This was maintained throughout the event and for >24 hr following streamflow recession. Downward wetting front propagation may be detected between t_0 and t_1, but thereafter, lower tensiometers responded higher than expected, due to a rising groundwater table. After t_2, matric potential versus depth relationships approached unit gradient, resulting in a change from vertical to lateral flow. Water-table elevation at Site 3 was sensitive to rainfall input. At times t_2-t_4, the water-table shifted from 70 cm (extrapolated) to 40 cm and back to 53 cm respectively. Near unit gradients were maintained and most flow

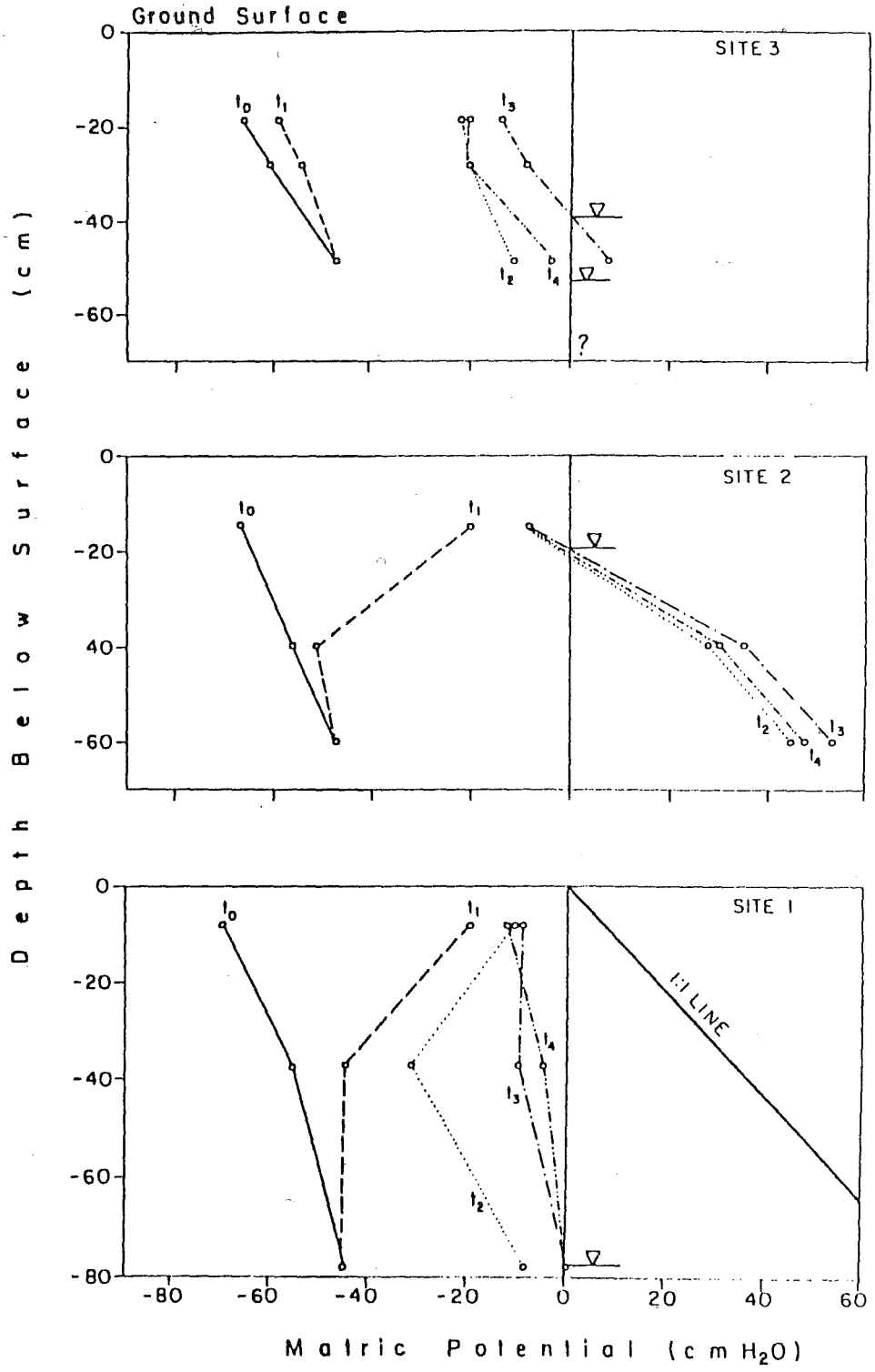

Figure 5.6 Near-stream matric potential versus depth below surface for the 24 October event.

was laterally downslope. The longevity of the water-table in the near-stream zone was maintained by further drainage from upslope zones and because of the effect of the underlying impermeable bedrock.

Total potential (ϕ) contours for the near-stream cross-section (Sites 1-3) are plotted with possible flow lines in Figure 5.7. Total potentials are computed from equation 2.2, with the stream channel bed as a zero datum. The flow lines are drawn normal to the equipotential lines. Figure 5.7 and subsequent plots of ϕ contours are drawn with vertical exaggeration of between 2 and 4. Although this enables a more detailed view of water-table fluctuations, it distorts slightly the actual ϕ contour angle. With this in mind, lateral flow through both the saturated and unsaturated zones prevailed before, during and after the event, with some increase in the downward component near the channel. Total potential gradients increased (i.e. equipotential lines became more closely spaced) with depth, as a water-table developed (especially at Site 2).

5.2.2 Moderate magnitude rainfall: 29 October event

Fifty-eight millimetres of rain fell during two short intense bursts on 29 October, with peak 10 min intensities in the order of 14 mm hr^{-1}. Streamflow response was rapid and peak specific discharge was 3 mm hr^{-1} (Figure 5.8). Thirty millimetres of runoff was produced, 29 mm of which was in the form of quickflow. API_7 and API_{14} were relatively high (4.7 mm and 5.0 mm respectively) and QF/P was 50%. The stream hydrograph had fully recovered from the preceding 24 October event, and baseflow conditions were maintained prior to rain input. Pit A throughflow response mirrored that of the main channel, and produced a peak discharge of 1250 ml min^{-1}. Seep discharge peaked 3.5 hr after both Pit A and the main channel. Peak flow was only

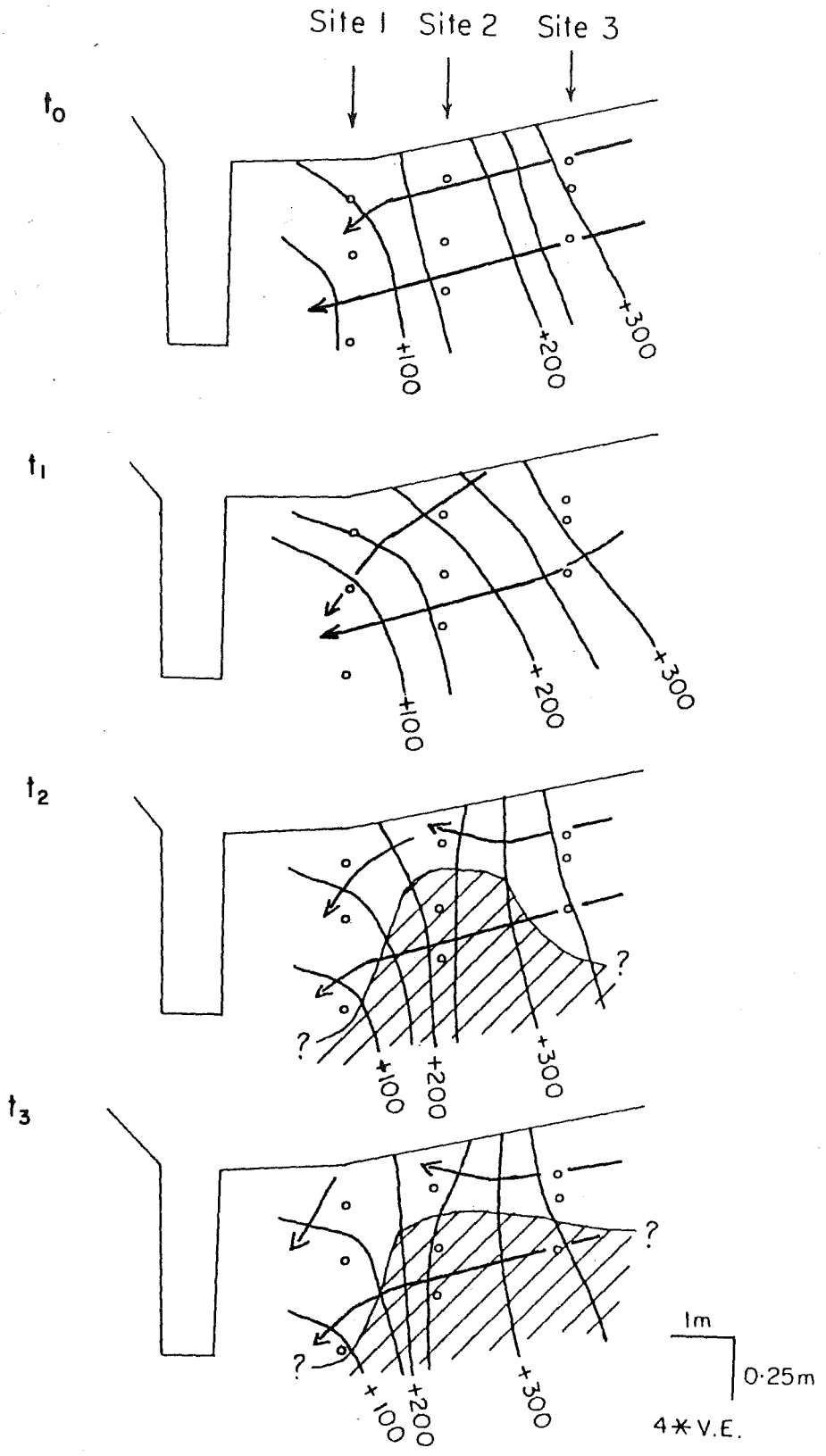

Figure 5.7 Flow lines and total potential in the near-stream cross section.

Figure 5.8 Rainfall-runoff relationships and near-stream tensiometric response for the 29 October event.

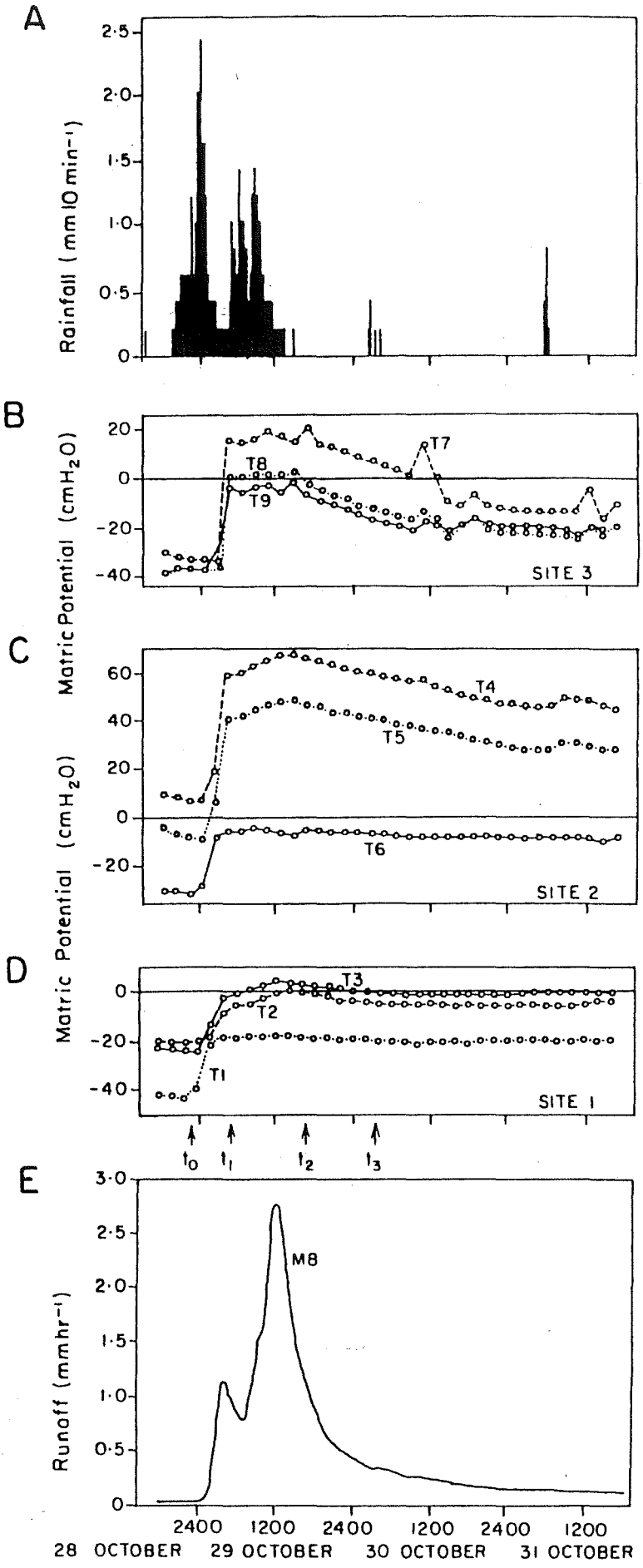
A
Rainfall (mm 10 min⁻¹)
2·5
2·0
1·5
1·0
0·5
0
B
Matric Potential (cmH2O)
20
0
-20
-40
T7
T8
T9
SITE 3
C
Matric Potential (cmH2O)
60
40
20
0
-20
T4
T5
T6
SITE 2
D
Matric Potential (cmH2O)
0
-20
-40
T3
T2
T1
SITE 1
t0
t1
t2
t3
E
Runoff (mmhr⁻¹)
3·0
2·5
2·0
1·5
1·0
0·5
0
M8
2400
1200
2400
1200
2400
1200
28 OCTOBER
29 OCTOBER
30 OCTOBER
31 OCTOBER

12.5 ml min^{-1}, and the hydrograph shape showed an extremely steep rise and recession.

Tensiometric response in the near-stream zone was very similar to the 24 October event, except that initial ψ was less negative, reflecting wetter antecedent conditions. Pre-storm ψ ranged from -45 to 10 cm H_2O, with average pre-storm suction of about 30 cm H_2O. At Sites 1, 2 and 3, all tensiometers responded at the same time (with no appreciable lag with depth), but about 6 hr after the start of the storm (Figure 5.8B-D). This contrasts with the 24 October response where strong lags were observed, reflecting lower rainfall intensities and the drier antecedent conditions. In this case, about 90% of the total ψ shift occurred in response to the first rainfall burst at 2400 hr 28 October.

Peak tensiometric response coincided with the stream hydrograph peak. Once peak ψ values were reached, approximately constant values persisted at Site 1 and near the surface at Site 2 (T6), while the rest gradually declined. Some variation in ψ recession can be seen in Figure 5.8B, where the upslope Site 3 tensiometers (T7-T9) showed a more rapid decline from peak positive ψ (0 to 20 cm H_2O) to negative ψ. Similarly, Site 2 ψ recession was more rapid than Site 1 ψ recession.

A plot of ψ versus soil depth for T1-T9 gives some indication of the infiltration-groundwater relationship (Figure 5.9). For t_0, t_1, t_2 and t_3, representing 2330 hr 28 October, 0830 hr 29 October, 1700 hr 29 October and 0230 hr 30 October, a water-table was established at each site (from previously unsaturated conditions throughout the profile, except site 2). Water-table elevation moved from undefined with the zone of measurement to approximately 40 cm from the ground surface at Site 1, within 8 hr. At Sites 2 and 3, groundwater table position shifted from -50 cm to -15 cm (Site 2), and from undetected to

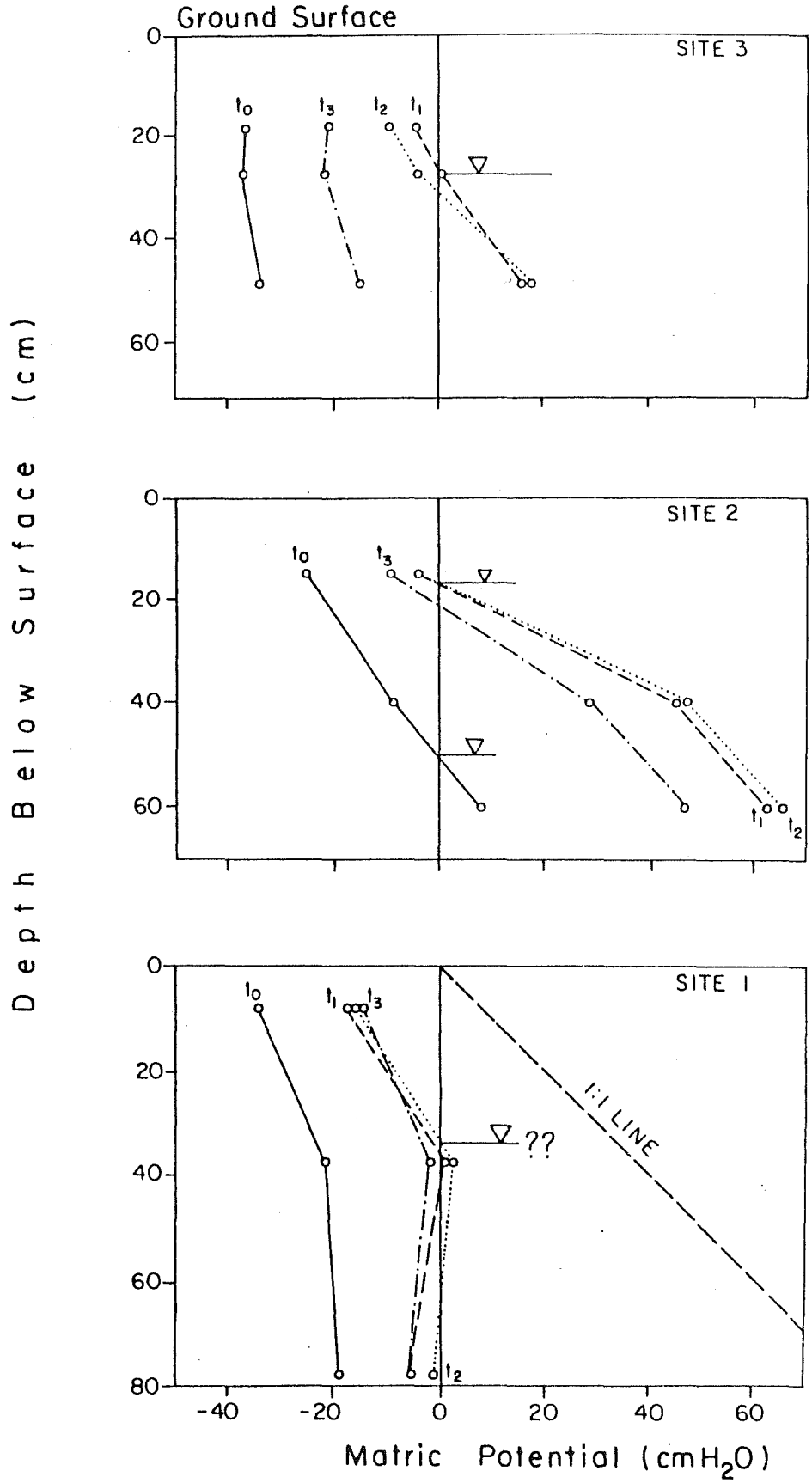

Figure 5.9 Near-stream matric potential versus depth below surface for the 29 October event.

-28 cm (Site 3), each within 8 hr.

Plotted cross-sectionally (Figure 5.10), water-table position can be seen to be quite irregular through time, partly due to surface microtopographical variations and irregular underlying bedrock topography. Even with these problems, however, a clearly substantial rise and development is noticeable, with a ridge developing at Site 2, sloping toward the stream channel. Lateral ϕ gradients prior to the event were rapidly shifted downward as the event progressed (Figure 5.10). Again, gradients become more lateral upslope, with downward flow predominating closer to the channel.

5.2.3 High magnitude rainfall: 13 October event

One hundred and three millimetres of rain fell over the M8 catchment between 0200 hr 13 October and 0200 hr 14 October, with average rain intensities in the order of 7 mm hr^{-1} (Figure 5.11). This same event was discussed in section 4.4.3, in relation to water chemistry and isotopic characteristics. API_7 and API_{14} were high (35.1 and 37.5 mm respectively), reflecting wet conditions produced by approximately 100 mm of intermittent rainfall from the previous week. Eighty-one millimetres of runoff was produced during the event, and peak specific discharge was 6.5 mm hr^{-1} (Figure 5.11). QF/R was almost 80% and QF/P was 62%. Data logging failure resulted in the loss of rainfall, streamflow, pit throughflow and tensiometric data for the period 0200 hr to 1700 hr 13 October. Both rainfall and streamflow data were able to be digitized from back-up charts, but all other data were lost completely. Tensiometric and pit throughflow response are therefore shown only from 1700 hr 13 October onward, which misses the main hydrograph peak at 1200 hr 13 October. This period does cover the second 25 mm burst after the initial 10 hr 75 mm burst, and gives some indication of the catchment condition immediately

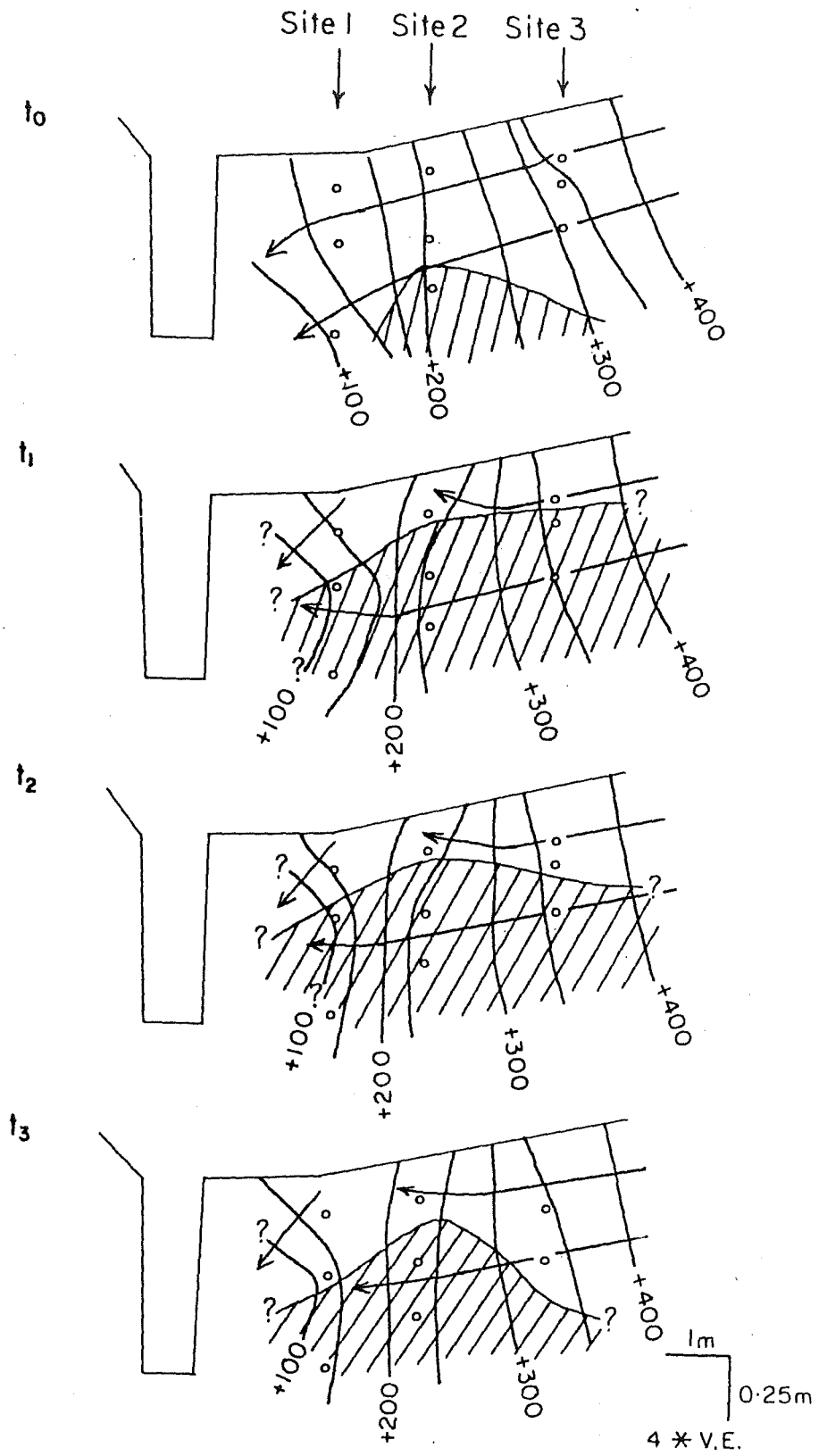

Figure 5.10 Flow lines and total potential in the near-stream cross section.

Figure 5.11 Rainfall-runoff relationships and near-stream tensiometric response for the 13 October event.

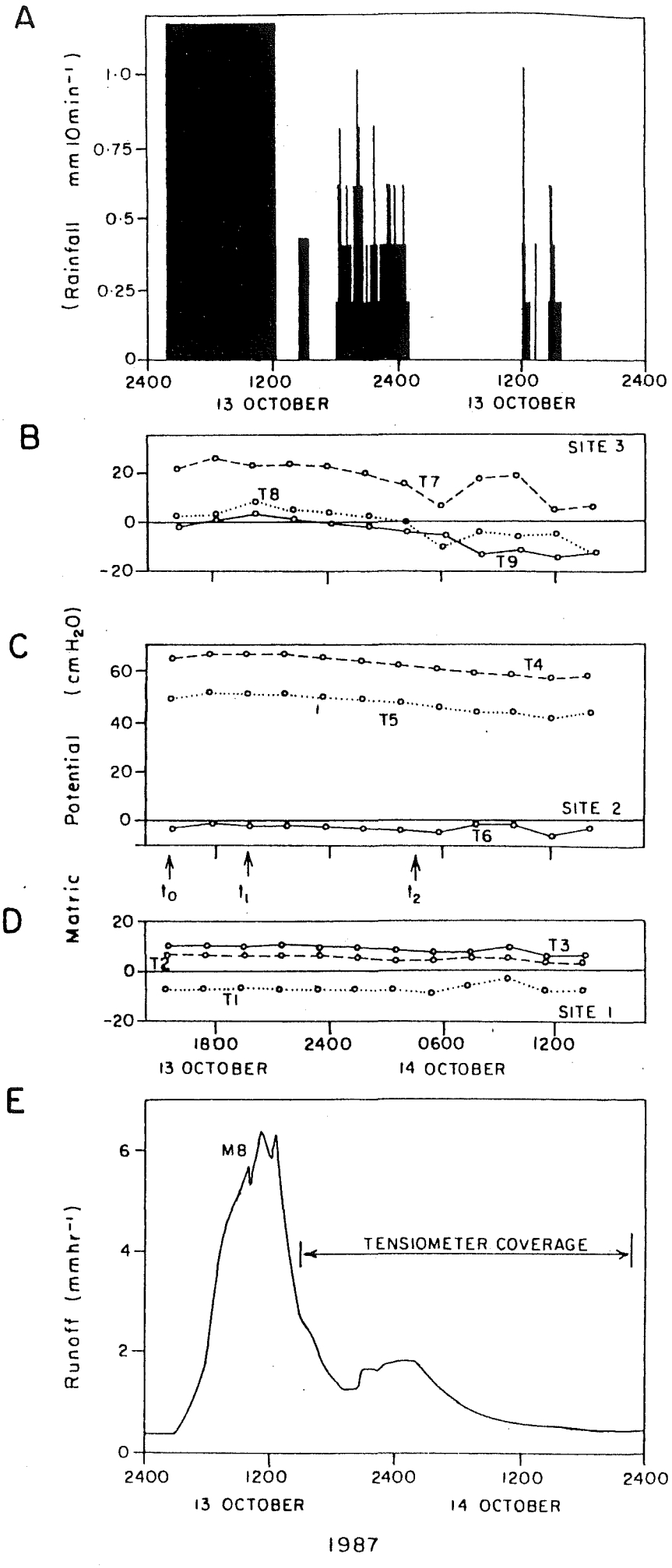
A
(Rainfall mm10min⁻¹)
1·0
0·75
0·5
0·25
0
2400
1200
2400
1200
2400
13 OCTOBER
13 OCTOBER
B
SITE 3
T7
T8
T9
20
0
-20
C
Potential (cmH₂O)
60
40
20
0
T4
T5
SITE 2
T6
t₀
t₁
t₂
D
Matric
20
0
-20
T3
T2
T1
SITE 1
1800
2400
0600
1200
13 OCTOBER
14 OCTOBER
E
Runoff (mmhr⁻¹)
6
4
2
0
M8
TENSIOMETER COVERAGE
2400
1200
2400
1200
2400
13 OCTOBER
14 OCTOBER
1987

following a high magnitude event with high antecedent wetness conditions.

Tensiometers in the near-stream zone, during the period of data coverage, were insensitive to the second 25 mm burst and showed a stable ψ through time. Some ψ shift at Site 3 between 1900 hr 13 October and 0500 hr 14 October can be detected (Figure 5.11B). Each site exhibited positive ψ through much of the soil profile, and a water-table was sustained throughout the period of coverage. It is assumed that initial ψ response to the first 75 mm rain burst occurred rapidly (as per 24 and 29 October events), and that values shown in Figure 5.11 are roughly equal to peak ψ caused by the large burst.

Three specfic time periods are discussed for the event: 1430 hr 13 October (t_0), 2030 hr 13 October (t_1), and 0400 hr 14 October (t_2). Water-table sloped toward the stream channel at t_1 and formed a mound at Site 2 (similar to 29 October event) for most of the duration of data coverage (Figure 5.12). Water-table elevations were higher in this event than any others observed throughout the entire study period, but show only slight variation in height with time (<10 cm), except at Site 3 where surface saturation occurred. Even under these very wet conditions, near-stream surface saturation was not observed at the Site 1 location. Total potential gradients show a substantial downward component (more than for the 24 or 29 October events) at Site 1 and Site 2, with a more lateral flux component at Site 3 (Figure 5.12). Gradients remained constant throughout the limited period of data coverage.

5.2.4 Summary

Tensiometric response to storm rainfall in the near-stream zone for a complete range of storm magnitudes and intensities is consistent with the type of response that Sklash et al. (1986)

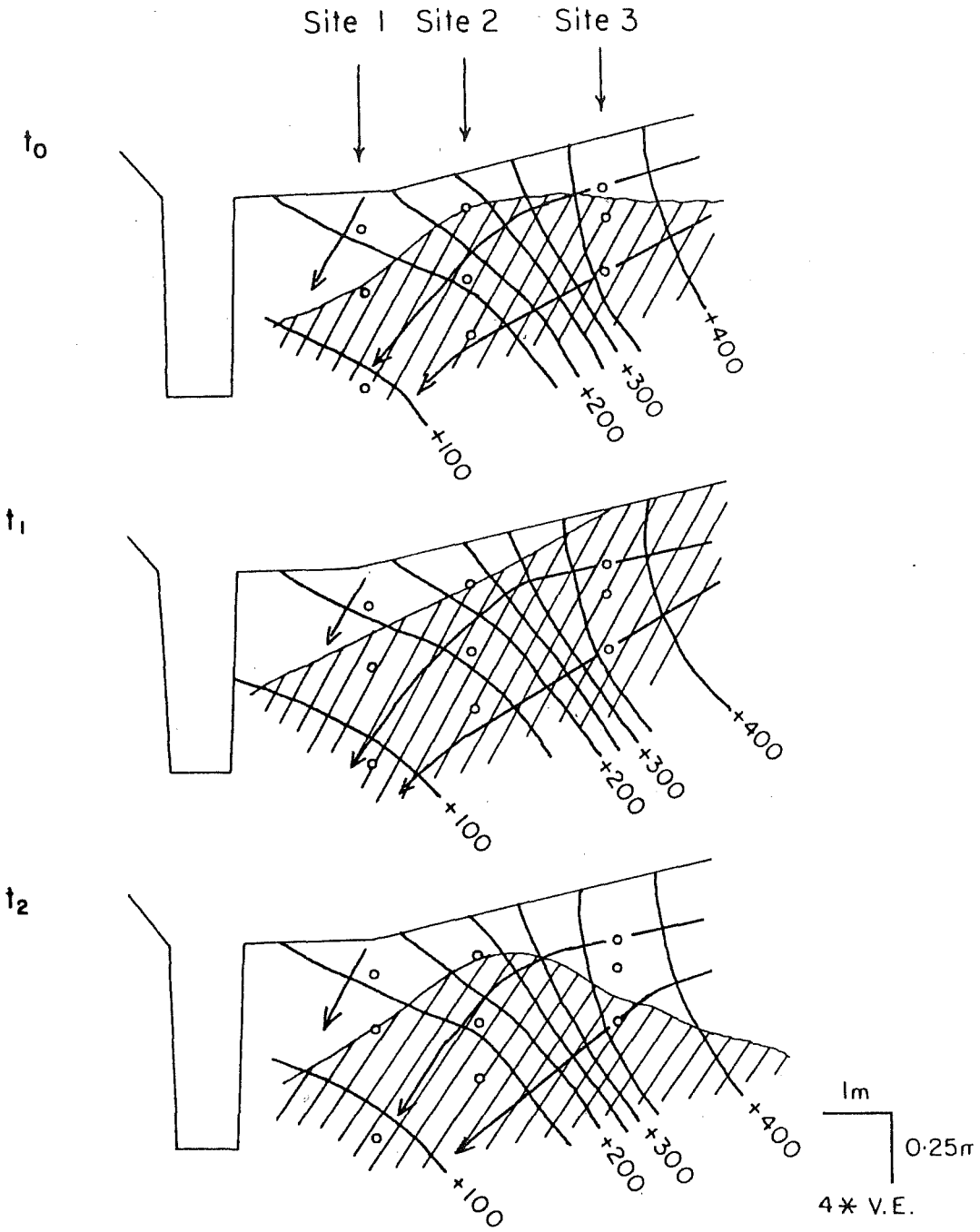

Figure 5.12 Flow lines and total potential in the near-stream cross section.

anticipated on the basis of the existence and properties of a capillary-fringe. Analysis of moisture release characteristics of the near-stream soils in section 5.1.3, however, showed that these soils do not sustain a tension-saturated zone, but tend to release water gradually with applied suction. As a result, rapid water-table responses in the near-stream zone and changes in soil matric potential are a result of the small differential water capacity or limited storage effects of the near-stream soils and not capillary-fringe properties. Furthermore, the rate of development and longevity of water-tables and changes in total and matric potential are affected by the presence of underlying impeding surface (Old Man Gravels) and drainage into the near-stream zone from upslope areas.

In each storm example, ψ response to rainfall input was very rapid through the complete profile for each site location, and water-tables were quickly established and maintained at depth. Rapid transition from matric to pressure potential occurred generally within 6 hr, and promoted increased downward ϕ gradients toward the stream channel at Site 1. Some lag in ψ response to rainfall input with depth was observed, consistent with the notion of initial downward wetting front propagation through the soil matrix. This pattern rapidly changed to accelerated low magnitude in ψ in the lower soil profile, due to perching of groundwater at the mineral soil-Old Man Gravel interface. During higher intensity rainfall bursts (cf. 29 October event), the complete profile responded at the same rate. This may be a function of air encapsulation during infiltration (Fayer and Hillel, 1986) also resulting in rapid water-table rise), or possibly some bypassing to depth, as short-term rainfall intensities exceeded mineral soil surface infiltration capacities.

Once peak ψ was reached within the profile, values persisted for 1-3 days, before gradually returning to pre-storm ψ. The maintenance of saturated zones in the near-stream location is a function of the shallow soil cover, underlain by impermeable Old Man Gravels. Additional subsurface flow from upslope zones and low slope angles would also have contributed to persistent low ψ.

The ridge or mound of groundwater observed at Site 2 for each monitored storm, is similar to that described by Ragan (1968). In this case, rain infiltrated the soil, rapidly filled available storage, and produced a rapid but localised groundwater response to rain input. When rainfall stopped, the ridge slowly drained and produced a more typical groundwater profile. The groundwater table at Site 1 did not respond as rapidly, because of the larger soil depth. The rapidity of Site 2 groundwater development may also reflect its topographic position near a break in slope. It is difficult to quantify the relationships between water-table rise and slope position, since soil depths at each site are unknown, and surface microtopographical variations were not measured.

5.3 MID-SLOPE TENSIOMETRIC RESPONSE TO STORM RAINFALL

Tensiometer porous cup depths and heights above datum for the Pit 5 location are shown in Figure 5.13. Depending on local soil depths, tensiometers were installed at depths of approximately 15, 40, 80 and 100 cm. These depths were rarely achieved and were adjusted if roots or stones interfered with augering. Site numbers are also shown, and will be referred to in the following discussion on tensiometer response. The following three storms (already discussed for the near-stream zone) are discussed in detail: a low magnitude rainfall on 24 October, a moderate magnitude rainfall on 29 October and a high magnitude rainfall on 13 October. Those times examined in detail for each

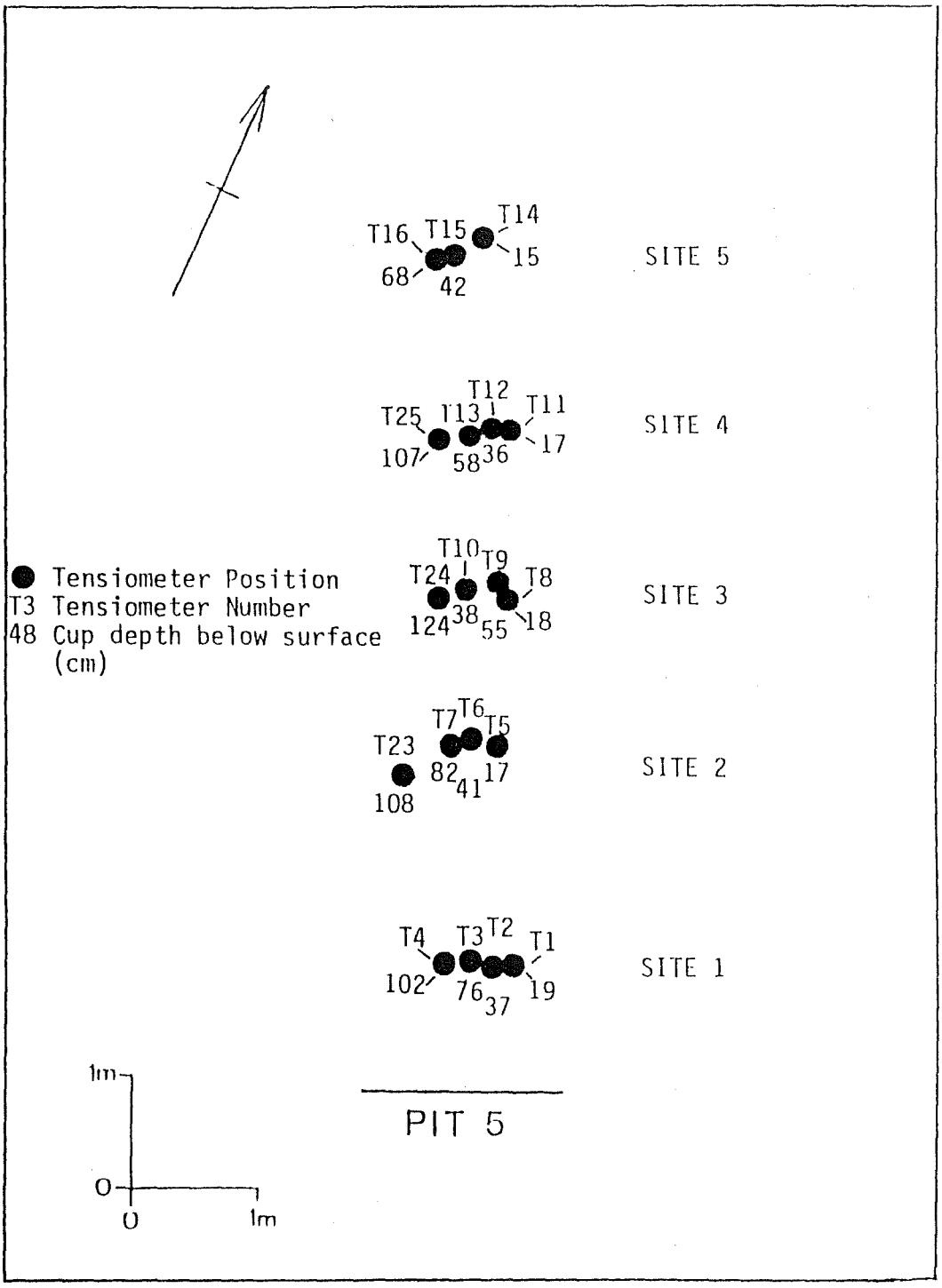

Figure 5.13 Tensiometer numbering and porous cup depths for the Pit 5 mid-slope site.

event discussed in section 5.2 (i.e. t_0, t_1, t_2 etc) will also be used for the following discussion of mid-slope response to storm rainfall.

5.3.1 Low magnitude rainfall: 24 October event

Hydrometric relationships for the 24 October event were given in section 5.2.1. Pit 5 throughflow rates were not available for this event, so ψ-Q comparisons cannot be made. It is assumed, however, that Pit 5 throughflow response was somewhere midway between that of Pit A and the Seep (Figure 5.14F).

Soil matric potential is plotted as a continuous function of time for tensiometer Sites 1-5 (Figure 5.14). Mid-slope ψ response was generally more subdued than the near-stream location, but some shallow tensiometers responded almost instantaneously to the rainfall input. Matric potential conditions prior to the rainfall input were similar to the near-stream zone. Response varied throughout the plot, reflecting variations in both slope position and soil physical characteristics (Figure 5.14A-E). One major difference between the near-stream and mid-slope sites for the 24 October event was the time taken to regain equilibrium through the profile. Near-stream soils are about 50 cm thinner, and the whole profile responded rapidly; a new equilibrium was reached within 18 hr. Mid-slope soils at Pit 5, because of their deeper soil horizons, took roughly double this time to regain a vertical drainage profile after initial wetting.

At Site 1, T1 (19 cm) and T2 (37 cm) responded almost immediately to the rainfall input, while the deeper tensiometers T3 (76 cm) and T4 (102 cm) peaked approximately 24 hr after the initial rainfall input (Figure 5.14E). T2 showed an initial ψ peak of -22 cm H_2O at c.2250 hr, followed by a rapid decline to

Figure 5.14 Pit throughflow and mid-slope tensiometric response for the 24 October event.

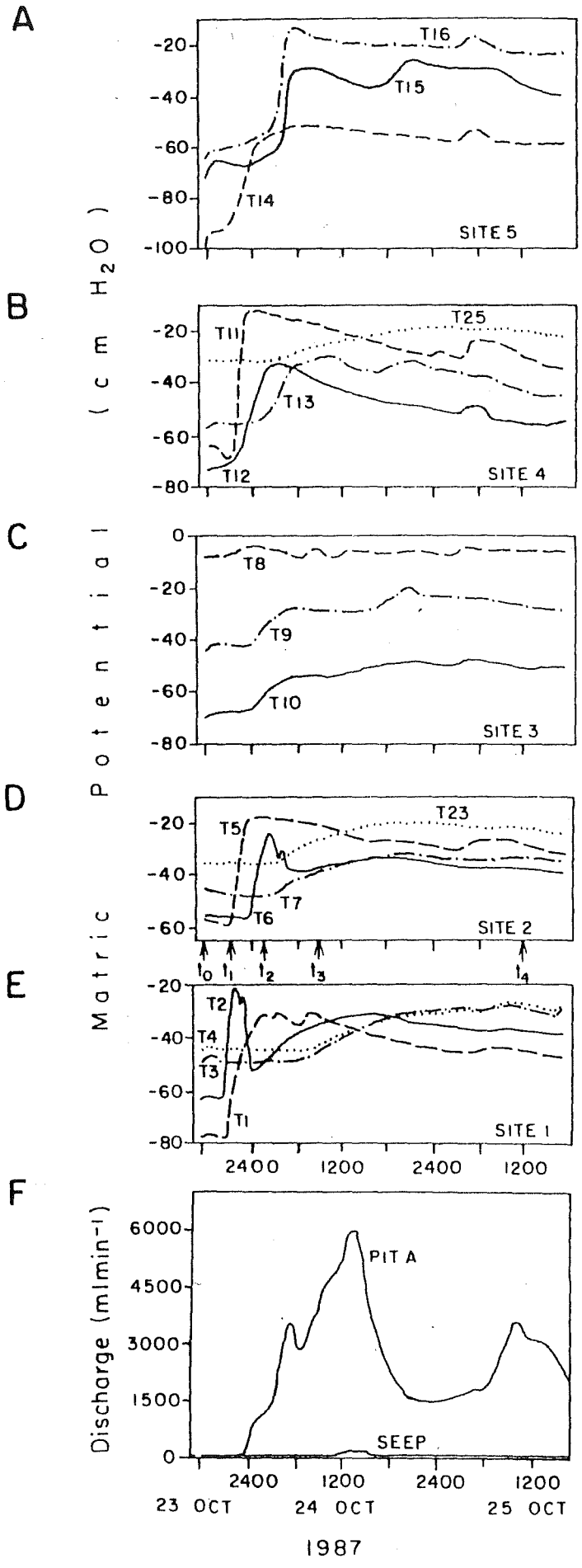
A
B
C
D
E
F
Matric Potential (cm H_2O)
-20
-40
-60
-80
-100
T16
T15
T14
SITE 5
T25
T11
T13
T12
SITE 4
0
T8
T9
T10
SITE 3
T23
T5
T7
T6
SITE 2
t_0 t_1 t_2 t_3 t_4
T2
T4
T3
T1
SITE 1
2400 1200 2400 1200
Discharge (ml min^{-1})
6000
4500
3000
1500
0
PIT A
SEEP
2400 1200 2400 1200
23 OCT 24 OCT 25 OCT
1987

-52 cm H_2O and then a gradual rise to a secondary peak of -30 cm H_2O at c.1400 hr 24 October. This tensiometer was particularly sensitive to rainfall input, as the timing of the response coincides with abrupt changes in rainfall intensity. T1 was also sensitive to rainfall input, and showed a slight secondary response (similar to the Pit A hydrograph) to the second rainfall burst at about 0900 hr 24 October. It is interesting that both T1 and T2 peaked and declined before T3 and T4 reached their respective peak ψ. This trend is apparent at Sites 2 and 4, but does not occur at sites farther upslope.

Site 2 response was similar to Site 1, but lacked the immediate ψ shift at c.50 cm depth (Figure 5.14D). The rate and magnitude of ψ response at Site 2 decreased with depth. Moving further upslope, Sites 3-5 (Figure 5.14A-C) showed readings consistent with a downward wetting front propagation, with similar ψ response to Site 2. Some of the shallow tensiometer ψ responses to rain input at T8 (18 cm), T5 (17 cm) and T11 (17 cm) show constant low suction, much lower than would be expected for an equilibrium profile, where suction decreases with depth. These tensiometers were installed at the base of the organic layer, slightly into the upper mineral soil matrix. The anomalous values may possibly be related to conditions described by Webster (1977), where high water contents of the humus layer in the Maimai area were observed for much of the year. Webster (1977) measured weekly variations in humus matric potential for a 12-month period using a manual tensiometer system. Mean matric potential over her entire 2 m by 2 m study plot was -7.4 +/-1 cm H_2O, and for individual tensiometers ranged from -12 +/-0.5 to -13 +/-4 cm H_2O. Minimum mean monthly suction was only 33 cm H_2O, and it is evident from this work that the water content of the humus remains high throughout the year.

Water-tables were not detected at any of the sites, although some of the lower tensiometers indicated a possible water-table at depth. This situation is difficult to determine because of the large variability of soil depth over very short distances. Generally, the pattern of wetting-front propagation is indicative of matrix flow, although some bypassing may be evident in the upper 50 cm of soil. In this case, water seems to be moving very rapidly to an intermediate depth (c.25-50 cm), and then being adsorbed by the matrix and moving further to depth through capillary pores. At each site, unsaturated vertical drainage occurred prior to the event.

During the rising limb of the hydrograph (t_o-t_x), ϕ gradients in the Pit 5 zone shifted from completely lateral to a more downward component, especially near the pit face (Sites 1 and 2). Farther upslope, ϕ gradients were close to lateral in a downslope direction for the complete storm period (Figure 5.15).

5.3.2 Moderate magnitude rainfall: 29 October event

Hydrometric relationships for the 29 October event were given in section 5.2.2. Pit 5 throughflow rates were not available for this event, so ψ-Q comparisons cannot be made. It is assumed, however, that Pit 5 throughflow response was somewhere midway between that of Pit A and the Seep (Figure 5.16F).

Matric potential response to storm rainfall at Pit 5 was very different from the previous 24 October event. In this case, lags to peak ψ with depth were shorter (Figure 5.16), reflecting the higher rainfall intensities and larger storm magnitude. Response was much greater throughout the profile, and positive ψ was established at most sites within 8 hr of the start of the event. The mid-slope site also differed in the timing of response, compared with the near-stream location. In this case, ψ

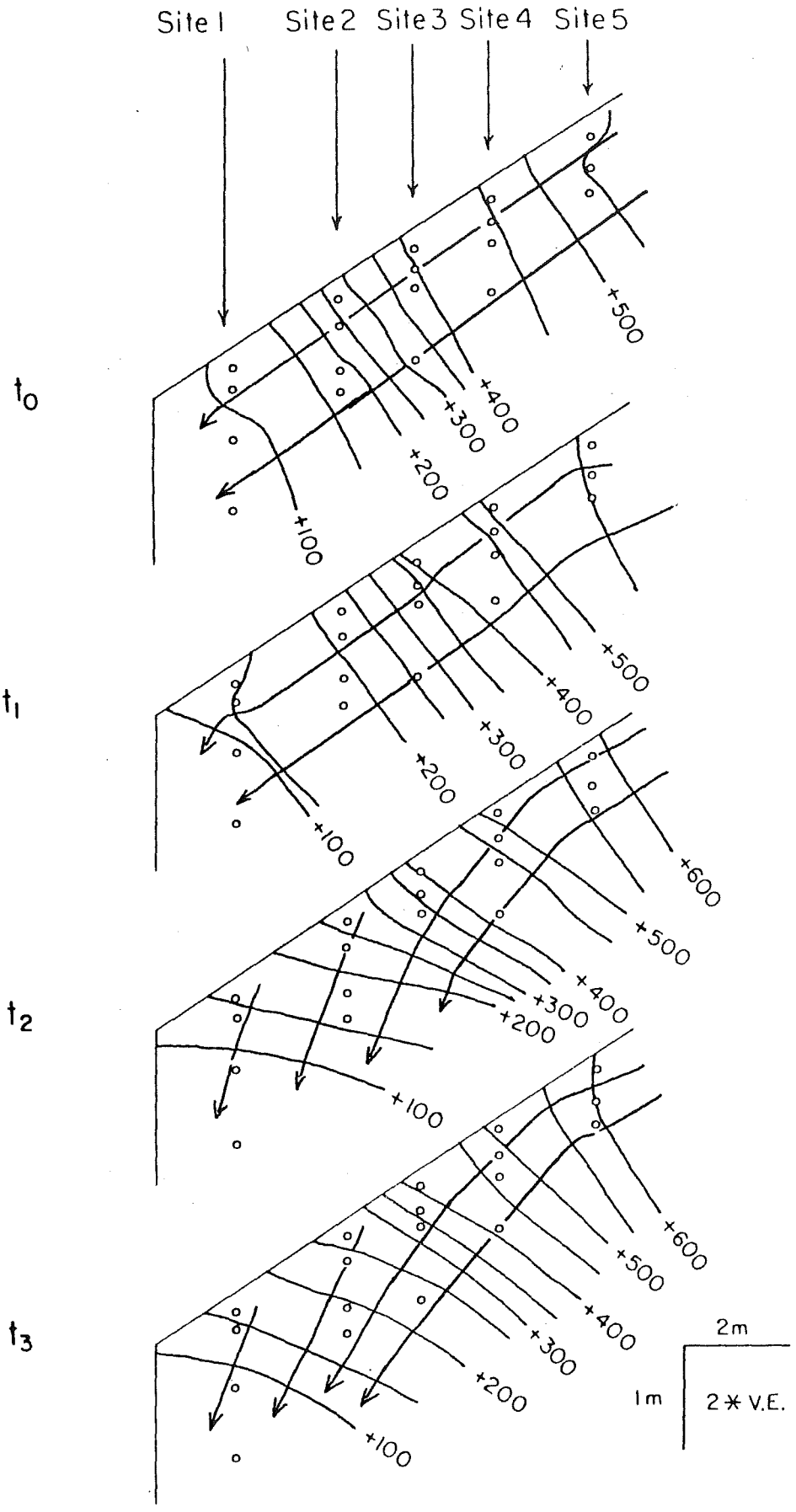

Figure 5.15 Flow lines and total potential in the mid-slope cross section.

Figure 5.16 Pit throughflow and mid-slope tensiometric response for the 29 October event.

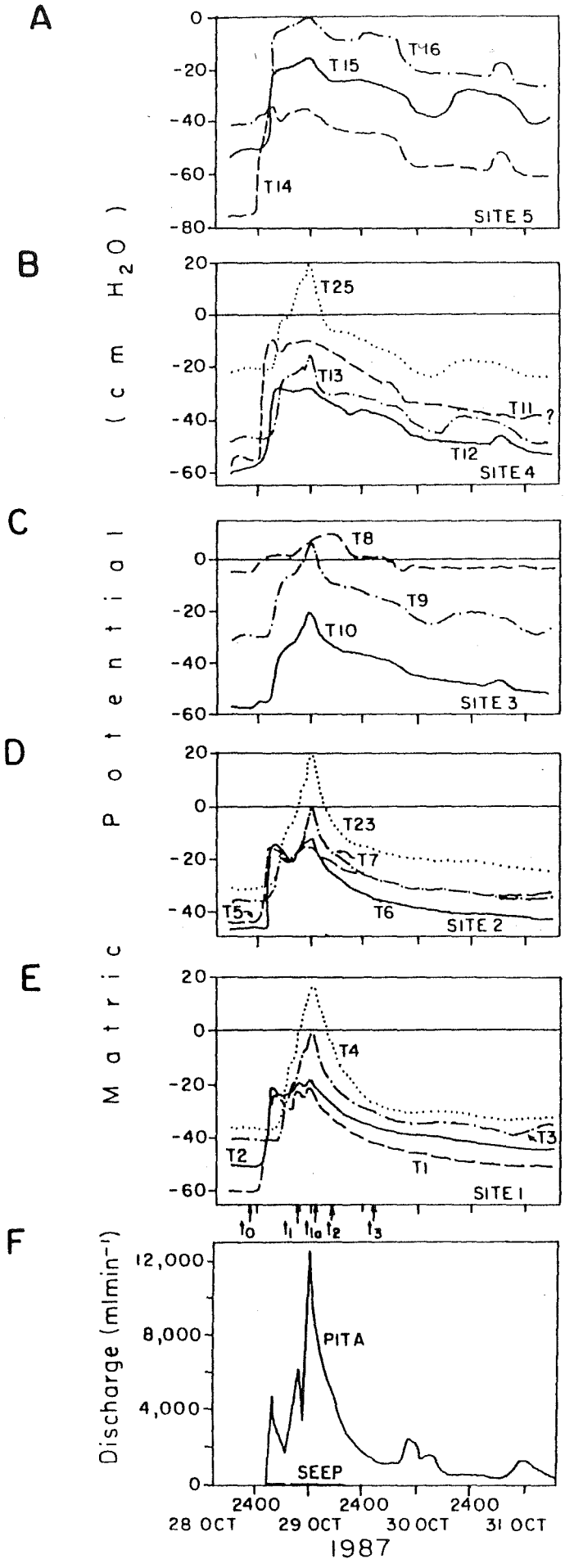
A
B
C
D
E
F
Matric Potential (cm H2O)
T16
T15
T14
SITE 5
T25
T13
T11
T12
SITE 4
T8
T9
T10
SITE 3
T23
T7
T5
T6
SITE 2
T4
T3
T2
T1
SITE 1
t0 t1 t1a t2 t3
Discharge (ml min-1)
12,000
8,000
4,000
0
PITA
SEEP
2400
28 OCT
2400
29 OCT
2400
30 OCT
31 OCT
1987

response shapes were closely aligned with the main Pit A and Seep hydrograph (Figure 5.16F), exhibiting both a steep rise and recession. In response to the second rainfall burst 0600-1200 hr 29 October, Sites 1-4 showed an immediate and large shift into positive ψ conditions, with no lag with depth.

At Site 1, T1 (19 cm) and T2 (37 cm) reached peak ψ within 3 hr of the first rainfall burst (Figure 5.16E). A second ψ peak of equal magnitude occurred at 1200 hr, corresponding to the second rainfall burst. T3 (76 cm) and T4 (102 cm) showed no ψ peak in response to the first rainfall burst, and only began to respond at this time. T3 and T4 rose sharply between 2400 hr 28 October and 1200 hr 29 October, and then receded at the same rate for another 12 hr, before declining more slowly. Low magnitude ψ were maintained only briefly, as compared to both the near-stream conditions and the 24 October event conditions at the mid-slope site.

Site 2, ψ response to storm rainfall was almost identical to Site 1 (Figure 5.16D). Moving further upslope, peak ψ response at depth was more subdued and showed a rise to peak, followed by constant low magnitude ψ. The variation in response, particularly at depth, may be a function of a build-up of saturation near the pit face, as described by Atkinson (1978), where a saturated wedge is established upslope of the face. Nevertheless, much of the profile throughout the mid-slope zone became saturated, and maintained positive ψ through the peak catchment runoff response.

Plots of matric potential versus depth (Figure 5.17) show a very rapid appearance and disappearance of water-tables throughout the zone, but particularly near the pit face (i.e. Sites 1 and 2). Total potential gradients during the 29 October event show a consistent lateral flux component, with some downward flux near the pit face at t_1 (Figure 5.18). Highest ϕ

Figure 5.17 Mid-slope matric potential versus depth below surface for the 29 October event.

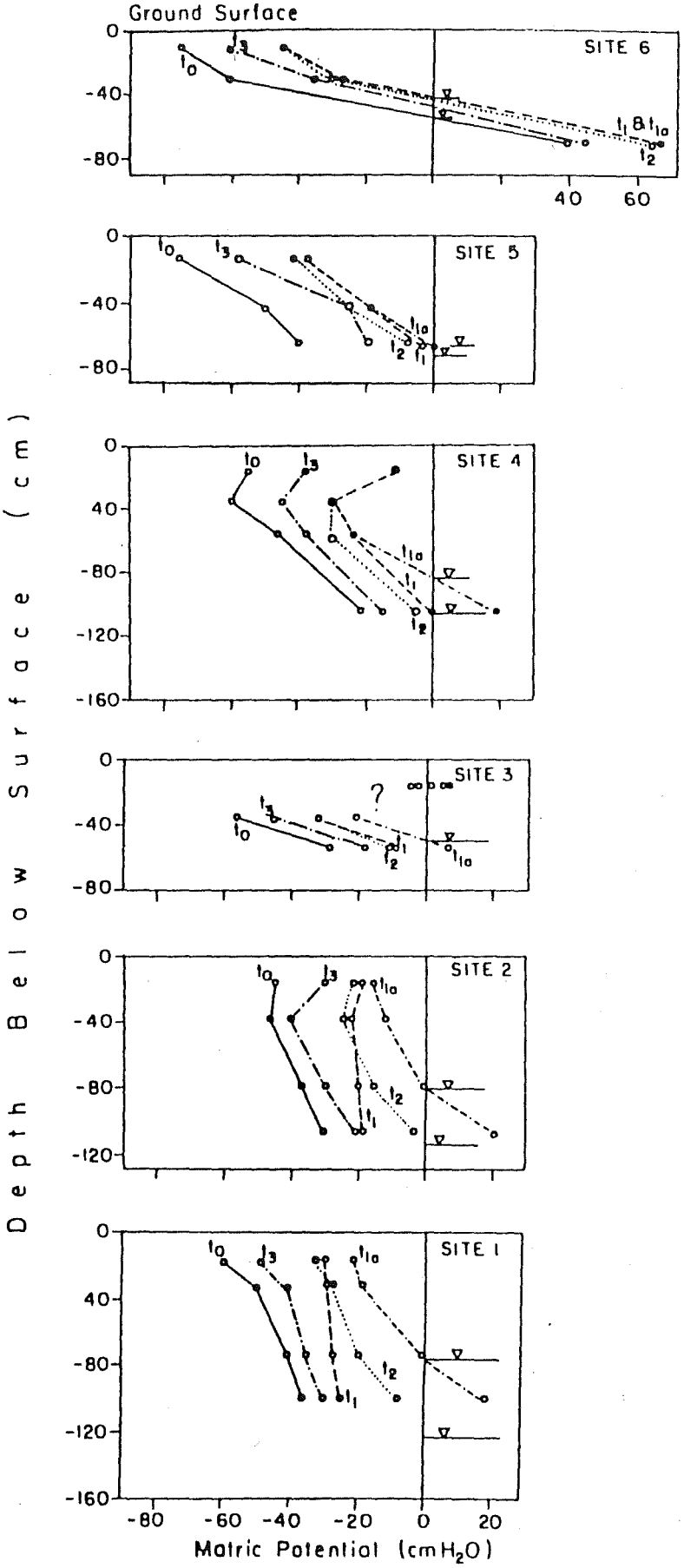
Ground Surface
SITE 6
SITE 5
SITE 4
SITE 3
SITE 2
SITE 1
Depth Below Surface (cm)
Matric Potential (cm H2O)

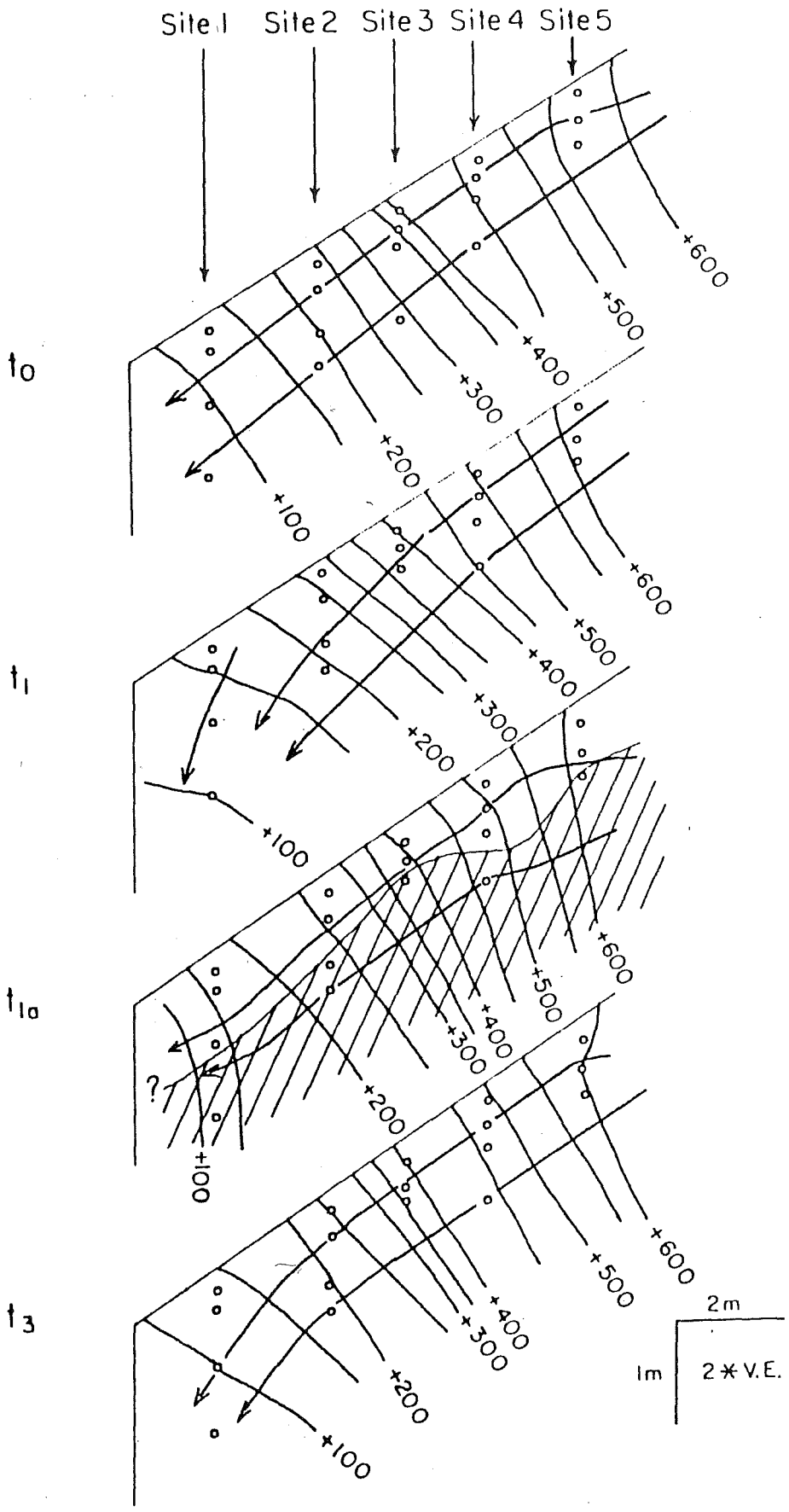

Figure 5.18 Flow lines and total potential in the mid-slope cross section.

gradients were established at t_{1m} (1200 hr 29 October), coinciding with peak ψ and peak pit throughflow. A detectable water-table (i.e. somewhere above the deepest tensiometer at each site) was only observed at t_{1m}. This rapid appearance and disappearance of water-table at depth is very different to the near-stream situation (where water tables persist for some time), and shows that the mid-slope zone is very well drained, despite very low K_{mat}.

5.3.3 High magnitude rainfall: 13 October event

Hydrometric relationships for the 13 October event were given in section 5.2.3. Data recording problems outlined in section 5.2.3 mean that pit throughflow data are not available for comparison to matric potential data. Furthermore, the period of tensiometric coverage (as in the near-stream discussion for this event), is limited to the period following the main 13 October runoff event.

Matric potential response to storm rainfall in the mid-slope zone for the period of data coverage was much more sensitive to small rainfall inputs than the near-stream location (Figure 5.19). Sites 1-4 showed a steep lowering of ψ magnitude in response to the second 25 mm burst. No lag with depth was observed, indicating that water may have bypassed much of the upper soil matrix en route to depth. Contrary to the near-stream situation, peak ψ response (coinciding with peak stormflow 1200 hr 13 October) may have been substantially higher than conditions portrayed in Figure 5.19. Nearby maximum rise piezometer data from the Pit 5 zone indicates that water table elevations may have risen to somewhere midway between T2 and T3 at Site 1.

For the period of data coverage, water-table elevations fluctuated <25 cm, except near the pit face (Site 1), where a

Figure 5.19 Mid-slope tensiometric response for the 13 October event.

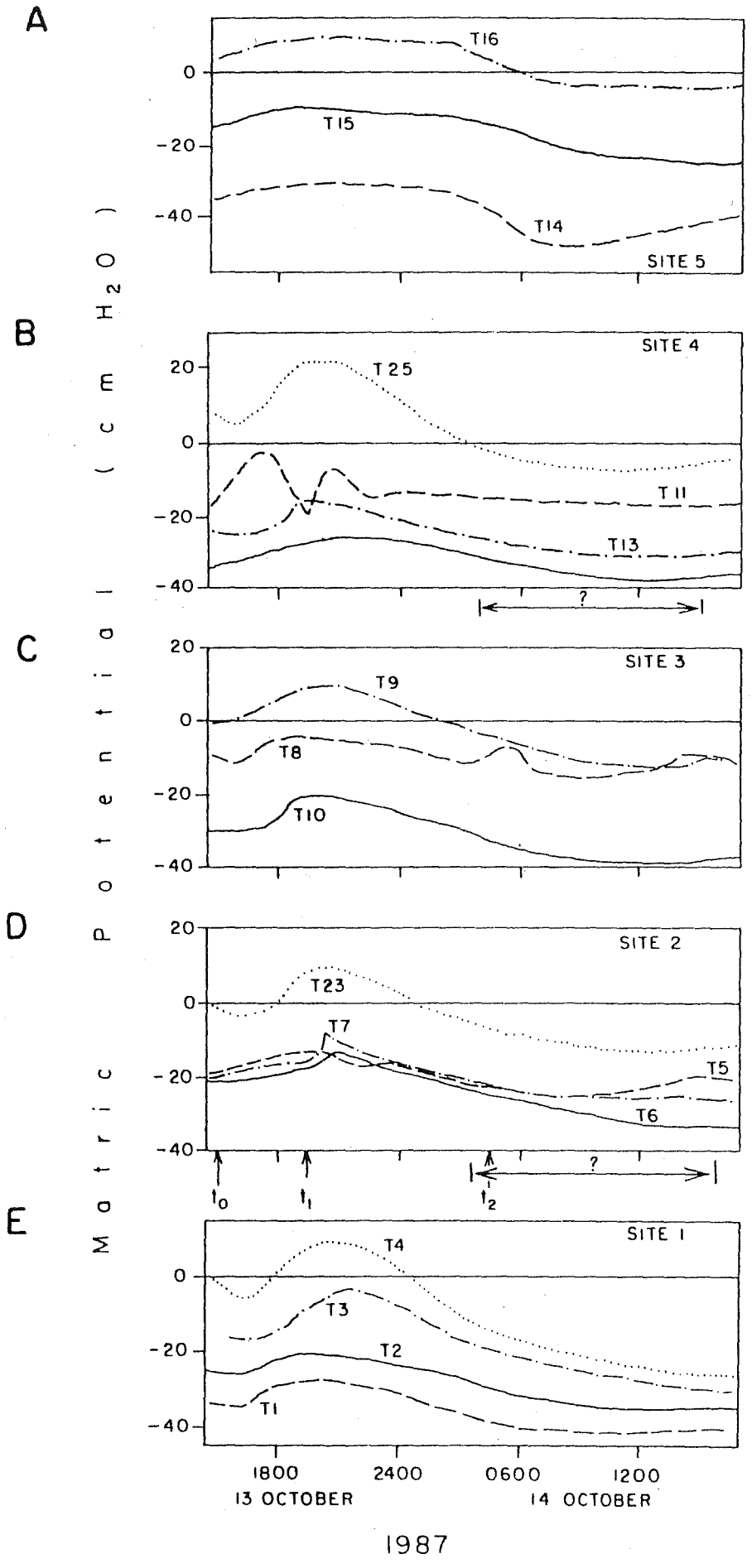
A
T16
T15
T14
SITE 5
B
SITE 4
T25
T11
T13
?
C
SITE 3
T9
T8
T10
D
SITE 2
T23
T7
T5
T6
?
t_0
t_1
t_2
E
SITE 1
T4
T3
T2
T1
0
-20
-40
20
Matric Potential (cm H_2O)
1800
2400
0600
1200
13 OCTOBER
14 OCTOBER
1987

water-table was formed at -80 cm and then disappeared at t_{22} (Figure 5.20). Even under very wet conditions in this case, saturation of the lower profile varied considerably, possibly reflecting variations in soil depth and underlying bedrock topography. Total potential gradients changed very little throughout the period of coverage, even with changes in ψ. Gradients remained lateral for t_{20}-t_{22}, and showed only a small downward component at the pit face (Figure 5.21).

5.3.4 Summary

Mid-slope response was highly variable for different storm magnitudes, intensities and pre-storm soil ψ conditions. Even though most of the soil profile at this site was affected by limited storage effects (as described for the near-stream site), response seemed to indicate a more erratic infiltration-ψ relationship than the near-stream zone. During low magnitude events (cf. 24 October), tensiometric data are consistent with a semi-constant wetting front propagation through the profile and with strong ψ response lags with depths. Although some bypass flow seemed to occur in the upper soil horizon (<50 cm), rainfall depth and soil moisture content was low enough so that the lower soil depths did not receive appreciable moisture from above until streamflow response had subsided. Water-tables therefore, did not develop at the Pit 5 site, and subsurface stormflow volumes were negligible.

During larger magnitude events, matric potential in the lower soil horizons (>75 cm) responded almost instantaneously to infiltrating rain. This seems to result from two processes: rapid wetting because of limited storage effects (as described in section 5.2.4), and rapid wetting from bypass flow. When rainfall intensities are low, but pre-storm soil water content is high (as in the 13 October event), any additional rainfall input rapidly

Figure 5.20 Mid-slope matric potential versus depth below surface for the 13 October event.

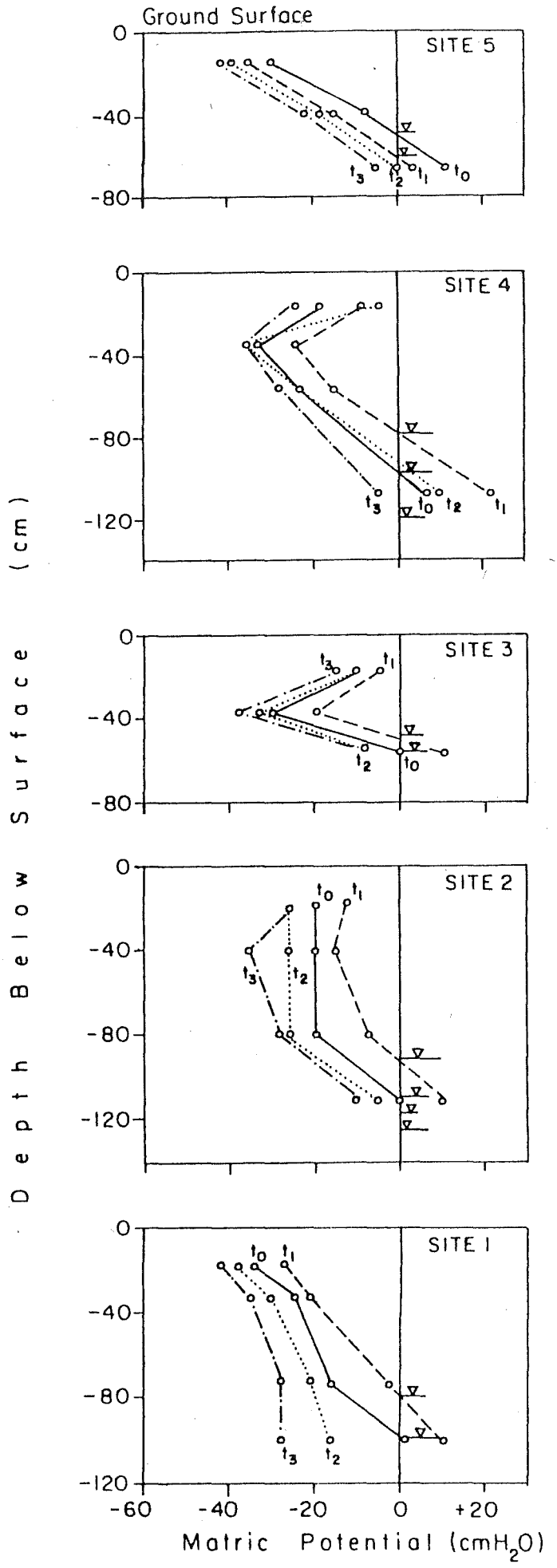
Ground Surface
SITE 5
SITE 4
SITE 3
SITE 2
SITE 1
0
-40
-80
-120
t_0
t_1
t_2
t_3
Depth Below Surface (cm)
-60
-40
-20
0
+20
Matric Potential (cmH_2O)

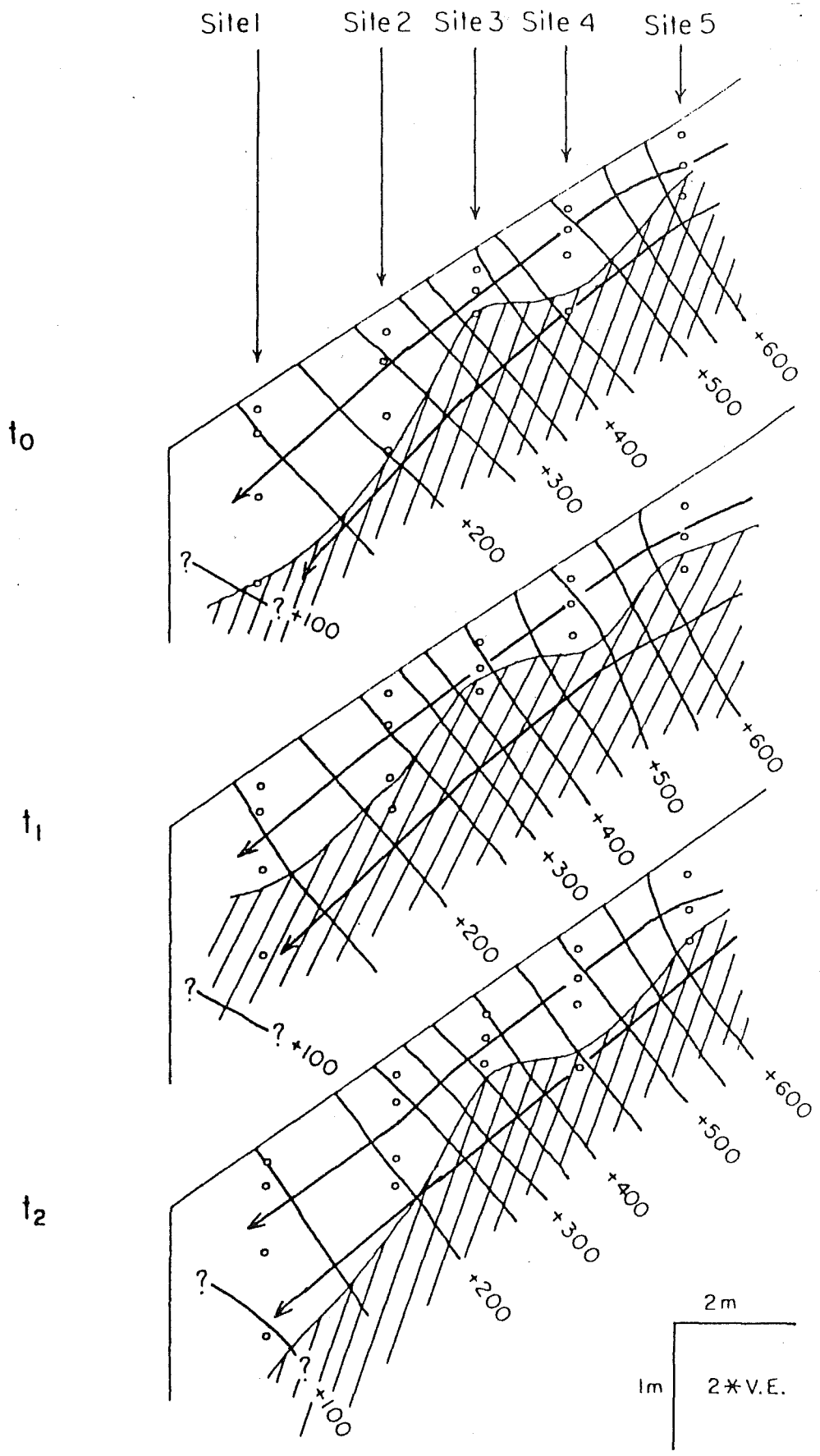

Figure 5.21 Flow lines and total potential in the mid-slope cross section.

fills the limited soil moisture storage, and perched water-table conditions quickly develop at the bedrock interface, as described by Hammermeister et al. (1982a). Matric potential response to rain input is rapid and consistent throughout the profile, with no appreciable lags with depth. On the other hand, if short-term rainfall intensities are high (as in the 29 October event), rainfall may bypass the upper soil horizons (<50 cm) and move to the profile base via vertical cracks, so that tensiometers in the lower half of the profile respond ahead or independent of the upper tensiometers, as described by DeVries and Chow (1978). The occurrence of bypass flow seems to be related to short-term rainfall intensity, rather than total rainfall depth. This effect has been reported by Bouma et al. (1981) and Bouma and DeLaat (1981). This non-uniform wetting also contributed to perched water-table conditions at the mineral soil-Old Man Gravel interface.

In each storm, elevational potential dominated total potential computations, and total potential gradients were strongly lateral in the downslope direction. Water-table longevity was very short (as compared to the near-stream zone) and showed a close correspondence with Pit 5 throughflow rate. Downslope drainage of perched groundwater was extremely efficient and showed no lag with recorded pit throughflow for storms where this data was available. This indicates that lateral saturated flow was rapid, and probably moved through pipes formed at the mineral soil-Old Man Gravel interface (details of which are discussed in section 6). The rapidity of tensiometric recession in the lower half of the soil profile in events with perched water-table conditions, supports the idea of rapid downslope drainage through pipes.

The relationship between rapid water-table development and pipeflow drainage is such that saturated conditions at the mineral soil base are required for pipeflow initiation, and consequently pipeflow is required for rapid water-table decline. The interconnectedness of pipes in this zone must be high to account for the rapidity of water-table decline.

5.4 UPSLOPE TENSIOMETRIC RESPONSE TO STORM RAINFALL

The near-stream Scanivalve unit was moved to the Pit A location on 23 November. Tensiometer deployment and individual cup depths are shown in Figure 5.22. Data logging at the new site commenced 1700 hr 25 November, immediately prior to the rainfall at 0300 hr 26 November. Forty-seven millimetres of rain fell in two separate bursts during 26 and 27 November and produced a rapid stream and pit throughflow response. A total of 9.8 mm of runoff was generated, 93% of which was in the form of QF. Peak 10 min rainfall intensities were >12 mm hr^{-1}, and would have temporarily exceeded mineral soil surface infiltration capacities in the Pit A hollow. API_7 and API_{14} were low (1.5 mm and 4.1 mm respectively), and as a result, QF/P was only 19%.

The two rain bursts were treated as separate events, in order to compare ψ response under dry and wet antecedent conditions. In each case, only matric potential versus time is examined, since shallow soil depths prevented detailed hillslope cross-sectional analysis.

5.4.1 26 November event: Part A

During Part A of the 26-27 November event (0000 hr to 2300 hr 26 November), 22 mm of rainfall produced a peak MB specific discharge of about 0.4 mm hr^{-1}. Peak ψ response at the Pit A site coincided with peak Pit A throughflow (800 ml min^{-1} at 2000 hr), except for some tensiometer positions, where peak ψ

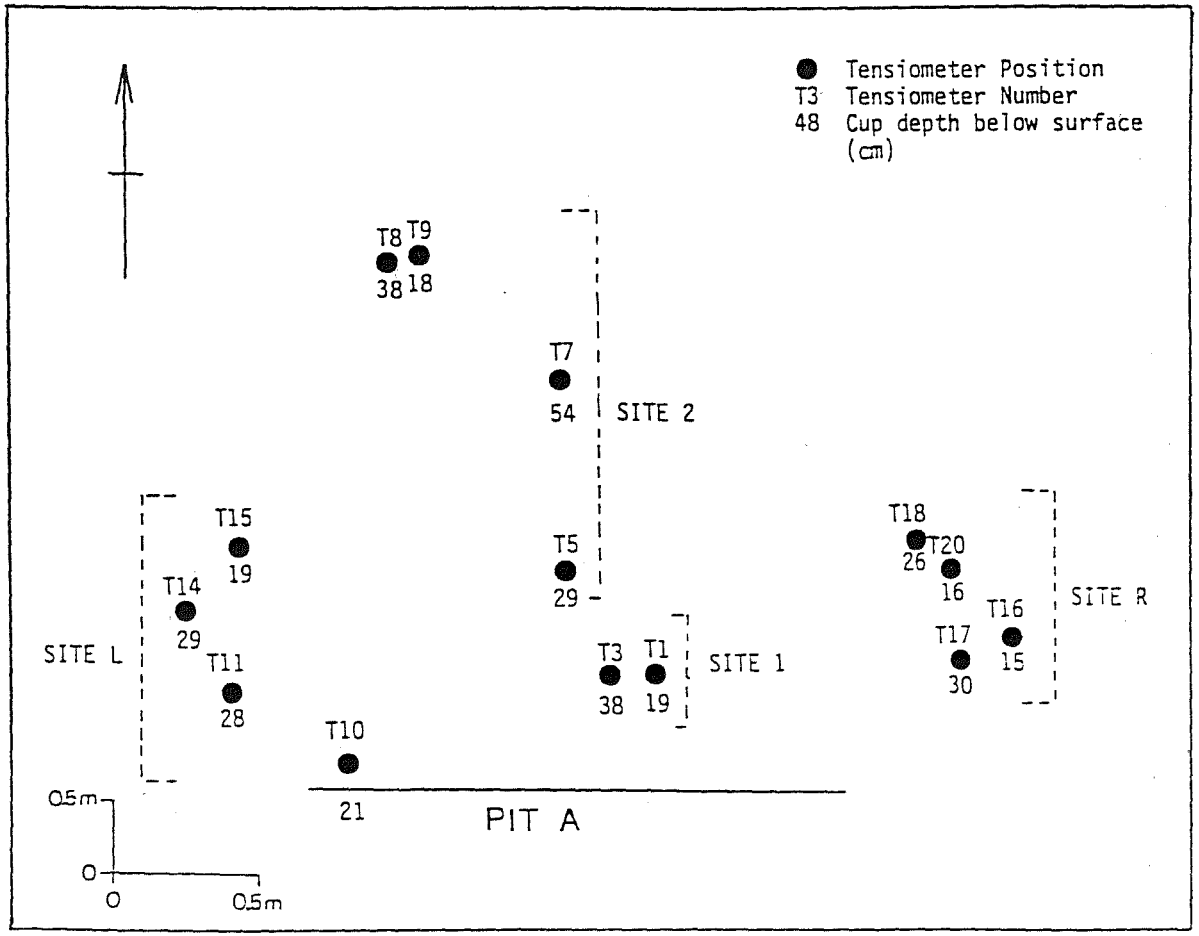

Figure 5.22 Tensiometer numbering and porous cup depths for the Pit A upslope site.

preceded pit throughflow peak by approximately 3 hr (Figure 5.23). Pre-storm ψ for most tensiometer positions was between -60 and -150 cm H_2O. The lowest magnitude ψ attained was -20 cm H_2O and no saturation was detected in any portion of the profile. Near the Pit A face at Site 1 (Figure 5.23C), equilibrium conditions were maintained prior to the event. T1 (19 cm) responded immediately to the rain input at 0300 hr. Matric potential shifted from -60 cm H_2O to a peak value of -35 cm H_2O over the following 9 hr, and then remained constant for the duration of the event. T3 (38 cm) matric potential response to storm rainfall lagged T1 by c.11 hr, but response was more rapid (-90 to -45 cm H_2O in 7 hr) and peaked at the same time as pit throughflow. This response is consistent with previous mid-slope and near-stream locations where ψ shift was lagged with depth. Matric potential response to rainfall from other tensiometer locations (Figure 5.23) is similar to Site 1. Sites 2, L and R (shown in Figure 5.22) maintained higher magnitude pre-storm ψ, but showed similar response magnitudes and timing to Site 1.

5.4.2 27 November event: Part B

Approximately 5 hr after the 26 November rain burst (Part A), another 18 mm of rain fell on the M8 catchment (Part B; Figure 5.24). Peak M8 specific discharge was 0.68 mm hr^{-1}, and again peak 10 min rainfall intensities exceeded 12 mm hr^{-1}. Peak discharge from the Pit A face was 6000 ml min^{-1} and lagged peak M8 flow by c.4 hr.

No saturation was observed in any portion of the soil profile and ψ response to rain input for each tensiometer group was minimal. Pre-storm ψ was equivalent to 26 November post-storm ψ, and no significant soil profile drainage occurred between events. At Site 1, ψ remained constant for the complete 27

Figure 5.23 Rainfall-throughflow relationships and upslope tensiometric response for the 26 November event.

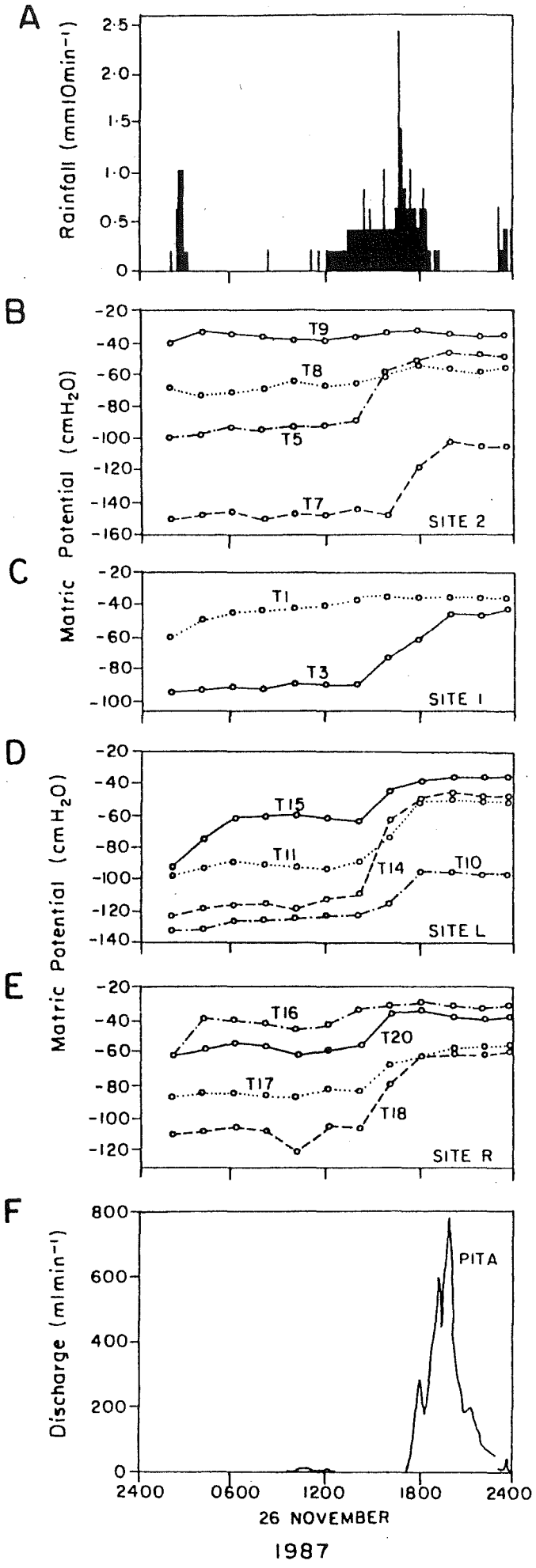
A
Rainfall (mm10min⁻¹)
2·5
2·0
1·5
1·0
0·5
0
B
Matric Potential (cmH2O)
-20
-40
-60
-80
-100
-120
-140
-160
T9
T8
T5
T7
SITE 2
C
-20
-40
-60
-80
-100
T1
T3
SITE 1
D
Matric Potential (cmH2O)
-20
-40
-60
-80
-100
-120
-140
T15
T11
T14
T10
SITE L
E
-20
-40
-60
-80
-100
-120
T16
T20
T17
T18
SITE R
F
Discharge (mlmin⁻¹)
800
600
400
200
0
PITA
2400
0600
1200
1800
2400
26 NOVEMBER
1987

Figure 5.24 Rainfall-throughflow relationships and upslope tensiometric response for the 27 November event.

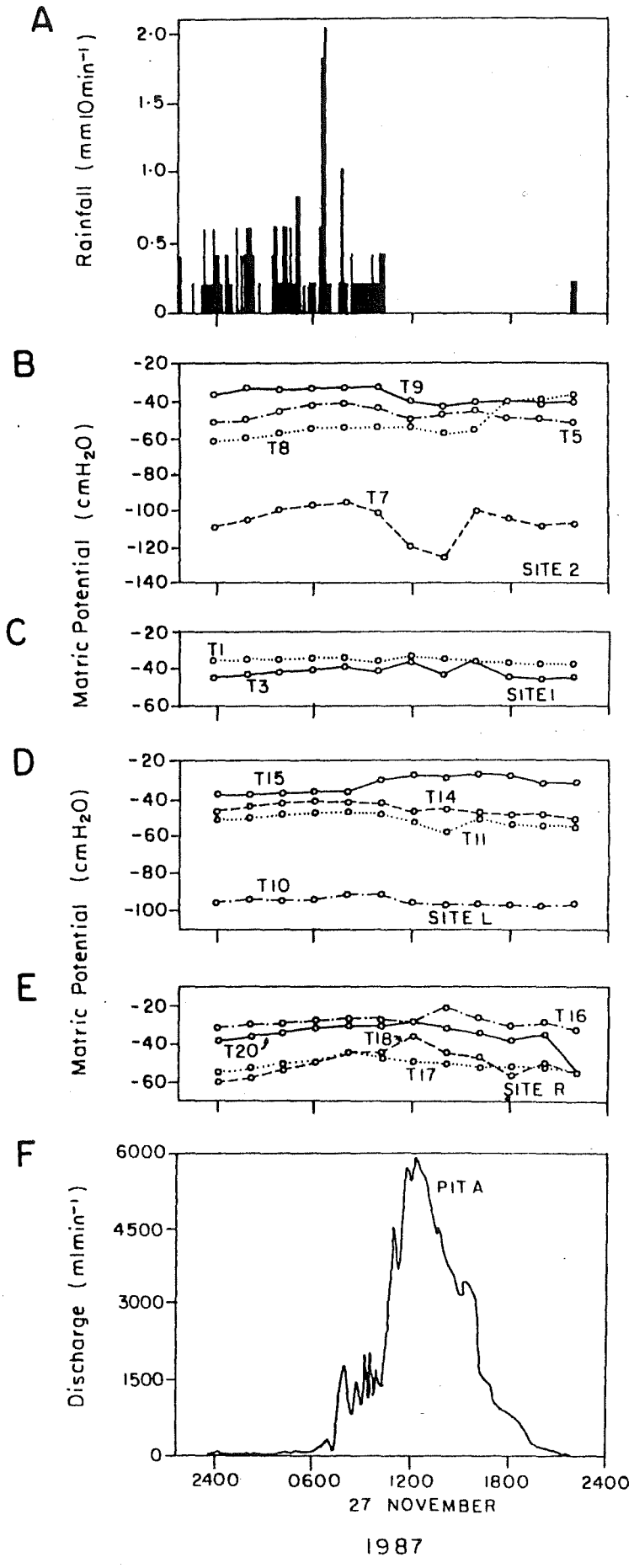
A
Rainfall (mm10min⁻¹)
2·0
1·5
1·0
0·5
0
B
Matric Potential (cmH2O)
-20
-40
-60
-80
-100
-120
-140
T9
T8
T5
T7
SITE 2
C
-20
-40
-60
T1
T3
SITE1
D
Matric Potential (cmH2O)
-20
-40
-60
-80
-100
T15
T14
T11
T10
SITE L
E
Matric Potential (cmH2O)
-20
-40
-60
T16
T18
T20
T17
SITE R
F
Discharge (mlmin⁻¹)
6000
4500
3000
1500
0
PIT A
2400
0600
1200
1800
2400
27 NOVEMBER
1987

November event and did not significantly deflect from pre-storm values. Site 2 tensiometers showed some decrease in ψ magnitude at 0900 hr, which coincided with the end of rain input. Sites L and R registered no response.

5.4.3 Summary

Both tensiometric and throughflow response for the 26-27 November events are consistent with the interpretation of Mosley (1979, p.802), whereby "a large portion [of runoff] runs downslope above the surface of the A horizon. A distinct saturated zone 1-2 cm deep in the base of the organic layer is frequently observed during storm conditions, and it is inferred that water moves downslope through this saturated highly porous layer in a manner intermediate between free surface flow and flow through a porous medium." This interpretation is verified by the fact that considerable volumes of throughflow were produced, without any soil saturation or significant change in soil ψ. In this case, rain intensities exceeded mineral soil infiltration capacities and forced water to flow over the mineral soil surface to produce the measured throughflow response. No bypass flow (as identified at Pit 5) was detected.

Although rain amounts and intensities for Parts A and B were similar, Part B produced 7.5 times more throughflow at Pit A. The tensiometer data seem to indicate that during Part A, a large portion of the rain input infiltrated into the soil matrix, with possibly some mineral soil surface flow during the most intense short burst at 1800 hr. As a result, only about 90 l of throughflow was produced. Presumably, the Part A rain input would also have filled the unsatisfied water storage capacity in the organic layer (5-15 mm from data in Webster, 1977). Part B throughflow rates and volumes indicate that the majority of

rainfall did not enter the soil matrix, but rapidly flowed over the mineral soil surface to the Pit A face. Without the unsatisfied moisture deficits in both the organic and mineral soil to fulfill, runoff production was much higher (>1000 l at the Pit A face).

Throughflow and matric potential variations between Parts A and B of this storm confirm the above interpretation. Soil ψ remained unchanged between cessation of 26 November rain and the start of 27 November rain. During this time, Pit A throughflow ceased, indicating that matrix flow could not sustain or supply earlier throughflow volumes. Then, during high rainfall intensities on 27 November, peak throughflow was 6000 ml min^{-1} without any measureable change in soil ψ. Again, soil matrix flow could not have accounted for runoff volumes and did not alter from pre-storm conditions. The majority of runoff therefore had to be produced by flow over the mineral soil surface. Contrary to Pit 5 response, water did not bypass to depth, because no increase in ψ in the lower soil profile (in response to perched water-table conditions) was observed.

5.5 SOIL POTENTIAL-THROUGHFLOW-STREAMFLOW RECESSION LINKAGES

In the preceding analysis of tensiometric data, the various controls on near-stream, mid-slope and upslope response to storm rainfall have been identified. In order to relate this information to the streamflow hydrograph, soil matric potential-throughflow-streamflow recession linkages are examined. This analysis also provides some indication of pipe versus matrix drainage conditions.

Throughflow-streamflow recession linkages have been determined in some previous investigations, in order to relate slope inputs to streamflow recession. Hewlett and Hibbert (1963) observed a 5-day transition period for a 1 m deep repacked soil

mass, where subsurface drainage shifted from saturated to unsaturated conditions. They observed a two-phase process, where during the initial 1.5 days, drainage occurred mainly through the large pores. After 5 days, rate of drainage decreased and they observed that subsequent slow drainage occurred only from the small pores. Weyman (1970; 1973) found that drainage from a natural slope was dominated by non-capillary saturated flow during the first day, and after a 4-day transition period, was dominated by unsaturated lateral flow in small pores, in a zone near the base of the slope. Harr (1977) observed much faster drainage characteristics than the two previous examples, which seemed to relate to differences in pore-size distribution and slope angle. He observed a clear transition from saturated to unsaturated drainage at around 10 hr from peak flow values.

Mosley (1979) showed that for a 90 mm rain event in the M8 catchment on 4-5 July 1978, throughflow hydrograph peaks were closely coincident, with lag times from rainfall centre of mass to runoff peak in the order of 1-2 hr. Peak discharge and total flow from the pit faces increased downslope, and total hillslope flow was more than sufficient to account for M8 runoff. The 0.3 ha subcatchment, while occupying 8% of the total M8 catchment area, produced 11% of the peak flow for Mosley's 1978 storm. Cumulative runoff curves (Mosley, 1979; Figure 9) showed that in many events, subsurface flow exceeded cumulative runoff at the main weir.

The results from this investigation support the data presented by Mosley (1979), but also highlight the important relationships between ψ changes in the near-stream, mid-slope and upslope zones and their relation to streamflow rise, peak and recession. Mosley (1979) examined the times at which flow ceased at the lower slope sites and found that it roughly coincided with

flow cessation at the main weir. This implies that subsurface flow is important in generating both stormflow and baseflow to the main channel, the first of which is via macropore flow and the latter by the slow release through the soil matrix. Data from the Pit 5 zone for this study show that mid-slope groundwater development (i.e. water-table height) and pit throughflow are strongly related (in the form of a power curve). Recession linkages for throughflow, streamflow and soil ψ (Figure 5.25) support this concept and identify transition times between the flow processes.

Logarithmic scales are used in each plot, since several studies (e.g. Wilcox, 1959; Nixon and Lawless, 1960; Hewlett and Hibbert, 1963) have shown that the logarithm of unsaturated drainage is linearly related to the logarithm of time. In each plot, three separate periods exist, during which linear relationships exist between the log of the Y variable and the log of time (except for the ψ plot). For throughflow and streamflow, the Y variable is related to time by:

$$Y = at^{-b} \qquad (5.1)$$

where Y is the flow rate, t is the time after peak flow, and a and b are constants specific to the drainage period (Figure 5.25). In the plot of ψ versus the logarithm of time, relationships are not quantified because of negative Y-values. Transition times, at which the rate of ψ recession changes abruptly, can, however, be identified and related to flow information.

For the 29 October event, M8 streamflow and Pit A throughflow follow a consistent three-stage pattern of decline after peak flow values at 1200 hr. M8 streamflow showed a sharp transition at 4 hr, followed by another truncation in the recession line at c.10 hr. Pit A throughflow also displays a

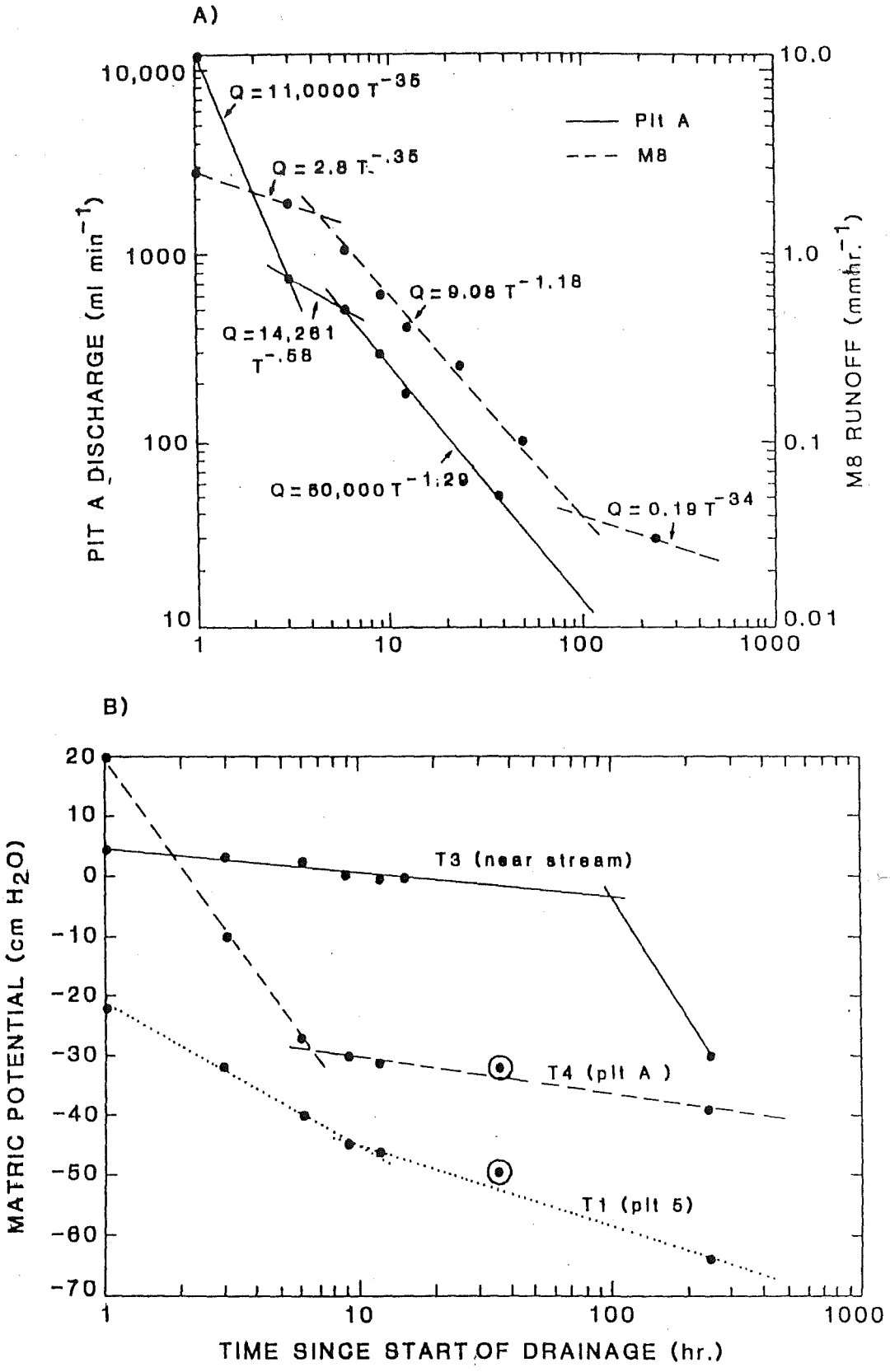

Figure 5.25 Relationship of throughflow and M8 runoff (A) and matric potential (B) with time since the start of drainage for the 29 October event.

three-stage pattern of decline, but out of phase with M8. In this case, an abrupt change in recession occurred at 3 hr and then again at 6 hr, before declining to zero flow. A semilogarithmic plot of ψ versus time (Figure 5.25B) provides some explanation of the flow recession relationships. The marked transition in Pit A throughflow at 3 hr (considered representative of Pit 5 throughflow decline in this example; from data in Mosley, 1979) coincides with ψ shift at Pit 5 from saturated to unsaturated conditions, as indicated by tensiometer T4 (102 cm) at Site 1. The second transition at 6 hr matches the marked change in slope of T4 recession at that time, again demonstrating a sensitive ψ-throughflow relationship. The ψ recession shift probably relates to the change from pipe drainage of perched groundwater to matrix-dominated drainage of soil water.

The initial change in M8 recession is midway between the two stage recession of Pit A. These conditions reflect hillslope flow drainage, but also near-stream contributions, that would have continued after hillslope flow decline. Nevertheless, the break in slope, although lagged, probably represents the decline of hillslope inputs, and the main recession slope matches Pit A decline. The transition of M8 recession at 10 hr coincides with a transition in near-stream water-table conditions. Figure 5.25B shows that the near-stream tensiometer T3 (38 cm) at Site 1 experienced an abrupt change in ψ recession somewhere near 100 hr. This time also roughly coincides with a shift from a partly saturated near-stream soil profile to unsaturated conditions.

6 HILLSLOPE TRACER EXPERIMENTS

6.1 INJECTION AND COLLECTION PROCEDURES

Mosley (1979) conducted 8 dye tracing experiments in a 0.38 ha sub-catchment, at the end of a storm that delivered 34 mm of rainfall in 48 hr. Dye was applied to the soil surface approximately 0.5-4 m upslope from a pit face through a 150 mm diameter cylinder pressed vertically into the organic horizon. These experiments were followed by another series of injections (Mosley, 1982), where dyed water was applied to the soil surface at 51 different sites within the Tawhai State Forest, through line-source troughs 1 m upslope from a pit face. By computing subsurface flow velocities of water movement from the point of injection to the pit face, Mosley concluded that in most cases, applied water 'short-circuited' the soil matrix (via macropores) en route to the pit face, and moved at rates up to 2 orders of magnitude greater than the soil K_{sat}.

Isotopic tracing results of Pearce et al. (1986) and Sklash et al. (1986), reviewed in section 2.5.2, explicitly refuted Mosley's interpretations by showing that old water dominated throughflow both between and during storm runoff events. More importantly perhaps, Pearce et al. (1986, p.1270) criticised dye tracing techniques by stating that "the appropriateness of field methods which have demonstrated rapid throughflow velocities is placed in serious doubt". Sklash et al. (1986, p.1282) also questioned the applicability of dye tracing by stating that "conclusions from dye tracer tests in the M8 catchment and other watersheds are in serious doubt".

The tracer experiments of Mosley (1979; 1982) were repeated in an attempt to reconcile his results with the Pearce et al. (1986) isotopic results and to observe directly, the possible

flow of water out of macropores at the pit faces. In addition to simple injection and collection of water (as performed by Mosley), soil water potentials were monitored in some cases, together with outflow water chemistry and isotopic characteristics. Travel velocities were not computed, but rather general outflow hydrograph shapes and timing were related to chemical and isotopic variations in throughflow. Due to logistical constraints, isotopically labelled water was not available for injection. A nearby stream was used as a water source, with the hope that isotopic concentrations would be sufficiently distinct from hillslope soil water to enable isotopic separation of input and ouput water.

In each experiment, water was applied to the soil surface through a 1.5 m wide trough, with holes drilled at 100 mm intervals along the base. Injection rates averaged 3 l min^{-1}, with total application volumes ranging from 15-60 l. Troughs were positioned at 1-3 m distances upslope from the pit faces. Rates of application were consistent with the range of subsurface flow discharges observed by Mosley (1979) under natural rain events (c. up to 5 l min^{-1} m of $contour^{-1}$). Tracer outflow from the pit face was monitored by timing and filling varying combinations of 100, 250 and 1000 ml beakers for periods of 5-60 sec. Water samples were also collected at various times throughout the tracer hydrograph. In some cases, Rhodomine B and Rhodomine WT dyes were incorporated into the injection water. Dye travel pathways were monitored at the pit face, the point of outflow. In later experiments, soil upslope of the pit was excavated to determine travel pathways through the soil. Organic soil was also removed to determine the relative importance of organic layer versus mineral soil water movement.

Tracer experimental results are presented below for 10 different applications at three selected pits within the 0.3 ha sub-catchment. Data is analysed following the procedure of Mosley (1979; 1982), and then discussed in relation to the work of Pearce et al. (1986) and Sklash et al. (1986) in section 6.3. Specifically, the question of how isotopically new input water rapidly acquires an old water signature is addressed.

6.2 TRACER EXPERIMENT RESULTS

6.2.1 Experiment 1

A 30 l application was performed 1 m upslope from Pit A on 11 November. API_7 and API_{14} were 7.9 mm and 11.7 mm respectively and no rain had fallen within 3 days of application. The first trace of water appeared at the pit face at 2.5 min (Figure 6.1A). The outflow hydrograph responded very rapidly, with peak outflow (3400 ml min^{-1}) at 6-8 min after initial application. Audible rushing of water through the organic layer and over the mineral soil was observed, particularly within the first 10 min of hydrograph response. Approximately 68% of the supply water reached the pit face within 50 min, at which time flow rate had dropped to only trace amounts.

Cl variations through the event show considerable flushing of supply (event) water. Pre-event seepage from the pit face was 7.299 ppm. The first water sample (4 min) showed considerable event water flushing (supply water = 3.241 ppm), with Cl concentrations dropping to 4.015 ppm. Cl concentration reached its lowest value at 6 min (3.794 ppm) and then rose gradually for the next 50 min to a value of 4.488 ppm (Figure 6.1B). δD values reflect the Cl changes but show some increase in old water discharge at c.20 min and then back to event water values (Figure 6.1C). δD interpretation is limited in this case because the supply water δD value (-35.3‰) was only 1.3‰ away from the

Figure 6.1 Experiment 1 water volume, chloride and deuterium relationships, Pit A.

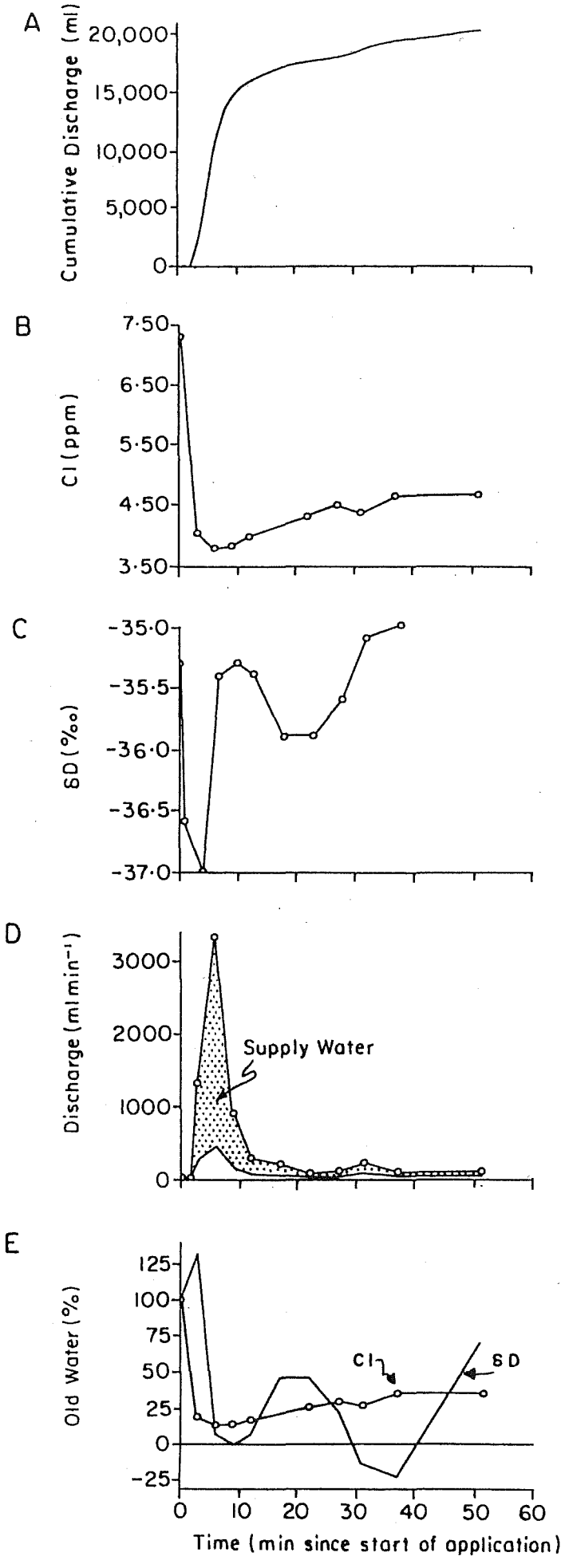
A
Cumulative Discharge (ml)
20,000
15,000
10,000
5,000
0
B
Cl (ppm)
7·50
6·50
5·50
4·50
3·50
C
δD (‰)
-35·0
-35·5
-36·0
-36·5
-37·0
D
Discharge (ml min⁻¹)
3000
2000
1000
0
Supply Water
E
Old Water (%)
125
100
75
50
25
0
-25
Cl
δD
0
10
20
30
40
50
60
Time (min since start of application)

pre-event flow value (-36.6‰). Since the analytical precision is +/-1‰, δD trends in this case must be treated with caution. For this reason also, hydrograph separation was not performed based on δD values.

Hydrograph separation using the Cl values in the mass balance is shown in Figure 6.1D. Very large new (supply) water volumes are evident in the separation, particularly during the peak hydrograph response. This is again indicative of rapid flushing of new water as described above. Old water percentages are plotted in Figure 6.1E and show that using the Cl separation, old water moved from a minimum of 10% at peak flow, steady upward to a peak value of approximately 35% as the soil slowly drained after the application. Old water percentages based on the δD mass balance are also shown in Figure 6.1E and re-inforce the problems noted earlier regarding its relevance for this experiment. Old water percentages were unrealistic in many cases (i.e. <100% and >0%), as noted in the plot.

6.2.2 Experiment 2

A 30 l application trial was conducted 1 m upslope from Pit 5 on 11 November in order to compare responses from experiment 1. API_7 and API_{14} values were very similar to experiment 1, and no rain occurred between the two experiments. Peak discharge was 40 times less than Pit A for the same application (Figure 6.2A), mainly due to much thicker local soil characteristics (c.1.5 m). A small amount of flow through the 150 mm organic layer, perched on the mineral soil surface, was observed during the early stages of application. No visible flow occurred through the soil matrix, although a saturated layer at the mineral soil-Old Man Gravel interface seemed to produce most of the flow.

Hydrograph response (Figure 6.2B) was quite erratic and did not show a typical sinusoidal rise to peak and recession curve.

Figure 6.2 Experiment 2 water volume, chloride and deuterium relationships, Pit 5.

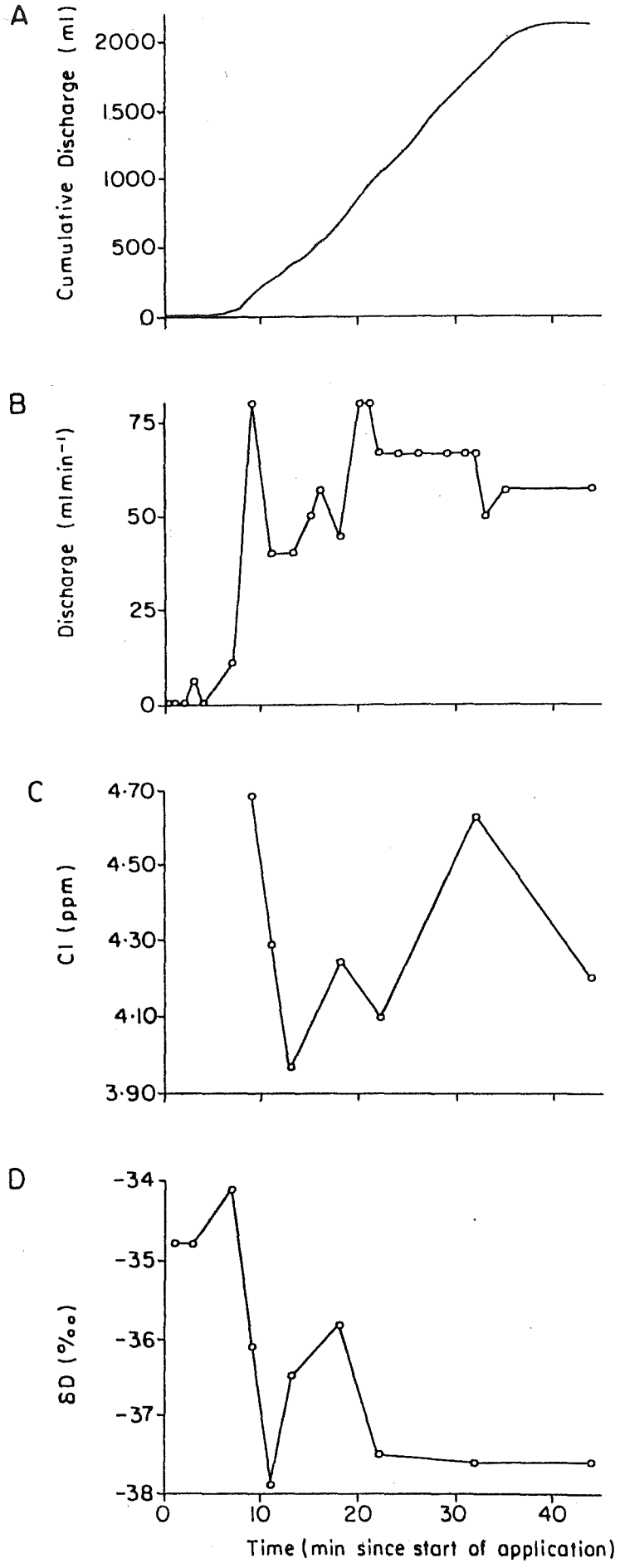
A
Cumulative Discharge (ml)
2000
1500
1000
500
0
B
Discharge (mlmin⁻¹)
75
50
25
0
C
Cl (ppm)
4·70
4·50
4·30
4·10
3·90
D
δD (‰)
-34
-35
-36
-37
-38
0
10
20
30
40
Time (min since start of application)

Rather, flow peaked immediately after application finished, subsided slightly, and then increased and maintained a constant flow. In this case, outflow Cl variations through the event were less than 1 ppm, indicating little if any flushing of applied water (Figure 6.2D). δD values corroborate Cl trends, by indicating large exfiltration of old stored matrix water. Since there was no pre-event seepage from Pit 5, suction lysimeter δD values from SL3, SL4 and SL5 were used to portray pre-event soil water δD conditions. Soil δD values for the 3 lysimeters averaged -40.0°/$_{oo}$ (SD=0.4°/$_{oo}$). When plotted with δD variation for the hydrograph (Figure 6.2D), the pit flow δD signature moved from a supply value of c.-28°/$_{oo}$ toward a soil water value of -37.5°/$_{oo}$.

Site 1 (Figure 5.13) tensiometric response to the experiment 2 application is shown in Figure 6.3. Soil water potential is plotted as a function of soil depth (Figure 6.3A) and as a continuous function of time (Figure 6.3B) for tensiometers T1-T4. Prior to the application, unsaturated conditions were maintained, with downward drainage through most of the profile. Non-steady state flow occurred immediately following water input, at 10 (t_{10}) and 20 (t_{20}) minutes. T1 (19 cm) showed negligible change during this period, but deeper tensiometers (T2-T4) responded substantially, indicating bypass flow of input water to depth. Water bypassed the upper mineral soil and moved to the T2 (37 cm) depth at t_{10}. At t_{20}, much of the bypass continued to move through the profile, and T3 (76 cm) and T4 (102 cm) responded with lower magnitude matric potential values.

6.2.3 Experiment 3

On 19 November, experiment 1 was repeated at Pit A using the same application volume, but this time moving the trough to 3 m upslope from the pit face. Rhodomine B dye was incorporated into the supply, and water pathways were traced as much as possible

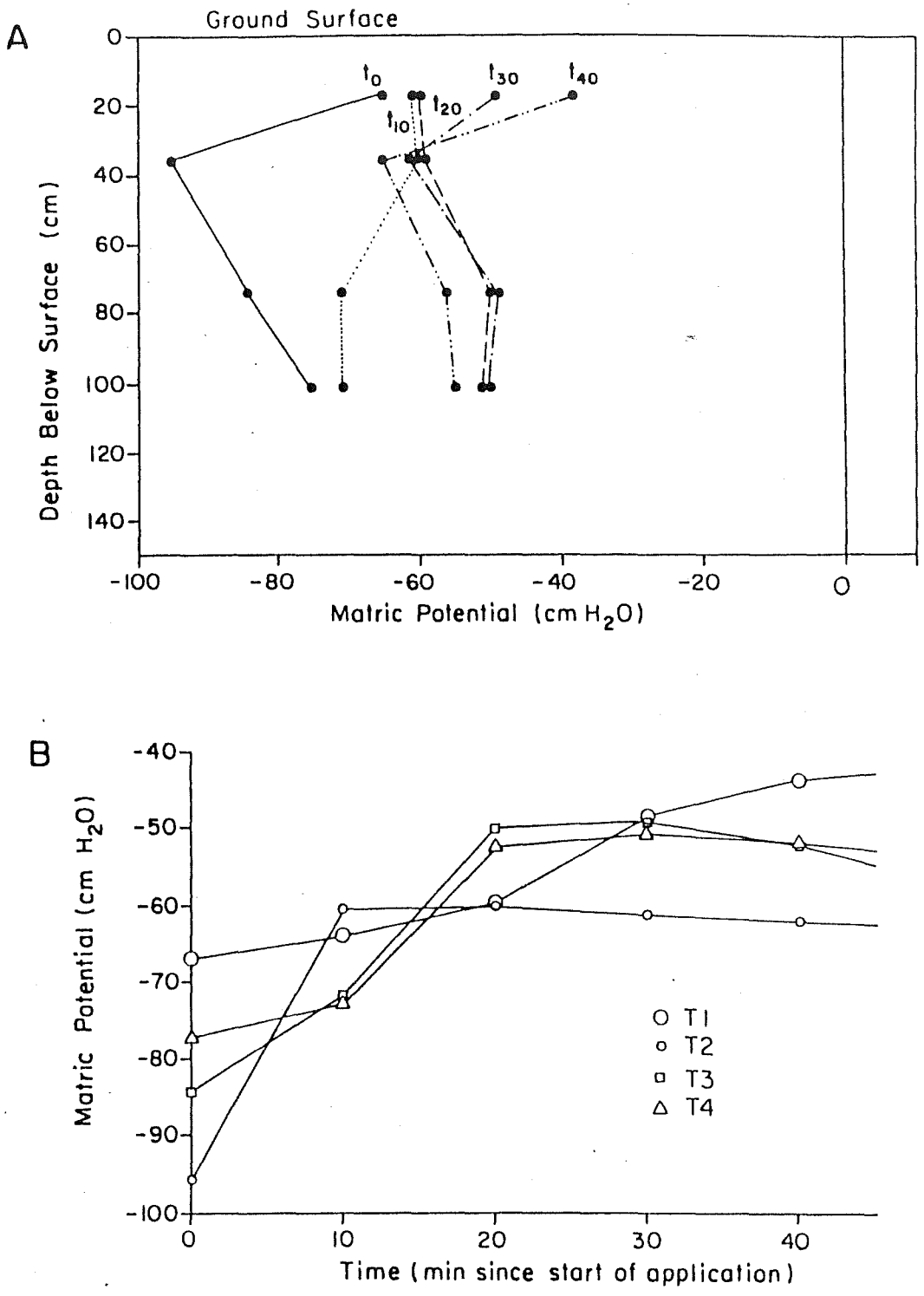

Figure 6.3 Experiment 2 matric potential response to water input, Pit 5.

without disturbing the soil structure. Flow to the pit face was notably reduced significantly to 1% of total application water (Figure 6.4A), indicating much larger losses to the matrix. The first appearance of flow at the pit face occurred at 11 min. Dyed water emanated from both the soil-organic layer interface and the soil-Old Man Gravel interface. Flow through the organic layer perched on the mineral soil was considerably less important than in experiment 1, with much more water entering the matrix. Most of the flow to the pit face followed a distinctly concentrated zone, reflecting local microtopographic conditions. Seepage at the pit face was concentrated in an area roughly 200 mm x 200 mm, even though the injection was spread 1.5 m across the slope. At 23 min, some clear water appeared in the concentrated seepage area, and by 37 min most of the water was clear.

Cl concentrations varied less than 1 ppm, indicating very little supply water flushing (Figure 6.4C). Unfortunately, δD supply and Pit A pre-event flow were within 1‰ of each other. It is interesting to note that δD signatures immediately prior to the hydrograph rise, move away from the supply and pre-event flow values (Figure 6.4D), to a value very close to SL6 (-38.8‰). Dye was noticed at the pit face 6 min previous to this, indicating that deeper soil water was initially displaced. During the rising limb of the hydrograph, δD values rose steadily to almost pre-storm values. This could represent two processes: (i) a return to pre-event δD conditions, or more realistically, (ii) the supply water moving through the system. Given the amount of dyed water making its way to the pit face, the second interpretation seems valid.

6.2.4 Experiment 4

A 60 l injection of water was made 1 m upslope from Pit 5 on 19 November. The experiment was conducted to see what effect

Figure 6.4 Experiment 3 water volume, chloride and deuterium relationships, Pit A.

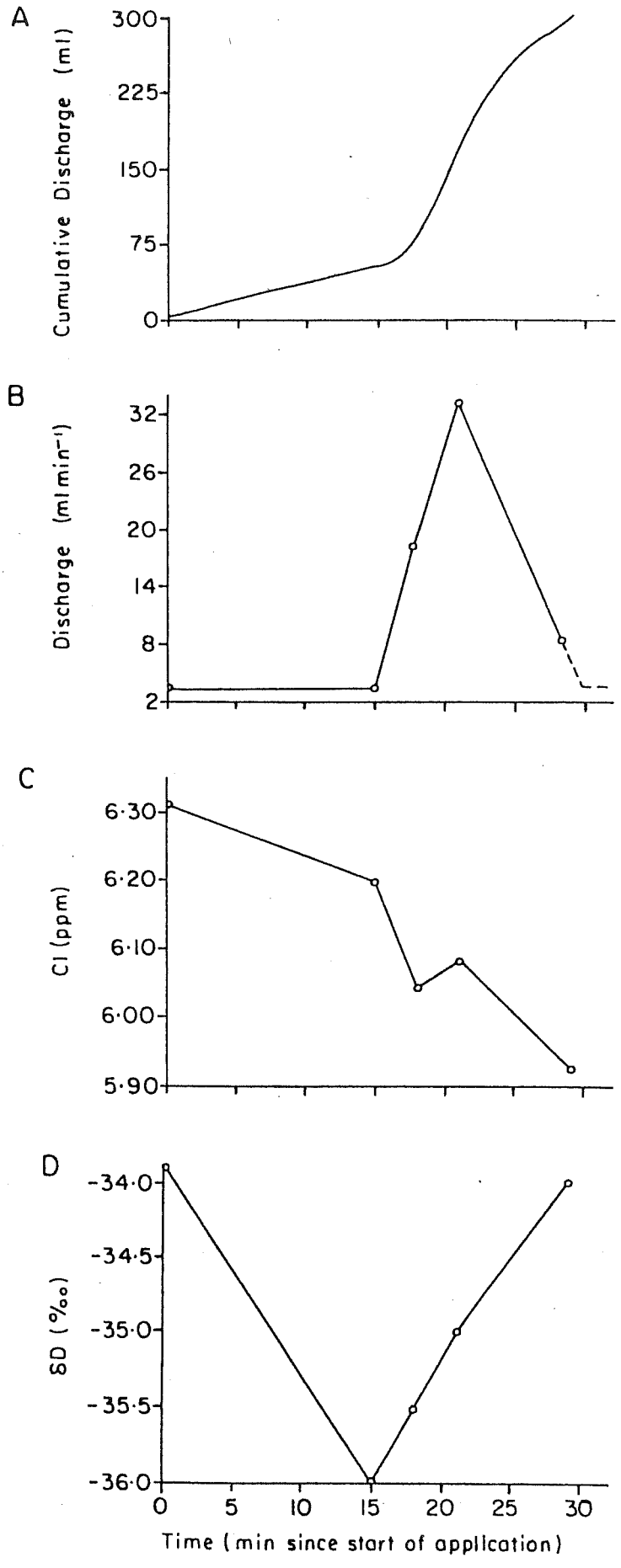
A
Cumulative Discharge (ml)
300
225
150
75
0
B
Discharge (ml min⁻¹)
32
26
20
14
8
2
C
Cl (ppm)
6·30
6·20
6·10
6·00
5·90
D
δD (‰)
-34·0
-34·5
-35·0
-35·5
-36·0
0
5
10
15
20
25
30
Time (min since start of application)

doubling the input of experiment 2 would have on pit throughflow response. Peak flow rate increased by a factor of 5 (Figure 6.5A), and the hydrograph shape was much more regular in form than the irregular response from experiment 2. The pit hydrograph was bimodal, with an initial peak response of 400 ml min^{-1}, followed by a second more attenuated peak of c.300 ml min^{-1} (Figure 6.5B). From observations made at the pit face, it seemed that the first peak was due to rapid shallow flow through the organic layer, perched on the mineral soil, while the latter response was attributable to deeper flow from the mineral soil-Old Man Gravel interface.

Both Cl and δD data seem to confirm the notion of initial supply water flushing followed by displacement of old water. Outflow Cl values showed elevated concentrations (i.e. >4.5 ppm) during the initial hydrograph peak, and then a slow but constant rise from 3.8 ppm to 4.1 ppm. Since supply water Cl and suction lysimeter Cl concentrations were within 1.0 ppm, it is difficult to quantify these changes. δD shifts provide a clearer picture of old water displacement, as indicated by a shift from supply water (-35.9°/$_{oo}$) to a value close to SL5 (-41°/$_{oo}$). δD values also show some flushing of shallow soil water (or organic layer water), because δD concentrations were actually lighter than the supply, and more characteristic of SL4 (-33.1°/$_{oo}$).

Soil matric potential (Figure 6.6) responded rapidly to water input. Matric potential shifts were similar to experiment 2 and indicated bypassing of the upper soil depths during initial wetting, followed by drainage characteristics similar to pre-input conditions. This interpretation corroborates chemical and isotopic evidence, which also suggests that water moved quickly to depth and then displaced older water toward the pit face.

Figure 6.5 Experiment 4 water volume, chloride and deuterium relationships, Pit 5.

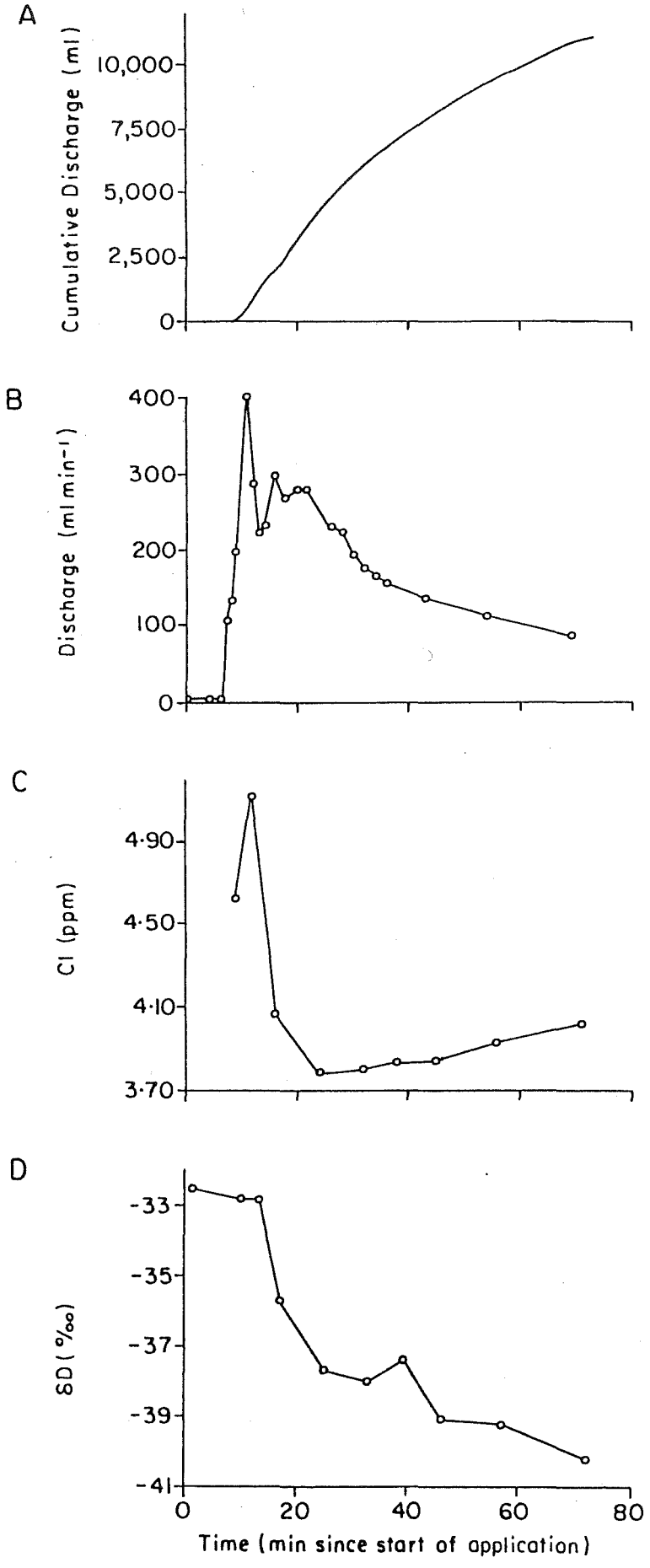
A
Cumulative Discharge (ml)
10,000
7,500
5,000
2,500
0
B
Discharge (ml min⁻¹)
400
300
200
100
0
C
Cl (ppm)
4·90
4·50
4·10
3·70
D
δD (‰)
-33
-35
-37
-39
-41
0
20
40
60
80
Time (min since start of application)

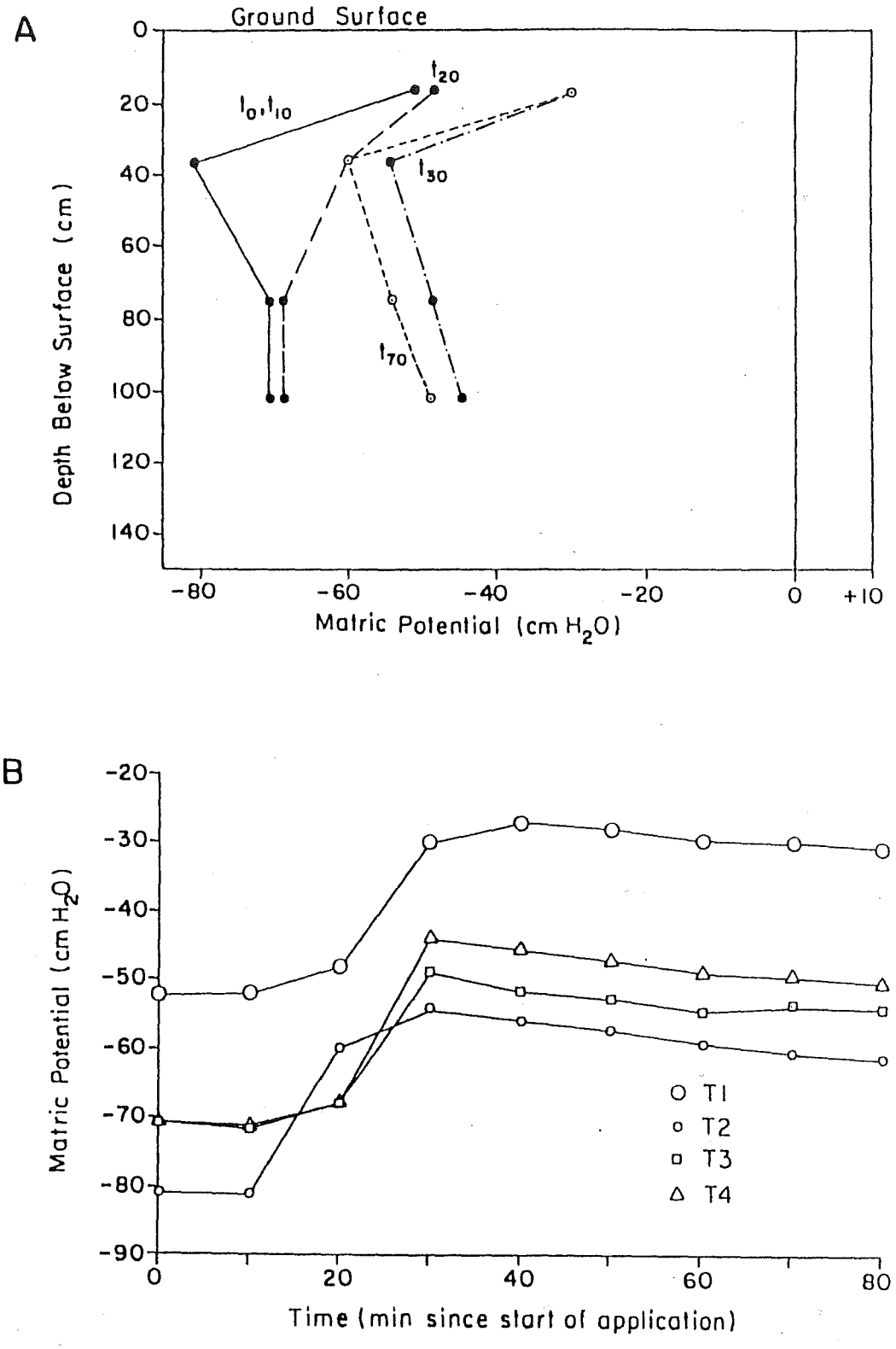

Figure 6.6 Experiment 4 matric potential response to water input, Pit 5.

6.2.5 Experiment 5

On 16 December, a series of applications (experiments 5, 6 and 6A) were conducted at Pit A, with various configurations of trough location and injection rate. Figure 6.7 shows the pit hydrograph for the three applications and provides some comparison for event time and response magnitude.

Prior to experiment 5, Pit A seepage was roughly 1 drip from the outflow hose every 2 sec. Six litres of Rhodomine B dyed water was applied through a 150 mm diameter cylinder, 1 m upslope from the pit face. This was the first time a cylinder injection was used, and was done to provide some basis for comparison between the methods of Mosley (1979; 1982) and their effect on throughflow rates and interpretations. The cylinder was pressed downward through the organic layer and into the mineral soil. Water ponded in the ring and no infiltration occurred within the first 15 min (Figure 6.8A). The ring was then raised out of the mineral soil, so that its base rested in the organic horizon, immediately above the mineral soil surface. Water flowed freely from the cylinder at this point and produced an immediate and large hydrograph rise (Figure 6.8B). Forty-two percent of the supply flowed from the pit face within 50 min, at which time flow returned to its pre-application rate.

Cl and δD concentrations through the hydrograph are difficult to explain. δD signatures shifted from a pre-application value of c.-36°/$_{oo}$ (very similar to SL6 δD), towards a supply water signature of -34.6°/$_{oo}$ and then increased to c.-32°/$_{oo}$ (similar to SL7 δD), before returning to a more constant level between that of the supply δD and pre-event flow δD (Figure 6.8D). This effect may be representative of rapid flushing through the organic horizon, incorporating isotopically lighter shallow soil water (as indicated by a shift towards SL7

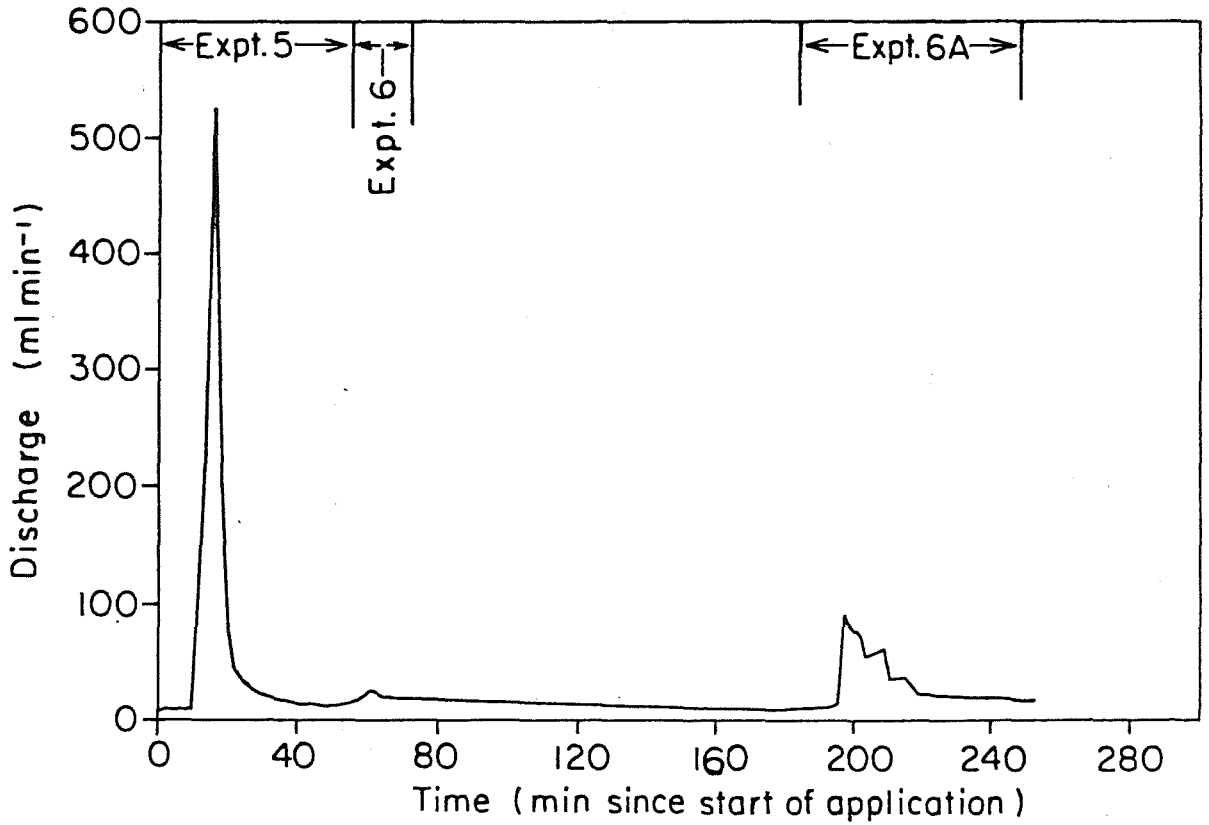

Figure 6.7 Experiments 5, 6 and 6A water volume relationships, Pit A.

Figure 6.8 Experiment 5 water volume, chloride and deuterium relationships, Pit A.

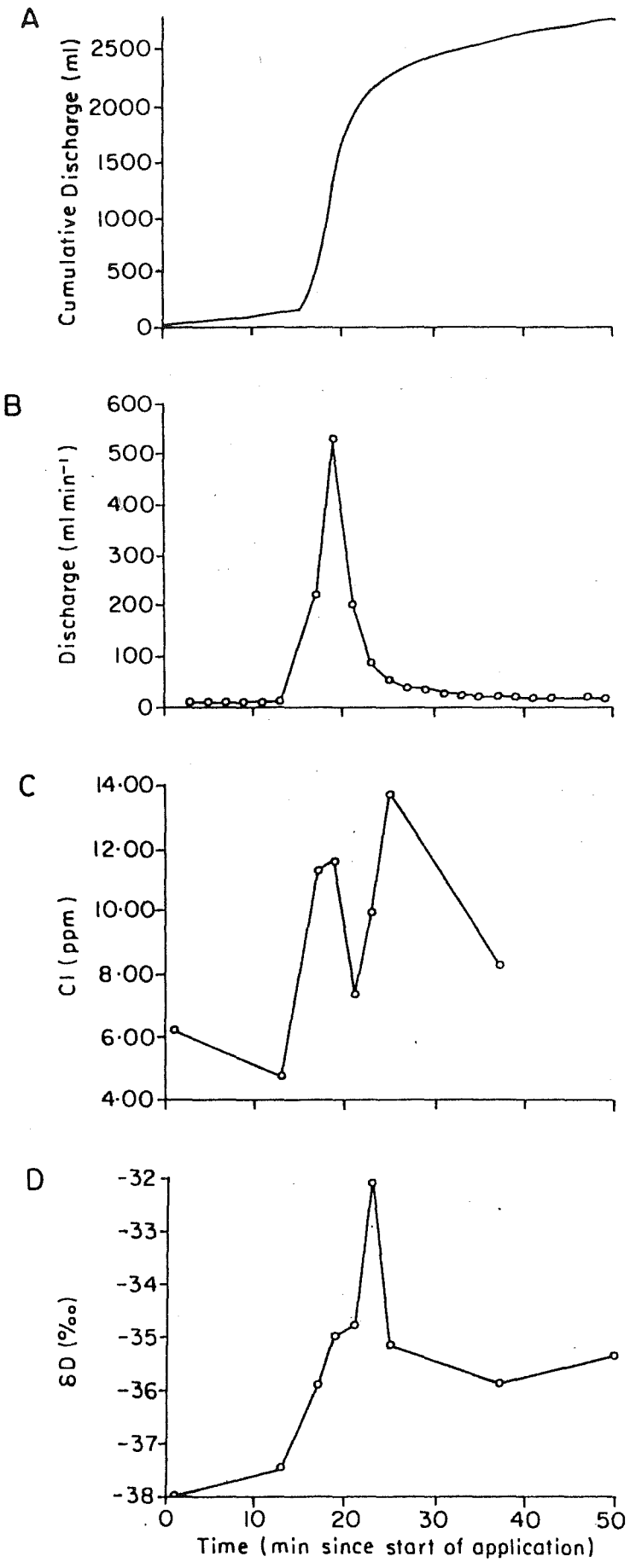
A
Cumulative Discharge (ml)
2500
2000
1500
1000
500
0
B
Discharge (ml min⁻¹)
600
500
400
300
200
100
0
C
Cl (ppm)
14·00
12·00
10·00
8·00
6·00
4·00
D
δD (‰)
-32
-33
-34
-35
-36
-37
-38
0
10
20
30
40
50
Time (min since start of application)

values), in the downslope movement to the pit face. Cl values on the other hand, show a shift away from the supply Cl concentration (3.865 ppm) toward 14.000 ppm, a value more than double that of the pre-storm flow (6.214 ppm) and SL6 (4.727 ppm; Figure 6.8C).

6.2.6 Experiment 6

Forty-five minutes after the initial experiment 5 application, 15 l of water was applied through the 1.5 m wide trough, 3 m upslope from the Pit A face (Figure 6.9A). The general goal was to see if additional dyed water from the preceding application would be displaced by the upslope water input. Based on the results of experiment 3, where the ratio of matrix flow (both capillary and non-capillary) to organic layer flow (over the mineral soil surface) was relatively high, it was expected that infiltrated experiment 5 water would be displaced by this movement.

Response to the 15 l application was negligible; from a pre-storm flow rate of 11 ml min^{-1} to 28 ml min^{-1} (Figure 6.9B). A typical hydrograph shape was produced and showed a slightly bimodal response. At approximately 60 min (i.e 15 min after the new injection), flow appeared at the organic layer-mineral soil interface. This first 150 ml of flow had a δD value of -37°/$_{oo}$, indicative of the supply water value of c.-38°/$_{oo}$ (Figure 6.9D). Subsequent to the first flow sample, δD moved back toward a pre-application value of -35.4°/$_{oo}$. Cl values (Figure 6.9C) cannot be explained.

6.2.7 Experiment 6A

One hundred and ninety minutes after the first application in experiment 5, and 145 min after the second application in experiment 6, an additional 15 l was applied through the trough, 3 m upslope from the pit face. 9 min after this application,

Figure 6.9 Experiment 6 water volume, chloride and deuterium relationships, Pit A.

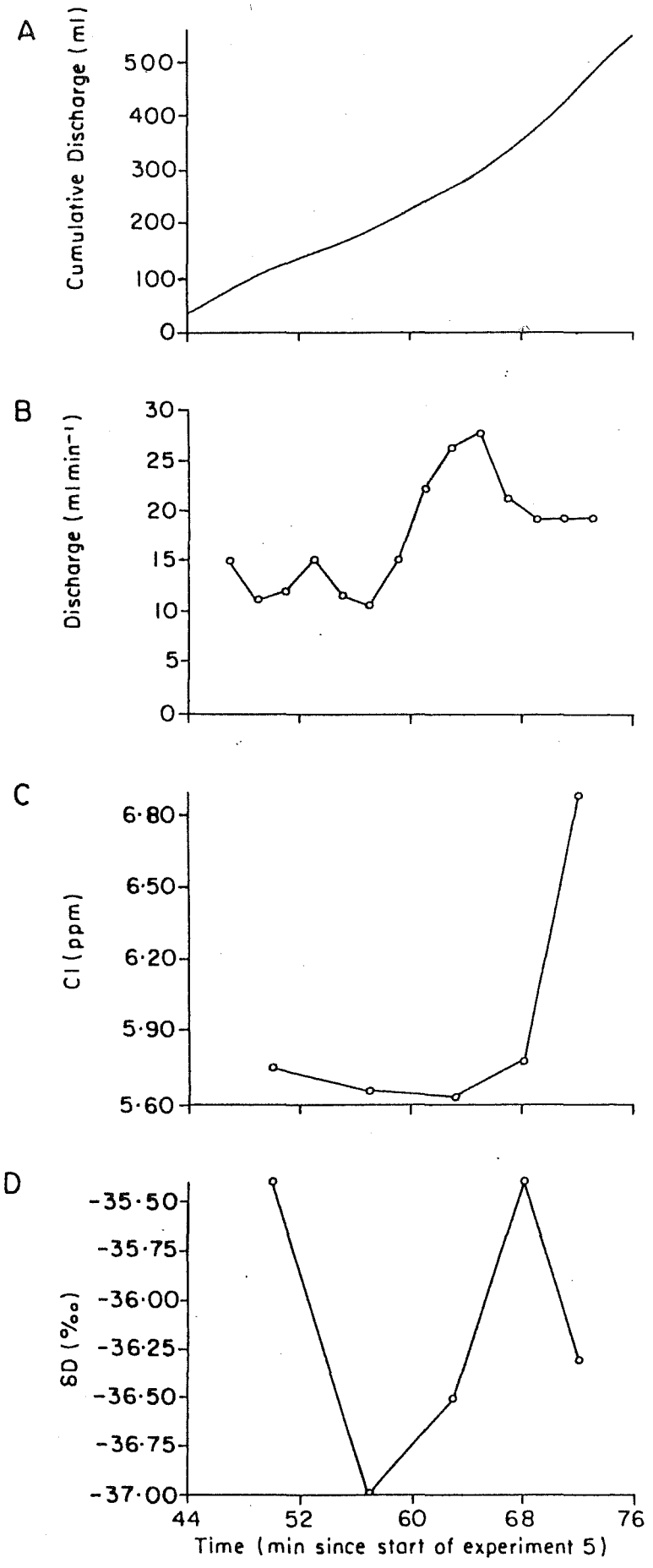
A
Cumulative Discharge (ml)
500
400
300
200
100
0
B
Discharge (ml min⁻¹)
30
25
20
15
10
5
0
C
Cl (ppm)
6·80
6·50
6·20
5·90
5·60
D
δD (‰)
-35·50
-35·75
-36·00
-36·25
-36·50
-36·75
-37·00
44
52
60
68
76
Time (min since start of experiment 5)

water appeared at the face. Less than 5% of the applied water was recovered after 250 min (Figure 6.10A), and presumably this would also include some water from the previous 2 applications. Dyed water (from experiment 5) dominated the flow until 210 min, when flow cleared considerably. Even after the hydrograph peak, almost all flow seemed to move through the organic layer, perched on the mineral soil surface. Flow and chemical data are shown in Figure 6.10B-D. Cl and δD are not analysed because of the small water volumes involved.

6.2.8 Experiment 7

Forty-five litres of water was applied through two troughs, 2 and 4 m upslope from the Pit 5 face on 16 December. No pit flow occurred prior to the application, and there was no change up to 50 min after injection. It is assumed that all water infiltrated and was absorbed into the unsaturated matrix.

6.2.9 Experiment 8

In order to examine matric response to water input at the Pit A site, a Scanivalve recording tensiometer unit was moved from the near-stream site to the Pit A location. Four tensiometers were inserted 0.5 m (T2, T13) and 1 m (T1, T3) upslope from the pit face at depths of 19, 31, 38, and 16 cm respectively. On 17 December, 15 l was applied to the soil surface, 1.25 m upslope from Pit A. Pre-application throughflow was 10 ml min^{-1} and reflected a small 7 mm rain event from the previous day. Cumulative flow (Figure 6.11A) was 39.3%. of total water input. Most flow (as in previous experiments) was from the organic layer over the mineral soil surface. Water flowed from the pit face within 3.5 min and peaked within 5 min (Figure 6.11B).

Figure 6.10 Experiment 6A water volume, chloride and deuterium relationships, Pit A.

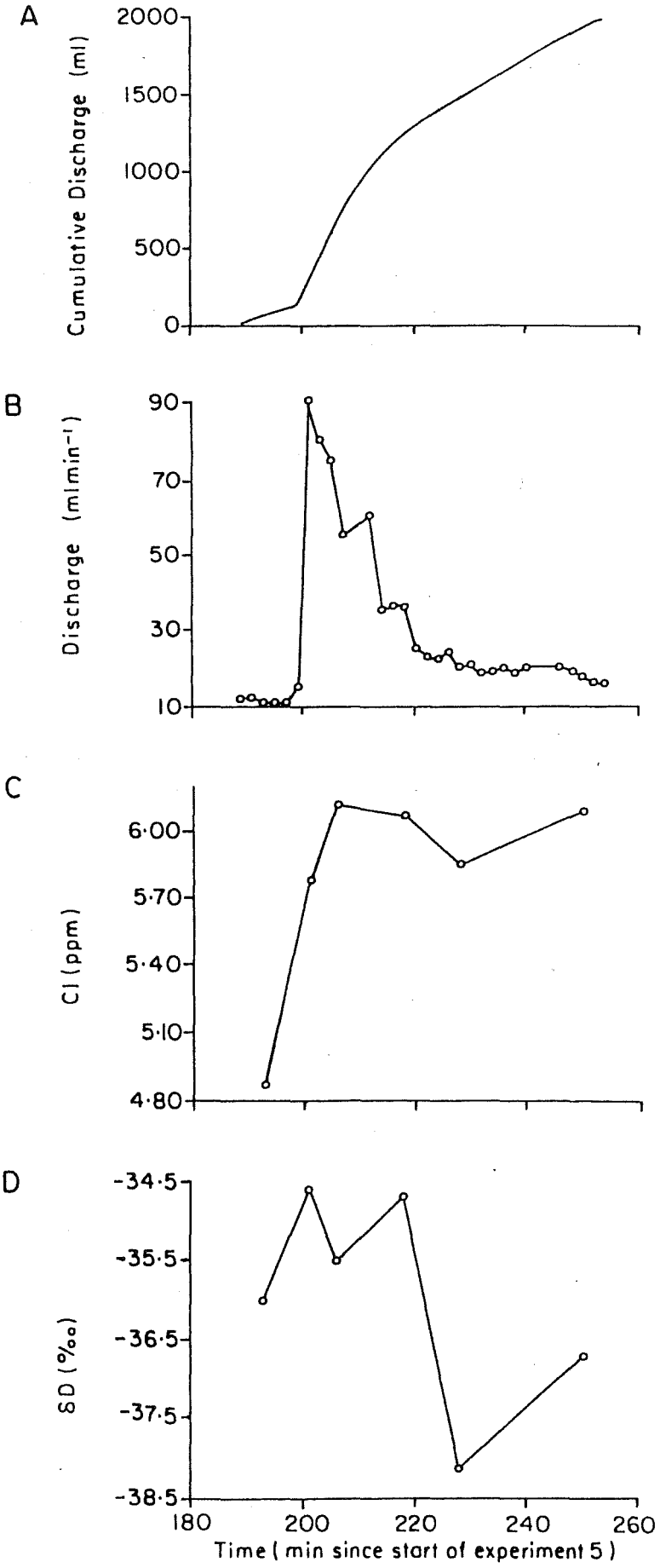
A
Cumulative Discharge (ml)
2000
1500
1000
500
0
B
Discharge (ml min⁻¹)
90
70
50
30
10
C
Cl (ppm)
6·00
5·70
5·40
5·10
4·80
D
δD (‰)
-34·5
-35·5
-36·5
-37·5
-38·5
180
200
220
240
260
Time (min since start of experiment 5)

Figure 6.11 Experiment 8 water volume, chloride and deuterium relationships, Pit A.

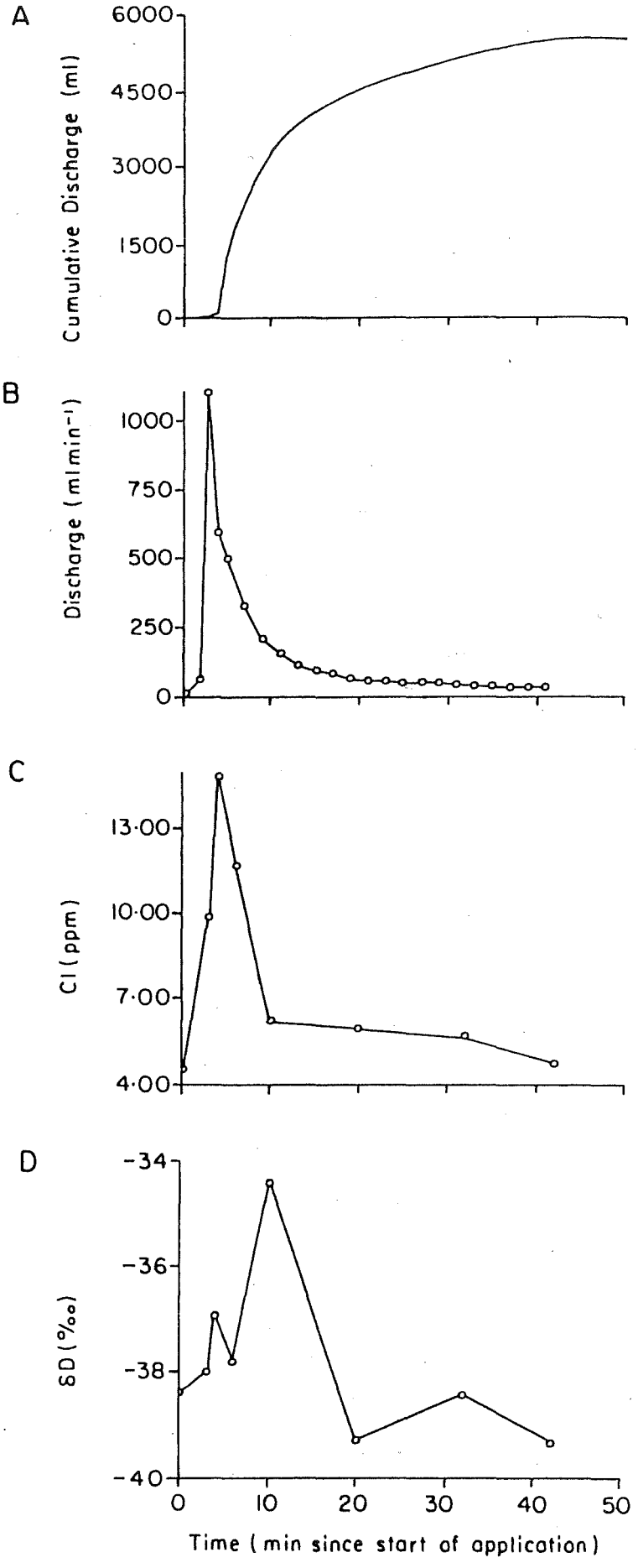
A
6000
4500
3000
1500
0
Cumulative Discharge (ml)
B
1000
750
500
250
0
Discharge (ml min⁻¹)
C
13·00
10·00
7·00
4·00
Cl (ppm)
D
-34
-36
-38
-40
δD (‰)
0
10
20
30
40
50
Time (min since start of application)

Cl response mirrored the pit throughflow hydrograph, but elevated concentrations are difficult to interpret (Figure 6.11C). Cl shifted rapidly from a pre-application 4.432 ppm to c.17.500 ppm and then quickly back to a constant c.8.000 ppm. Supply water Cl concentration was only 2.900 ppm and cannot account for such high values during peak flow. δD variations through the hydrograph show rapid flushing of supply and shallow soil water, with a shift from pre-storm δD (-38.4°/$_{oo}$) to -34.5°/$_{oo}$ (cf. SL4=-33.1°/$_{oo}$), and then back to deeper matrix water signatures (SL3=-38.9°/$_{oo}$).

Tensiometer response was negligible and reinforces the isotopic interpretation of rapid flushing over the mineral soil surface (Figure 6.12) without contacting the soil matrix. T1 and T13 (representing the deeper soil zone) showed no response within 50 min of application (Figure 6.12A) or even 200 min after application (Figure 6.12B). T2 and T3 showed a very slow ψ shift of c.10 cm H_2O over 50 min (Figure 6.12A), and then peaked roughly 100 min after application. This peak represents slow vertical drainage through the profile, which would presumably continue propagating downward to the T1 and T13 tensiometer sites, sometime after 200 min.

6.2.10 Experiment 9

In order to compare the response of pits located in topographic hollows (Pits 5 and A) to pit response on nose slopes, Pit 2 (Mosley, 1979, p.797) was used for an experimental run. Fifteen litres of water was applied in the usual manner, 1 m upslope from the pit face on 17 December. Soil depth at the pit face was 350 mm, including a 30 mm organic layer. Although mineral soil K_{sat} values were almost 2 orders of magnitude greater than those at Pits A and 5 (for equivalent topographic positions from data given in Table 5.4), most flow occurred

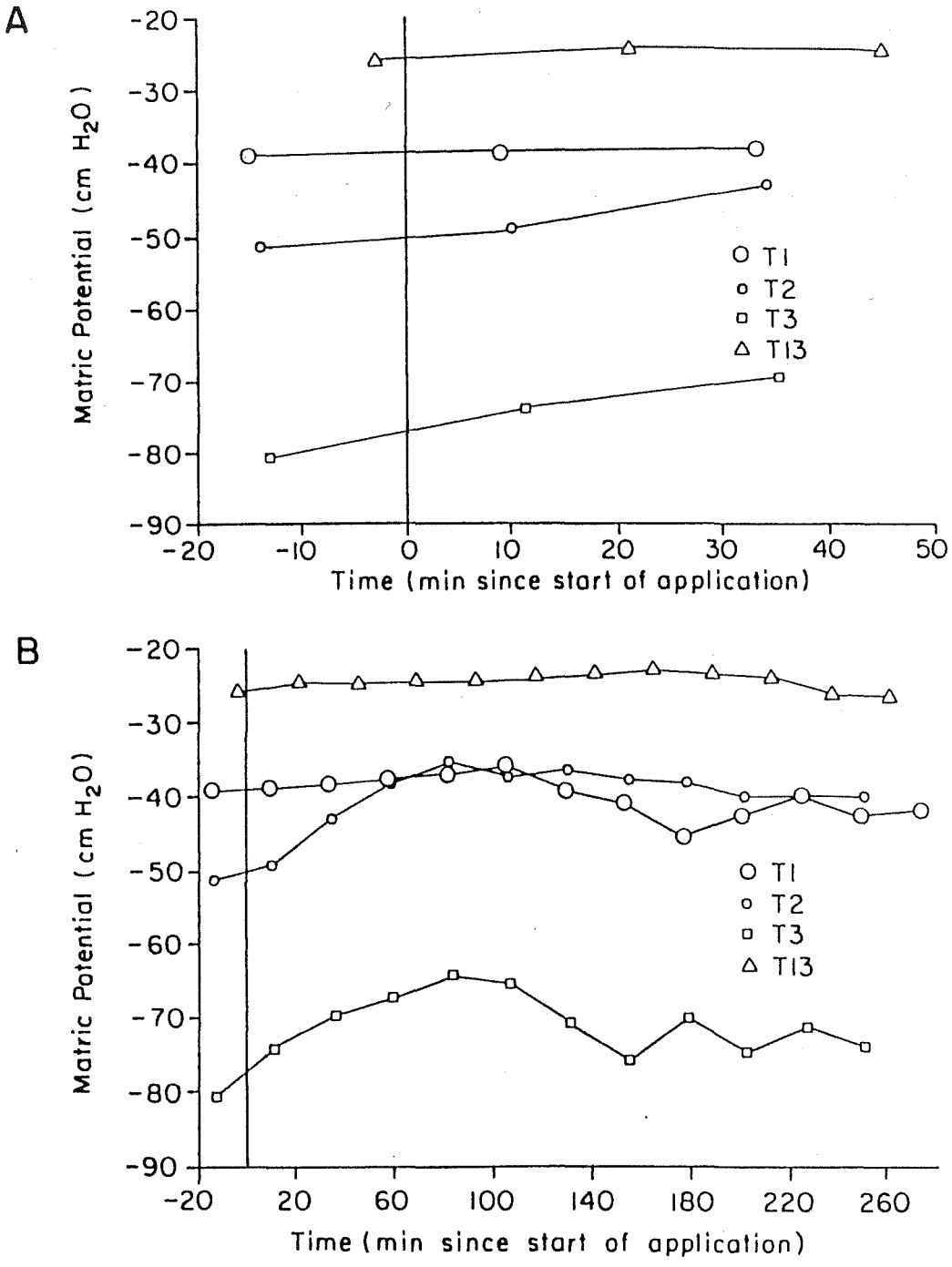

Figure 6.12 Experiment 8 matric potential response to water input, Pit A.

through the organic layer and over the mineral soil surface. However, a significant portion of the introduced water did flow through the complete depth of the mineral soil matrix and extended over the full width of the pit face. Prior to application, the pit face was completely unsaturated and pre-event pit flow was zero. Of the total application volume, 80% flowed through the trough within 30 min (Figure 6.13A). This represents the largest recovery of any of the experimental runs and gives some indication of the transmission properties of this soil/slope situation.

Both Cl and δD variations show remarkably similar and consistent patterns, with an initial steep rise toward soil water signatures, followed by a slight trend toward supply water values and then back toward soil water values again. Soil water Cl and δD concentrations were assumed to be equivalent to SL4 values, since slope positions and soil depths were roughly similar. Although Cl did mirror δD response, the magnitude of the shift (from 3.500 ppm to 7.000 ppm) is difficult to rationalise, since SL4 was 2.330 ppm (Figure 6.13B). Suction lysimeter values from other similar slope positions were somewhat higher (i.e. SL6=4.727 ppm and SL7=3.917 ppm), but again are not high enough to explain peak Pit 2 Cl of 7.000 ppm.

δD trends are more readily explicable and are consistent with suction lysimeter information. Initial flow from Pit 2 showed rapid flushing of supply water (-37.7‰), followed by a rapid shift toward soil water δD values (SL4=-33.1‰; Figure 6.13C). Hydrograph separation was performed using SL4 as the old water component in pit throughflow (Figure 6.13D). Although isotopic values reinforce the notion of rapid supply water flushing, it is interesting to note the rapid increase in old

Figure 6.13 Experiment 9 water volume, chloride and deuterium relationships, Pit 2.

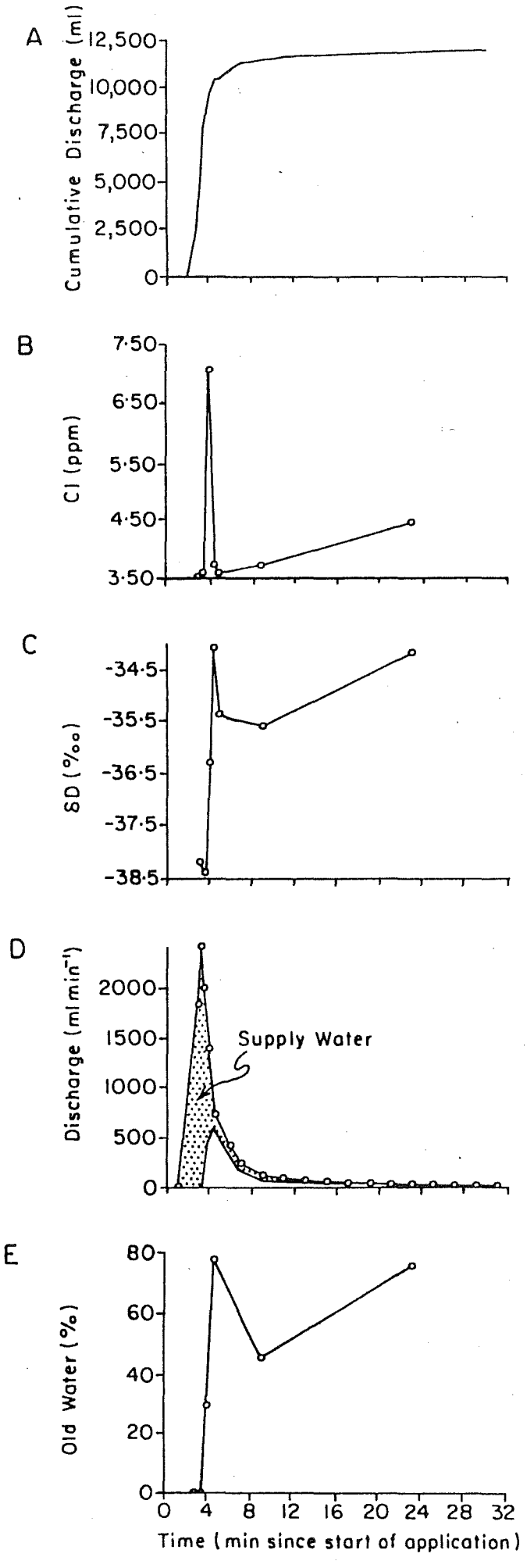
A
Cumulative Discharge (ml)
12,500
10,000
7,500
5,000
2,500
0
B
Cl (ppm)
7·50
6·50
5·50
4·50
3·50
C
δD (‰)
-34·5
-35·5
-36·5
-37·5
-38·5
D
Discharge (ml min⁻¹)
2000
1500
1000
500
0
Supply Water
E
Old Water (%)
80
60
40
20
0
0 4 8 12 16 20 24 28 32
Time (min since start of application)

water discharge after 3.5 min. At 5 min, old water dominates the hydrograph and this trend continues until flow ceases at 30 min. The percentage of old water peaked at 5 min at almost 80% and then maintained values in the 50-75% range (Figure 6.13E). The timing of old water displacement is very different to experiment 1, in which the hydrograph separation showed at least some old water from the start of hydrograph rise onward.

6.2.11 Experiment 10

The final experiment was conducted at Pit 5 on 17 December. The experiment was designed to examine the effects of a very large water application on throughflow response. Thirty litres of water (supply 1) was applied 1.5 m upslope from the pit face. 20 min later, another 30 l of water (supply 2) was applied in a similar manner. Prior to application, a 50 mm saturated layer was apparent in the mineral soil at the Old Man Gravel interface. Matric potentials at this seepage face must have been less than atmospheric, however, because no actual seepage was observed and pre-storm pit flow was zero. Of the total supply input, 20% was recovered after 100 min (Figure 6.14A).

Water started seeping from the lower portion of the pit face at 7 min. A very low flow rate (c. 1 drip every 6 sec) was maintained until 26 min, at which time flow increased rapidly to a peak rate of 350 ml min^{-1} (Figure 6.14B). During the hydrograph rising limb, much of the flow emanated from the mid-profile, seeping from c.1 mm root channels and worm burrows. At 35 min (peak flow), 85% of the total pit flow came from a 100 mm diameter pipe at the mineral soil-Old Man Gravel interface. Saturated zone thickness at this site increased to approximately 250 mm, and seemed to supply the recession limb flow for the next several hours. No flow through the organic layer was observed at

Figure 6.14 Experiment 10 water volume, chloride and deuterium relationships, Pit 5.

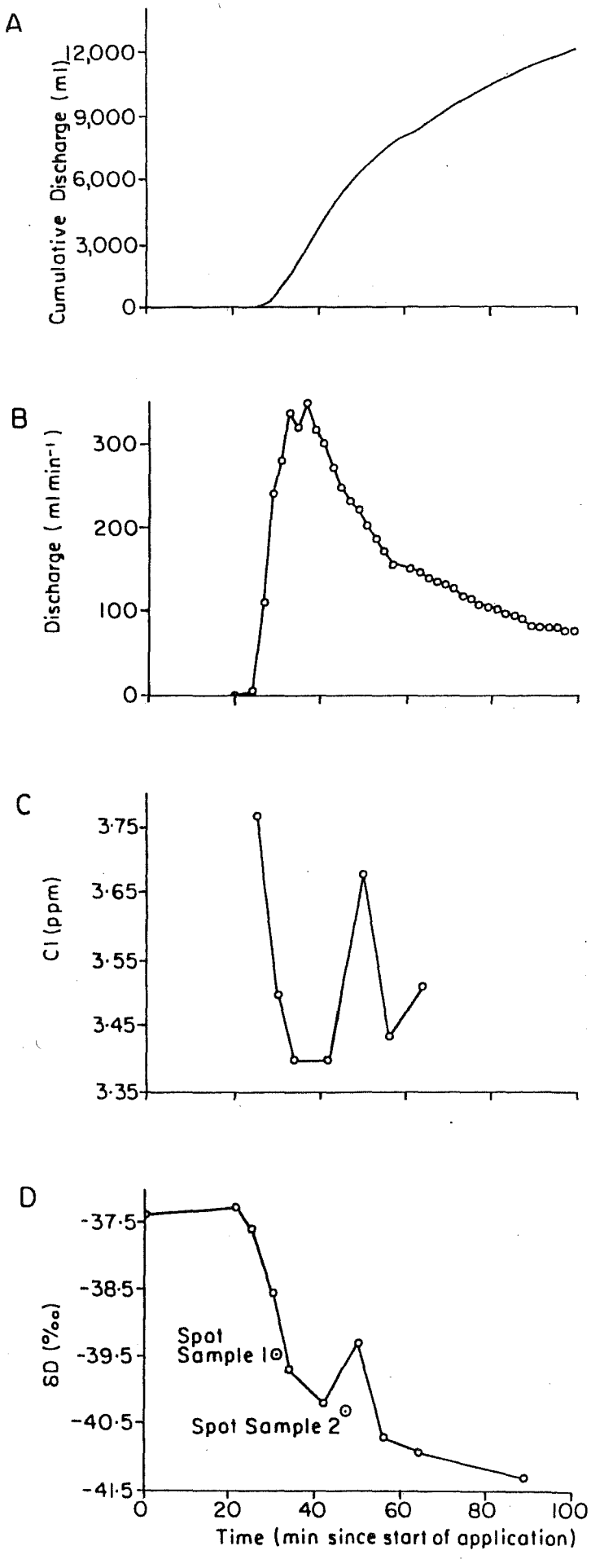
A
Cumulative Discharge (ml)
12,000
9,000
6,000
3,000
0
B
Discharge (ml min⁻¹)
300
200
100
0
C
Cl (ppm)
3·75
3·65
3·55
3·45
3·35
D
δD (‰)
-37·5
-38·5
-39·5
-40·5
-41·5
Spot Sample 1
Spot Sample 2
0
20
40
60
80
100
Time (min since start of application)

the pit face, although much of the lower organic layer 0.5-1.5 m upslope was damp to the touch.

Cl concentrations through the hydrograph are difficult to explain. Unfortunately supplies 1 and 2 were only 1 ppm apart, and most of the Cl fluctuation occurred within this range (Figure 6.14C). Of particular interest, however, were the values for the pipeflow samples, taken at 35 min and 44 min. These values were 8.194 ppm and 9.462 ppm respectively, much higher than nearby suction lysimeter sites (SL3-5, range 2.333 to 3.422 ppm). This discrepancy is difficult to explain, but may indicate a concentration of Cl immediately above the Old Man Gravels, possibly due to weathering of elevated Cl conglomerates.

Variations in δD concentrations show a steady shift from supply δD (average -38.4‰) to deep soil water δD (i.e. SL5=-41‰; Figure 6.14D). Pipeflow spot samples at 35 and 44 min are remarkably consistent with the trend in total pit flow δD, and reinforce the notion of pipe domination of flow. Hydrograph separation was not performed because supply 1 δD was 3.2‰ heavier than supply 2. This creates some problems with the preceding interpretation, because the trend toward the SL5 δD could in fact be displacement of supply 1 water, followed by some displacement of SL5-type water. If this was the case, however, a later shift toward supply 2 water would be expected. Spot sample 2 (44 min) from the pipe shows no sign of supply 2 water and indicates a further shift toward SL5 δD.

Tensiometer data from site 1 corroborates the interpretation that water moved rapidly to depth, bypassing much of the shallow soil layers. Prior to the application, the top 80 cm of soil was in an almost fully drained state, as indicated by the slope of the line of ψ versus depth below surface (Figure 6.15A). T3 and T4 responded rapidly to the injection (Figure 6.15B) and peaked

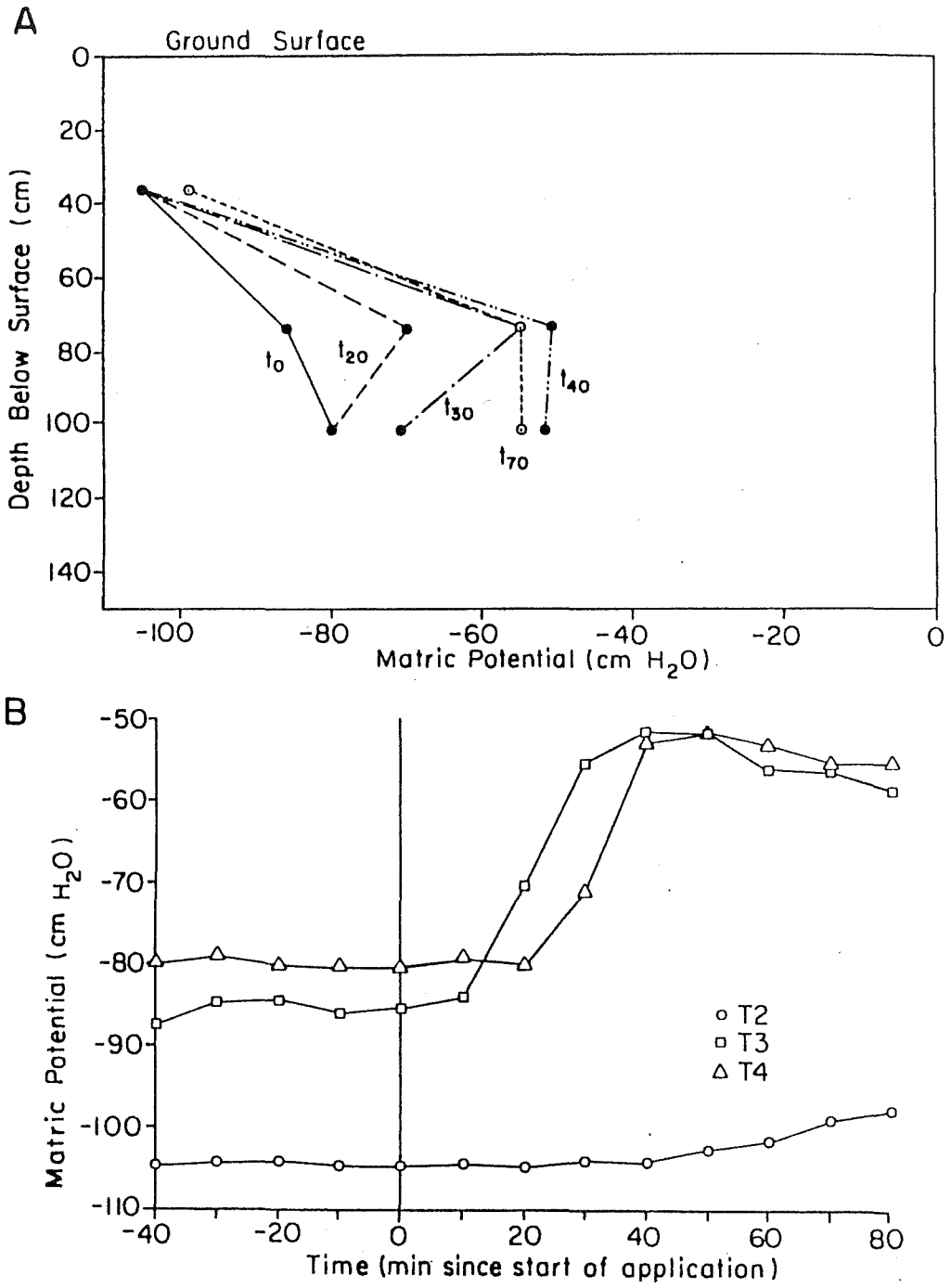

Figure 6.15 Experiment 10 matric potential response to water input, Pit 5.

at the same time as pit throughflow response. T1 malfunctioned during this experiment and is not shown in Figure 6.15. At peak ψ for T3 and T4, a strong lateral gradient was established (since both maintained similar ψ). T3 continued a slow shift from -105 (0 min) to -98 cm H_2O (80 min), reflecting slow unsaturated drainage of matrix water from above.

6.3 TRACER EXPERIMENT DISCUSSION

Mosley (1979; 1982) conducted injection trials similar to experiments 1-10 described above, in order to determine the rate of water moving downslope. From repeated measurements, he computed transmission rates and also observed various pathways of dyed water movement (Mosley, 1982, Figure 5, p.77). Pearce et al. (1986) questioned the appropriateness of Mosley's approach and refuted his interpretation of macropore flow by showing large old water displacement. Results from this study confirm Mosley's observations of pathways through the soil. Results also confirm findings of Pearce et al. (1986) and Sklash et al. (1986) using isotopic data. The reasons for this are discussed below.

At Pit 5, each experiment showed that most of the pit throughflow volume emanated from the mineral soil-Old Man Gravel interface. Injected water moved over the mineral soil surface, beneath the organic layer, until it encountered a crack. Once water entered the crack, it moved very rapidly to depth, and then flowed along the soil-bedrock interface to the pit face. This interpretation is confirmed by visual observation, flow data, soil matrix tensiometric response, and chemical and isotopic variations in pit throughflow and suction lysimeters. In addition to this rapid response, water slowly infiltrated vertically through the matrix, producing a shift in ψ.

The interpretation of these runoff pathways is consistent with those of Mosley (1982), but does not agree with his

conclusion on water origin. Mosley (1979; 1982) observed injected dyed water appearance immediately at the pit face, and made the conjecture that it was the same water injected minutes earlier. On the other hand, Sklash et al. (1986) used this observation by Mosley as the basis for their criticism of his work, suggesting that throughflow δD variations could be explained without recourse to a macropore flow process. They interpreted the old displaced throughflow as being matrix water, translated to the face by matrix flux in the capillary zone.

The experiments conducted in this study seem to show that the dyed water used by Mosley may have completely misled both Mosley and Sklash et al. in their understanding of the processes. Experiments at Pit 5 show that throughflow at the pit face was mainly displaced old water, even though the dyed water moved rapidly to depth and then downslope, independent of the soil matrix. If only dyed water appearance was used as the basis for judging injection water breakthrough, this water could be diluted by mixing with soil water up to several times the original volume before any significant visual change in colour concentration was noticed. In fact, the injection water could possibly exchange with a much larger volume of stored water, and still maintain a dyed appearance at the pit face. Some simple computations are described below.

Suppose 30 l of dyed water was applied in the usual manner, 1.5 m upslope from the Pit 5 face. If only quantifiable cracks and pipes are considered (i.e. not discontinuous worm channels etc), the potential store of old soil water within 5 mm of the macropore wall (asuming ψ=-75 cm H_2O and θ=0.54 along the length of the crack opening and ψ=0 cm H_2O, θ=0.63 in lower saturated zone, Figure 5.3) is 261 l. Cracks were observed at Pit 5, extending from the soil surface to the Old Man Gravel interface.

The presence of organic staining, combined with fine root systems, indicates frequent water movement in this zone, confirmed by injection experiments described earlier. If vertical cracks are spaced at regular 150 mm intervals, and bypass water is assumed to exchange with matrix-water within 5 mm of the crack wall (on both sides of the crack face), then the 30 l of injected water (assuming all 30 l flow through the cracks), would show only c.25% new water input by the time it reached the mineral soil base. Frequently, the lower 100 mm of mineral soil, overlying the Old Man Gravel, maintained positive ψ. If the infiltrated water then mixed with the possible old water store at the soil base (either through lateral pipeflow, as per experiment 10, or other bypass mechanisms), then new water would equal only 12% of total flow at the pit face, assuming complete exchange with the saturated base.

The conditions described above are clearly artificial and simplistic, but do demonstrate the potential significance of the old matrix water store in the macropore wall. In the MB context, this exchange is important because of regularly high volumetric water contents (>85%). These interpretations are developed further in section 7, as they relate to natural rain events.

Experiments conducted at the Pit A site showed that most of applied water rapidly infiltrated through the organic layer and then flowed laterally over the mineral soil surface toward the pit face. Much more of the applied water volume was retrieved and under most conditions, only a small volume of water entered the soil matrix. This interpretation was confirmed by visual observations, flow data, soil matrix tensiometric response and chemical and isotopic analysis of throughflow and suction lysimeter water.

Applying the same logic used in the Pit 5 discussion, and acknowledging the results of both Mosley and Sklash et al., some simple computations can be made to rationalise water flow pathways and dyed water appearance with throughflow δD-values. If 30 l of water was applied 1.5 m upslope of the Pit A face in the usual manner, and one assumed that mineral soil surface overland flow (constituting 100% of total runoff) exchanged with 50 mm of mineral soil matrix water (ψ=-75 cm H_2O and θ=0.52) and 50 mm of organic soil water (θ=50%, 86% porosity), then flow at the pit face would constitute c.45% new water. Here again, dyed water outflow could easily be diluted to form only 45% of original dyed water input, without any noticeable visual change in dyed water concentration. The notion of rapid flow (this time over the mineral soil surface and through the organic layer) can be reconciled with the displacement of old soil water, without considering matrix flow.

7 TOWARD A CONCEPTUAL MODEL OF STORM RUNOFF PRODUCTION IN A STEEP HUMID HEADWATER CATCHMENT

The following section attempts to integrate results from the preceding sections, in order to formulate a general model of runoff production in the M8 watershed. Catchment representativeness is addressed and M8 rainfall-runoff response is summarised in relation to other documented humid headwater catchments. The importance of near-stream versus mid-slope and upslope response is examined in relation to storm events of varying magnitude and intensity. Long-term rainfall data for the Maimai area are then used to indicate the overall significance of observed processes. Finally, geomorphological implications of identified runoff processes are discussed, in relation to a case study of debris flow initiation in the M8 catchment.

7.1 CATCHMENT REPRESENTATIVENESS

Most isotopic tracing studies have been conducted in areas characterised by gentle to moderate terrain. These areas are less hydrologically responsive than the steeper slope regions, where macropore flow processes have been interpreted as the dominant storm runoff response mechanism. Pearce et al. (1986) note that there has been some scepticism about the applicability of these findings to highly responsive catchments where rapid flow of infiltrated rain from the current storm through macropores has traditionally been acknowledged as the main response mechanism. The work of Sklash et al. (1986) has shown that even in a catchment as responsive as M8, old water dominates channel stormflow. This study has attempted to explain how this process operates, in an environment at the extremely responsive end of the hydrologic spectrum.

7.1.1 Rainfall-runoff relationships

The M8 catchment exceeds the quickflow responsiveness of any documented forested headwater catchment (Pearce et al., 1986). Dunne (1978) reported that quickflow response (QF/P) for most well-vegetated catchments is less than 20%. Harr (1977) showed that QF/P for a large number of storms on a forested hillslope plot in Oregon averaged 38%. M8 QF/P is approximately twice that of many responsive study basins in the eastern USA (Hewlett and Hibbert, 1967; Woodruff and Hewlett, 1970; Bryan, 1979; Olszewski, 1980). The QF/P averaged for runoff events from rainfalls >25% (i.e. R-index; 46% for M8) is 11-43% higher than those values collected for 11 basins distributed between Georgia and New Hampshire (Hewlett et al., 1977), and 27-41% higher than values obtained for catchments in Natal, South Africa (Hope, 1984).

Part of the reason for such high runoff response is the high subsurface runoff rates. Table 7.1 shows that measured subsurface flow velocities by Mosley (1979; 1982) for the M8 hillslope soils are up to 2 orders of magnitude greater than any other documented values. This includes other environments where continuous downslope macropore flow has been cited as being the major factor in hillslope response. The M8 catchment K_{sat} information from Webster (1977), Mosley (1979; 1982) and this study shows that M8 soils maintain a large range in K_{sat} topographically, but show some very high values (in ridge areas) compared with other documented catchment soils. Only those data reported by Beasley (1976), Harr (1977) and Megahan and Clayton (1983) exceed M8 measured values for ridge sites, as a result of either highly aggregated soil structure or high sand contents.

Very little data regarding pre-storm matric potential-soil moisture content relationships have been presented in the

Table 7.1. Measured and calculated K_{sat} and subsurface velocities for various hillslope soils (supplemented with data from Sidle et al., 1985).

Data source	Soil Type	K_{sat} mm hr^{-1}	V_{sub} mm hr^{-1}	Method
Ahuja and ElSwaify (1979)	Clay loam	11.2	---	A
Beasley (1976)	Sandy loam	640.0	---	A
Bonell et al. (1983)	Aggregated clay	7.0	---	B
Dunne (1978)	Varved sandy silt	---	48.0*	A
Dunne and Black (1970b)	A horizon, sandy loam	---	343.0	A
Hammermeister et al. (1982b)	B horizon, 12-35cm depth, convex slope	19.1	3.8	B
Hammermeister et al. (1982b)	B horizon, 10-38cm depth, convex slope	55.6	7.8	B
Hammermeister et al. (1982b)	B horizon, 12-39cm depth, convex slope	43.9	7.0	B
Hammermeister et al. (1982b)	B horizon, 12-45 cm depth, convex slope	103.3	16.5	B
Harr (1977)	Well-aggregated gravel clay silty loam	2875.0**	3.8**	B
Harr (1977)	Massive structure gravel clay loam	190.0**	0.5**	B
Hewlett and Hibbert (1963)	Sandy loam	---	305.0*	A
Megahan and Clayton (1983)	C horizon, loamy sand	1155.0**	452.0**	A
Mosley (1979); Webster (1977)	Upper 60cm of forest soil	265.0**	57600*	A
Mosley (1982)	Shallow forest soil	---	10800*	A
Mosley (1982)	Tussock sites, silt loam, organic surface	---	4540*	A
Palkovics and Petersen (1977)	B horizon, above fragipan	3.4	1.2	B
Roberge and Plamondon (1987)	Till	100.0	---	A
Weyman (1973)	Entire profile	---	3.0*	A
Whipkey (1965)	Sandy loam, 56-90cm depth	---	286.0*	A
Whipkey (1965)	Clay loam, 120-150cm depth	---	2.0*	A
Present study	Forest soil, 30cm depth hollow	3.0	---	B
Present study	Forest soil, 30cm depth ridge	300.0	---	B

A and B represent interception and indirect methods respectively
V_{sub} is the linear subsurface flow velocity
* Measured directly in the field
** Averaged values

literature. It is assumed that M8 conditions are as wet or wetter than other reported 'rapid response' environments. Rainfall at M8 is evenly distributed throughout the year and events are generally protracted with low hourly rainfall intensities. Pearce and Rowe (1981) examined a 2 yr rainfall record from M8 and identified a relatively uniform distribution of storms between 18 and 36 hr, and a somewhat scattered distribution between 36 and 130 hr. Rainless periods between storm events for the 1987 season averaged less than 7 days, and reflected the constant passage of westerly depressions across the Tasman Sea. One study that may be comparable in terms of pre-storm soil matric potential and soil moisture content is that reported by Harr (1977). He showed that during moderate size winter storms on the west coast of Oregon, fronts moved in a wavelike fashion from the Pacific Ocean at 24 to 48 hr intervals. Average matric potential for a slope position during a December 1973 storm, maintained values in the order of -10 to -20 cm H_2O depending on soil depth.

Table 7.2 lists a number of field studies that have separated catchment stormflow into old and new water components. Results from the present study, and those results obtained by Pearce et al. (1986) and Sklash et al. (1986), indicate that average M8 new water stormflow contributions are similar to or even less than most other documented catchments (40 ha to 62000 ha in area), even though catchment responsiveness is much higher. In fact, only those storms analysed by Jacks et al. (1986) in central Sweden and Turner et al. (1987) in western Australia were possibly less than the new water values for the M8 catchment.

Table 7.2. Estimated new water inputs to storm runoff determined from stable isotope tracing.

Data source	Location	Area ha	Tracer	Event	Qn %
Bonell et al. (1989)	S. Island New Zealand	125	δD	R	20-60
Bottomley et al. (1984)	C. Ontario, Canada	114	^{18}O	R	10-60
Bottomley et al. (1984)	N. Ontario, Canada	1050	^{18}O	S	30
Bottomley et al. (1986)	N. Ontario, Canada	1050	^{18}O,δD	S	40-50
Christophersen et al. (1984)	Birkenes, Norway	41	^{18}O	S	40
Crouzet et al. (1970)	S.E. France	--	T	R	?
Dincer et al. (1970)	N. Czechoslovakia	265	T,^{18}O	S	40
Fritz et al. (1976)	Manitoba, Canada	2200	^{18}O	R	40
Fritz et al. (1976)	Ontario, Canada	180	^{18}O	R	50-70
Fritz et al. (1976) Sklash et al. (1976)	Ontario, Canada	8000	^{18}O	R	40
Fritz et al. (1976)	Ontario, Canada	70000	^{18}O	R	50
Herrmann et al. (1978); Herrmann and Stichler (1980)	W. Germany	1870	T,^{18}O	S,R	30
Hooper and Showmaker (1986)	New Hampshire, USA	42	δD	S	?
Jacks et al. (1986)	C. Sweden	3400	^{18}O	S	10
Krouse et al. (1978)	Alberta, Canada	1100	δD,^{18}O	S,R	20
Kennedy et al. (1986)	California, USA	62000	δD,T,^{18}O	R	20
Martinec (1975)	Switzerland	4330	T	S	30-40
Pearce et al. (1986)	S. Island, New Zealand	4	^{18}O	R	3
Rodhe (1981)	C. Sweden	680	^{18}O	S	25
Rodhe (1981)	C. Sweden	400	^{18}O	S	10-40
Rodhe (1987)	C. Sweden	3-660	^{18}O	S	5-68
Sklash and Farvolden (1979)	Quebec, Canada	120	^{18}O	R	25-35
Sklash and Farvolden (1979)	Quebec, Canada	390	^{18}O	R	20
Sklash et al. (1986)	S. Island New Zealand	4	δD,^{18}O	R	<25
Turner et al. (1987)	W. Australia	82	δD,^{18}O	R	5-40
This study	S. Island New Zealand	4	δD	R	0-12

7.1.2 Effects on interpretations

The ultimate goal of any field hydrological investigation is to generalise observed processes in the form of a model, and then apply this understanding to other catchments. Catchment representativeness therefore, becomes an important issue, and must be understood before interpretations can be applied to other areas. The preceeding paragraphs demonstrated that the M8 catchment is not typical of other documented headwater catchments, in terms of pre-storm wetness condition and runoff responsiveness, and yet new water contributions to stormflow are similar to other less responsive environments.

Rather than the question of generality of conclusions becoming a problem, the notion of starting with an apparent 'end member' has definite advantages for testing specific hypotheses of runoff production. The value of this work is seen not in its 'transportability' of results to other study catchments, but its ability to answer specific questions for an extremely responsive catchment (with no significant aquifer storage), where new water contributions to storm runoff are negligible. Furthermore, although the responsiveness of the M8 catchment exceeds most documented studies, it nevertheless represents physiographic and climatological conditions of much of New Zealand and many other parts of the world; where slopes are short and steep, soils are thin and underlain by impermeable bedrock and annual rainfall is high. The fact that M8 is atypical compared to other documented catchments, is probably related more to the dominance of hydrologic research in lower relief in parts of the U.K. and North America. Very recent work reported by Bras et al. (1988) shows that many small humid headwater catchments in Japan, may exhibit similar catchment physiographic characteristics and runoff response rates to the M8 catchment.

7.2 DISCUSSION ON RUNOFF PRODUCTION

This study confirms the results of Sklash et al. (1986) by demonstrating that rapid macropore flow of new water (as suggested by Mosley, 1979) is not needed to account for the volume of new water in M8 stormflow. Old water accounted for 85-100% of channel stormflow, for all monitored 1987 events. New water contributions in each case could be accounted for by near-stream saturation overland flow and headwater zone new water subsurface inputs. Present results show, however, that a rapid macropore flow mechanism is required to account for the total runoff and quickflow volumes in most stormflow events, because valley bottom near-stream soil matrix flux rates cannot sustain measured runoff response. Isotopic data indicate that macropores (mainly pipes) are conducting isotopically old soil water and groundwater rapidly downslope and discharging into 1st order surface channels during storm events.

The following sub-sections discuss the observed relationships between limited storage effects and macropore flow, and show that the limited storage effect (analagous to the capillary-fringe effect) has the ability to explain seemingly diverse runoff phenomena which characterises M8 stormflow response. Given the high variability of soil characteristics and other controlling functions, the discussion is limited to a general level and suggested models are simplified versions of probable complex interactive mechanisms. A generalised model of runoff response is presented below, and then is followed by a set of sub-sections which address specific aspects of runoff production.

7.2.1 A simple model of runoff response

Any model of runoff response in the M8 catchment must acknowledge and support data presented in the previous sections

on subsurface water isotopic composition, within storm matric potentials, throughflow rates and tracer injection experimental results. Furthermore, this model must satisfy two apparently divergent phenomena: (i) runoff production is extremely rapid and characterised by macropore flow, and (ii) the groundwater component in channel stormflow is in excess of 85%.

The answer to this problem may simply relate to the large soil water store (350-500 mm) relative to rainfall input during individual storms (typically 25-75 mm). Sklash et al. (1986) argue that since less than 30% (in their monitored events) of the rainfall amount appears as quickflow, about 70% of the rainfall either infiltrates or is intercepted, and this is sufficient to supply the subsequent low-flow discharge and transpiration until the next storm. Furthermore, only a small amount of the soil water store must be discharged to obtain the quickflow yield in most storms. Tensiometric evidence shows that much of the catchment is within 10% of soil saturation for most of the year. Therefore, all that is required to satisfy the rapidity of catchment runoff response is an efficient transport system to bring stored water quickly from the hillslopes to the surface channels.

Soil moisture content in the M8 catchment increases substantially in the downslope direction, because of steep slope angles and relatively permeable soils. The near-stream valley bottom zone, along the main channel, represents the only zone of semi-permanent aquifer storage. During the initial wetting of the profile, available moisture storage in zones closest to the channel are filled, and resident groundwater begins to discharge into the channel, assisted by groundwater ridging (or mounds) along the channel margins. Soil water overlying the near-stream groundwater body is rapidly converted to groundwater because of

limited storage effects, and is then displaced into the channel. This process is seen as a near-stream response and would probably only occur in the valley-bottom zone of the main channel section.

As the hydrograph starts to rise, near-stream zones along the steep 1st order channels would also start to discharge groundwater into the ephemeral channels. The majority of this input would come from hollow zones (small zero-order basins) upslope from the channel bank. Initially, matrix flow from a growing saturated wedge would contribute to channel inflow, but then as perched water-table conditions developed on the slopes, pipes would conduct the majority of saturated flow downslope. Depending on the total depth of rainfall, hollow saturated zones would expand upslope and increase in local saturated zone thickness, feeding a well-connected system of pipes, that would route the water quickly downslope and into the 1st order channels. At the same time, valley-bottom near-stream zones would continue to exfiltrate groundwater into the main channel, with increasing contributions from upslope zones.

At peak flow, water-table elevations in the near-stream and hillslope hollow zones would be at their maximum elevation. Once rainfall inputs ceased, hillslope zones would quickly drain via pipeflow, such that hillslope subsurface flow rates would decrease faster than M8 hydrograph recession. The recession limb of the hydrograph would operate like a sponge whereby drainage from the pipes would 'shut-down' as soon as water-tables in the hillslope hollows were dissipated. The majority of the recession after this point would be fed by valley-bottom near-stream zones, whose deeper aquifer storage (and any additional drainage from upslope) would continue to supply the receding limb.

The simplified model follows the Hewlett and Hibbert (1967) notion of an expanding contributing zone through the event. The

difference in the two models lies in the mechanism of response, whereby once a rainfall magnitude threshold is exceeded during the hydrograph rising limb, the system converts from a matrix-dominated near-stream flux, to a pipeflow dominated hillslope hollow system. Depending on the rainfall intensity, perched water-table conditions on the hillslope would develop rapidly because of limited storage effects (low intensity rain) or by a combination of this and bypass flow (high intensity rainfall).

7.2.2 Near-stream limited storage effects

While limited storage effects such as those due to soil capillary-fringe properties, have been demonstrated in laboratory models (Abdul and Gillham, 1984), wetland situations (Heliotis and DeWitt, 1987; Novakowski and Gillham, 1988) and computer simulations (Sklash and Farvolden, 1979), only Ragan (1968) provides comprehensive field evidence of the capillary-fringe effect on storm runoff response. Ragan observed that along the perimeter of transient and perennial discharge areas of an experimental catchment in the eastern USA, the water-table and its associated capillary-fringe occurred close to the ground surface. Soon after rain commenced, infiltrating water readily converted the near-stream tension saturated capillary-fringe into a pressure saturated zone or groundwater ridge. This groundwater ridge affected groundwater response in two ways: (i) it provided the early increased impetus for the displacement of groundwater already in a discharge position (as further outlined in Sklash and Farvolden, 1979), and (ii) it increased the size of the groundwater discharge area that was essential in producing large groundwater contributions to measured channel stormflow. In this study, tensiometric response to storm rainfall monitored in the valley bottom near-stream zone, seems to fit this general model,

but shows that groundwater ridging is affected by limited storage characteristics rather than capillary-fringe effects. Nevertheless, the rate and magnitude of water-table response to rainfall input is very similar to other field studies, where capillary-fringe induced water-table rise has been recorded.

Figure 7.1 shows water-table rise data for several studies reporting capillary-fringe effects. M8 near-stream water-table rise, arbitrarily selected from tensiometer T4 (60 cm) at Site 2 for the 24 October event, is plotted in Figure 7.1A. Near-stream water-table rise is similar in shape and form to data reported in Heliotis and DeWitt (1987; Figure 7.1B), Sklash and Wilson (1982; Figure 7.1C), Novakowski and Gillham (1988; Figure 7.1D) and Ragan (1968; Figure 7.1E). In each reported case of rapid hydrograph rise, the maximum height attained by the water-table was several times greater than that expected, based on the specific yield of the soil or overburden material involved. Dividing the amount of water added (25 mm) in the 24 October event by the rise in water-table gives an effective specific yield of about 8%. From data given in Freeze and Cherry (1979) and Linsley et al. (1982), this is in the range of specific yields for materials similar to the near-stream soils (3-8%). Therefore, limited moisture storage characteristics of the near-stream site seem to resemble the capillary-fringe effect, itself a function of limited storage phenomenon.

Sklash and Wilson (1982) have summarised the essential points of the groundwater ridging effect as: (i) groundwater is frequently a major contributor to channel stormflow, (ii) near-stream groundwater is responsible for the early contribution to high runoff events, (iii) near-stream groundwater responds quickly to storm rainfall, and its response is a function of pre-storm water-table elevation in the near-stream and seep areas

Figure 7.1 Water-table rise data for field studies reporting capillary-fringe phenomenon.

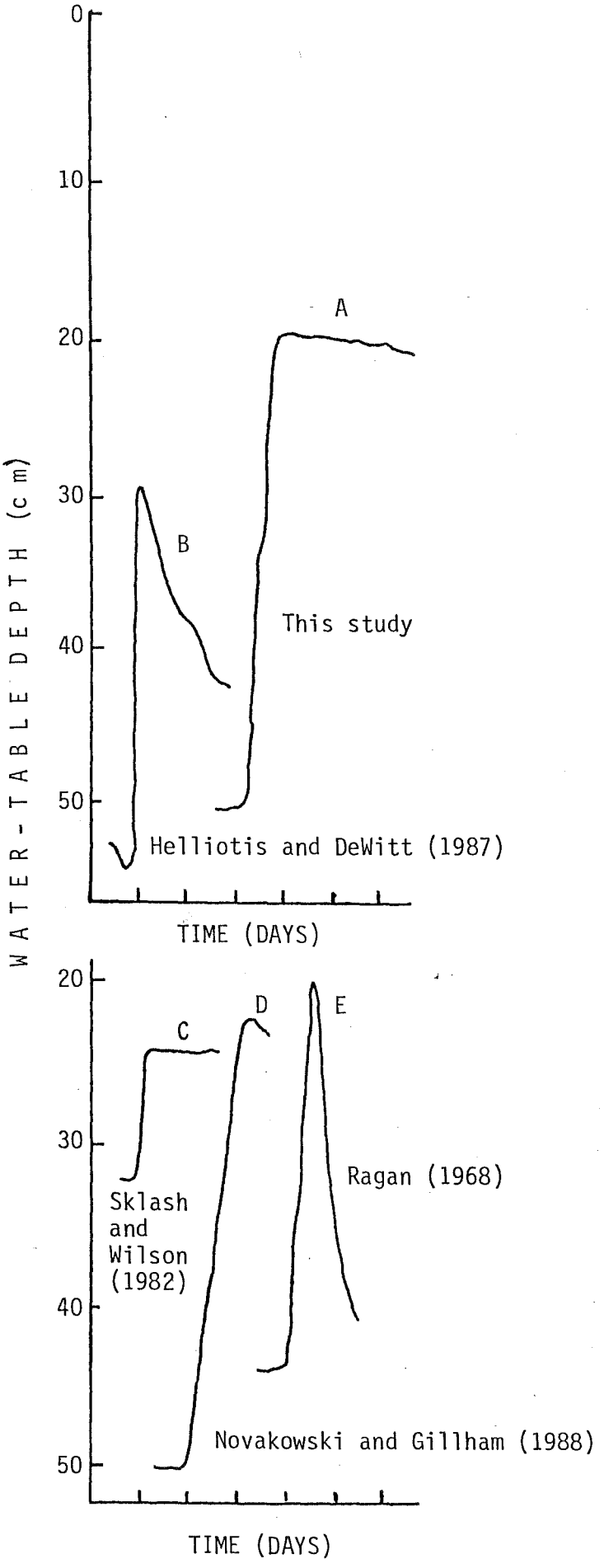
0
10
20
30
40
50
WATER-TABLE DEPTH (cm)
A
B
This study
Helliotis and DeWitt (1987)
TIME (DAYS)
20
30
40
50
C
D
E
Ragan (1968)
Sklash
and
Wilson
(1982)
Novakowski and Gillham (1988)
TIME (DAYS)

only, and (iv) overland flow may consist of some combination of rainfall and exfiltrating groundwater. Sklash and Farvolden (1979) noted that under capillary-fringe (or limited storage) dominated conditions, the response of upland area groundwater may become important at later times in the runoff event, but has little influence during hydrograph rise. Ragan (1968) observed that only a small portion of the watershed ever contributed flow to the storm hydrograph and that groundwater contributing zones existed in the form of localised zones of intense contribution (seeps). Although the limited storage conditions described above are applicable to the M8 catchment, their overall significance to channel stormflow is much less than Ragan (1968) or Sklash and Farvolden (1979) suggest.

In the steep M8 catchment, groundwater contributions from upper hillslope zones have a considerable effect on the timing and isotopic composition of hydrograph rise, if rainfall amounts exceed roughly 10 mm. The area producing the near-stream groundwater ridging response in the M8 catchment, only represents approximately 8% of the catchment area, in a valley bottom zone along either side of a 125 m section of the main channel. More than 80% of the total channel length (measured from a map in Sklash et al., 1986, Figure 1, p.1274), is characterised by steep channel slopes and highly incised channel bottoms. These areas did not respond in the manner described above and were dominated by rapid hillslope subsurface flow directly into the channel, with negligible near-stream storage or flow attenuation. This observation is verified by the fact that many of these first-order channels are ephemeral, while the main channel is perennial.

If the near-stream groundwater ridging mechanism is to explain total catchment runoff, then sufficient volumes of old

water must be discharged through this limited near-stream zone to account for measured runoff volumes at the M8 weir. A crude calculation of potential near-stream groundwater flux (v) can be made using measured K_{sat} values from Table 5.2, along with typical near-stream ϕ values (measured from the near-stream tensiometer plot) and computed channel dimensions:

$$v = -K_{sat} \text{ grad } \phi \qquad (7.1)$$

where: v is the flux rate in mm hr^{-1} and grad ϕ is the gradient of ϕ toward the channel. Assuming a K_{sat} of 3-30 mm hr^{-1}, and a typical ϕ gradient of 0.67 mm hr^{-1} (from the 29 October event), v=2.0 mm hr^{-1}. If groundwater ridging is important along 125 m of the stream channel (as outlined above) and the saturated depth through which water seeps into the channel is 1 m, then the potential seepage face would be 250 m^2 (assuming water entered from both sides of the channel). Combining the flux rate with the seepage area and then dividing by the catchment area (3.8 ha), produces a near-stream runoff contribution of 0.013-0.13 mm hr^{-1}.

Although a number of simplifying assumptions have been made, the v-value gives some indication of the importance of near-stream flux. For most rain events, near-stream channel inputs, as described above, could accommodate all runoff production for rain events <c.10mm (from data given in Mosley, 1979) if the 30 mm hr^{-1} K_{sat} value is used in equation 7.1. This K_{sat} value is clearly an overestimate of probable conditions. Therefore, for rain events greater than 10 mm, another flux mechanism is required to explain channel stormflow.

7.2.3 Matrix flow versus pipeflow of old water

(a) Low flow conditions

Under low flow (baseflow) conditions, M8 streamflow is sustained by the slow continual unsaturated downslope drainage toward the channel from mid and upslope zones. This would also

include a thin (<10 mm) layer of saturated drainage at the mineral soil-Old Man Gravel interface. Local catchment characteristics such as steep side-slopes, shallow soils, incised valley bottoms with little aquifer storage, and impermeable underlying bedrock, augment this process and result in the continual priming of near-stream zones. Soil moisture content increases downslope, such that saturated or near-saturated conditions regularly occur in the near-stream zone (cf. near-stream tensiometer data in section 5.2). This constant downslope movement during non-storm conditions produces two key features: (i) hydrograph rise and the timing of channel response is accelerated because the near-stream zone is so well-primed, and (ii) the age of subsurface water increases considerably downslope (see model results in section 4.3.3), so that large old water volumes are in a discharge position and ready for quick displacement into the channel.

The process of continual downslope mixing and progressive displacement of subsurface water has been outlined by Horton and Hawkins (1965) and Zimmerman et al. (1966). From laboratory experiments using tritiated water, both studies showed that drainage from the upslope zone in sloping soil profiles displaced downslope soil water. Despite high δD variability between different hillslope zones and soil depths within the M8 catchment (as shown in section 4.3.1), under long-term conditions (i.e. August to December, 1987), these differences disappear if one simply averages weekly values. Although all suction lysimeter sites showed a somewhat dampened response to the sinusoidal high amplitude rain δD input, each varied according to slope position and depth within the soil profile.

Exponential model results (section 4.3.3) showed that mean age increased downslope, such that near-stream zones were >100

days old, while upslope zones were roughly 2 weeks old. Theoretically, if soil water from upslope zones (with discrete δD values) drains into the mid-slope zone and then into the near-stream zone, as proposed by the exponential model, then the long-term average δD of each site must be the same (disregarding the 1-100 day lag for water to move from the ridge to the channel). Suction lysimeter δD for all sites, averaged over the complete period, was -39.9‰ (SD=1.4‰). All individual site averages, including M8 baseflow, were within +/-1‰ of the mean value.

To verify residence time computations made in section 4.3.3, exponential model results are compared with computed low flow hillslope flux rates. If an average representative slope length of 75 m is selected (from ridge to main channel) and a water residence time of 100 days is used (from model results), then flux rate would equal 31 mm hr^{-1}. Although K_{sat} measurements overestimate unsaturated K (for reasons outlined in section 5.1.4), some comparison of measured K_{sat} values and isotopic flux rates can be made. It is assumed that unsaturated drainage from the hillslope profile would move partly as a thin saturated layer at the base of the soil profile. Results indicate that computed reservoir flux is in the range of K_{sat} values listed in Table 5.4 (i.e. from approximately 3 mm hr^{-1} for hollow zones to approximately 300 mm hr^{-1} for ridge sites). Although very approximate, these results seem to verify residence time computations.

(b) Storm runoff events

Near-stream zones adjacent to 1st order channels were characterised by highly incised, steep-sided banks. In many locations, the sloping soil mass simply formed a face, at which water seeped into the channel (roughly analagous to a pit face). Figure 5.2 showed an example of this type of channel section,

where macropores at the base of the mineral soil layer, issue directly into the channel zone. Although this example is from a newly-formed stream section (discussed in detail in section 7.3.2), it characterises much of the steep first-order channel zones within M8. Hillslope hydrological processes, identified at Pit 5 and Pit A, therefore, are assumed to be directly comparable to processes controlling water movement to stream areas within these steep 1st order channel zones. Furthermore, these processes are seen as distinctly different to valley bottom near-stream behaviour.

Mosley (1982) determined mean subsurface flow velocities of 0.3 cm sec^{-1} for a range of artificial sprinklings and natural rain events. This means that with a mean slope length of 30 m, water could travel from the divide to the stream channel in 2.8 hr. Mosley (1982) notes that these rates of flow would be restricted to areas of saturated soils where water could enter macropores, and hence during the early stages of a storm are more likely to apply to the lower slopes where a saturated wedge persists during rain-free periods. During a storm, saturation builds at the profile base. Limited storage effects in the hillslope hollows and lower slope zones would accelerate this process.

Sklash et al. (1986), although correctly identifying the mechanism that allows rapid hillslope water-table development, did not properly acknowledge the mechanism that limits its longevity. Pipes at the mineral soil base are considered to be reasonably continuous downslope because: (i) they allow rapid dissipation of perched water-table conditions, and (ii) there is close correspondence of water-table rise and fall with pit throughflow.

Mosley (1979) discovered two pipes at the mineral soil base, at a site on the 28 m contour between Pit 5 and the Seep. He observed that during a natural storm event, water gushed from these pipes in the order of 20 l sec^{-1}. Mosley (1979) inferred that this water eventually appeared at the Seep. Mixing processes identified in section 6 have shown that Mosley's notion of new water movement for 10s of metres is unrealistic. Soil water contents and mixing processes outlined in section 6.3 are such that only a short distance of pipeflow movement is required to change to isotopic signature from new water to old.

7.2.4 Frequency of observed processes

(a) Near-stream versus hillslope dominance of channel stormflow

Pearce et al. (1986) noted that storms with high response ratios in the M8 catchment are frequent, and roughly 25 storms per year produce quickflow yields of >5 mm. In order to determine the frequency of near-stream versus hillslope dominance of channel stormflow and therefore their overall relative significance, a detailed study was made of 13 years of collected F.R.C. Maimai rainfall data (01 December 1974 to 19 January 1988). More than half of the rain events occurring within this period were <6.3 mm. This means that at least 50% of rainfall events could be accommodated entirely by near-stream processes.

Rather than derive cumulative frequency data for all events (upward of 0.1 mm), a value of 7.5 mm was selected as the critical rainfall depth for producing measureable quickflow at the M8 weir. Although quite arbitrary, this value seems to be the threshold for initiating roughly 0.5-1.0 mm of quickflow in storms presented in Mosley (1979), under a wide range of antecedent wetness conditions. For storms producing >7.5 mm of quickflow, over 90% would be controlled by hillslope flow

processes, based on analyses presented in section 7.2.2. It should also be noted that large storms were rather infrequent during the 13 yr period covered in Table 7.3. Over 50% of the events >7.5 mm were less than 30 mm total rainfall and only 15% were greater then 75 mm (8% of all events).

It appears that the study of Mosley (1979) was oriented towards infrequent, high magnitude events, where hillslope flow processes dominated and much of the runoff was conducted through pipes. Although 13 rainfall events were examined, Mosley focussed the discussion of runoff mechanisms on one event of 90 mm total rainfall. On the other hand, Pearce et al. (1986) and Sklash et al. (1986) may have examined runoff processes operating near or below the threshold for hillslope pipeflow dominance. Pearce et al. (1986) examined one event of 19 mm total depth and Sklash et al. (1986) examined four events between 33.2 and 43.7 mm total rain. Therefore, it seems likely that their interpretation of flow pathways are divergent from those of Mosley (1979), partly due to these factors alone.

Table 7.3. Cumulative frequencies for Maimai storm rainfall depth for a 13 yr period.

Rainfall mm	Cumulative % (>7 mm total)	Cumulative % (all values)
7.5	0.0	52.4
10	9.0	56.7
15	23.5	63.6
20	34.7	68.9
25	46.4	74.5
30	52.9	77.4
40	61.3	81.6
50	71.4	86.4
75	84.9	92.5
100	93.5	96.8

(b) Rapid water-table response due to bypassing

Bypass flow phenomenon were identified at the Pit 5 zone for rainfall events with high 10 min intensities. Unfortunately, only hourly rainfall intensity data are available on a long-term basis, so direct comparison to 10 min intensity data from this study cannot be made. Nevertheless, Table 7.4 suggests that average hourly rainfall intensities are extremely low, with over 65% of measured events between 01 December 1974 and 19 January 1988 less than 1 mm hr^{-1}. Less than 2% of the monitored events maintained hourly rainfall intensities that might induce bypass flow. Again, it must be noted that within these coarse hourly intensity figures, much higher short-term intensities might prevail. It appears, however, that significant bypass flow phenomenon may be much less important than dye water injection experimental results (from Mosley, 1979; 1982; and this study) may imply.

Table 7.4. Cumulative frequencies for Maimai storm rainfall hourly intensities by clock hour for a 13 yr period.

Hourly intensity mm hr^{-1}	Cumulative %
1	68.1
2	83.2
3	90.1
4	94.4
5	97.0
6	98.3
7	99.1
9	99.9

While bypass flow would certainly augment rapid water-table response in some storms, it seems clear that limited storage effects would be much more important in intiating this same response on a regular basis. Again, it appears that the

interpretations of Mosley (1979) may have been oriented toward infrequent high intensity storms. Hourly rainfall intensities reported for the 4-5 July 1978, 90 mm event (examined in detail by Mosley and used for discussion of runoff production) were over 15 mm hr^{-1} (Mosley, 1979; Figure 2.3). During the 13 yr period identified in Table 7.4, hourly intensities greater than 15 mm were only recorded for 29 clock hours. This highly infrequent occurrence compares with maximum hourly rainfall intensities reported by Pearce et al. (1986) and Sklash et al. (1986) of 0.6 and 3.2 mm hr^{-1}. Again, it seems likely that their interpretations of flow pathways are divergent, partly due to these factors.

7.2.5 Effects of varying K_{sat} on water movement into hollows

Runoff mechanisms and the relationships between matrix and macropore flow have been examined in two-dimensions. In steep catchments, three-dimensional topographic covergence of subsurface flow exerts a strong influence on hillslope runoff production. Several studies (Beven, 1978; O'Loughlin, 1981; Beven et al., 1988) have shown that convergent zones may yield earlier and higher peak subsurface flows than planar or convex slope segments. Anderson and Burt (1978a) noted that in a catchment with 25° slope angles and 1.5-2.0 m deep soils, nose slope contributions/m of channel length/m^2 drained area, were almost an order of magnitude less than hollow contributions. Although spur reaches along the stream comprised 60% of the basin area, Anderson and Burt (1978a) noted that these zones only contributed 40% of the total discharge under the most favourable of conditions.

In the M8 catchment, up to 75% of the total channel length is fed by either planar sideslope zones or nose slopes. The

catchment itself, however, is strongly dissected, and hollow zones, and sideslopes draining into hollow zones, comprise roughly 85% of the total catchment area. In addition to simple topographic influences on suburface water disposition, varying K_{sat} characteristics strongly influence the magnitude and direction of water movement. Section 5.1.4 showed that K_{sat} in the mid-slope zone near Pit 5, varied almost 2 orders of magnitude, from within the hollow (approximately 3 mm hr^{-1}) to the ridge (approximately 300 mm hr^{-1}). While nose and side-slope sections transmit matrix water much more efficiently, most of this flow is toward a slope hollow, from which it continues to move downslope toward the channel. During a storm event, drainage density increases considerably and extends into the lower footslopes of the hollow zones. This promotes more efficient drainage and increased channel contributions, than would be expected from low-flow drainage density patterns.

This study has concentrated on hollow zones within the M8 catchment. Some comparison between hollow, nose or planar slope runoff volumes and timing, can be gathered from data presented in Mosley (1979). He showed a large difference between quickflows from Pit 1 and Pit A, which are only 4 m apart. Pit 1 is on a planar slope with a 20 cm deep soil cover, whereas the catchment area of Pit A (used in this study) is bowl shaped, and the soil is 45 cm deep. Mosley also determined regression relationships between peak specific discharge in l sec^{-1} ha^{-1} at the main weir and at the Pit 1 and Pit A sites:

$$Q_m = 0.799Q_1^{0.82} \qquad r^2 = 0.92 \qquad (7.2)$$

$$Q_m = 1.98Q_A^{0.54} \qquad r^2 = 0.83 \qquad (7.3)$$

where: Q_m, Q_1 and Q_A is the discharge at the main weir, Pit 1 and Pit A, respectively. For several storms during 1978, equality was attained at:

$$Q_m = Q_1 = 0.3 \text{ l sec}^{-1} \text{ ha}^{-1} \text{ (1.15 l sec}^{-1}\text{)} \quad (7.4)$$

$$Q_m = Q_A = 1.42 \text{ l sec}^{-1} \text{ ha}^{-1} \text{ (5.45 l sec}^{-1}\text{)} \quad (7.5)$$

where: the value in brackets is the discharge at the M8 weir.

These relationships show that Pit A produces smaller quantities of quickflow than the main weir, up to about 10 mm. Furthermore, Pit 1 quickflow volumes are higher than Pit A for small events, because of thinner and more permeable soils. For a 17 mm rain event, Mosley (1979) showed that quickflow at the main weir, Pit 1 and and Pit A were 1.9, 2.6, and 0.2 mm, respectively. For larger events (>10 mm quickflow), Pit A quickflow depth exceeded both Pit 1 and M8. This suggests two important factors: (i) for small events, hillslope flow does not significantly account for channel storm flow, and this is verified by computations made in section 7.2.2, and (ii) hollows dominate runoff production during high flow. This phenomenon also contributes to the longevity of hollow saturation and pipeflow drainage.

Although not explicitly recognised in previous investigations (e.g. Sklash et al., 1986), topographic convergence of subsurface water into hollows will have a strong influence on soil water and groundwater isotopic mixing. If one accepts that hillslope hollows dominate channel stormflow in moderate to large events, then they must also control resulting streamflow isotopic compositions. Suction lysimeter data demonstrated large δD differences between shallow (SL4) and deep (SL3) zones and ridge (possible SL7) and hollow zones (possible SL6). In addition to mixing at a point during an event, hollow zones receive new water from surrounding slope segments, which mixes with older hollow water before being transmitted to the channel.

7.3 GEOMORPHOLOGICAL IMPLICATIONS

7.3.1 Subsurface flow and debris flow mass movement

Although many studies have documented the physical properties of failed hillslopes (e.g. Shlemon et al., 1987) and their rheology (e.g. Fisher, 1971), few have examined the role of subsurface water movement pathways on debris flow initiation. In steep areas, debris flows generally occur in response to low matric potential and high rainfall intensities and magnitudes. As the pressure potential in a sloping soil mass increases, the frictional component of the shear forces holding the soil on-slope decreases. Neary and Swift (1987) have noted that this, combined with decreased cohesion due to water displacing air in soil interstices, reduces shear resistance force enough to produce slope failure. Several studies have also shown (e.g. Costa, 1984) that factors such as thin soil conditions, steep slopes, concentrated drainage, shallow-rooted vegetation and high soil clay content, will promote increased susceptibility to failure.

Notwithstanding, increased pressure potentials (positive matric potentials) and soil water movement seem to be the major control on slope stability. Sidle et al. (1985) note that few data exist on matric potential in the soil mantle at the time of hillslope failure. Some studies (O'Loughlin and Pearce, 1976; Sidle and Swanston, 1981; 1982) have suggested that near-saturation of shallow soils (<1 m thick) may be necessary to induce slope failure. O'Loughlin and Pearce (1976) showed that pressure potential in excess of 100 cm H_2O was required to initiate failure in soils underlain by late-Tertiary sandstone (slopes >25°) in North Westland, New Zealand. Sidle and Swanston (1982) reported that a pressure potential shift from 0 to

25 cm H_2O in hillslope depression in coastal Alaska, reduced the factor of safety from 1.49 to 1.00. Anderson and Kneale (1980) observed hillslope soil pressure potential values in the order of 12 to 67 cm H_2O, adjacent to a slope failure, while Rogers and Selby (1980) computed a pressure potential of 110 cm H_2O associated with slope failure. Finally, Pierson (1980) found complete saturation of the soil mantle along axes of hillslope depressions in the Coastal Ranges of Oregon during a winter storm with an estimated return period of 4 years.

The rate of water movement through unstable soil mantles is probably the most significant hydrologic function affecting soil mass movement (Sidle et al., 1985). Although sparse data do exist for pre-failure ψ, subsurface runoff pathway effects on failure initiation has not been addressed. The data and interpretations of this thesis present a unique opportunity to speculate as to the ψ and pathway controls on slope failure. Furthermore, the local environment is highly suited to debris flow phenomena, as a result of high annual rainfall and steep slopes. The following sub-section presents a case study of debris flow movement in the M8 catchment, with the objective of relating experimental subsurface flow results to possible failure initiation processes.

7.3.2 The 19 May 1988 debris flow event

(a) Rainfall and streamflow characteristics

On 19 May 1988, 160 mm of rain fell over the M8 catchment, after a prolonged 11 day period of intermittent rainfall totalling approximately 250 mm. API_7 and ALI_{14} were 29 and 37 mm respectively and Figure 7.2 shows the general rainfall-runoff relationship for the 27 April to 27 May period. A debris flow was initiated in a small north-east facing hillslope hollow, normal to the main channel, roughly 25 m upstream from the main weir. Over 1000 m^3 of debris moved rapidly downstream, destroying the

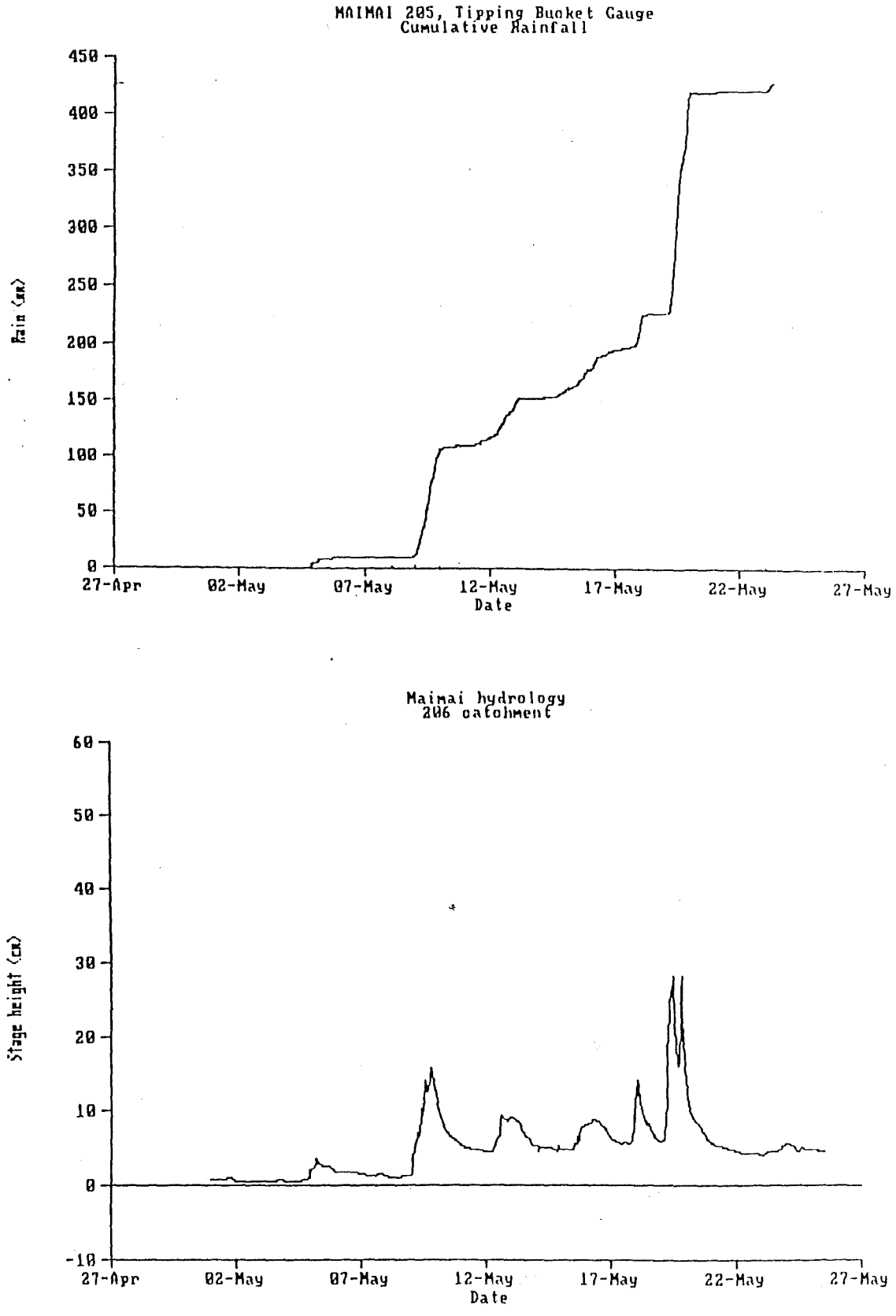

Figure 7.2 Rainfall-runoff relationships for the 19 May debris flow event.

weir, stilling well and stage recorder. M6 streamflow data are used as a surrogate for M8 streamflow in Figure 7.2, because of lost M8 records. M6 is a 1.6 ha unlogged control catchment in the Maimai Experimental area, and as such, produces less quickflow than M8. Sklash et al. (1986) note that M6 produces approximately 11% less runoff and 27% less quickflow than the logged and burnt M8 catchment. Nevertheless, the catchments are physiographically similar and are expected to operate similarly in a hydrological context.

The rainfall intensities plotted in Figure 7.2 were extracted from an uncalibrated Forest Research Centre tipping bucket gauge. Subsequent calibration of the device has shown that these values may be up to 8% higher than actual observed data (S. Kitchingmen, personal communication, 1988). None the less, these values are used in the following examination of storm conditions and are considered representative of actual conditions. The 19 May event has an estimated 24 hr return period of about 10 to 20 years, from maps presented in Tomlinson (1980). Rowe (1988) compiled data from 3 previous extreme rainfall events recorded at Maimai (from a Lambrecht raingauge 2 km from the M8 site; Table 7.5), which shows that the 19 May storm is not exceptional (compared to other large recorded events), in terms of 1,3,6,12 or 24 hr intensities. Maximum 1 hr rainfall for the 19 May event was 16 mm, which was exceeded by only 0.008% of events tabulated over a 13 yr period (see Table 7.3). Although this intensity is high compared to most protracted low intensity events experienced at Maimai, maximum 10 min rainfall intensites would often reach the 16 mm hr^{-1} value (cf. monitored 1987 events). Therefore, it was the effect of prolonged steady rain, high antecedent wetness conditions, and to a lesser extent rainfall intensity, which made the 19 May storm one of the more extreme events.

Table 7.5. Rainfall intensity characteristics for large storms monitored at Maimai (data from Rowe, 1988).

Date	24 hr mm	12 hr mm	6 hr mm	3 hr mm	1 hr mm
April 1975	177	153	104	59	22
December 1979	110	107	79	58	26
July 1983	216	134	75	41	15
May 1988	145	98	66	34	16

The 19 May storm started at 0100 hr and maintained low rain totals (<11 mm) and intensities (2 mm hr^{-1}) for the first 4 hr. Between 0500 hr and 1200 hr, 77 mm of rain fell with average 1 hr intensities in the order of 10 mm hr^{-1}. M6 streamflow response was rapid and peak runoff was 12.4 mm hr^{-1}. M8 peakflow would be within 10% of this value, but it is difficult to determine its exact value. Table 7.6 shows that for previous 1987 events, the relationship between M8 and M6 peak runoff is non-linear. In small to moderate events (e.g. 24 and 29 October 1987), M8 and M6 response followed the observation made by Sklash et al. (1986) cited above. For the 13 October 1987 event, however, M6 produced higher peak runoff values than M8. The reasons for this are not fully understood. With this in mind, the M6 hydrograph for the 19 May event was bimodal, with a second peak (also 12.4 mm hr^{-1}) occurring approximately 8 hr after the first peak, in response to a further 20 mm burst between 1830 hr and 2000 hr.

Table 7.6. Comparison of peak runoff rates for M8 and M6 for selected 1987 events.

Date	M8 Q_{pk} mm hr^{-1}	M6 Q_{pk} mm hr^{-1}
13 October	6.4	8.8
24 October	0.26	0.20
29 October	2.6	2.1

(b) Debris flow characteristics

The failure occurred in a small undrained hollow on the east side of the main catchment (Figure 7.3). The movement initiated about 40 m from the catchment divide, and extended 113 m downslope from the 300 m contour. Average width was 10 m, but showed noticeable remnants of super-elevation of gully walls down the main axis of the flow, and at the base, where the flow entered the main channel. Table 7.7 shows that the total surface area of the flow was 0.11 ha and total mobilised sediment volume was about 1000 m^3.

The source area of the failure was 391 m^2 and occupied 35% of the overall flow area (Figure 7.4). Slopes surrounding the bowl-shaped hollow (16 m by 30 m) were steep (>40°), and soils were 1 to 1.5 m deep; equivalent to other similar physiographic positions within the catchment (cf. Pit 5 area). The failed material consisted of slope-derived colluvium (similar to Pit 5 area), and the main shearing occurred at the mineral soil-Old Man Gravel interface. The large intact mass of soil broke away from the slope and left a well-defined headscarp. The exposed Old Man Gravel surface slope was 30° and no scour of the bedrock surface was observed within the source area. A 5 mm allophane-rich organic clay layer was observed throughout the source area, overlying the exposed bedrock surface. This layer probably functioned as a lubricant during the sliding process. Subsequent soil erosion around the source perimeter obscured exposed soil face structural characteristics. Some large pipes could be identified in the exposed soil face. These are discussed in detail in section 7.3.3.

The main track of the flow extended 75 m downslope from the source area. A constriction in the gulley width and transition from concave to convex slope, marked the change in slope between

Figure 7.3 Photograph of debris flow triggered during 19 May storm event, showing source area and main track.

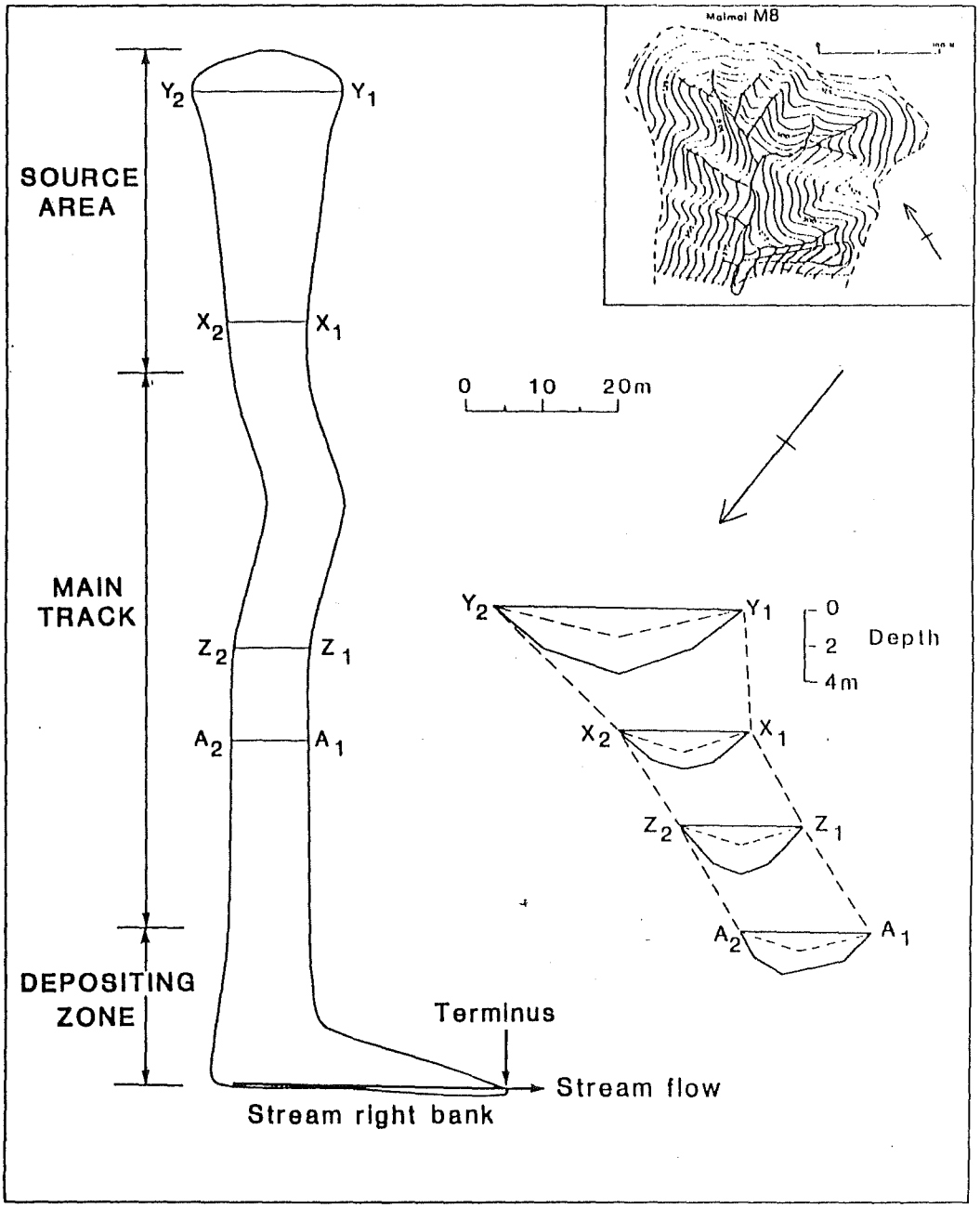

Figure 7.4 Map of the 19 May 1988 debris flow.

the source area and main track. The slope of the main track averaged c.40°, and considerable incision down through the Old Man Gravel surface was observed. In some cases, up to 1.5 m of conglomerate was excavated from the central track channel. The main track was v-shaped in cross-section (Figure 7.4) and showed signs of super-elevation. The physical destruction observed in the main track area and downslope zone, combined with the super-elevation remnant in the main track and runout zone, suggest that the flow travelled downslope at possibly 5-10 m sec^{-1} (from similar flows reported in the literature). Track walls maintained very steep angles (>40°), with some asymmetry of channel form farther downslope. The main track occupied 480 m^2, representing 35% of the total debris flow area.

The deposition zone was located in and around the M8 main stream channel bed, and extended c.40 m downstream from where the debris flow intersected the channel. Failed debris covered 232 m^2, representing 21% of the debris flow area. Poorly sorted, hyper-concentrated depositional material average 2 to 3 m deep, and dammed streamflow in the main channel for several days. Failed material was still in its original position on 31 October 1988.

Table 7.7. Debris flow physical characteristics.

			Total	-----Surface Area--------		
Length m	Width m	Volume m^3	Surface m^2	Hollow m^2	Track m^2	Dep'n m^2
113	10	1,050	1,102	391	480	231

(c) Possible pre-storm soil matric potential conditions

Although all tensiometric recording equipment had been removed from the M8 catchment prior to the 19 May debris flow,

some general inferences can be made regarding the possible pre-storm ψ conditions in the failed hollow. The topographic position, elevation, soil characteristics and soil depths are roughly similar to the Pit 5 zone. It is assumed that soil structure characteristics and macropore development were also similar at both sites.

Pre-storm ψ conditions can be readily compared to the post 10 October event period, when catchment API conditions were roughly similar. In this case, the lower mineral soil in the Pit 5 hollow was near saturation. The deepest tensiometer at about 100 cm below the ground surface showed ψ in the order of -10 to -25 cm H_2O. Closer to the ground surface, soil ψ was -35 to -45 cm H_2O. Bypass flow and piping, however, would affect the development and longevity of perched water-table conditions on the slope. As shown in previous storm event analyses, groundwater development in the mid-slope zone is extremely rapid and transient. Given the high rainfall intensities, bypass flow would have augmented limited storage response to perched water-tables. It is assumed that during the 19 May event, complete saturation of the soil matrix would probably have occurred in the failed hollow, given the magnitude of the rainfall and low magnitude pre-storm ψ conditions.

7.3.3 A slope failure mechanism

The mineral soil-Old Man Gravel interface represents a structurally weak part of the regolith profile, and is where most shearing failures are located in the Maimai study area (O'Loughlin and Pearce, 1976). This zone is also the location for rapid development of perched water-table conditions, where infiltrating rainfall is rapidly translated to depth via cracks or as a result of limited storage effects. Hillslope failure probably occurred at this site because of a number of

contributing factors: (i) perched groundwater was rapid and sensitive to increases in rainfall intensity, (ii) complete saturation of the soil mantle developed, (iii) three-dimensional drainage (i.e convergence) into the hollow from highly conductive sideslopes would have further exacerbated the build-up of saturated conditions, (iv) the highly concave shape of the hollow base was such that it could not distribute the perched groundwater enough to prevent rapid water-table elevational increases, and finally (v) the failure zone was underlain by a thin layer of allophane-rich organic clay.

Bypassing and pipeflow, in association with those factors described above, were probably the most important causal factors in initiating slope failure. In some situations, pipes may improve slope stability by increasing the rate of soil drainage and limiting the development and longevity of perched water-table conditions. On the other hand, if bypass flow increases the rate of vertical infiltration and exceeds the rate at which the anastomosing pipes transmit recently infiltrated water downslope, then a rapid perched water-table condition will develop. In this case, bypass flow would certainly have occurred under the storm rainfall intensities experienced and probably exceeded pipeflow drainage.

Only a few studies have examined the role of macropores (mainly pipes) on slope stability. Perhaps the most detailed study which examined these processes was a laboratory study conducted by Pierson (1983). He used a Hele-Shaw (viscous flow) model to demonstrate the effect of a single pipe on the overall flow regime of a slope. Pierson's analogue showed that when a pipe was blocked or was a dead-end passageway (a closed pipe), the cavity could be readily filled with water during a rain event, increasing pressure potentials in the surrounding matrix.

Furthermore, it was observed that if pipes were continuous downslope for some distance, they could generate pressure potentials much greater than those generated by total saturation of the soil, enabling failure initiation at sites that would otherwise be stable.

Brand et al. (1986) documented the effect of constricted or silt-filled pipes on Hong Kong hillslopes, which resulted in a total potential increase of 4 m in 6 hr and subsequent slope failure. The 'blocking-up' of normally hydraulically efficient pipes was seen as the major contributing factor to frequent landsliding. Anderson et al. (1982) showed that vertical bypassing in clay shrinkage cracks in a roadway embankment, resulted in a faster than expected increase in matric potential at a mid-soil profile depth. Water movement through seasonally-active cracks led to the development of an upper zone where matric potentials exceeded zero, and produced a concomitant decrease in slope stability.

The relative hydraulic efficiency of bypass flow and pipeflow in the M8 catchment hillslope zones is such that under 'normal' rainfall conditions, a rapid perched water-table develops (also assisted by limited storage effects) and is quickly dissipated by pipe drainage. Even under reasonably high rainfall depths (cf. 13 October event), perched water-tables in the Pit 5 area disappeared <12 hr after rainfall cessation. Several studies (e.g. Pierson, 1980) have shown, however, that soils in apparently similar hollows (even on the same slope), may vary greatly in their susceptibility to slope failure, due to subtle differences in soil moisture retention capacity, macropore configuration etc. Blockage of pipes in the hollow area could be a possible factor, particularly since pipes were identified near the headscarp fracture zone.

The build-up of hydrostatic pressures, both along the vertical cracks and at the mineral soil base, may also be a contributing factor in flow initiation for the 19 May event. If water moves rapidly to depth along a vertical crack, in excess of pipeflow transmission rates, water 'backs up' within the crack, exerting hydrostatic pressure on the crack walls and contributing to the overall disturbing forces. At the same time, rapidly moving pipeflow at the mineral soil base may produce upthrust pressures or buoyancy effects (Rogers and Selby, 1980). This, combined with drainage from surrounding topographic units would serve to generate failure. This could also have been aided by macropore blockage as outlined by Pierson (1983).

O'Loughlin et al. (1982) note that the geomorphic work (mass wasting, channel changes and sediment transport) performed during large events, such as the 19 May storm, account for years to decades of work accomplished by 'normal' rainfall and streamflow. Finally, a mention must be made of the effects of clearfelling on slope stability. A general decline in slope stability has probably been caused by the reduction in the strength of the tree root network. These effects are beyond the scope of the present analysis, but it should be noted that for the high magnitude storms summarised in Table 7.5, no landslides occurred in the nearby undisturbed forested control catchments. Therefore, the magnitude and types of geomorphic change during large events (as outlined by O'Loughlin et al., 1982), depend closely on slope environments, particularly slope vegetation conditions.

8 CONCLUSIONS

8.1 SUMMARY OF MAJOR FINDINGS

Hydrometric and dye tracer studies by Mosley (1979) suggested that macropore flow of new water dominates storm runoff in the M8 catchment. Subsequent isotopic investigations by Sklash et al. (1986) and Pearce et al. (1986) explicitly refuted Mosley's interpretation by showing that all new water contributions in the M8 catchment could be accounted for by saturation overland flow. They argued that there is little need to subscribe to a macropore flow concept to explain new water contributions to storm runoff. The present study has re-examined the age, origin and pathways of subsurface runoff in the M8 catchment using a combined hydrometric, recording tensiometric, chemical and isotopic tracing approach. By integrating methods previously used in isolation to each other, this study has clearly demonstrated the value of using independent observations of storm runoff. Furthermore, a mechanism has been proposed that links the idea of macropore flow with the notion of old water displacement, which satisfies both slope-oriented hydrometric and stream-oriented isotopic approaches.

The following paragraphs summarise the major findings of this study by addressing the series of questions posed in section 2.6:

1. Large variations in the isotopic composition of subsurface water were observed, both on a between storm and within storm basis. These large variations, however, did not affect the isotopic composition of stormflow at the main weir. New water inputs to the main channel during storm events were 0-30%, reflecting the dominance of pre-storm soil water and groundwater. Differences in suction lysimeter deuterium concentrations related

to a fluctuating rainfall isotopic input and mixing processes in the subsurface reservoir. Although the subsurface zone was not fully mixed, downslope water movement within and between storms resulted in mixing within the soil matrix and along macropore walls. Even under conditions of rapid flux through cracks and pipes, enough mixing of input and soil water occurred to completely shift stormflow compositions toward stored water.

(i) Rain isotopic variations had a large effect on soil water and groundwater deuterium concentrations. Modelling attempts were able to exploit the cyclical deuterium variations in rainfall to determine soil water and groundwater residence times within the catchment. Using an exponential model, mean residence times were computed for various slope positions and soil depths, and showed a mean residence time of >100 days for water entering the main channel in the valley- bottom zone. Because of high volumetric water contents, large old water volumes were available for contact with infiltrating new water. As a result, old water signatures, by virtue of their dominance volumetrically, completely overshadowed new water input.

(ii) Within the saturated and unsaturated zones, variations in stored water deuterium concentration were observed in a downslope direction and with increasing soil depth. Simple volumetric mixing models showed that shallow unsaturated soil zones (<20 cm) reflected rainfall inputs of 7 to 14 days, while deeper within the profile or further downslope, the age of water increased dramatically to >100 days. Cluster analysis showed that suction lysimeter water deuterium concentrations, could be grouped according to soil depth and distance from the catchment divide.

2. In the M8 catchment there is enough old water in a near-stream discharge position to account for the old water component

in a runoff event for most rain events <10 mm. Under rainfall conditions >10 mm, however, runoff response and runoff volumes are such that large upslope contributions to channel stormflow occur. The soil hydraulic conductivity of valley-bottom near-stream discharge areas is too low to account for these stormflow volumes, and major contributions of old water come from hollow zones several tens of metres from the channel. Although not readily in a discharge position for rapid exfiltration into a surface channel, transient hillslope groundwater perched at the mineral soil-Old Man Gravel interface, is rapidly moved to a first order channel via pipeflow.

(i) Although Sklash et al. (1986) noted that several trends in the deuterium values of M8 stream and throughflow indicate that soil water and groundwater are isotopically similar, suction lysimeter data from different slope positions have shown that they are not equal in the M8 catchment. This feature is a result of different residence times, produced by downslope and down-profile mixing processes summarised above in 1.

(ii) Subsurface isotopic mixing processes within the M8 catchment occur in two forms: slow diffusive mixing within the soil matrix, and rapid mixing of turbulent flow through cracks and pipes with matrix water stored within the macropore walls. Depending on input rates and volumes, substantial mixing occurs in each situation, and the resulting throughflow solution is isotopically old water.

3. Moisture release measurements conducted on the M8 soils showed that they do not exhibit capillary-fringe characteristics similar to other environments where groundwater ridging phenomena has been cited. Soil matric potentials are, however, highly sensitive to rainfall input because of the small differential water capacity or 'limited storage effect'. As a result, rapid

water-table rise frequently occurs in the near-stream and mid-slope zones.

(i) Limited storage effects operate similarly in hillslope and near-stream locations, but are significantly affected by soil depth and pre-storm wetness. Near-stream soils are generally wetter and up to 1 m thinner than mid-slope hollow soils, resulting in less available storage. Within 10 m of the main channel, matric potential response to rainfall is very rapid.

(ii) Limited storage effects and the rate of water-table response are markedly influenced by rainfall intensity. Antecedent wetness conditions also affect the rapidity of water-table response by controlling the degree of available storage.

(iii) Groundwater ridging seems to occur along the perimeter of near-stream valley bottom zones. The maintenance of high water-table conditions in the near-stream zone is assisted by drainage from upslope areas and increased groundwater flux into the main channel persists for several days.

4. Storm event tensiometric data and water injection experimental results from the mid-slope hollow, indicate that short-term high rainfall intensities occasionally exceed the hydraulic conductivity of the mineral soil. Water moved hundreds of millimetres downslope over the mineral soil surface until it encountered a vertical crack. Under intense bursts lasting perhaps 15 to 30 min, bypass flow rapidly moved to the base of the soil profile.

(i) Bypass flow outlined above augments rapid water-table rise on hillslope areas where vertical cracks occur. The relatively low frequency of high hourly rainfall, however, ensures that this is not a regular occurrence in the M8 catchment.

(ii) The valley-bottom near-stream zone and slope areas draining into small first order channels, operate differently in terms of runoff mechanisms and timing. Valley-bottom near-stream zones account for the early increase in old water discharge into the main channel, and control initial hydrograph response during the rising limb. As rain exceeds a threshold of approximately 10 mm (depending on antecedent wetness conditions), hillslope zones develop perched water-table conditions, and pipeflow rapidly transmits this water to small first order channels. Once rainfall ceases, hillslope subsurface stormflow decreases rapidly as water-tables disappear. Valley-bottom near-stream zones continue to supply the old water discharge during hydrograph recession.

8.2 SUGGESTIONS FOR FUTURE RESEARCH

8.2.1 Within the M8 catchment

Although the M8 catchment has probably received more detailed field study into subsurface stormflow processes than any other documented experimental catchment, many questions remain unanswered. This study has resolved some previous conflicts, but has also uncovered several questions and areas of research which could not be addressed.

1. Simple isotopic mixing models were examined in section 4. Modelling should be continued in the form of a more detailed lumped-parameter approach. This interpretive method could be undertaken using steady-state lumped parameter models (Kreft and Zuber, 1978; Maloszewski and Zuber, 1982) to transform the input (deuterium concentration of rainfall) to allow simulation of the outputs (deuterium concentration of soil moisture and throughflow) and to provide more detailed information on the residence time distributions in the system. In this manner, dispersion parameters could be varied to fit the simulated to the

actual output, and macropore flow (with a short turnover time) and other flow paths could be incorporated into the model structure. Dispersion models would be very flexible, because they would permit a wide variation of possible residence time distributions. In other studies (e.g. Zuber, 1986), it has been an effective simulator for a wide variety of hydrological systems.

2. Although some aspects of soil variability were considered in this thesis, a much greater effort could be made in identifying spatial variability of soil parameters, including saturated and unsaturated hydraulic conductivity, macropore distributions etc. Recent work in other areas (e.g. Ahuja et al., 1988) have utilized geostatistical methods and conditional probability approaches to quantify the variability of soil properties. These data could be incorporated into a kinematic wave approach (e.g. Germann and Beven, 1985) for modelling macropore flow (both bypassing and pipeflow) in the mid and upper hillslope zones, in an effort to better quantify its movement. This presumably could be incorporated into a chemical model of macropore flow displacement processes, similar to that outlined in 1.

3. Near-stream limited storage effects and their influence on old water displacement and saturation overland flow process could be examined further through chemical tracer experiments. It may be possible to inject lithium bromine at the top of the saturated zone, at a known distance upslope from where limited storage effects are most important. Travel times to the stream channel could be computed, from extracted streamflow at some point downstream. V. Kennedy (personal communication, 1987) notes that lithium would be slightly delayed by adsorption, but bromine would not be delayed unless there was an unusually high anion adsorption. The tracer would be easily detected since both have

very low background levels, and concentrations could be analysed easily using ion chromatography.

3. The process of pipeflow should be examined in more detail and modelling should be attempted. Jones (1988) notes that the four key features to successful pipeflow modelling include: (i) water movement into the pipe wall, (ii) rate of pipeflow, (iii) continuity of the pipe network, and (iv) the position of the pipe outflow relative to open channels. Following the methods of Nieber and Warner (1986), the presence of a pipe could be incorporated into a hillslope model by treating the soil pipe as if it were a drain tile lying on the slope. The mathematical boundary value problem could be solved by coupling a two-component matrix flow and bypass flow model (for flux into the pipe, (i) above) with a turbulent pipe flow model (for in-pipe travel times, (ii) above). This study has identified pipe outflow along the banks of several 1st order channels ((iv) above), and presumably intensive dye or radioactive tracing could be conducted to quantify the continuity or connectedness of the pipe network ((iii) above).

8.2.2 In other areas

There remains a tremendous scope for future investigations into runoff processes, together with opportunities to integrate these results with other fields (i.e. hillslope geomorphology, acquatic ecology, hydrogeology etc). This thesis has underscored the importance of a combined hydrometric, soil physics, stable isotope and chemical tracing approach in identifying the mechanisms, as well as the origins of storm runoff. Future catchment runoff investigations should adopt a similar holistic approach if further progress is to be made in quantifying runoff production. Individually, these techniques are limited. Isotopic tracing is a black-box approach and can only resolve inputs and

outputs of water components. On the other hand, hydrometric approaches allow analysis of water movement pathways, but cannot determine the age or origin of runoff components. Furthermore, the combination of field experimentation and model development (as emphasised by Dunne, 1983) is seen as crucial to the testing of more detailed hypothesis of catchment behaviour.

1. Laboratory studies of macropore flow, limited storage effects and slope development, are required for testing specific hypotheses of catchment response. The advantage of laboratory experiments lies in the controlled initial boundary conditions and in the high precision of measurement of all relevant parameters and variables needed (Stauffer and Dracos, 1986).

Although unrealistic in many ways, laboratory models have the advantage of enabling control of rainfall rate, tracer concentrations, soil variability etc. The experimental approach outlined in this study could be easily converted to a laboratory model. A large scale rainfall simulator and runoff plot would be required and the system could be instrumented with devices similar to the M8 experiment. Known concentrations of specific tracers could be incorporated into the rainfall, and then water could be extracted from soil below, using modified suction lysimeters. Multiple experiments could be run using different soil packing, rainfall intensities and magnitudes. Artificial macropore systems could be incorporated into the soil structure to enable tests of hillslope response using known macropore configurations. Tensiometers could also monitor changes in matric potential. Using a rainfall simulator similar to the Utah Water Research Laboratory model, varying slope angles could also be incorporated into experimental runs.

Specific questions, unique to a laboratory experiment of this kind, could address what effect varying rainfall intensity

and isotopic composition, slope angle, antecedent wetness, soil textures and hydraulic conductivity would have on: (i) resulting subsurface isotopic concentrations, (ii) runoff pathway, rate and timing, and (iii) quickflow-delayed flow relationships. Furthermore, these subsurface flow processes could be incorporated into newly-developed hillslope models (Sharma et al., 1987; Hillman and Verschuren, 1988), since boundary conditions could be easily specified.

2. It would be important to check the experimental and numerical results with observations in natural systems. Although these systems are characterised by a much higher degree of complexity, measurement could be directed at obtaining specific information relevant to laboratory model results. Field verification of rainfall simulator results would be crucial to the overall understanding of observed processes. Key factors identified in model runs could be tested on natural slopes, in gauged catchments where considerable work had already been conducted on subsurface flow hydrology. In this way, knowledge of hillslope behaviour would be a cumulative process, building (in a single catchment) on previous work.

Also, results obtained from highly responsive catchments (or lab models) could be tested on less responsive catchments, to see if observed processes continue to dominate runoff production. The system of laboratory investigation, numerical modelling and field experimentation would clearly address many problems confronted by catchment experiments criticised by Church (1984). Finally, since proper operation of this experimental system would be expensive, it should be designed as a multiple purpose experiment, allowing other investigators to make use of the facilities. In this way, investigations into such diverse phenomenon as solute or

microbial transport, rain-splash erosion, soil creep and debris flow initiation could also be accommodated.

REFERENCES

Abdul, A.S. and R.W. Gillham (1984). Laboratory studies of the effects of the capillary-fringe on streamflow generation. Water Resour. Res., 20:691-698.

Ahuja, L.R., S.A. El-Swaify (1979). Determining soil hydrologic characteristics on a remote forest watershed by continuous monitoring of soil-water pressures, rainfall and runoff. J. Hydrol., 44:135-147.

Ahuja, L.R., J.W. Naney, R.D. Williams and J.D. Ross (1988). Vertical variability of soil properties in a small watershed. J. Hydrol., 99:307-318.

Allison, G.B., C.J. Barnes, M.W. Hughes and F.W.J. Leaney (1983). Effect of climate and vegetation on oxygen-18 and deuterium profiles in soils. In: Isotope Hydrology 1983, IAEA, Vienna, pp.105-123.

American Public Health Association, A.P.H.A. (1976). Standard methods for the examination of water and waste water, 14th ed., American Public Health Association, Washington, D.C., 1193pp.

Anderson, M.G. and T.P. Burt (1977). Automatic monitoring of soil moisture conditions in a hillslope spur and hollow. J. Hydrol., 33:27-36.

Anderson, M.G. and T.P Burt (1978a). Experimental investigations concerning the topographic control of soil water movement on hillslopes. Z. Geomorph. N.F. Suppl. Bd., 29:52-63.

Anderson, M.G. and T.P Burt (1978b. Toward a more detailed field monitoring of variable source area. Water Resour. Res., 14:1123-1131.

Anderson, M.G. and T.P. Burt (1978c). The role of topography in controlling throughflow generation. Earth Surf. Proc., 3:331-344.

Anderson, M.G., M.G. Hubbard and P.E. Kneale (1982). The influence of shrinkage cracks on pore-water pressures within a clay embankment. Q. J. Eng. Geol., 15:9-14.

Anderson, M.G. and P.E. Kneale (1980). Topography and hillslope soil water relationships in a catchment of low relief. J. Hydrol., 47:115-128.

Atkinson, T.C. (1978). Techniques for measuring subsurface flow on hillslopes, In. M.J. Kirkby (ed.), Hillslope Hydrology, Wiley, Chichester, pp.73-120.

Aubertin, G.M. (1971). Nature and extent of macropores in forest soils and their influence on subsurface water movement. Forest Ser. Res. Pap., 192PS, 33pp.

Bache, B.W. (1984). Soil-water interaction. Trans. Roy. Soc. London Series B, 305:393-407.

Beasley, R.S. (1976). Contribution of subsurface flow from the upper slopes of forested watersheds to channel flow. Soil Sci. Soc. Am. J., 40:955-957.

Betson, R.P. (1964). What is watershed runoff? J. Geophys. Res., 69:1541-1551.

Betson, R.P. and J.B. Marius (1969). Source areas of storm runoff. Water Resour. Res., 5:574-582.

Betson, R.P., J.B. Marius and R.T. Joyce (1968). Detection of saturated interflow in soils with piezometers. Soil Sci. Soc. Am. J., 32:602-604.

Beven, K. (1978). The hydrological response of headwater and sideslope areas. Hydrol. Sci. Bull., 23:419-437.

Beven, K. (1981). Micro-, meso-, macroporosity and channeling flow phenomenoa in soils. Soil Sci. Soc. Am. J., 45:1245.

Beven, K.J. and P. Germann (1982). Macropores and water flow in soils. Water Resour. Res., 18:1311-1325.

Beven, K.J., R. Warren and J. Zaoui (1980). SHE: Towards a methodology for physically based distributed forecasting in hydrology. IAHS Publ., 129:133-137.

Beven, K., E.F. Wood and M. Sivapalan (1988). On hydrological heterogeneity: Catchment morphology and catchment response. J. Hydrol., 100:353-375.

Blowes, D.W. and R.W. Gillham (1988). The generation and quality of streamflow on inactive uranium mine tailings near Elliot Lake, Ontario. J. Hydrol., 97:1-22.

Bonell, M., D.A. Gilmour and D.S. Cassells (1983). A preliminary survey of the hydraulic properties of rainforest soils in tropical north-east Queensland and their implications for the runoff process. Catena Suppl., 4:57-78.

Bonell, M., D.A. Gilmour and D.F Sinclair (1981). Soil hydraulic properties and their effect on surface and subsurface water transfer in a tropical rainforest catchment. Hydrol. Sci. Bull., 26:1-18.

Bonell, M., M. R. Hendricks, A.C. Imeson and L. Hazelhoff (1984). The generation of storm runoff in a forested clayey drainage basin in Luxembourg. J. Hydrol., 71:53-77.

Bonell M., A.J. Pearce and M.K. Stewart (1989). The determination of runoff-production mechanisms using environmental isotopes in a tussock grassland catchment, eastern Otago, New Zealand. Hydrol. Proc., submitted.

Bonell, M. and J. Williams (1986). The generation and redistribution of overland flow on a massive Oxic soil in a eucalypt woodland within the semi-arid tropics of north Australia. Hydrol. Proc., 1:31-46.

Bottomley, D.J., D. Craig, and L.M. Johnston (1984). Neutralization of acid runoff by groundwater discharge to streams in Canadian Precambrian Shield watershed. J. Hydrol., 5:1-26.

Bottomley, D.J. D. Craig and L.M. Johnston (1986). Oxygen-18 studies of snowmelt runoff in a small Precambrian Shield watershed. Implications for streamwater acidification in acid-sensitive terrain. J. Hydrol., 88:213-234.

Bouma, J. (1981). Soil morphology and preferential flow along macropores. Agric. Water Manag., 3:235-250.

Bouma, J. and J.L. Anderson (1973). Relationships between soil structure characteristics and hydraulic conductivity. In. Field Soil Water Regime, Soil Sci. Soc. Am. Spec. Publ., 5:77-105.

Bouma, J., L.W. Dekker and C.J. Muilwijk (1981). A field method for measuring short-circuiting in clay soils. J. Hydrol., 52:347-354.

Bouma, J. and P.J.M DeLaat (1981). Estimation of the moisture supply capacity of some swelling clay soils in The Netherlands. J. Hydrol., 49:247-259.

Bouma, J., A. Jongerius, O. Boersma, A. Jager and D. Schoonderbeek (1977). The function of different types of macropores during saturated flow through four swelling soil horizons. Soil Sci. Soc. Am. J., 41:945-950.

Bouma, J., A. Jongerius and D. Schoonderbeek (1979). Calculation of saturated hydraulic conductivity of some pedal clay soils using micromorphometric data. Soil Sci. Soc. Am. J., 43:261-264.

Bouma, J. and J.H.L. Wosten (1979). Flow patterns during extended saturated flow in two undisturbed swelling clay soils with different macro structures. Soil Sci. Soc. Am. J., 43:16-22.

Brand, E.W., M.J. Dale and J.M. Nash (1986). Soil pipes and slope stability in Hong Kong. Q. J. Eng. Geol., 19:301-303.

Bras, R.L., M. Hino, P.K. Kitanidis and K. Takeuchi, eds. (1988). Hydrologic research: The U.S.-Japan experience. Special Issue, J. Hydrol., Vol. 102, 528pp.

Brewer, R. (1964). Fabric and Mineral Analysis of Soils. John Wiley and Sons, New York.

Brown, M.J. (1986). Use of stream chemistry to estimate hydrologic parameters. Water Resour. Res., 22:805-811.

Bryan, B.A. (1979). Effects of strip mining on stormflow and peakflow from experimental basins in eastern Kentucky. M.Sc. Thesis, Univ. of Georgia, Athens, 60pp.

Bullock, P. and A.J. Thomasson (1979). Rothamsted studies of soil structure, 2: Measurement and characterisation of macroporosity by image analysis and comparison with data from water retention measurements. J. Soil Sci., 30:391-414.

Burt, T.P. (1978). An automatic fluid-scanning switch tensiometer system. Brit. Geomorph. Res. Group. Tech. Publ., 21:1-30.

Burt, T.P. (1979). The relationship between throughflow generation and the solute concentration of soil and stream water. Earth Surf. Proc., 4:257-266.

Burt, T.P. (1985). Slopes and slope processes. Prog. in Phys. Geog., 7:583-599.

Burt, T.P. and D.P. Butcher (1985). On the generation of delayed peaks in stream discharge. J. Hydrol., 78:361-378.

Calles, U.M. (1985). Deep groundwater contribution to a small stream. Nord. Hydrol., 16:45-54.

Childs, E.C. (1969). An Introduction to the Physical Basis of Soil Water Phenomena. Wiley, New York, 493pp.

Church, M. (1984). On experimental method in geomorphology. In. Burt, T.P. and D.E. Walling (eds.), Catchment Experiments in Fluvial Geomorphology, Geo Books, Norwich, U.K., pp.563-580.

Clothier, B.E. and I. White (1981). Measurement of sorptivity and soil water diffusivity in the field. Soil Sci. Soc. Am. J., 45:241-245.

Coleman, M.L., T.J. Shepherd, J.J. Durham, J.E. Rouse and G.R. Moore (1982). Reduction of water with zinc for hydrogen isotope analysis. Anal. Chem., 54:993-995.

Conca, J.L. and A.M. Astor (1987). Capillary moisture flow and the origin of cavernous weathering in dolerites of Bull Pass, Antarctica. Geology, 15:151-154

Cooke, R.U., D. Brunsden, J.C. Doornkamp, and D.K.C. Jones (1982). Salinity, groundwater and salt weathering. In. Urban Geomorphology in Drylands. Oxford Univ. Press, Oxford, pp.168-189.

Corbett, E.S., W. Sopper and J.A. Lynch (1975). Watershed response to partial area applications of simulated rainfall. IAHS Publ., 117:63-73.

Costa, J.E. (1984). Physical geomorphology of debris flows. In. Costa, J.E. and P.J. Fleisher (eds.), Developments and Applications of Geomorphology, Springer-Verlag, Berlin, pp. 268-313.

Crabtree, R.W. and S.T. Trudgill (1985). Hillslope hydrogeochemistry and stream response on a wooded permeable bedrock: The role of stemflow. J. Hydrol., 80:161-178.

Craig, H. (1961). Isotope variations in meteoric waters. Science, 133:1702-1703.

Crouzet, E., P. Hubert, P. Olive and E. Siwertz (1970). Le tritium dans les mesures d'hydrologie de surface: Determination experimentale du coefficient de ruissellement. J. Hydrol., 11:217-229.

Danielson, R.E. and P.L. Sutherland (1986). Porosity. In. Klute, A. (ed.), Methods of Soil Analysis, Part 1. Agron. Monog., 9:443-461.

Dansgaard, W. (1964). Stable isotopes in precipitation. Tellus, 16:436-468.

DeVries, J. and T.L. Chow (1978). Hydrologic behaviour of a forested mountain soil in Coastal British Columbia. Water Resour. Res., 14:935-942.

Dillon, P.J., D.S. Jeffries and W.A. Scheider (1982). The use of calibrated lakes and watersheds for estimating atmospheric deposition near a large point source. Water Air Soil Pollut., 18:241-258.

Dincer, T., B.R. Payne, T. Florkowski, J. Martinec amd E. Tongiorgi (1970). Snowmelt runoff from measurements of tritium and oxygen-18. Water Resour. Res., 6:110-124.

Dunne, T. (1969). Runoff production in a humid area. Ph.D. Thesis, Dept. of Geog., Johns Hopkins Univ., Baltimore, Maryland, 255pp.

Dunne, T. (1978). Field studies in hillslope flow processes. In. M.J. Kirkby (ed.), Hillslope Hydrology. Wiley, Chichester, pp.227-293.

Dunne, T. (1983). Relation of field studies and modelling in the prediction of storm runoff. J. Hydrol., 65:25-48.

Dunne, T. and R.D. Black (1970a). An experimental investigation of runoff production in permeable soils. Water Resour. Res., 6:478-490.

Dunne, T. and R.D Black (1970b). Partial area contributions to storm runoff in a small New England watershed. Water Resour. Res., 6:1296-1311.

Durum, W.H. (1953). Relation of mineral constituents in solution to streamflow, Saline River near Russel, Kansas. Trans. Am. Geophys. Union, 34:435-442.

Duysings, J.J.H.M., J.M. Verstraten and L. Bruynzeel (1983). The identification of runoff sources of a forested lowland catchment: A chemical statistical approach. J. Hydrol., 64:357-375.

Edwards, A.M.C. (1973). The variation of dissolved constituents with discharge in some Norfolk rivers. J. Hydrol., 18:219-242.

Egboka, B.C.E. (1985). Appropriate monitoring techniques using bomb tritium and other geochemical parameters in hydrogeological investigations. Hydrol. Sci. J., 30:207-224.

Ehhalt, D.K., K. Knott, J.F. Nagel and J.C. Vogel (1963). Deuterium and oxygen-18 in rain water. J. Geophys. Res., 68:3775-3780.

Elrick, D.E., W.D. Reynolds, D.M. Lee and B.E. Clothier (1984). The 'Guelph Permeameter' for measuring the field-saturated soil hydraulic conductivity above the water table, 1: Theory, procedures and applications. Proc. Can. Hydrol. Symp., Quebec City, pp.643-655.

Eriksson, E. (1965). Deuterium and oxygen-18 in precipitation and other natural waters. Some theoretical considerations. Tellus, 17:498-512.

Everitt, B.S. (1974). Cluster Analysis. Heinemann Educational Books, London.

Fayer, M.J. and D. Hillel (1986). Air encapsulation, 2: Profile water storage and shallow water table fluctuation. Soil Sci. Soc. Am. J., 50:572-577.

Fisher, R.V. (1971). Features of coarse-grained high concentration fluids and their deposits. J. Sed. Petrol., 41:916-927.

Freeze, R.A. (1972a). Role of subsurface flow in generating surface runoff, 1. Baseflow contributions to channel flow. Water Resour. Res., 8:609-623.

Freeze, R.A. (1972b). Role of subsurface flow in generating surface runoff, 2. Upstream source areas. Water Resour. Res., 8:1272-1283.

Freeze, R.A. and J.A. Cherry (1979). Groundwater. Prentice-Hall, Englewood Cliffs, New Jersey, 604pp.

Fritz, P., J.A. Cherry, K.U. Weyer and M. Sklash (1976). Storm runoff analyses using environmental isotopes and major ions. In. Interpretation of Environmental Isotope and Hydrochemical Data In Groundwater Hydrology, IAEA, Vienna, pp.111-130.

Gat, J.R. and W. Dansgaard (1972). Stable isotope survey of the fresh water occurrences in Isreal and the northern Jordan rift valley. J. Hydrol., 16:177-212.

Germann, P.F. (1986). Rapid drainage response to precipitation. Hydrol. Proc., 1:3-13.

Germann, P.F. and K. Beven (1981). Water flow in soil macropores 1: An experimental approach. J. Soil Sci., 32:1-13.

Germann, P.F. and K. Beven (1985). Kinematic wave approximation to infiltration into soils with sorbing macropores. Water Resour. Res., 21:990-996.

Gillham, R.W. (1984). The capillary-fringe and its effect on water-table response. J. Hydrol., 67:307-324.

Gradwell, M.W. (1978). Pore-size distributions of some New Zealand soil groups. NZ J. Agric. Res., 21:603-613.

Hammermeister, D.P., G.F. Kling and J.A. Vomocil (1982a). Perched water tables on hillsides in Western Oregon 1; Some factors affecting their development and longevity. Soil Sci. Soc. Am. J., 46:811-818.

Hammermeister, D.P., G.F. Kling and J.A. Vomocil (1982b). Perched water tables on hillsides in Western Oregon 2; Preferential downslope movement of water and anions. Soil Sci. Soc. Am. J., 46:819-826.

Hanks, R.J. and G.L. Ashcroft (1986). Applied Soil Physics. Springer-Verlag, Berlin, 159pp.

Harr, R.D. (1977). Water flux in soil and subsoil on a steep forested slope. J. Hydrol., 33:37-58.

Hartley, P.E. (1981) Deuterium/hydrogen ratios in Australian rainfall. J. Hydrol., 50:217-229.

Heathcote, J.A. and J.W. Lloyd (1986). Factors affecting the isotopic composition of daily rainfall at Driby, Lincolnshire. J. Climat., 6:97-106.

Heliotis, F.D. and C.B. DeWitt (1987). Rapid water table responses to rainfall in a northern peatland ecosystem. Water Resour. Bull., 23:1011-1016.

Herrmann, A., J. Martinec and W. Stichler (1978). Study of snowmelt-runoff components using isotope measurements. In. Colbeck, S.C. and M.Ray (eds.), Proc. Modelling of Snow Cover Runoff, U.S. Army Cold Regions Res. and Eng. Lab., pp.288-296.

Herrmann, A. and W. Stichler (1980). Groundwater-runoff relationships. Catena, 7:251-263.

Hewlett, J.D. (1961). Soil moisture as a source of base flow from steep mountain watershed. US Dept. Agric. Forest Ser., Southeastern Forest experiment Station, Asherville, North Carolina, Station Paper 132, 11pp.

Hewlett, J.D. (1982). Principles of Forest Hydrology. Univ. of Georgia Press, Athens, 183pp.

Hewlett, J.D., G.B. Cunningham and C.A. Troendle (1977). Predicting stormflow and peakflow from small basins in humid areas by the R-index method. Water Resour. Res., 13:231-253.

Hewlett, J.D. and A.R. Hibbert (1963). Moisture and energy conditions within a sloping soil mass during drainage. J. Geophys. Res., 68:1081-1087.

Hewlett, J.D. and A.R. Hibbert (1967). Factors affecting the response of small watersheds to precipitation in humid areas. In. W.E. Sopper and W.H. Lull (eds.), International Symposium on Forest Hydrology, Pergamon, New York, pp.275-290.

Hillel, D. (1987). Unstable flow in layered soils: A review. Hydrol. Proc., 1:143-147.

Hillman, G.R. and J.P. Verschuren (1988). Simulation of the effects of forest cover, and its removal, on subsurface water. Water Resour. Res., 24:305-314.

Hooper, R.P. and C.A. Shoemaker (1986). A comparison of chemical and isotopic hydrograph separation. Water Resour. Res., 22:1444-1454.

Hope, A.S. (1984). Estimation of stormflow volumes from small semi-arid catchments using the R-index method. J. Hydrol., 67:129-139.

Horton, J.H. and R.H. Hawkins (1965). Flow path of rain from the soil surface to the water table. Soil Sci., 100:377-383.

Horton, R.E. (1933). The role of infiltration in the hydrological cycle. Trans. Am. Geophys. Union, 14:446-460.

Jacks, G., E. Olofsson and G. Werme (1986). An acid surge in a well-buffered stream. Ambio, 15:282-285.

Jackson, R.J. (1987). Hydrology of an acid wetland before and after draining for afforestation, western New Zealand. IAHS Publ. 167:465-474.

Jones, J.A.A. (1971). Soil piping and stream channel initiation. Water Resour. Res., 7:602-610.

Jones, J.A.A. (1979). Extending the Hewlett model of storm runoff generation. Area, 11:110-114.

Jones, J.A.A. (1987). The effects of soil piping on contributing areas and erosion patterns. Earth Surf. Proc., 12:229-248.

Jones, J.A.A. (1988). Modelling pipeflow contributions to stream runoff. Hydrol. Proc., 2:1-17.

Kennedy, V.C., G.W. Zellweger and R.J. Avanzino. (1979). Variation of rain chemistry during storms at two sites in Northern California. Water Resour. Res., 15:687-702.

Kennedy, V.C., C. Kendall, G.W. Zellweger, T.A. Wyerman and R.J. Avanzino (1986). Determination of the components of stormflow using water chemistry and environmental isotopes, Mattole River Basin, California. J. Hydrol., 84:107-140.

Kirkby, M.J. (ed.) (1978). Hillslope Hydrology. John Wiley and Sons, Chichester, 389pp.

Klute, A. (1986). Water retention: Laboratory methods. In. Klute, A. (ed.), Methods of Soil Analysis, Part 1, Soil Sci. Soc. Am, Agron. Monog., 9:635-662.

Knapp, B. (1973). A system for the field measurement of soil water movement. Brit. Geomorph. Res. Gp. Tech. Publ., 9:1-26.

Kneale, W.R. and R.E. White (1984). The movement of water through cores of a dry (chalked) clay-loam grassland topsoil. J. Hydrol., 67:361-365.

Kreft, A. and A. Zeuber (1978). On the physical meaning of the dispersion equation and its solutions for different initial and boundary conditions. Chem. Eng. Sci., 33:1471-1480.

Krouse, H.R., G. Hollecek, and H. Steppuhn (1978). Detecting snow water in streamflow by D/H and $^{18}O/^{16}O$ abundances in two Western Canadian Basins. In. B.W. Robinson (ed). Stable Isotopes in the Earth Sciences. NZ DSIR Bull., 220:87-95.

Langbein, W.B. and D.R. Dawdy (1964). Occurrence of dissolved solids in surface waters in the United States. US Geol. Surv. Pap., 501-D.

Likens, G.E., F.H. Bormann, R.S. Pierce, J.S. Eaton and N.M. Johnson (1977). Biogeochemistry of a Forest Ecosystem. Springer-Verlag, New York, N.Y., 146pp.

Linsley, R.K., M.A. Kohler and J.L.H. Paulhus (1982). Hydrology for engineers. McGraw Hill Internat., Tokyo, 508pp.

Lundin, L. (1982). Mark-och grundvatten i moranmark och marktypens betydelse for avrinningen. UNGI Report 56, Uppsala Univ., Dept. of Phys. Geog., 216pp. (in Swedish, quoted in Rodhe, 1987).

Luxmoore, R.J. (1981). Micro-, meso- and macroporosity of soil. Soil Sci. Soc. Am. J., 45:671.

Maloszewski, P., W. Rauert, W. Stichler and A. Herrmann (1983). Application of flow models in an alpine catchment area using tritium and deuterium data. J. Hydrol., 66:319-330.

Maloszewski, P. and A. Zuber (1982). Determining the turnover time of groundwater systems with the aid of environmental tracers, 1. Space models and their applicability. J. Hydrol., 57:207-231.

Marshall, T.J. (1959). Relations between water and soil. Tech. Comm. 50, Commonwealth Bur. Soils, Harpenden, U.K.

Marthaler, H.P., W. Vogelsanger, F. Richard and R.J. Wierenga (1983). A pressure transducer for field tensiometers. Soil Sci. Soc. Am. J., 47:624-627.

Martinec, J. (1975). Subsurface flow from snowmelt traced by tritium. Water Resour. Res., 11:496-498.

Matsuo, S. and I. Friedman (1967). Deuterium content in fractionally collected rainwater. J. Geophys. Res., 72:6374-6376.

McCaig, M. (1983). Contributions to storm quickflow in a small headwater catchment - The role of natural pipes and soil macropores. Earth Surf Proc., 8:239-252.

McCord, J.T. and D.B. Stevens (1987). Lateral moisture flow beneath a sandy hillslope without an apparent impeding layer. Hydrol. Proc., 1:225-238.

McDonald, P.M. (1967). Disposition of soil moisture held in temporary storage in large pores. Soil Sci., 103:139-143.

McKie, D.A. (1978). A study of soil variability within the Blackball Hill Soils, Reefton, New Zealand. M.Ag.Sc. Thesis, University of Canterbury, 180pp.

Megahan, W.F. (1983). Hydrologic effects of clearcutting and wildfire on steep granitic slopes in Idaho. Water Resour. Res., 19:811-819.

Megahan, W.F. and J.L. Clayton (1983). Tracing subsurface flow on roadcuts on steep, forested slopes. Soil Sci. Soc. Am. J., 47:1063-1067.

Mew, G., T.H. Webb, C.W. Ross and J. Adams (1975). Soils of Ignangahua Depression, South Island, New Zealand. NZ Soil Surv. Rep. No. 17.

Miyake, H., O. Matsubaya and C. Nishihara (1968). An isotopic study of meteoric precipitation. Pap. Meteorol. Geophys., 19:243-266.

Mosley, M.P. (1979). Streamflow generation in a forested watershed, New Zealand. Water Resour. Res., 15:795-806.

Mosley, M.P. (1982). Subsurface flow velocities through selected forest soils, South Island, New Zealand. J. Hydrol., 55:65-92.

Mullins, C.E., O.T. Mandiringana, T.R. Nisbet and M.N. Aitken (1986). The design, limitations and use of a portable tensiometer. J. Soil Sci., 37:691-700.

Neary, D.G. and L.W. Swift (1987). Rainfall thresholds for triggering a debris avalanching event in the southern Appalachian Mountains. Rev. in Eng. Geol., Geol. Soc. Am., 7:81-92.

Nelson, W.R. and L.D. Baver (1940). Movement of water through soils in relation to the nature of the pores. Soil Sci. Soc. Am. J., 5:69-76.

Nieber, J.L. and G.S. Warner (1986). Partitioning subsurface stormflow between soil matrix flow and soil pipe flow. EOS, 67(44):956.

Nixon, P.R. and G.P. Lawless (1960). Translocation of moisture with time in unsaturated soil profiles. J. Geophys. Res., 65:655-661.

Novakowski, K.S. and R.W. Gillham (1988). Field investigations of the nature of water-table response to precipitation in shallow water-table environments. J. Hydrol., 97:23-32.

New Zealand Soil Bureau (1968). General survey of the soils of the South Island, New Zealand. NZ Soil Bur., Bull. No. 4, 404pp.

Nutter, W.L. (1971). The role of soil water in the hydrologic behaviour of upland basins. In. Field Soil Water Regime, Soil Sci. Soc. Am. J., Spec. Publ., pp.181-193.

O'Brien, A.L. (1982). Rapid water table rise. Water Resour. Bull., 18:713-715.

O'Loughlin, C.L. and A.J. Pearce (1976). Influence of Cenozoic geology on mass movement and sediment yields in small forest catchments, North Westland, New Zealand. Bull. Int. Assoc. Eng. Geol., 14:41-46.

O'Loughlin, C.L., L.K. Rowe and A.J. Pearce (1980). Sediment yield and water quality responses to clearfelling of evergreen mixed forests in western New Zealand. IAHS Publ., 130:285-292.

O'Loughlin, C.L., L.K. Rowe and A.J. Pearce (1982). Exceptional storm influences on slope erosion and sediment yield in small forest catchments, North Westland, New Zealand. In Proc. Nat. Symp. on Forest Hydrology, Melbourne, Australia, pp.84-91.

O'Loughlin, E.M. (1981). Saturated regions in catchments and their relations to soil and topographic properties. J. Hydrol., 53:229-246.

Olszewski, R.J. (1980). Stormflow and peakflow prediction in northeast Georgia with the R-index method. M.Sc. Thesis, Univ. of Georgia, 50pp.

Omoti, U. and A. Wild (1979). Use of fluorescent dyes to mark the pathways of solute movement through soils under leaching conditions, 2. Field experiments. Soil Sci., 128:98-104.

Overrein, L.N., H.M. Seip and A. Tollar (1980). Acid precipitation-effects on forest and fish. Final Rep. of the SNSF Project, 1972-80 SNSF Proj. FR19/80, Norwegian Inst. Water Res., Oslo.

Palkovics, W.E. and G.W. Petersen (1977). Contribution of lateral soil water movement above a fragipan to streamflow. Soil Sci. Soc. Am. J., 41:394-400.

Pearce, A.J. and A.I. McKerchar (1979). Upstream generation of storm runoff. In. D.L Murray and P. Ackroyd (eds.), Physical Hydrology The New Zealand Experience. NZ Hydrol. Soc., pp.165-192.

Pearce, A.J., C.L. O'Loughlin and L.K. Rowe (1976). Hydrologic regime of small, undisturbed beech forest catchments, North Westland. In. Proc. 3rd Soil and Plant Water Symp., NZ DSIR Publ., pp150-158.

Pearce, A.J., L.K. Rowe and C.L. O'Loughlin (1980). Effects of clearfelling and slash-burning on water yield and storm hydrographs in evergreen mixed forests, western New Zealand. IAHS Publ., 30: 119-127.

Pearce, A.J., L.K.Rowe, and C.L. O'Loughlin (1984). Hydrology of mid-altitude tussock grasslands, Upper Waipori catchment: II - Water balance, flow duration and storm runoff. J. Hydrol. (NZ), 23:60-72.

Pearce, A.J. and L.K. Rowe (1981). Rainfall interception in a multi-storied, evergreen mixed forest: Estimates using Gash's analytical model. J. Hydrol., 49:341-353.

Pearce, A.J., M.K. Stewart and M.G. Sklash (1986). Storm runoff generation in humid headwater catchments 1: Where does the water come from? Water Resour. Res., 22:1263-1272.

Phillip, J.R. (1968). The theory of absorption in aggregated media. Aust. J. Soil Res., 6:1-19.

Pierson, T.C. (1980). Piezometric responses to rainstorms in forested hillslope drainage depressions. J. Hydrol. (NZ), 19:1-10.

Pierson, T.C. (1983). Soil pipes and slope stability. Q. J. Eng. Geol., 16:1-11.

Pilgrim, D.H., D.D. Huff and T.D. Steele (1978). A field evaluation of subsurface runoff 2. Runoff processes. J. Hydrol., 38:319-341.

Pilgrim, D.H., D.D. Huff and T.D. Steele (1979). Use of specific conductance and contact time relations for separating flow components in storm runoff. Water Resour. Res., 15:329-339.

Pinder, G.F. and J.F. Jones (1968). Determination of the groundwater component of peak discharge from the chemistry of total runoff. Water Resour. Res., 5:438-445.

Price, A.G. and B.O. Bauer (1984). Small-scale heterogeneity and soil-moisture variability in the unsaturated zone. J. Hydrol., 70:277-293.

Ragan, R.M. (1968). An experimental investigation of partial area contribution. IAHS Publ., 76:241-249.

Rahe, T.M., C. Hagedorn, E.L. McCoy and G.F. Kling (1978). Transport of antibiotic-resistant Escherichi coli through a western Oregon hillslope soil under conditions of saturated flow. J. Environ. Qual., 7:487-494.

Ranken, D.W. (1974). Hydrologic properties of soil and subsoil on a steep forested slope. M.Sc. Thesis, Oregon State Univ, Corvallis.

Reeves, M.J. (1980). Recharge of the English chalk, a possible mechanism. Eng. Geol., 14:231-240.

Reynolds, W.D. and D.E. Elrick (1985). Measurement of field-saturated conductivity, sorptivity and the conductivity-pressure head relationship using the Guelph Permeameter. Proc. Nat. Water Well Assoc. Conf. on Characterization and Monitoring of the Vadose (Unsaturated) Zone, Denver, Colorado, pp.1-25.

Ringrose-Voase, A.J. (1987). A scheme for the quantitative description of soil macrostructure by image analysis. J. Soil Sci., 38:343-356.

Rodhe, A. (1981). Spring flood meltwater or groundwater. Nord. Hydrol., 12:21-30.

Rodhe, A. (1987). The origin of streamwater traced by oxygen-18. Uppsala Univ., Dept. of Phys. Geog., Div. Hydrol., Report Series A41, 260pp. Appendix 71pp.

Rogers, N.W. and M.J. Selby (1980). Mechanisms of shallow translational landsliding during summer rain-storms: North Island, New Zealand. Geogaf. Ann., 62:11-21.

Rowe, L.K. (1979). Rainfall interception by a Beech-Podocarp-Hardwood forest near Reefton, North Westland, New Zealand. J. Hydrol. (NZ), 18:63-72.

Rowe, L.K. (1988). Maimai hydrological study: Report on the storm of 19 May 1988. Unpub. Rep., pp.1-4.

Scotter, D.R. (1978). Preferential solute movement through larger soil voids 1: Some computations using simple theory. Aust. J. Soil Res., 16:257-267

Sharma, M.L., R.J. Luxmoore, R. DeAngelis, R.C. Ward and G.T. Yeh (1987). Subsurface water flow simulated for hillslopes with spatially dependent soil hydraulic characteristics. Water Resour. Res., 23:1523-1530.

Shlemon, R.J., R.H. Wright and D.R Montgomery (1987). Anatomy of a debris flow, Pacifica, California. Rev. in Eng. Geol., Geol. Soc. Am., 7:181-199.

Sidle, R.C., A.J. Pearce and C.L. O'Loughlin (1985). Hillslope stability and land use. Water Resour. Monograph 11, Am. Geophys. Un., 140pp.

Sidle, R.C. and D.N. Swanston (1981). Storm characteristics affecting piezometric rise in unstable hillslopes of southeast Alaska (abstract). EOS Trans., AGU, 62:856.

Sidle, R.C. and D.N. Swanston (1982). Analysis of a small debris slide in coastal Alaska. Can. Geotech. J., 19:167-174.

Sklash, M.G., R.N. Farvolden and P. Fritz (1976). A conceptual model of watershed response to rainfall, developed through the use of oxygen-18 as a natural tracer. Can. J. Earth Sci., 13:271-283.

Sklash, M.G. and R.N. Farvolden (1979). The role of groundwater in storm runoff. J. Hydrol., 43:45-65.

Sklash, M.G. and R.N. Farvolden (1980). The use of environmental isotopes in the study of high-runoff episodes in streams. In. E.C. Perry Jr. and C.W. Montgomery (eds.), Isotope Studies of Hydrologic Processes. North. Illinois Univ. Press, DeKalb, Ill., pp.65-73.

Sklash, M.G., M.K. Stewart and A.J. Pearce (1986). Storm runoff generation in humid headwater catchments 2: A case study of hillslope and low-order stream response. Water Resour. Res., 22:1273-1282.

Sklash, M.G. and B.A. Wilson (1982). An investigation of the groundwater ridging hypothesis for storm runoff generation. Proc. Canadian Hydrol Symp., Fredericton, N.B., pp.575-595.

Skopp, J., W.R. Gardner and E.J. Tyler (1981). Solute movement in structured soils: Two-region model with small interaction. Soil Sci. Soc. Am. J., 45:837-842.

Smettem, K.R.J., S.T. Trudgill and A.M. Pickles (1983). Nitrate loss in soil drainage waters in relation to bypassing flow and discharge on an arable site. J. Soil Sci., 34:499-509.

Smith, M.S., G.W. Thomas, R.E. White and D. Ritonga (1985). Transport of Escherchia coli through intact and disturbed columns of soil. J. Environ. Qual., 14:87-91.

Stauffer, F. and T. Dracos (1986). Experimental and numerical study of water and solute infiltration in layered porous media. J. Hydrol., 84:9-34.

Stanley, K., G.L. Lyon and M.K. Stewart (1984). Hot shot reduction of water to hydrogen for isotopic analysis. Rep. INS-R-322, Inst. of Nucl. Sci., DSIR, Lower Hutt, New Zealand.

Stephenson, G.R. and R.A. Freeze (1974). Mathematical simulation of subsurface flow contributions to snowmelt runoff, Reynolds Creek watershed, Idaho. Water Resour. Res., 10:284-294.

Stewart, M.K. (1975). Stable isotope fractionation due to evaporation and isotopic exchange of falling water drops: Application to atmospheric processes and evaporation of lakes. J. Geophys. Res., 80:1138-1146.

Systat (1985). Software manual. Systat Inc., Evanston, Illinois, 417pp.

Talsma, T. and P.M. Hallam (1980). Hydraulic conductivity measurement of forest catchments. Aust. J. Soil Res., 30:139-148.

Thomas, G.W. and R.E. Phillips (1979). Consequences of water movement in macropores. J. Environ. Qual., 8:149-152.

Thomas, G.W., R.E. Phillips and V.L. Quisenberry (1978). Characterisation of water displacement in soils using simple chromographic theory. J. Soil Sci., 32:32-37.

Thony, J.L. and G. Vachaud (1980). Automatic measurement of soil-water pressure using a capacitance manometer. J. Hydrol., 46:189-196.

Tomlinson, A.I. (1980). The frequency of high intensity rainfalls in New Zealand, Part 1. Water and Soil Tech. Publ., 19.

Turk, L.K. (1975). Diurnal fluctuations of water tables induced by atmospheric pressure changes. J. Hydrol., 26:1-16.

Turner, J.V., D.K. Macpherson and R.A. Stokes (1987). The mechanisms of catchment flow processes using natural variations in deuterium and oxygen-18. J. Hydrol., 94:143-162.

Van Stiphourt, T.P.J., H.A.J. Van Lanen, O.H. Boersma and J. Bouma (1987). The effect of bypass flow and internal catchment of rain on the water regime in a clay loam grassland soil. J. Hydrol., 95:1-11.

Walling, D.E. and I.D.L. Foster (1975). Variations in the natural chemical concentration of river water during flood flows, and the lag effect: Some further comments. J. Hydrol., 26:237-244.

Ward, R.C. (1984). On the response to precipitation of headwater streams in humid areas. J. Hydrol., 74:171-189.

Watson, K.K. (1967). A recording field tensiometer with rapid response characteristics. J. Hydrol., 5:33-39.

Webster, J. (1977). The hydrologic properties of the forest floor under beech/podocarp hardwood forest, North Westland. Unpubl. MSc thesis, University of Canterbury, Chrsitchurch, 77pp.

Wellings, S.R. and J.P. Bell (1980). Movement of water and nitrate in the unsaturated zone of upper chalk near Winchester, Hants, England. J. Hydrol., 48:119-136.

Wellings, S.R. and J.P. Bell (1982). Physical controls of water movement in the unsaturated zone. Q. J. Eng. Geol., 15:235-241.

Weyman, D.R. (1970). Throughflow on hillslopes and its relation to the stream hydrograph. Int. Assoc. Hydrol. Sci. Bull., 15:25-33.

Weyman, D.R. (1973). Measurements of the downslope flow of water in a soil. J. Hydrol., 20:267-288.

Wheater, H.S., S.J. Langan, J.D. Miller and R.C. Ferrier (1987). The determination of hydrological flow paths and associated hydrochemistry in forested catchments in central Scotland. IAHS Publ., 167:433-449.

Whipkey, R.Z. (1965). Subsurface flow on forested slopes. Bull. Int. Assoc. Sci. Hydrol., 10:74-85.

Whipkey, R.Z. (1967). Theory and mechanics of subsurface stormflow. In. W.E. Sopper and H.W. Lull (eds.). Int. Symp. on Forest Hydrology, Pergamon Press, pp.255-260.

Whipkey, R.Z. and M.J. Kirkby (1978). Flow within the soil. In. M.J. Kirkby (ed.), Hillslope Hydrology, Wiley, Chichester, pp.121-144.

Wilcox, J.C. (1959). Rate of soil drainage following an irrigation. 1: Nature of soil drainage curves. Can. J. Soil Sci., 39:107-119.

Wilson, G.V. and R.J. Luxmoore (1988). Infiltration, macroporosity and mesoporosity distributions on two forested watersheds. Soil Sci. Soc. Am. J., 52:329-335.

Wilson, C.A. and P. Smart (1984). Pipes and pipeflow in an upland catchment. Catena, 11:145-158.

Woodruff, J.F. and J.D. Hewlett (1970). Predicting and mapping the average hydrologic response for the eastern United States. Water Resour. Res., 6:1312-1326.

Zaltsberg, E. (1986). Comment on 'Laboratory studies of the effects of the capillary-fringe on streamflow generation' by A.S. Abdul and R.W. Gillham. Water Resour. Res., 22:837-838.

Zanger, C.N. (1953). Theory and problems of water percolation. Eng. Monog., Bureau of Reclam., Denver, Colorado, pp.48-71.

Zimmerman, U., K.O. Munnich, W. Roether, W. Kreutz, K. Schubach and O. Siegel (1966). Tracers determine movement of soil moisture and evapotranspiration. Science, 152:346-347.

Zuber, A. (1986). Mathematical models for the interpretation of environmental radioisotopes in groundwater systems. In. Fritz, P. and J.C. Fontes (eds.), Handbook of Environmental Isotope Geochemistry, Vol. 1, Part B., Elsevier, Amsterdam.

A LABORATORY CALIBRATIONS

Laboratory calibrations of the electronically multiplexed recording tensiometer system were conducted to examine tensiometer response time. Three factors were tested in relation to tensiometer tubing effects on pressure response and attenuation downline: tube material, length and diameter. A cheap, readily available non-toxic tubing (4.2 mm OD) was initially selected as a tubing to connect the tensiometer pipes to transducer port. Lab tests showed, however, that the flexible-walled tubing exhibited large pressure attenuation (in a 15 m length of tube) in response to 360 mm head changes (Figure A.1). This concern led to a test of two new rigid-walled nylon vacuum tubing configurations in order to reduce these effects; 3/16" (4.7 mm) OD, and 1/16" (1.6 mm) OD.

Both tube diameters were subjected to multiple increases and decreases in head by simply raising and lowering a water reference bottle. The CR21X was used as a volt meter and recorded voltage output changes in the SCX15DN sensors. Figure A.2 shows that although the 1.6 mm OD tubing displayed immediate response at varying lengths (and therefore no pressure attenuation), the relative voltage difference between the 15 m length and 1 m length increased with increasing head. The 4.7 mm OD diameter showed no pressure attenuation and low relative voltage change between 15 and 1 m lengths (Figure A.2B). These data, combined with the potentially higher latent heat store in the 4.7 mm OD tubing (i.e. in relation to possible freezing in winter months) led to the selection of the 4.7 mm OD nylon vacuum tubing for field experimentation.

The Soil Moisture Corp. 1 bar (1×10^5 Pa) cup was chosen to enable rapid equilibrium between the soil and cup. A porous

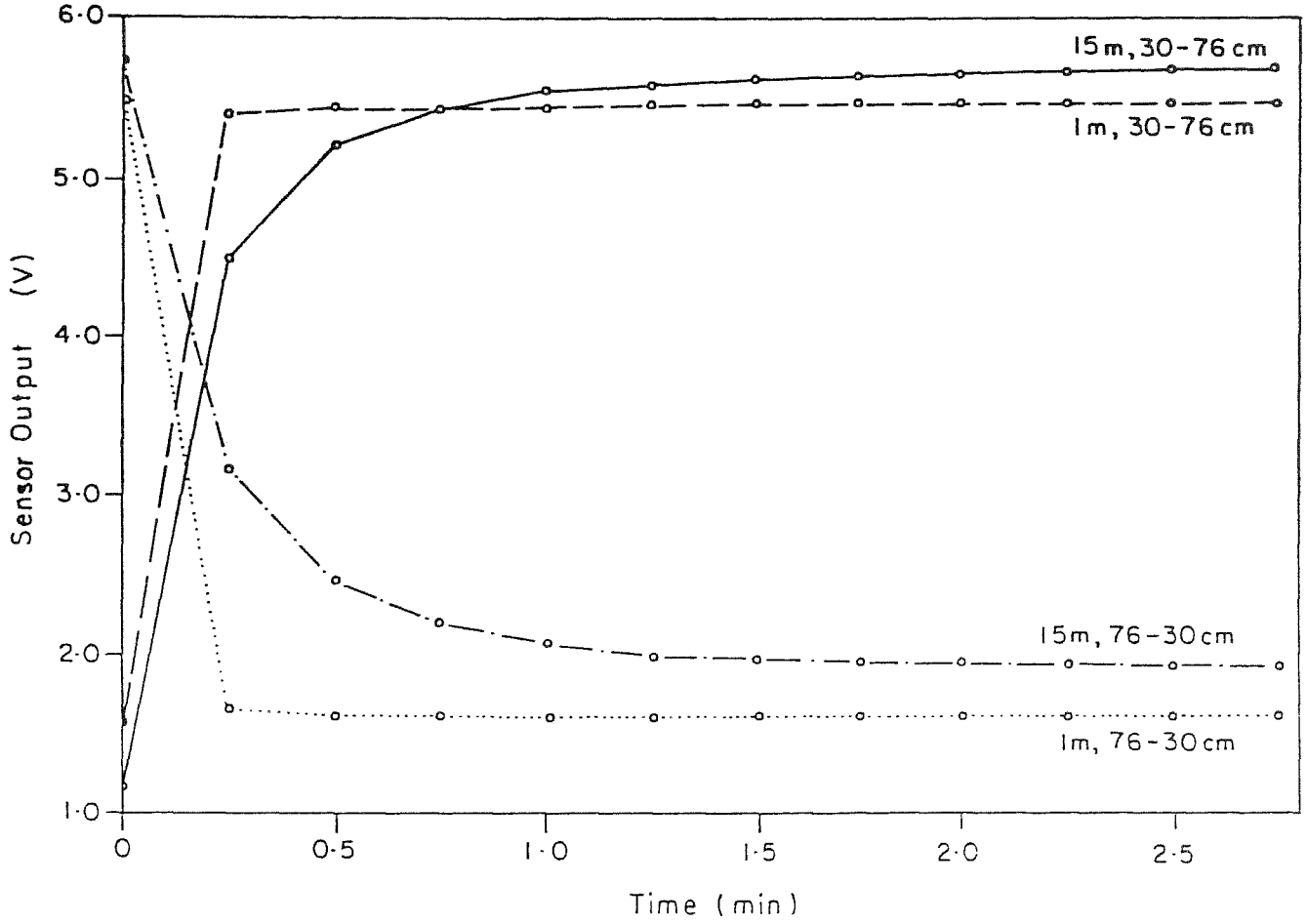

Figure A.1 Effect of +/-360 mm head change on 1 m and 15 m flexible tubing.

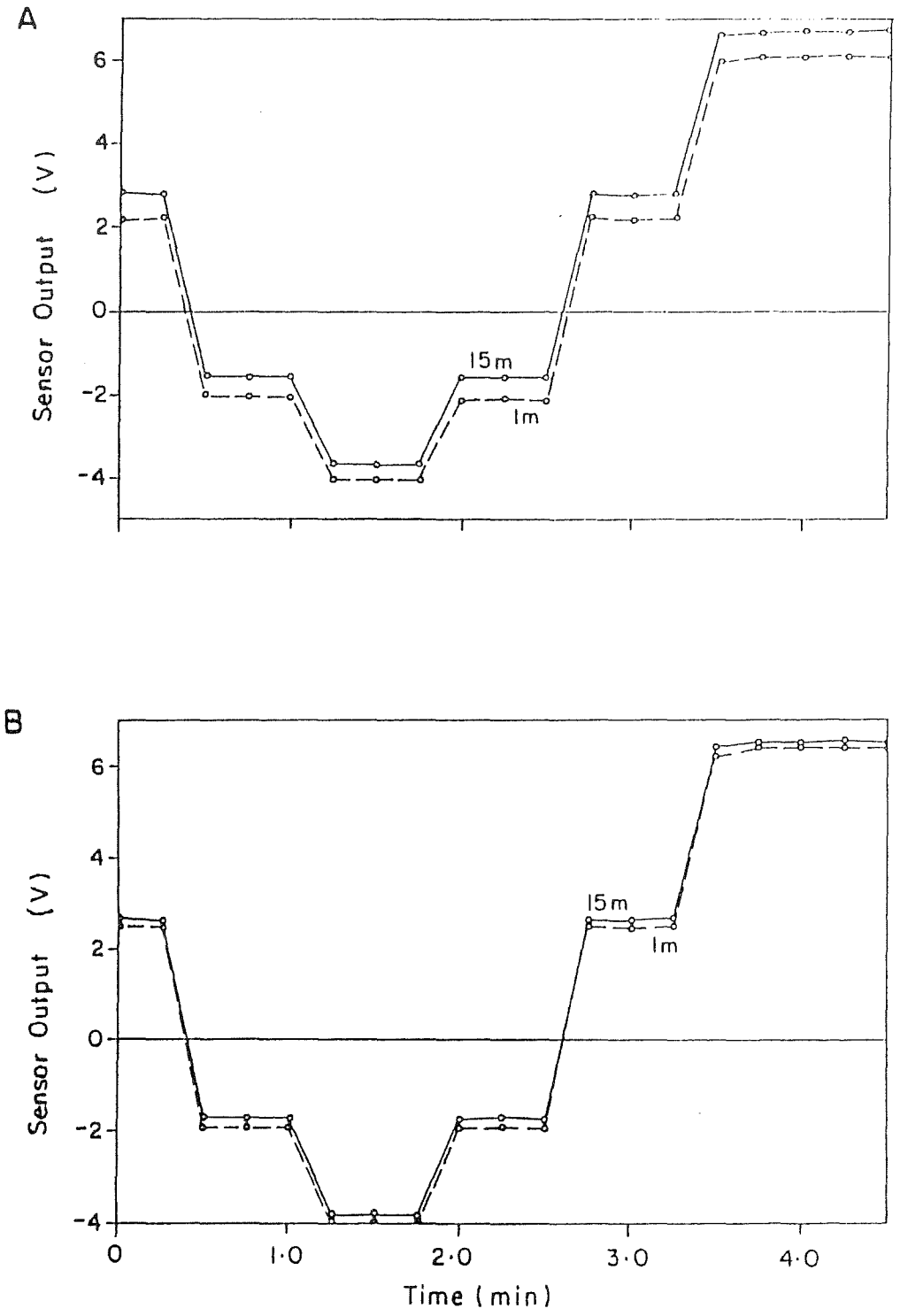

Figure A.2 Effect of head changes on pressure response through 1 m and 15 m tubing for 1.6 mm (A) and 4.7 mm (B) diameters.

ceramic, with the largest possible pore size that still maintained a bubbling pressure higher than the maximum equilibrium pressure used, was required to facilitate this. The 1 bar cup showed a bubbling pressure (air entry value) of 20-30 psi (1.38×10^{5}-2.07×10^{5} Pa) and flow rate of c.2 ml hr^{-1} cm^{-2} (Soil Moisture Corporation, unpublished data, 1978). Hydraulic conductivity of the porous cup was determined using Darcy's Law:

$$K = V\ L / A\ h'\ t \qquad (A.1)$$

where: K is the hydraulic conductivity, V is the volume of fluid that flows through a given area in a given time, L is the thickness of the porous cup, A is the area through which the fluid flows, h' is the pressure differential across the plate and t is the time interval of flow. Given a flow of 2 ml^{-1} hr^{-1} cm^{2} 14.7 psi^{-1} through a 1/4" (6.3 mm) wall thickness, K = 3.46×10^{-9} m sec^{-1}, with a pore size of c.2.1 microns.

Soil bin experiments were conducted to examine porous ceramic cup response time in relation to changing head within a medium sand porous media. In response to anticipated maximum head fluctuations in an M8 field situation, results showed an equilibrium time of c.5-10 min. (Figure A.3). On the basis of this information, the multiplexer scanning rate was set at 10 min intervals.

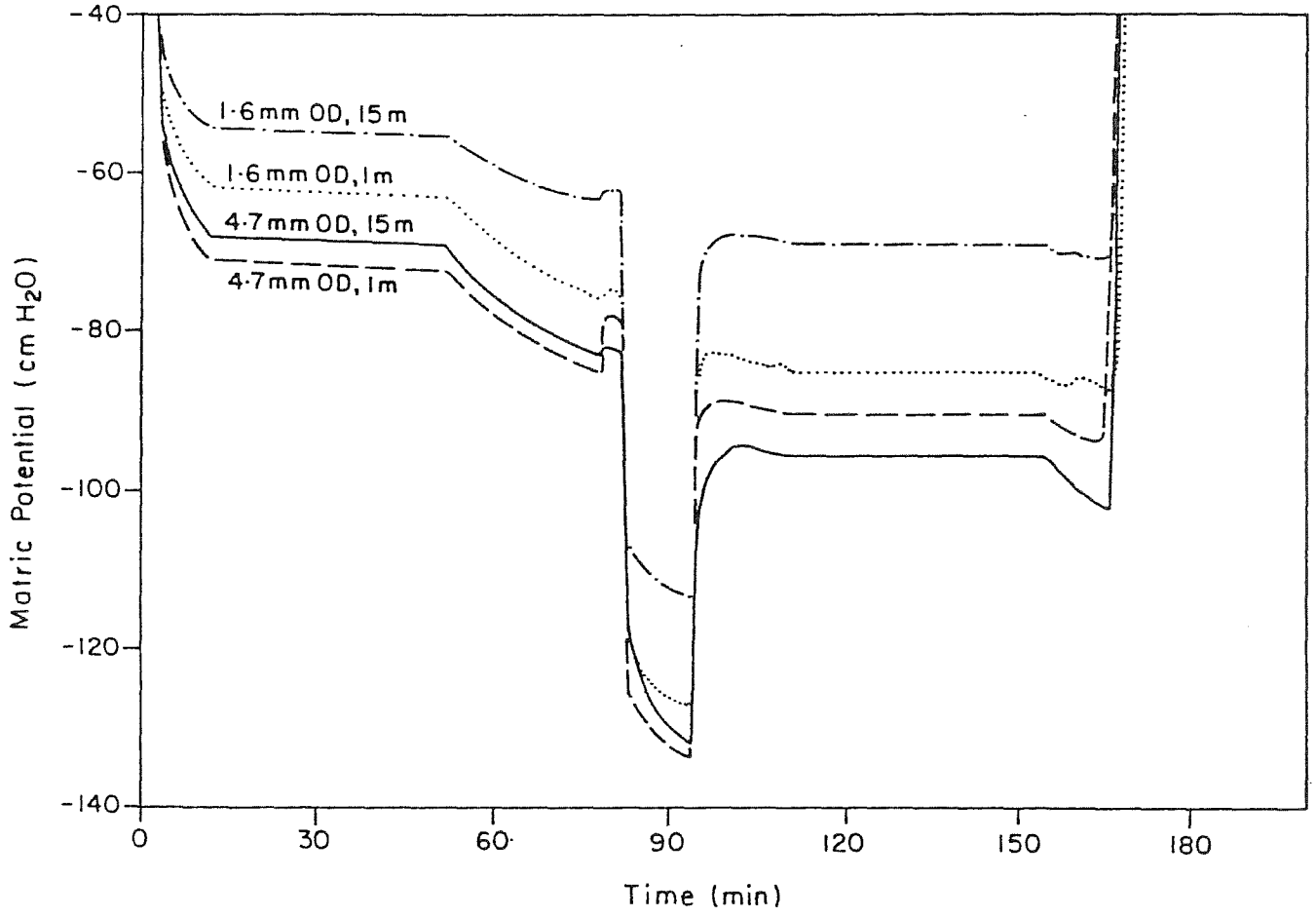

Figure A.3 Soil bin experiments for determining porous cup response time.

B THROUGHFLOW AND STREAMFLOW WEIR POOL RESIDENCE TIME

Water was sampled from the M8 weir pool because stream points immediately upstream and downstream were too shallow for intake hose placement. Similarly pit throughflow into the 210 l storage drums was sampled from the drum reservoir, because of the low intermittent flows involved. Water automatically sampled from shallow reservoirs at set time intervals may be altered isotopically by its residence time within the pool. Theoretical weir pool flushing time (FT) was computed to determine isotopic mixing as a function of weir or drum outflow:

$$FT = VOL_{pool} / VOL_{out} \qquad (B.1)$$

where: VOL_{pool} is the weir pool volume (m^3) and VOL_{out} is the weir outflow volume ($m^3\ hr^{-1}$), assuming that all inputs mix equally throughout the pool water column.

Figure B.1A shows an exponential fit of equation B.1 for the M8 weir. For low stage heights (>4-5 cm), flushing rate is very long (c.10-20 hr), which would significantly alter the true isotopic composition of the streamflow. Fortunately, a stage of 40-50 mm represented a baseflow condition within the M8 catchment (during the August to December period) and stormflow exceeded this value in every case within the first 30 min of flow. Since water samples were extracted from the weir pool on a 2, 4 and 8 hr basis, storm hydrograph separation using these samples are correct.

A theoretical flushing curve for the 210 l drum is shown in Figure B.1B. In this case, most flow events started from an initial stage of 0-2 mm, therefore initial flushing was extremely slow (no flushing to 36 days) resulting in substantial error during the early stages of storm hydrograph rise. For the 4 and

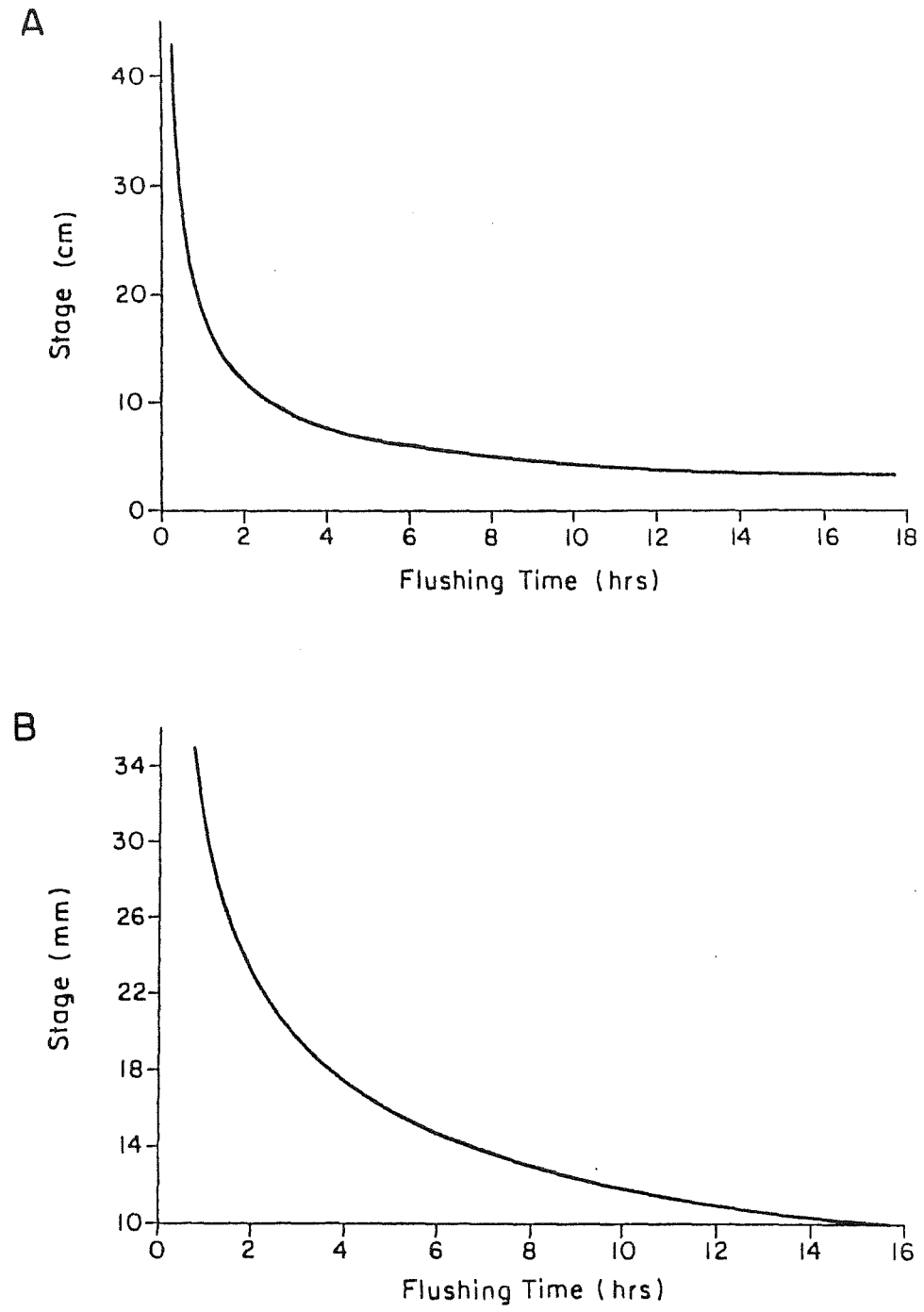

Figure B.1 Theoretical flushing rates for M8 weir pool (A) and 210 l drum pool (B).

8 hr sampling strategy adopted throughout the study, critical stage heights of 14 and 18 mm were required to maintain flushing within these time periods. However, instantaneous samples corresponding to flow at that point were desired, therefore stage heights of 24 and 18 mm were required to limit flushing-induced errors to 0.5 times the sampling interval for 4 and 8 hr sampling respectively.

Table B.1 shows δD differences for drum outflow versus hose input for varying flow-stage relationships sampled during the 26-28 November event. For the Pit 5 outflow, drum water was $-1.8°/_{oo}$ lighter than the input hose (i.e true pitflow δD) at 1600 hr 27 November. Proceeding through the event, drum and hose δD were equal ($+/-$ $0.1°/_{oo}$) at 1000 hr 29 November. By 1715 hr 01 December, drum water was again approximately equal ($+/-0.6°/_{oo}$). Pit A drum water was $-2.9°/_{oo}$ heavier than input water at 1600 hr 27 November. At 1000 hr 29 November, drum water was lighter than the input by $-1.9°/_{oo}$ and then approximately equal to input value $+/-0.1°/_{oo}$ by 1715 hr 02 December.

Given that the accuracy of δD mass spectroscopy is $+/-1.0°/_{oo}$, only the initial values for Pit 5 and Pit A are in error. Subsequent values are within experimental error and generally fit the hypothesis of complete theoretical drum flushing as expressed in equation B.1. Pit hydrograph separations in section 4 are examined in light of possible error during the rising limb.

Table B.1. Drum flushing experiment results.

Location	Date	Time hr	Drum δD ‰	Hose δD ‰
Pit 5	27 November	1600	-37.7	-39.5
	29 November	1000	-40.2	-40.1
	02 December	1715	-39.1	-38.5
Pit A	27 November	1600	-43.2	-40.3
	29 November	1000	-39.9	-41.8
	02 December	1715	-39.4	-39.3

C RAINFALL ISOTOPIC WEIGHTING TECHNIQUES

The following appendix is an abbreviated version of a manuscript in preparation. Data presented are from M. Bonell (personal communication, 1988) and ideas presented, form a joint venture with M. Bonell (James Cook University), M. Stewart (NZ Institute of Nuclear Sciences) and A. Pearce (NZ Forest Research Centre).

C.1 SUMMARY

Isotopic variation in storm rainfall is an important consideration in hydrograph separation using the mass balance approach, but is rarely considered when determining the accuracy of old water estimates. Results from a small watershed on the South Island of New Zealand show that in addition to the within storm isotopic variations themselves, rainfall weighting techniques may substantially influence estimates of old/new water as a function of both total runoff and total quickflow production. Two incremental approaches to rainfall weighting are presented. Results show that within storm incremental weighting is better than the standard weighting technique, which imposes a total storm rainfall value exogenously on the mass balance equation.

C.2 INTRODUCTION

C.2.1 Hydrograph separations based on D and ^{18}O

Recent studies in temperate (Fritz et al., 1976; Sklash et al., 1976; Sklash and Farvolden, 1979; Bottomley et al., 1984; Kennedy et al., 1986), arid (Turner et al., 1987) and high rainfall (Pearce et al., 1986; Sklash et al., 1986) environments, have utilised the natural stable isotope variations in the water balance to determine the 'old' water (groundwater and soil water) versus 'new' water (rainfall) components in storm runoff.

Hydrograph separations are based on the simple mass balance equation:

$$Qo = [(Cs - Cn)/(Co - Cn)]Qs \quad (C.1)$$

and,

$$Qn = Qs - Qo \quad (C.2)$$

where: Q is the stream discharge and C expresses the deuterium (D) or oxygen-18 (^{18}O) concentration of s (stream), o (old) water and n (new) water, generally expressed as the per mil ($^{o}/_{oo}$) variation with respect to standard mean ocean water (Craig, 1961). The use of equations C.1 and C.2 are based on the requirement that old and new water have distinct isotopic signatures. The conditions under which hydrograph separations can be successfully made are based on a further set of assumptions and requirements (Sklash and Farvolden, 1979; 1982) that: (i) groundwater and baseflow are characterized by a single isotopic content, (ii) rainfall is characterized by a single isotopic content or variations in the content are documented, (iii) vadose water contributions to the stream are negligible, and (iv) surface storage water contributions to the stream are negligible.

Although there are limitations associated with each of the above assumptions (Kennedy et al., 1986), isotopic variation in storm rainfall (assumption 2) has not been adequately addressed in previous isotopic separation studies, because bulk storm rainfall has been mainly used for estimating the new water signature. Under some circumstances, when fractional storm rainfall has been collected, standard weighting techniques have been shown to be inadequate, which leads to inaccurate assessments of old water volumes in stormflow (Rodhe, 1987, p. 179). Two alternative weighting techniques are presented for incrementally collected storm rainfall, in order to generate awareness of rainfall isotopic variations and the applicability

of different weighting techniques to varying hydrological situations.

C.2.2 Potential problems of δD rain variations

Large variations in the isotopic compositions of precipitation over short periods of time (hours or days) at individual locations are commonly observed. Factors influencing rainfall isotopic compositions are temperature of condensation (e.g. Dansgaard, 1964; Hartley, 1981), origin of air mass vapour (Gat and Dansgaard, 1972) and evaporation and isotopic exchange between falling raindrops and surrounding water vapour (Ehhalt et al., 1963; Stewart, 1975). Recently, Heathcote and Lloyd (1986) observed large variations in rainfall isotopic composition on a time scale of a few days, which showed no seasonal dependence nor any clear relationship with daily mean air temperature. Fractionally collected rainwater was also analyzed by Matsuo and Friedman (1967), who showed that storm rainfall isotope contents varied with time, especially at the beginning of a shower where the precipitation intensity was low. Constancy of the isotopic composition was observed only during high intensity rainfall.

In most storm runoff isotopic separations, bulk storm rainfall is collected and analysed to yield a single isotopic input value. When several rainfall samples have been collected during a storm, a weighted mean value for the storm rainfall has been computed as:

$$\delta D \text{ or } \delta^{18}O = \sum_{i=1}^{n} Pi\delta i / \sum_{i=1}^{n} Pi \qquad (C.3)$$

where: Pi and δi denote fractionally collected precipitation depth and δ value respectively. This weighted mean represents the average isotopic composition of the new water input, but does not address the within storm isotopic variability or its relation to rainfall intensity. Kennedy et al. (1986) argue that isotopic composition of overland flow may not match that of the average

rain isotopic composition because moderate-intensity rain may infiltrate completely, whereas more intense rainfall with a different isotopic composition may exceed infiltration capacities and runoff directly. In these circumstances, higher intensity rainfall, whose isotopic signature is different from lower intensity rainfall (Matsuo and Friedman, 1967), would have a greater effect on catchment hydrograph and isotopic response.

C.3 METHODS

C.3.1 Sequential rainfall sampler

A modified version of a Kennedy et al. (1979) sequential rainfall sampler was used to sample discrete rainfall increments during individual storm events. Rain samples were collected using a 39 cm diameter plastic funnel connected to individual 300 and 600 ml sample bottles, representing 2.5 and 5.0 mm increments respectively. Details of construction are given in section 3.4.2. A tipping bucket raingauge was located within 1m of the sequential sampler to enable sample volume to be related to rain intensity and time of rainfall burst. Water samples were removed from the bottles within 3-6 days and analyzed for deuterium composition. Samples were housed in cool shaded areas in sealed full bottles to prevent any fractionation prior to analysis. Isotope samples were prepared by the zinc reduction method (Stanley et al., 1984) and analyses were run on a V.G. Micromass 602 mass spectrometer.

C.3.2 Additional weighting techniques

In addition to the standard mean weighting (equation C.3), two other weighting techniques were employed: incremental mean and incremental intensity mean. An incremental mean rainfall isotopic value is a refinement of the standard weighted mean and allows the current rainfall isotopic composition to vary during the event as further rain falls, rather than being fixed at the

overall mean value. Cumulative mean values of sequentially sampled rainfall are computed at a time appropriate to when the stream sample was taken (either on a time sampling basis or runoff depth sampling basis), and are used directly in the mass balance separation. The incremental intensity mean is also an endogenous approach, but is based on the rationale that higher intensity rain produces more runoff under many circumstances and thus should be weighted accordingly. The procedure is similar to the incremental mean, but modifies equation C.3 to give:

$$\delta D \text{ or } {}^{18}O = \sum_{i=1}^{n} I_i \delta_i / \sum_{i=1}^{n} I_i \qquad (C.4)$$

where: Ii is the average mm hr^{-1} rainfall intensity during the sampling increment. In this way, the isotopic signatures of high intensity bursts assume a greater influence on the average storm isotopic weighting. If the rainfall intensity was constant throughout, the two incremental approaches would give the same result.

C.4 RESULTS AND DISCUSSION

Weighting technique effects on storm hydrograph isotopic separation are presented for a small catchment on the South Island of New Zealand (Figure C.1). Glendhu 2 is a moderately responsive catchment (310 ha) with rolling sideslopes (average 28°) and wide concave valley bottoms. Annual precipitation is 1303 mm and quickflow production averages 30% of the total runoff and 20% of the total precipitation (Pearce et al., 1984).

A 45.1 mm rain event on 23 February 1988 showed a 32.9‰ range in δD values with a weighted mean (equation C.3) of -80.3‰. Peak catchment specific discharge was 2.72 mm hr^{-1} with QF/R = 86.9% and QF/P = 35.2%. Hydrograph separations using the three weighted mean approaches are shown in Figure C.2. Peak old water specific discharges for the standard, incremental mean and incremental intensity were 0.56 mm hr^{-1}, 1.19 mm hr^{-1} and

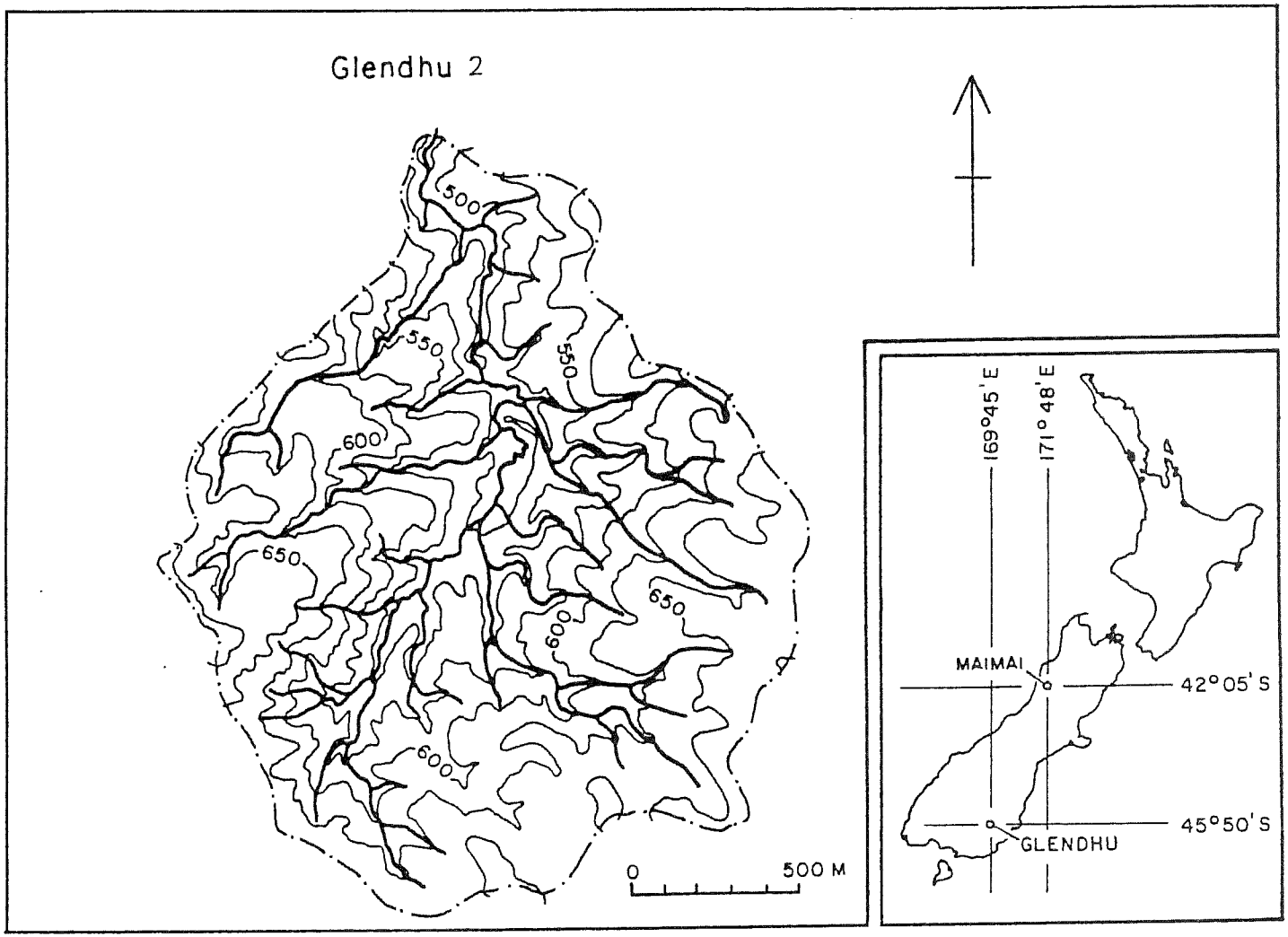

Figure C.1 The Glendhu 2 experimental catchment.

Figure C.2 Glendhu 2 response to the 23 February 1988 storm showing the effect of different weighting techniques on hydrograph separation.

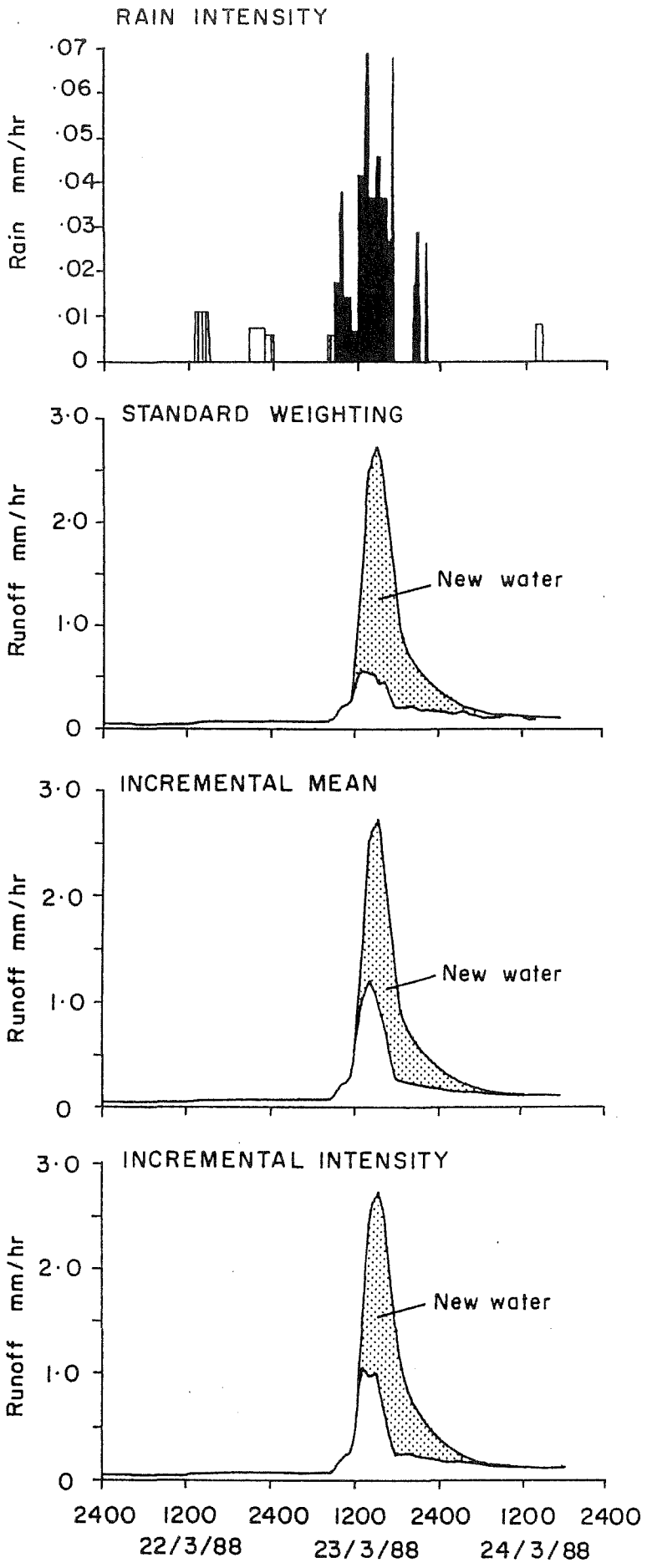
RAIN INTENSITY
·07
·06
·05
·04
·03
·02
·01
0
Rain mm/hr
STANDARD WEIGHTING
3·0
2·0
1·0
0
Runoff mm/hr
New water
INCREMENTAL MEAN
3·0
2·0
1·0
0
Runoff mm/hr
New water
INCREMENTAL INTENSITY
3·0
2·0
1·0
0
Runoff mm/hr
New water
2400 1200 2400 1200 2400 1200 2400
22/3/88 23/3/88 24/3/88

1.06 mm hr^{-1} respectively. The percent old water versus time is shown in Figure C.3 and clearly demonstrates the dependence on the method of rainfall weighting used. In this storm, the standard weighting technique overestimated the amount of new water entering the stream by up to 30%, with the highest differences being encountered during the rising limb of the hydrograph.

Tabulation of quickflow characteristics (Table C.1) as a function of new water volumes shows clear differences in the ratio of quickflow to gross precipitation (Qn/P) and total quickflow (Qn/QF). Here again, standard rainfall weighting produced a 14.5% and 10.7% overestimate of new water volumes in quickflow against the incremental mean and incremental intensity approaches respectively.

Less difference between calculations from incremental Pi and Ii is found in the monitored event because of persistent low rain intensities of similar magnitude between increments. Greater differences may occur in high rainfall areas like tropical rainforests (Bonell et al., 1981) or mid-latitude convective thunderstorm events. The differences that do occur are largest during the rising limb of the hydrograph. Each of the methods should and do merge toward a single value towards the end of the storm, once all the rainfall samples have been included into the cumulative mean.

Another rainfall 'weighting' technique may be appropriate under certain conditions. For example, a heavy 10 min burst of rainfall may occur within a protracted low intensity rain event, producing a large and rapid hydrograph response. If widespread saturation overland flow was occurring, as in the case of a semi-wetland (e.g. Jackson, 1987) or a high rainfall, high relief tropical rainforest catchment (e.g. Bonell and Williams, 1986),

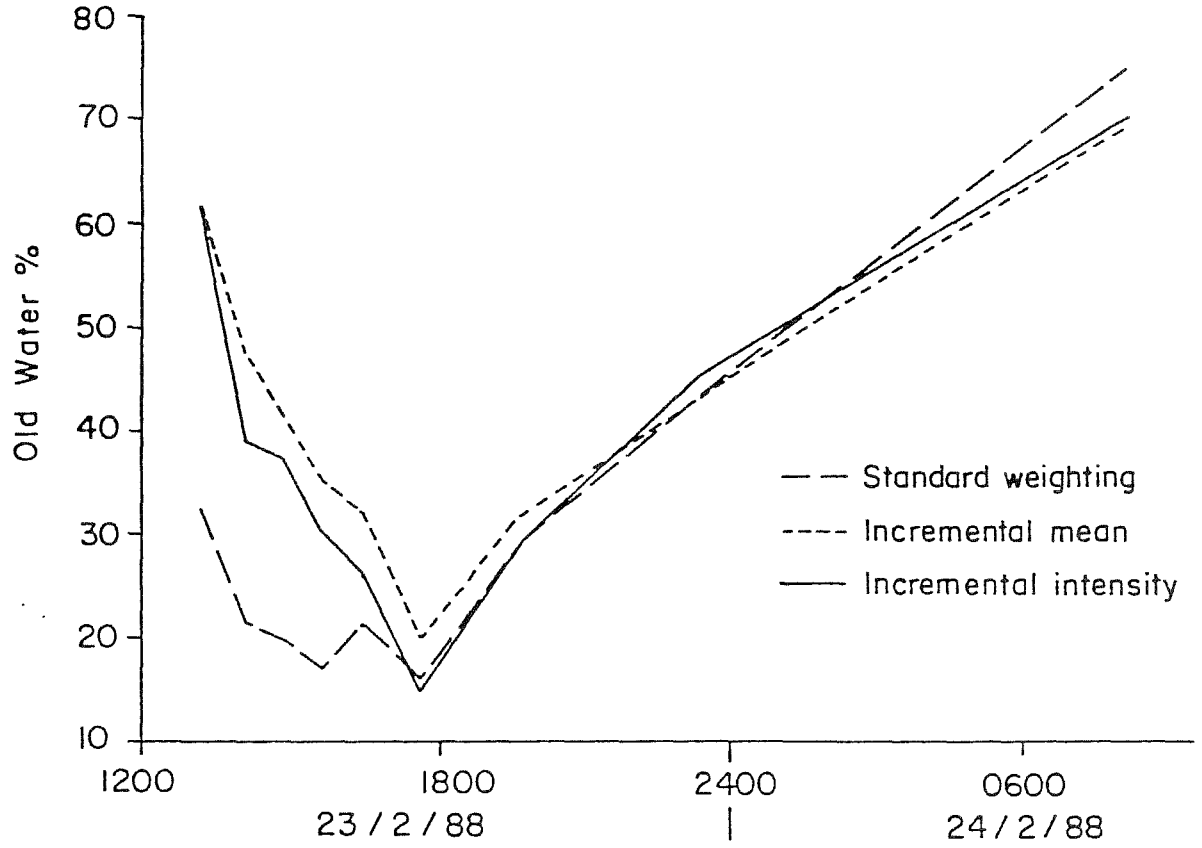

Figure C.3 Old water percentage estimates for the Glendhu 2, 23 February 1988 storm event.

only the 10 min burst could be realistically linked with the resulting sudden hydrograph rise. In this case, weighting rainfall to values that fell several hours previous to the intense burst or giving them any weighting at all would be unrealistic. Here again, if total storm rainfall was simply bulk-collected and used in the mass balance separation, major errors could occur if rain varied isotopically.

Table C.1. Weighting technique comparisons for the Glendhu 2, 23 February 1988 storm event.

Method	QF mm	Qo mm	Qn mm	Qn/P %	Qn/QF %
Standard	15.9	3.8	12.1	26.8	76.1
Incremental Mean	15.9	6.1	9.8	21.7	61.6
Incremental Intensity	15.9	5.5	10.4	23.1	65.4

C.5 CONCLUSIONS

Clearly, rainfall weighting techniques can make a large difference to old water computation if rainfall isotopic variability is high. Conclusions drawn from this appendix are:

1. Deuterium concentration in storm rainfall can vary significantly and therefore should be sampled sequentially during storm events if hydrograph separation is to be conducted.

2. The standard weighting technique employed in most isotopic hydrograph separations is unrealistic because it uses rain isotopic signatures for the entire event for point separations within the event. Therefore, old water estimates at any point before the end of the event are affected by the isotopic composition of rain that has not yet fallen, rendering the technique physically incorrect.

3. An incremental mean approach solves the above problem by computing a running mean through an event and using this more correct value in the mass balance separation.

4. An incremental intensity mean approach may be useful under conditions of variable rainfall intensity, particularly in mid-latitude continental situations with cold front or thunderstorm events and the high rain intensities experienced in tropical areas which produce intense bursts interspersed with lower intensity periods.

5. Individual sequential values through an event (or a single value within the event) may be used directly in the mass balance separation at that point, under some circumstances, when a very high intensity burst is isolated within a protracted low intensity period. This would be suited to a highly responsive catchment only, where saturation overland flow is produced over very large portions of the watershed.

Finally, it is not suggested that these additional weighting techniques are the only ones to consider or that they solve specific hydrograph separation problems. We merely wish to highlight the variability in rainfall isotopic composition and its implication for hydrograph separation. There are a number of errors associated with isotopic separation ranging from molecular exchange between overland flow and return flow (Rodhe, 1987), to soil water/groundwater definitions and isotopic determination (Kennedy et al., 1986). It remains for many of these problems to be isolated and analyzed and for proper error analysis to be conducted.